University of Missouri, St. Louis

IRL @ UMSL

Dissertations

UMSL Graduate Works

12-13-2010

Activation of Propargylic Alcohols by Piano-Stool Ruthenium Complexes Bearing Phosphoramidite Ligands

Stephen Andrew Costin
University of Missouri-St. Louis, sacz89@mail.umsl.edu

Follow this and additional works at: https://irl.umsl.edu/dissertation

Part of the Chemistry Commons

Recommended Citation

Costin, Stephen Andrew, "Activation of Propargylic Alcohols by Piano-Stool Ruthenium Complexes Bearing Phosphoramidite Ligands" (2010). *Dissertations*. 449.
https://irl.umsl.edu/dissertation/449

This Dissertation is brought to you for free and open access by the UMSL Graduate Works at IRL @ UMSL. It has been accepted for inclusion in Dissertations by an authorized administrator of IRL @ UMSL. For more information, please contact marvinh@umsl.edu.

Activation of Propargylic Alcohols by Piano-Stool Ruthenium Complexes Bearing Phosphoramidite Ligands

by

Stephen Costin

A dissertation submitted in partial fulfillment
Of the requirements for the degree of
Doctor of Philosophy
(Chemistry)

University of Missouri-St. Louis
Fall, 2010

Eike Bauer
Chairperson

Joyce Corey

George Gokel

Christopher Spilling

Acknowledgements

I would like to offer special thanks my adviser, Dr. Eike Bauer for his guidance and support. Thank you to my lab mate, Sergey Sedinkin, for many good ideas and for challenging me to be great. Thanks to Dr. Nigam Rath for assistance with X-ray structures and Dr. Rudolph Winter and Mr. Joe Kramer for help with mass spectrometry. I would also like to acknowledge Dr. Christopher Spilling and Dr. James Chickos for occasional guidance. Special thanks to my undergraduate research adviser, Dr. Robert Corcoran for convincing me to pursue my Ph. D. Thank you to my mother, Ginger Costin, for her unwavering support and for teaching me vision and self-motivation.

Thank you to the University of Missouri–St. Louis Research Board and the University of Missouri–St. Louis Research Award for funding.

This is dedicated to the memory of my father,

Frank Costin

I am sad that you could not be here for this.

Table of Contents

List of Tables iv

List of Figures v

List of Schemes vi

Structural listing of new compounds x

Abstract xii

Chapter 1: Introduction 1

Chapter 2: Synthesis and reactivity studies of η^6-arene piano-stool complexes 17

- 2.1. Aim 17
- 2.2. Introduction 17
- 2.3. Results 19
- 2.4. Discussion 27
- 2.5. Summary and Prospective 36
- References 36
- Experimental 38

Chapter 3: Synthesis and reactivity studies of η^5-cyclopentadienyl complexes 54

- 3.1. Aim 54
- 3.2. Introduction 54
- 3.3. Results 58
- 3.4. Discussion 62
- 3.5. Summary and Prospective 71
- References 72
- Experimental 74

Chapter 4: Synthesis and coordination chemistry of a new P-donor ligand class 82

4.1. Aim 82

4.2. Introduction 82

4.3. Results 83

4.4. Discussion 87

4.5. Summary and Prospective 90

References 91

Experimental 92

Chapter 5: Activation of propargylic alcohols by η^5-indenyl ruthenium complexes . . . 96

5.1. Aim 96

5.2. Introduction 96

5.3. Results 102

5.4. Discussion 119

5.5. Summary and Prospective 124

References 125

Experimental 127

Chapter 6: Electronic tuning of η^5-indenyl complexes via ligand substitution 147

6.1. Aim 147

6.2. Introduction 147

6.3. Results 151

6.4. Discussion 166

6.5. Summary and Prospective 169

6.6. Conclusions 170

References 172

Experimental 174

List of Tables

Table 2.1. β-Oxo ester formation. 22

Table 2.2. Cyclic β-oxo ester formation. 23

Table 2.3. Comparison of catalysts in β-oxo ester formation. 26

Table 3.1. Selected bond lengths and angles for complexes **69b** and **70**. 62

Table 3.2. Catalytic results of the Mukaiyama aldol reaction. 70

Table 5.1. Selected bond lengths and angles for complex **111b** 106

Table 5.2. Selected bond lengths and angles for complexes **116a, b**. 110

Table 5.3. Substitution of propargylic alcohols by electron-rich aromatics. 117

Table 6.1. Selected bond lengths and angles of **132**. 157

Table 6.2. Crystallographic parameters for **132**. 158

List of Figures

Figure 1.1. Chiral-at-metal allenylidene complexes. 11

Figure 1.2. Structure of some typical phosphoramidite ligands. 12

Figure 2.1. Crystal structure of **43a** 20

Figure 2.2. Sterically and electronically tuned phosphoramidite ligands. 24

Figure 2.3. Kinetic comparison of catalysts. 30

Figure 3.1. X-ray structures of **69b** and **70**. 61

Figure 5.1. Crystal structure of **111b**. 105

Figure 5.2. Allenylidenes bearing electron-donating and electron-withdrawing groups 107

Figure 5.3. Crystal structure of allenylidene complexes **116a**. .109

Figure 5.4. Crystal structure of allenylidene **116b**. 109

Figure 5.5. A space-filled model of complex **116b**. 111

Figure 6.1. Steric and electronic tuning sites in indenyl complexes. 148

Figure 6.2. Trimethylindenyl phosphine ruthenium complexes. 149

Figure 6.3. Crystal structure of **132**. 157

List of Schemes

Scheme 1.1. The Nicholas reaction.. 3

Scheme 1.2. Potential intermediates in catalytic propargylic substitution. 4

Scheme 1.3. Gold catalyzed propargylic substitution. 5

Scheme 1.4. Rh catalyzed propargylic amination. 5

Scheme 1.5. Rhenium catalyzed propargylic substitution reactions. 6

Scheme 1.6. Ruthenium catalyzed propargylic substitution reactions. 6

Scheme 1.7. Copper catalyzed propargylic amination. 7

Scheme 1.8. Selegue's allenylidene synthesis. 8

Scheme 1.9. Reactivity of a chiral allenylidene complex. 9

Scheme 1.10. Nucleophilic addition to a chiral-at-metal allenylidene. 11

Scheme 1.11. Tuned phosphoramidite ligands in catalysis. 13

Scheme 2.1. Watanabe's catalyst system for β-oxo ester formation. 18

Scheme 2.2. Phosphoramidite complex synthesis. 20

Scheme 2.3. Allenylidene cleavage by attack of H_2O. 22

Scheme 2.4. Synthesis of a novel ligand based on R-BIPHEN. 24

Scheme 2.5. Synthesis of complexes [$RuCl_2$(*p*-cymene)(phosphoramidite)]. 25

Scheme 2.6. Synthesis of a hexamethylbenzene (C_6Me_6) complex. 28

Scheme 2.7. Dissociation of the *p*-cymene ligand. 29

Scheme 2.8. Attempted synthesis of the allenylidene complex. 32

Scheme 2.9. Chloride abstraction in acetonitrile. 33

Scheme 2.10. Proposed mechanism of β-oxo ester formation 35

Scheme 3.1. Formation of allenylidenes from a *p*-cymene ruthenium complex. 55

Scheme 3.2. Formation of a vinylvinylidene complex. 56

Scheme 3.3. Formation of a cyclobutylidene complex. 56

Scheme 3.4. Nucleophilic attack on allenylidene complexes. 57

Scheme 3.5. Protonation of an allenylidene complex. 57

Scheme 3.6. Synthesis of new mixed phosphine/phosphoramidite complexes. 58

Scheme 3.7. Synthesis of diastereopure Cp ruthenium complexes. 59

Scheme 3.8. Synthesis of allenylidene complexes. 64

Scheme 3.9. Synthesis of a Cp allenylidene complex via activation with $AgPF_{6.}$ 66

Scheme 3.10. Attempted allenylidene formation from complex **70**. 67

Scheme 3.11. Formation of a reactive intermediate by chloride abstraction. 68

Scheme 3.12. A potential catalytic cycle for propargylic substitution. 69

Scheme 4.1. Attempted electronic tuning via phosphoramidite ligands. 83

Scheme 4.2. Synthesis of the first dithiaphosphoramidite. 83

Scheme 4.3. Synthesis of the new dithiaphosphoramidite ligand (rac)-**89**. 84

Scheme 4.4. Synthesis of the first dithiaphosphoramidite ruthenium complex **90**. 85

Scheme 4.5. Etherification of propargylic alcohols using (rac)-**90**. 86

Scheme 4.6. Double addition of methanol. 88

Scheme 4.7. Hydrolysis of **89** and **90**. 90

Scheme 5.1. Synthesis of an allenylidene complex. 97

Scheme 5.2. Addition of nucleophiles to an allenylidene complex. 98

Scheme 5.3. Unique reactivity of vinylvinylidene complexes. .99

Scheme 5.4. Evidence for an allenylidene-vinylvinylidene tautomerization. 99

Scheme 5.5. Formation of a bicyclic allenylidene complex. 100

Scheme 5.6. Stoichiometric enantioselective substitution of propargylic alcohols. . . .100

Scheme 5.7. Synthesis of a vinylalkylidene complex. 101

Scheme 5.8. Synthesis of new indenyl phosphoramidite complexes of ruthenium. . . .103

Scheme 5.9. New phosphoramidite ligand synthesis. 104

Scheme 5.10. Synthesis of new chiral complexes. 104

Scheme 5.11. Synthesis of the first phosphoramidite allenylidene complex. 107

Scheme 5.12. Allenylidene versus vinylvinylidene formation. 112

Scheme 5.13. Attempted synthesis of aliphatic allenylidenes. 113

Scheme 5.14. Synthesis of a secondary allenylidene. 113

Scheme 5.15. Synthesis of allenylidenes **120**. 114

Scheme 5.16. Catalytic propargylic substitution with electron-rich aromatics. 116

Scheme 5.17. Proposed catalytic cycle for propargylic substitution. 118

Scheme 5.18. Proposed mechanism of substitution. 119

Scheme 5.19. The indenyl effect in allenylidene formation. 121

Scheme 5.20. Nucleophilic attack on allenylidene **116b**. 123

Scheme 6.1. Substitution of PPh_3 by a chelating bis(phosphine) ligand. 150

Scheme 6.2. Synthesis of cationic complexes. 150

Scheme 6.3. Synthesis of mixed carbonyl phosphine complexes. 151

Scheme 6.4. Synthesis of indene derivatives. 152

Scheme 6.5. Attempted synthesis of new indenyl ruthenium complexes. 152

Scheme 6.6. Synthesis of [(Ind)RuCl(cod)] (**125**). 154

Scheme 6.7. Synthesis of a bis(phosphoramidite) complex. .154

Scheme 6.8. Synthesis of a tripyrrolylphosphine complex **132**. 156

Scheme 6.9. Attempted synthesis of a pyridyl complex. 160

Scheme 6.10. Synthesis of a new P,N-chelating phosphoramidite. 160

Scheme 6.11. Synthesis of a new P,N-phosphoramidite complex. 161

Scheme 6.12. Synthesis of an electronically tuned P,N-phosphoramidite ligand. 162

Scheme 6.13. Unexpected reactivity of the new bidentate ligand. 163

Scheme 6.14. Synthesis of a cationic complex **141a**. 166

Structural listing of new compounds

Chapter 2:

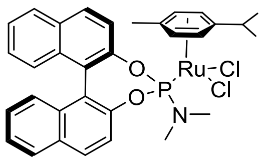
O
O
P
Ru
Cl
Cl
N

43a

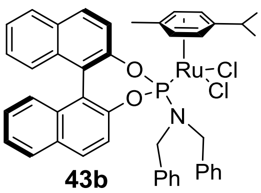
O
O
P
Ru
Cl
Cl
N
Ph
Ph

43b

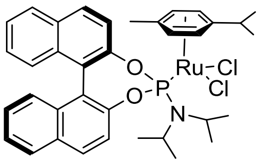
O
O
P
Ru
Cl
Cl
N

43c

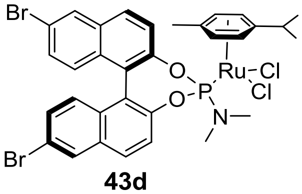
Br
Br
O
O
P
Ru
Cl
Cl
N

43d

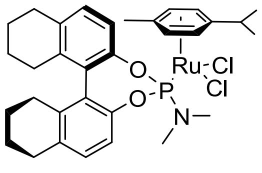
O
O
P
Ru
Cl
Cl
N

48a

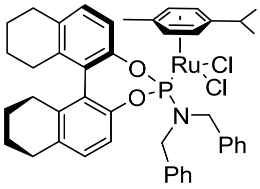
O
O
P
Ru
Cl
Cl
N
Ph
Ph

48b

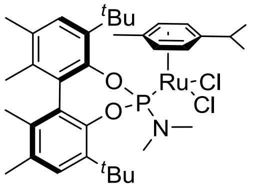
tBu
tBu
O
O
P
Ru
Cl
Cl
N

49

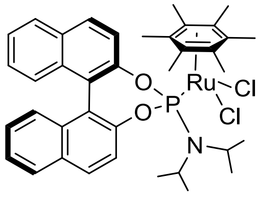
O
O
P
Ru
Cl
Cl
N
N

51

Chapter 3:

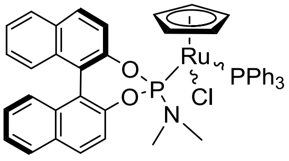
O
O
P
Ru
PPh3
Cl
N

69b

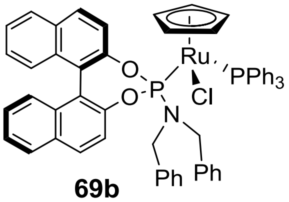
O
O
P
Ru
PPh3
Cl
N
Ph
Ph

69b

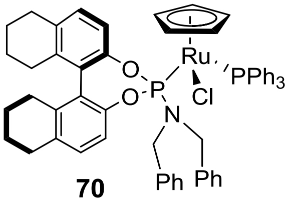
O
O
P
Ru
PPh3
Cl
N
Ph
Ph

70

Chapter 4:

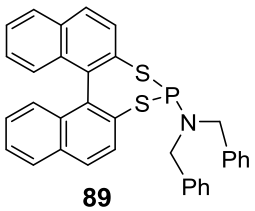

89

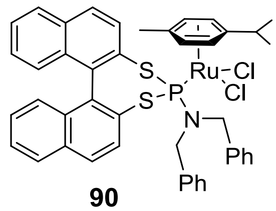
S
S
P
Ru
Cl
Cl
N
Ph
Ph

90

Chapter 5:

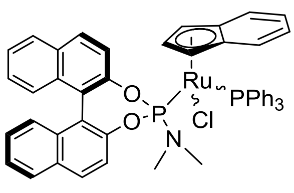
O
O
P
Ru
PPh3
Cl
N

111a

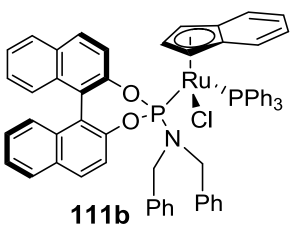
O
O
P
Ru
PPh3
Cl
N
Ph
Ph

111b

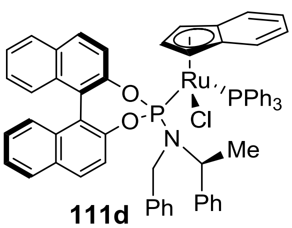
O
O
P
Ru
PPh3
Cl
N
Me
Ph
Ph

111d

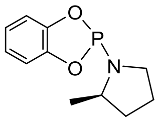

114

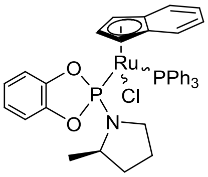

111c

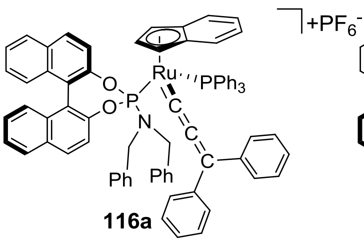

116a

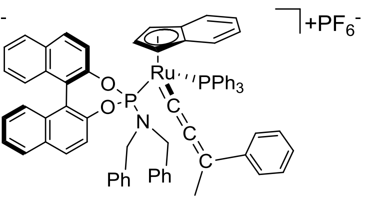

116b

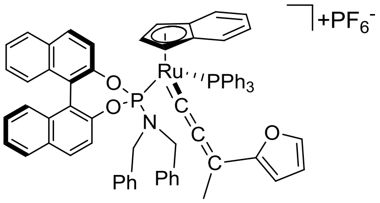

116c

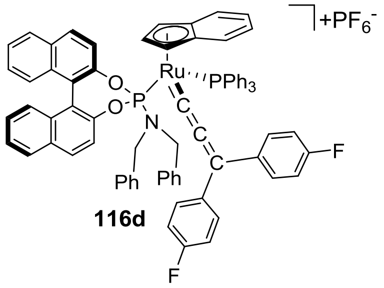

116d

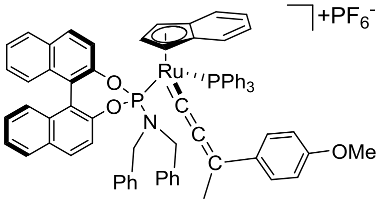

116e

Chapter 6:

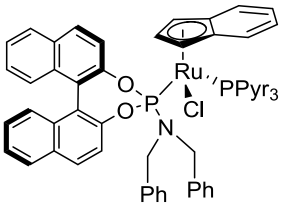

132

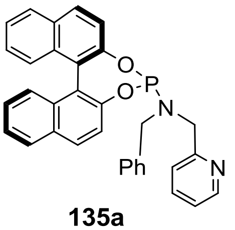

135a

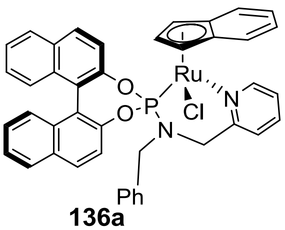

136a

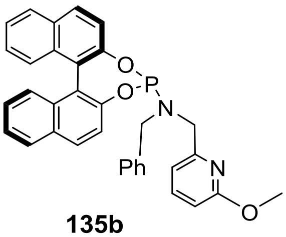

135b

Abstract

Various piano-stool ruthenium complexes bearing phosphoramidite ligands have been synthesized and characterized spectroscopically and in some cases structurally. Reaction of phosphoramidite ligands **41** with an appropriate metal precursor gave new piano-stool ruthenium complexes [RuCl(L)(arene)(phosphoramidite)], where L = Cl, PPh_3, or others. The novel complexes were tested for their ability to activate propargylic alcohols catalytically as well as stoichiometrically. Specifically, catalytic substitution of propargylic alcohols via allenylidene intermediates was envisioned. Stoichiometric reactions designed to form stable, isolable allenylidenes were sought as well.

η^6-*p*-cymene complexes of the type [$RuCl_2$(η^6-*p*-cymene)(phosphoramidite)] (**43, 45**) activate propargylic alcohols in the reaction with carboxylic acids to form β-oxo esters. The catalytic activity of the complexes is clearly related, in part, to the steric effects of the ligands with the more hindered complexes such as **43b** outperforming their less sterically crowded counterparts. In these complexes the arene ligand has been shown to be labile, dissociating at elevated temperatures or after prolonged times in solution (CH_2Cl_2, cyclohexane) or in the solid state. The complexes overall were shown to be inactive in reactions involving allenylidene intermediates.

η^5-arene complexes of the type [CpRuCl(PPh_3)(phosphoramidite)] (**43**) and [(Ind)RuCl(PPh_3)(phosphoramidite)] (**111**) are viable complexes for the activation of propargylic alcohols as well. Upon coordination of a chiral phosphoramidite ligand a new stereocenter is formed at the metal. The diastereoselectivity of complex formation is highly dependent on the steric effects of the incoming phosphoramidite ligand. The best

results were obtained for the complexes bearing the ligand **41b** (**69b**, **111b**), as they can be isolated in diastereomeric purity (**111b** forms as a single diastereomer). **111b** forms stable allenylidenes [(Ind)Ru(PPh_3)(**41b**)(=C=C=CR^1R^2)]PF_6 (**116**) in reaction with propargylic alcohols (**5**) after chloride abstraction using $(Et_3O)PF_6$ in CH_2Cl_2.

Bidentate phosphoramidite ligands utilizing a pyridyl moiety (**135**) can coordinate in a chelating fashion, favoring the double substitution due to entropic reasons. A potentially general synthetic route to this new class of ligands has been developed. The effectiveness of this method of electronic tuning is still uncertain, as the coordination chemistry of the analogous ligands is dissimilar for steric reasons. Synthesis of a small library of tuned, bidentate phosphoramidite ligands will give greater insight into the usefulness of this ligand class and will allow further tuning of the catalytic activity of the respective complexes.

Introduction

Organic chemistry has played and continues to play a fundamental role in shaping everyday life. As organic chemistry continues to have a considerable role in advancements in technology, medicine and elsewhere, it is important to continue to expand the base for chemistry and chemical reactions. The discovery of new reaction pathways is necessary for the development of better synthetic techniques, in turn allowing the synthesis of previously unattainable compounds. Organometallic catalysts utilizing transition metals have long been employed to achieve this goal.

Transition metal based organometallic catalysts can be used for transformations that otherwise would be impossible or would require multiple steps. Employment of chiral catalysts allows for stereoinduction as well. For example, hydrogenation of olefins is a common reaction that often employs organometallic catalysts. From the achiral Wilkinson's catalyst[1] in 1966 to modern rhodium catalysts employing asymmetric phosphoramidite ligands,[2] hydrogenation reactions are a representative case where organometallic catalysis is used to perform a reaction, with or without stereoinduction.

Formation of stereocenters with high enantioselectivity is one of the most fundamental and most difficult problems in organic chemistry. Modern methods for this process include use of chiral auxiliaries,[3] enzymatic catalysis,[4] kinetic resolution[5] and asymmetric catalysis.[6] All of these methods have drawbacks, however. Chiral auxiliaries generally have to be synthesized and add extra steps to the synthesis for attachment and removal following use. Enzymatic catalysis is limited by the enzymes available, and many reactions do not allow for formation of analogues. Resolution techniques have a theoretical yield of only 50%. Asymmetric catalysis also has drawbacks, e.g. cost and toxicity, but the benefits including the broad range of reactions available, the ability to tune catalysts for moderated activity, and minimization of waste frequently make it a preferred method for stereoinduction.

Modern concerns of diminishing carbon feedstocks, climate change and a potential energy crisis have caused a shift in the chemical industry centered on the principles of Green Chemistry.[7] Green chemistry is an ideal based on decreasing the negative environmental impact of doing chemistry. Its principles include reducing waste, decreasing energy usage and decreasing (or even eliminating toxic chemical use). Asymmetric catalysis fits with the tenets of Green Chemistry by preventing stoichiometric waste, potentially lowering energy costs (by lowering reaction temperatures) and preventing the necessity of extra steps that would require energy and consume more solvent waste. One such reaction where this may be possible is the Nicholas reaction.[8]

The Nicholas reaction is a cobalt mediated, multi-step reaction requiring the use of stoichiometric amounts of toxic $Co_2(CO)_8$ (Scheme 1.1). Overall, the Nicholas reaction substitutes the hydroxyl group of a propargylic alcohol by a general nucleophile. A number of carbon centered nucleophiles, including aromatics, β-keto esters, and β-diketones can be used. A metal stabilized propargylic carbocation is the key intermediate in the reaction. After addition of the nucleophile to the carbocation, the cobalt must be removed by oxidation in a final step. Replacing this stoichiometric, multi-step process that utilizes a highly toxic reagent with one that makes use of asymmetric organometallic catalysis presents a useful solution, not only for its Green Chemistry implications but for the advancement of chemical synthesis as well.

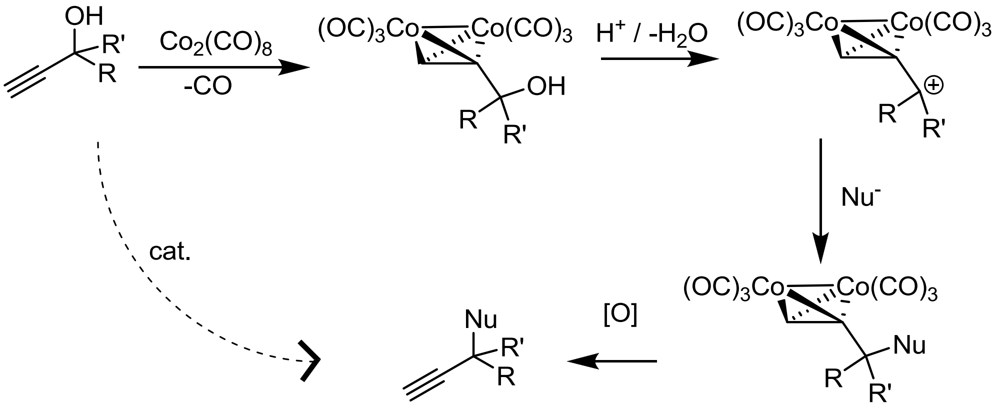

Scheme 1.1. The Nicholas reaction.[8]

The Nicholas reaction and related propargylic substitution reactions have been used in the total synthesis of many biologically active compounds, such as (+)-cis-lauthisan[9] as well as a β-pinene-neoclerodan hybrid.[10] Holman and Toste et al. utitilized a Re(V) catalyst for substitution of a propargylic alcohol in route to human lipoxygenase inhibitors.[11] In some cases, the products of these types of reactions are racemic mixtures,[11] whereas in others diastereoselectivity can be achieved by the presence of another stereocenter.[9] The ability to control the configuration at a given stereocenter is a key component to any total synthesis. However, diastereoselectivity is not always achieved and often gives rise to the undesired diastereomer. In this way, asymmetric catalysis is beneficial because achiral starting materials can be converted to chiral products of either enantiomer, simply by choosing a given catalyst configuration. Propargylic alcohols are important for industrial processes[12] in addition to their application in total synthesis. As a result, propargylic substitution reactions present a worthwhile challenge for catalysis to overcome.

Substitution reactions of propargylic alcohols are known to be catalyzed by complexes of Cu,[13] Re,[14] Rh,[15] Au,[16] Ru[17] and others.[18] Several different catalytic intermediates are proposed for the various catalystic cycles. In some cases, propargylic cations are theorized as intermediates, similar to that of the Nicholas reaction.[16] Other reactions are thought to proceed via allenolate[14] (bottom) or allenylidene[17] (top) intermediates (Scheme 1.2). Of these proposed intermediates, propargylic cations and allenolates can be formed using propargylic alcohols with terminal as well as internal alkynes. Allenylidenes can only be formed using terminal alkynes.

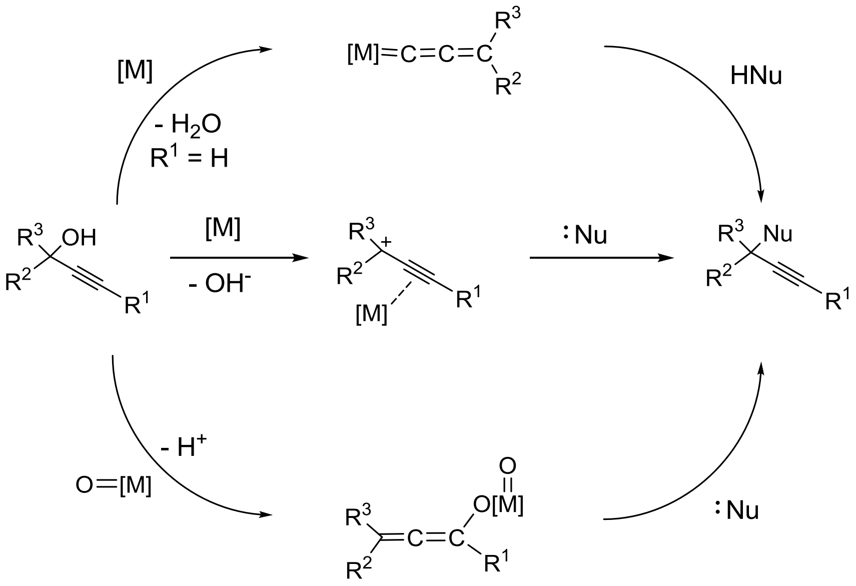

Scheme 1.2. Potential intermediates in catalytic propargylic substitution.[14,16,17]

Campagne et al. found that Au (III) salts catalyzed the substitution of propargylic alcohols by various O, S, and C centered nucleophiles in low to excellent yields (33–97%).[16] The electronic environment around the propargylic center has a significant impact on the activity of the catalyst. Reactivity is only observed for electron-rich propargylic alcohols with benzylic or tertiary propargylic centers. Beginning with an enantiomerically enriched propargylic alcohol (1,3-diphenyl-2-propyn-1-ol, 96% e.e.), allylation proceeds with racemization of the stereocenter. A propargylic cation is proposed as an intermediate in the catalytic cycle (Scheme 1.3).

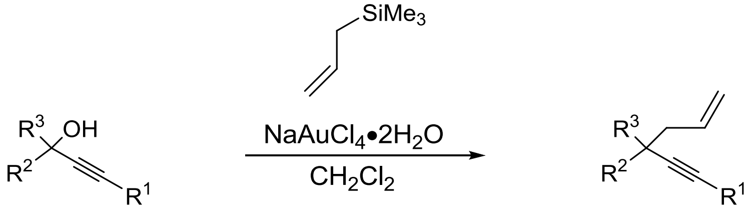

Scheme 1.3. Gold catalyzed propargylic substitution.[16]

Evans utilized a modified version of Wilkinson's catalyst for propargylic substitution using sulfonamides as nucleophiles.[15] Secondary propargylic carbonates derived from terminal propargylic alcohols were used in this reaction as the corresponding alcohols are unreactive. Interestingly, internal alkynes (with the exception of 1-phenyl-6-trimethylsilyl-4-pentyn-3-ol *t*-butylcarbonate) are unreactive under the same conditions. In some cases competing allene formation is observed along with propargylic substitution (Scheme 1.4).

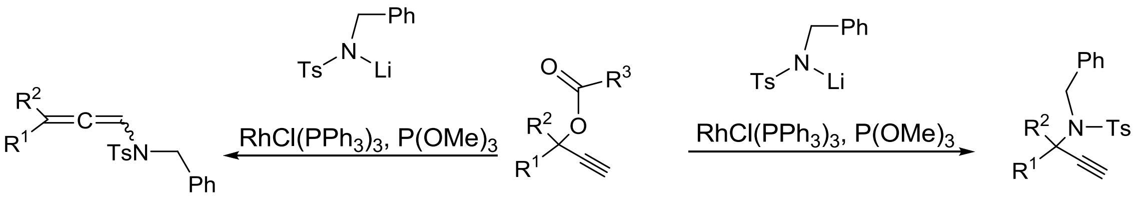

R^3 = Me, OMe, O^{t}Bu   Ts = *p*-toluenesulfonyl

Scheme 1.4. Rh catalyzed propargylic amination.[15]

Toste[14] reported that a rhenium(V)-oxo complex was also active in the catalytic substitution of propargylic alcohols with primary and secondary alcohols and amine nucleophiles. The isolated yields are good (between 53-93%), however the reaction is primarily used for secondary propargylic alcohols and shows some steric sensitivity. A chiral allenolate is proposed as a catalytic intermediate, but reactions beginning with an enantiomerically enriched propargylic alcohol gave racemic products (Scheme 1.5).

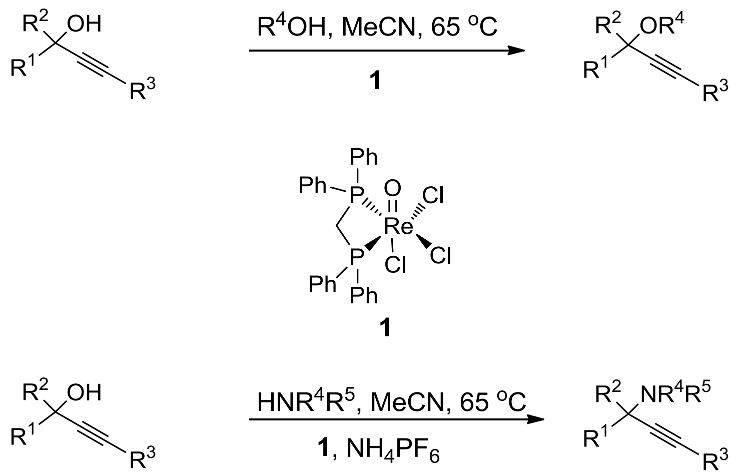

Scheme 1.5. Rhenium catalyzed propargylic substitution reactions.[14]

Selective substitution of terminal propargylic alcohols is of great interest. The most established chemistry in this area has been performed with a thiolate-bridged diruthenium complex developed by Nishibayashi and Uemura (**2** in Scheme 1.6).[17] Using this catalyst system, substitution of the hydroxyl group by C,[17b-e] N,[17i] S[17k] and O[17i] centered nucleophiles is possible (Scheme 1.6). Chirality has also been employed in the form of bridging chiral thiolate ligands.[17b] Again secondary propargylic alcohols are used primarily, and the yields show substrate dependence. An excess of the nucleophile is also necessary in many cases. Although high enantioselectivities can be achieved in some reactions (up to 97% e.e.),[17b] the stereoselectivity is substrate dependent (Scheme 1.6).

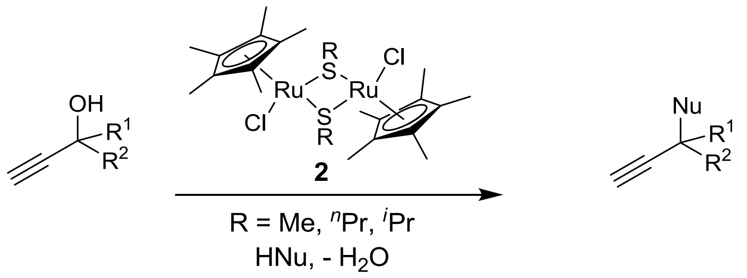

Scheme 1.6. Ruthenium catalyzed propargylic substitution reactions.[17]

Maarseveen also reported a propargylic substitution with various anilines utilizing chiral copper(I) complexes (Scheme 1.7).[13] Various chiral oxazoline based ligands are employed to give enantioselectivity. The active catalyst in this case is formed *in situ* and thus the active catalyst is ill-defined. The reaction gives good enantiomeric excesses (ee's) (up to 88%) but requires propargylic acetates be used as the starting material. Aliphatic amines give low to good yield (27–76%) with low enantioselectivity (<40%).

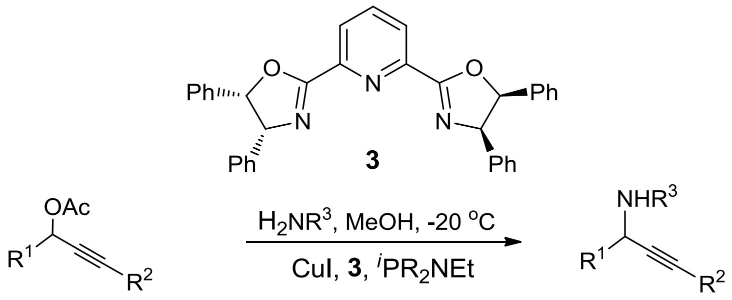

Scheme 1.7. Copper catalyzed propargylic amination.[13]

The ruthenium and copper catalyzed substitution reactions of propargylic alcohols described above are believed to proceed via allenylidene intermediates. Allenylidenes are three carbon cumulenylidene structures of the type $[M]=C=C=CR_1R_2$ (Scheme 1.8). First isolated in 1976 by Fischer and Berke,[19] the study of allenylidenes was significantly advanced when in 1982 Selegue[20] found that they were easily accessible utilizing an appropriate precursor complex and propargylic alcohols. Allenylidenes have an alternating $\delta+$, $\delta-$ character on the cumulene chain as shown by calculations and reactivity studies.[21] Thus, the α- and γ-carbons of the allenylidene chain can be attacked by nucleophiles, and the β-carbon can be protonated.[22] Bulky ligands at the metal center tend to favor attack at the γ-carbon for steric reasons. The reactivity pattern observed for allenylidenes makes them interesting both as catalytic intermediates[23] and as catalysts.[24]

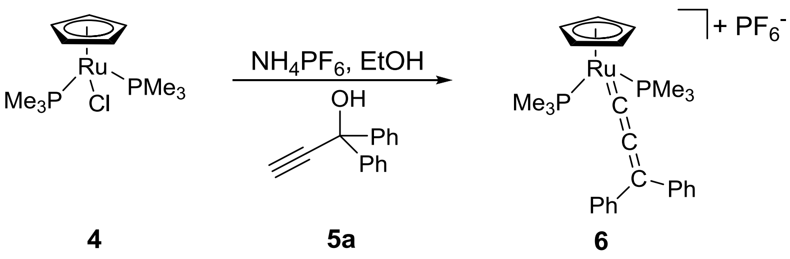

Scheme 1.8. Selegue's allenylidene synthesis.[20]

Optically active allenylidenes are little explored. In 2002, J. Gimeno et al. described an optically active allenylidene (**7**) derived from the fragment $[Ru(Ind)(PPh_3)_2]^+$ (Ind = indenyl anion) and a chiral propargylic alcohol (Scheme 1.9).[25] Nucleophilic attack by the cyclopentanone enolate occurs regioselectively and stereoselectively at the γ- carbon atom of the allenylidene to give the η^1-alkynyl derivative (**8**) as a 2:1 mixture of non-separable diastereomers. The alkynes can be liberated in a two-step process, formally giving the substituted propargylic compounds (**10**) in optically pure form. In 2003 it was shown that the same complex adds CN^-, Me^- and $PhC\equiv C^-$ nucleophiles in a highly stereoselective manner, giving a single diastereomer as product.[25] Again, the substituted alkynes can be liberated by a two-step procedure, giving the propargylic substituted products. The stereoselectivity of the nucleophilic attack in these cases is derived from the stereocenters on the allenylidene ligand itself, not from a ligand-based stereocenter. A more general synthesis of terminal alkynes of high optical purity was reported by Nishibayashi.[17a] Utilizing the chiral ligand (R)-1,1'-binapthyl-2,2'-bis(diphenylphosphine) ((R)-BINAP), the piano-stool ruthenium allenylidene complex $[(Ind)Ru(BINAP)(=C=C=CHPh)]PF_6$ can be formed by Selegue's method from the corresponding chloride complex. Nucleophilic addition of various arylmethyl ketone enolates to C_γ gives the corresponding η^1-alkynyl complexes as diastereomeric mixtures. The diastereomers can by separated by chromatography to give both diastereomers in excellent optical purity (>99% d.e.). Again, protonation with HBF_4 followed by demetalation in refluxing acetonitrile gave both configurations of the corresponding terminal alkynes in >99% e.e.

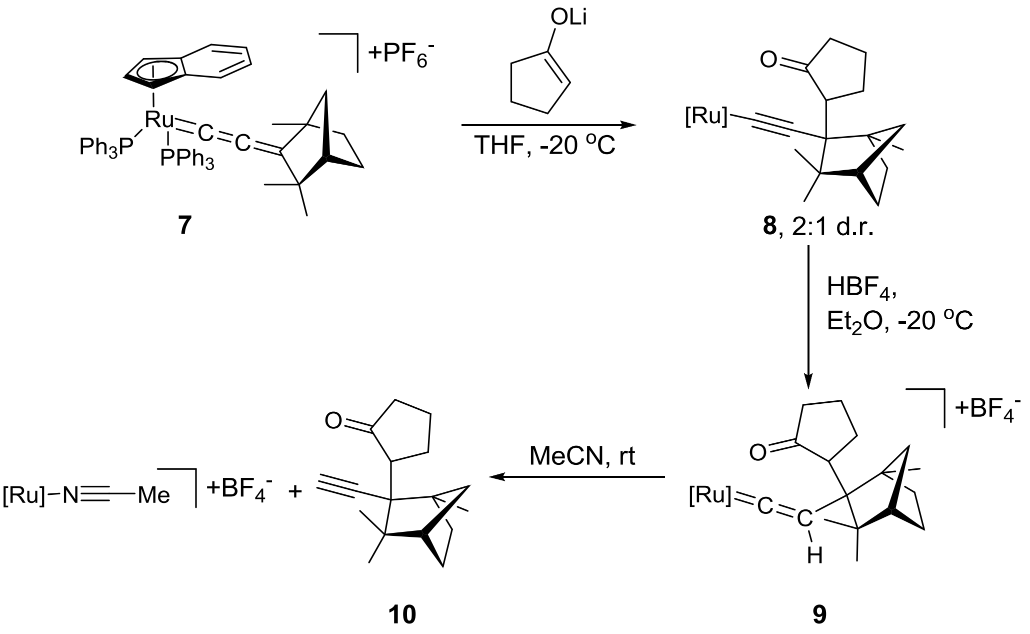

Scheme 1.9. Reactivity of a chiral allenylidene complex. [25]

Enantioselective propargylic substitution via an allenylidene intermediate requires selective attack of the nucleophile at one face of the allenylidene. As shown by stoichiometric experiments this can be difficult.[25] Although stereocenters on the allenylidene can direct nucleophilic attack stereoselectively, ligand stereocenters give lower selectivity of attack. The proximity of the stereocenter to the site of attack may have a direct correlation to stereoselectivity. A metal-based stereocenter may be better capable of inducing high enantioselectivity relative to reactions where stereocenters are only present on the ancillary ligands. Chiral at metal catalysts are used for a variety of organic transformations including transfer hydrogenation,[26,27] cyclopropanation,[28] 1,3-dipolar cycloaddition,[29] Diels-Alder cycloaddition[26,30] and others.[31,32] These reactions can proceed with high e.e.'s with the metal stereocenter sometimes being the determining factor in enantioselectivity.[29,31] In these cases, it is important to obtain the complex in high enantio- or diastereopurity. It is also necessary that the metal stereocenter be stable under the conditions for catalytic activity. Epimerization at the metal could cause loss of stereoselectivity in the products. Conversely, a chiral at metal catalyst with high diastereo-purity and a stable metal stereocenter could lead to products of high e.e. In the case of propargylic substitution reactions via allenylidene intermediates, formation of allenylidenes with optical purity is a must if high levels of stereoinduction are to be achieved.

In 2007 E. Lastra[33] and E. Nakamura[34] reported chiral allenylidene complexes of ruthenium for which stereocenters exist on at least one ancillary ligand as well as on the metal itself. Lastra employed a chiral phosphanylferrocenyloxazoline ligand to obtain the chiral-at-metal allenylidene (**11**) shown in Figure 1.1. The precursor complex is likely configurationally unstable with respect to the metal stereocenter as the diastereomeric ratio is dependent on solvent (^{31}P NMR). In Nakamura's allenylidene (**12**), the metal stereocenter is formed with complete diastereoselectivity. The complex bears a chiral fullerene as well as a chiral diphosphine ligand (Figure 1.1). Complete diastereoselectivity is observed in all cases even with asymmetric allenylidenes [Ru]=C=C=CHAr. Nucleophilic addition of Grignard reagents to the γ- carbon of the allenylidene chain proceed with low to high selectivity (20-90% d.e.) (Scheme 1.10).

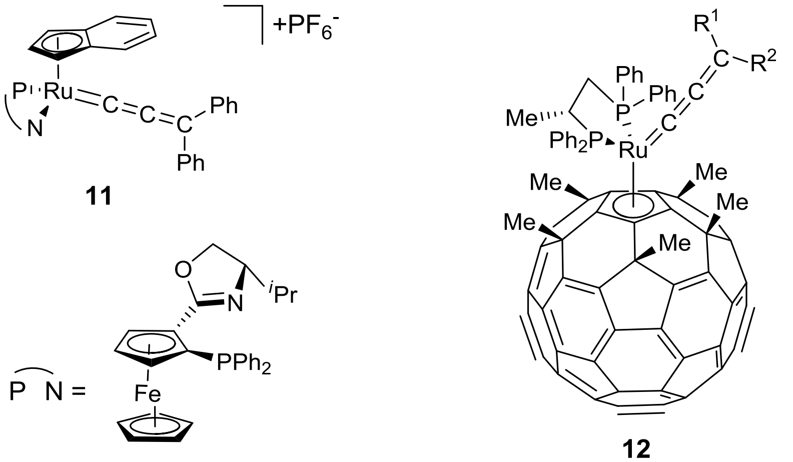
+PF6-
Ru
Ph
Ph
P N =
Fe
PPh2
O
N
iPr
R1
R2
Ph
Ph
P
Me
Ph2P
Ru
Me
Me
Me
Me
Me

11

12

Figure 1.1. Chiral-at-metal allenylidene complexes.[33,34]

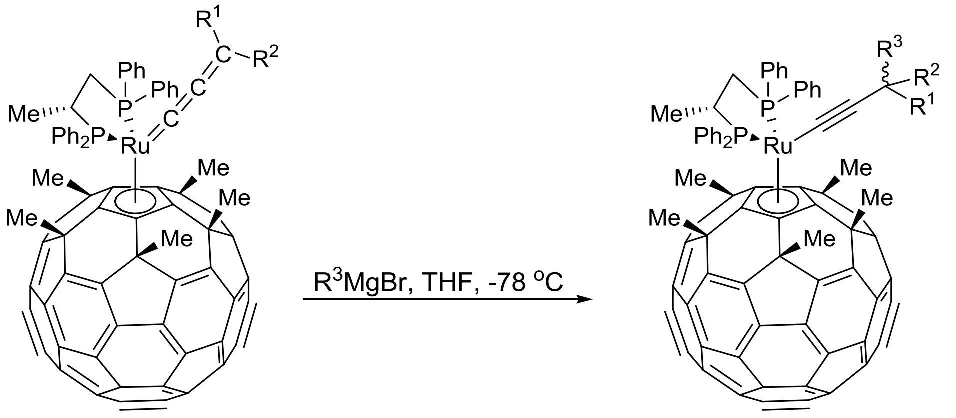
R1
R2
Ph
Ph
P
Me
Ph2P
Ru
Me
R3MgBr, THF, -78 °C
R3
R2
R1

12

13

Scheme 1.10. Nucleophilic addition to a chiral-at-metal allenylidene.[34]

A potential catalytic cycle involving an allenylidene intermediate must involve a complex capable of forming an allenylidene, but the allenylidene cannot be so stable that it would halt the catalytic cycle at this intermediate. Allenylidenes have been shown to be stabilized by electron-rich metal centers.[21] Many of the above mentioned complexes that are capable of forming stable allenylidenes (and in some cases allow for multi-step stoichiometric substitution of propargylic alcohols) bear phosphine ligands.

By replacing the good σ-donor phosphine ligands by relatively electron-poor two electron donors, the electron density at the metal center can be effectively decreased. Efficient steric and electronic tuning in this manner may allow for formation of an unstable allenylidene that would react with a nucleophile *in situ* and turn over in a catalytic cycle.

Phosphoramidites represent a potential alternative to phosphines as ligands in organometallic catalysis. Like phosphines, phosphoramidites are neutral, two electron P-donor ligands. Unlike phosphines, phosphoramidites have three electronegative atoms directly attached to the donating center. As a result phosphoramidites are less σ-donating and more π-accepting than phosphine ligands.[35] Most phosphoramidites are based on the commercially available diol 1,1-binapthyl-2,2'-diol (BINOL)[35] but others are based on (4*S*,5*S*)-2,2-dimethyl-α,α,α',α'-tetraphenyl-1,3-dioxolane-4,5-dimethanol (TADDOL)[36] or other alcohols (Figure 1.2).[37]

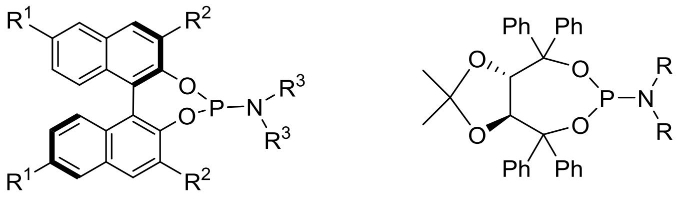

(BINOL)

(TADDOL)

Figure 1.2. Structure of some typical phosphoramidite ligands.[35,36]

As for the phosphoramidites based on BINOL, orthogonal steric and electronic tuning of the ligand is possible by changing the substituents on nitrogen and on the BINOL backbone. Addition of electron-donating or electron-withdrawing substituents to the backbone of the ligand can alter its σ-donating ability. Likewise, changing the substituents on nitrogen can have a direct impact on the steric environment of the resulting complexes.

Phosphoramidites have been employed as ligands on catalysts/catalyst precursors for allylation reactions,[38] cyclopropanations,[39] hydrogenation,[40] [2+2][41] and [4+2][42] cycloadditions, allylic substitutions[43] and others.[44] In some cases well defined catalysts are created and used in the catalytic reactions while in others the active catalytic species are formed *in situ*. Without well-defined catalysts, exact modes of reactivity cannot be determined. Likewise, catalyst tuning of ill-defined systems is more difficult.

The ability to tune catalyst activity via the phosphoramidite is clearly seen in Au(I) catalyzed [2+2] cycloaddition. The catalyst exhibits sensitivity to both steric and electronic tuning, giving in some cases very high e.e. (>99%) (Scheme 1.11).[41] Electron-poor ligands give lower conversion and significantly lower e.e. than their electron-rich counterparts. Conversely, the best stereoselectivity is observed for the most sterically crowded ligand (R^1 = Me, Ar = 4-^{t}BuPh in Scheme 1.11).

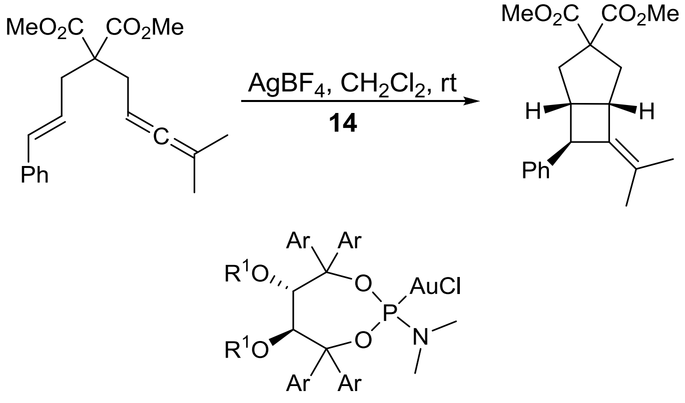

14

R^1_2 = isopropylidene, Ar = Ph, *p*-MeOPh, *p*-FPh
R^1 = Me, Ar = Ph, 4-^{t}BuPh

Scheme 1.11. Tuned phosphoramidite ligands in catalysis.[41]

The goal of this project is to create new well defined complexes for catalytic substitution of propargylic alcohols by a general nucleophile. Ruthenium complexes bearing phosphoramidite ligands are targeted because the corresponding phosphine complexes have been shown to form stable allenylidenes in reactions with propargylic alcohols.[21] Using ruthenium phosphoramidite complexes, reactions with propargylic alcohols intended to form stable allenylidenes will be performed. Once a complex capable of forming stable allenylidenes is found, steric and electronic tuning of the complex via the ligands will be used in an effort to destabilize the allenylidene to the point that it is possible to be used as an intermediate in a catalytic cycle. Catalytic substitution of propargylic alcohols will be tested for all isolated catalysts.

---

[1] Osborn, J. A.; Jardine, F. H.; Young, J. F.; Wilkinson, G. *J. Chem. Soc. A* **1966**, 1711.

[2] Xie, J.-H.; Zhou, Q.-L. *Acc. Chem. Res.* **2008**, *41*, 581.

[3] Evans, D. A.; Chapman, K. T.; Bisaha, J. *J. Am. Chem. Soc.* **1988**, *110*, 1238.

[4] Klibanov, A. M.; *Acc. Chem. Res.* **1990**, *23*, 114.

[5] Li, Y.-Y.; Zhang, X.-Q.; Dong, Z.-R.; Shen, W.-Y.; Chen, G.; Gao, J.-X. *Org. Lett.* **2006**, *24*, 5565.

[6] Blystone, S. L. *Chem. Rev.* **1989**, *89*, 1663.

[7] Anastas, P. T.; Kirchhoff, M. M. *Acc. Chem. Res.* **2002**, *35*, 686

[8] Nicholas, K. M. *Acc. Chem. Res.* **1987**, *20*, 207.

[9] Ortega, N.; Martín, T.; Martín, V. S. *Org. Lett.* **2006**, *8*, 871.

[10] Álvaro, E.; de la Torre, M. C.; Sierra, M. A. *Org. Lett*. **2003**, *5*, 2381.

[11] Ohri, R. V.; Radosevich, A. T.; Hrovat, K. J.; Musich, C.; Huang, D.; Holman, T. R.; Toste, F. D. *Org. Lett.* **2005**, *7*, 2501.

[12] Bonrath, W.; Eggersdorfer, M.; Netscher, T. *Catalysis Today* **2007**, *121*, 45.

[13] Detz, R. J.; Delville, M. M. E.; Hiemstra, H.; van Maarseveen, J. H. *Angew. Chem. Int. Ed.* **2008**, *47*, 3777.

[14] Sherry, B. D.; Radosevich, A. T.; Toste, F. D.*J. Am. Chem. Soc.* **2003**, *125*, 6076.

[15] Evans, P. A.; Lawler, M. J. *Angew. Chem. Int. Ed.* **2006**, *45*, 4970.

[16] Georgy, M.; Boucard, V.; Campagne, J.-M. *J. Am. Chem. Soc.* **2005**, *127*, 14180.

---

[17] (a). Nishibayashi, Y.; Imajima, H.; Onodera, G.; Uemura, S. *Organometallics* **2005**, *24*, 4106; (b). Inada, Y.; Nishibayashi, Y.; Uemura, S. *Angew. Chem. Int. Ed.* **2005**, *44*, 7715; (c). Matsuzawa, H.; Miyake, Y.; Nishibayashi, Y. *Angew. Chem. Int. Ed.* **2007**, *46*, 6488; (d). Matsuzawa, H.; Kanao, K.; Miyake, Y.; Nishibayashi, Y. *Org. Lett.* **2007**, *9*, 5561; (e). Daini, M. Yoshikawa, M.; Inada, Y.; Uemura, S.; Sakata, K.; Kanao, K.; Miyake, Y.; Nishibayashi, Y. *Organometallics* **2008**, *27*, 2046; (f). Yada, Y.; Miyake, Y.; Nishibayashi, Y. *Organometallics* **2008**, *27*, 3614; (g). Fukamizu, K.; Miyahe, Y.; Nishibayashi, Y. *J. Am. Chem. Soc.* **2008**, *130*, 10498; (h). Yamauchi, Y.; Miyake, Y.; Nishibayashi, Y. *Organometallics* **2009**, *28*, 48; (i). Tanabe, Y.; Kanao, K.; Miyake, Y.; Nishibayashi, Y. *Organometallics* **2009**, *28*, 1138; (j). Kanao, K.; Miyake, Y.; Nishibayashi, Y. *Organometallics* **2009**, *28*, 2920; (k). Inada, Y.; Nishibayashi, Y.; Hidai, M.; Uemura, S. *J. Am. Chem. Soc.* **2002**, *124*, 15172.

[18] Ljungdahl, N.; Kann, N. *Angew. Chem. Int. Ed.* **2009**, *48*, 642.

[19] (a). Fischer, E. O.; Halder, H.-J.; Franck, A.; Köhler, F. H.; Huttner, G. *Angew. Chem. Int. Ed. Eng.* **1976,** *15*, 623; (b). Berke, H. *Angew. Chem. Int. Ed. Eng*. **1976**, *15*, 624.

[20] Selegue, J. P. *Organometallics* **1982**, *1*, 217.

[21] Reviews: (a). Cadierno, V.; Gimeno, J. *Chem. Rev.* **2009**, *109*, 3512; (b). Che, C.-M.; Ho, C.-M.; Huang, J.-S. *Coord. Chem. Rev.* **2007**, *251*, 2145; (c). Rigaut, S.; Touchard, D.; Dixneuf, P. H. *Coord. Chem. Rev.* **2004**, *248*, 1585; (d). Winter, R. F.; Záliš, S. *Coord. Chem. Rev.* **2004**, *248*, 1565; (e). Werner, H. *Chem. Commun.* **1997**, 903.

[22] Bustelo, E.; Jiménez-Tenorio, M.; Mereiter, K.; Puerta, M. C.; Valerga, P. *Organometallics* **2002**, *21*, 1903.

[23] Bruneau, C.; Dixneuf, P. H. *Angew. Chem. Int. Ed.* **2006**, *45*, 2176.

[24] Dragutan, I.; Dragutan, V. *Platinum Metals Rev.* **50**, *2*, 81.

[25] (a). Cadierno, V.; Conejero, S.; Gamasa, M. P.; Gimeno, J.; Pérez-Carreño, E.; García-Granda, S. *Organometallics* **2001**, *20*, 3175; (b). Cadierno, V.; Conejero, S.; Gamasa, M. P.; Gimeno, J.; Falvello, L. R.; Llusar, R. M. *Organometallics* **2002**, *21*, 3716; (c). Cadierno, V.; Conejero, S.; Gamasa, M. P.; Gimeno, J. *Dalton Trans.* **2003**, 3060.

[26] Liu, J.; Wu, X.; Iggo, J. A.; Xiao, J. *Coord. Chem. Rev*. **2008**, *252*, 782.

[27] Carmona, D.; Lamata, M. P.; Oro, L. A. *Eur. J. Inorg. Chem.* **2002**, 2239.

[28] Lasa, M.; Lopez, P.; Cativiela, C.; Carmona, D.; Oro, L. A. *J. Mol. Catal. A*: *Chem.* **2005**, *234*, 129.

[29] Carmona, D.; Lamata, M. P.; Viguri, F.; Rodríguez, R.; Lahoz, F. J.; Fabra, M. J.; Oro, L. A. *Tetrahedron: Asymmetry* **2009**, *20*, 1197.

---

[30] Faller, J. W.; Grimmond, B. J. *Organometallics* **2001**, *20*, 2454.

[31] Chavarot, M.; Ménage, S.; Hamelin, O.; Charnay, F.; Pécaut, J.; Fontecave, M. *Inorg. Chem.*. **2003**, *42*, 4810.

[32] Tamm, M.; Baum, K.; Lügger, T.; Fröhlich, R.; Bergander, K. *Eur. J. Inorg. Chem*. **2002**, 918.

[33] García-Fernández, A.; Gimeno, J.; Lastra, E.; Madrigal, C. A.; Graiff, C.; Tiripicchio, A. *Eur. J. Inorg. Chem.* **2007**, 732.

[34] Zhong, Y.-W.; Matsuo, Y.; Nakamura, E. *Chem. Asian J.* **2007**, *2*, 358.

[35] (a). Hulst, R.; de Vries, N. K.; Feringa, B. L. *Tetrahedron: Asymmetry* **1994**, *5*, 699; (b). Rimkus, A.; Sewald, N. *Org. Lett.* **2003**, *5*, 79.

[36] Moteki, S. A.; Wu, D.; Chandra, K. L.; Reddy, D. S.; Takacs, J. M. *Org. Lett.* **2006**, *8*, 3097.

[37] Niu, J.-L.; Chen, Q.-T.; Hao, X.-Q.; Zhao, Q.-X; Gong, J.-F.; Song, M.-P. *Organometallics* **2010**, *29*, 2148.

[38] (a). Esteruelsa, M. A.; García-Yebra, C.; Oliván, M.; Oñate, E.; Valencia, M. *Organometallics* **2008**, *27*, 4892; (b). Wassenaar, J.; van Zutphen, S.; Mora, G.; Le Floch, P.; Siegler, M. A.; Spek, A. L.; Reek, J. N. H. *Organometallics* **2009**, *28*, 2714; (c). Stanley, L. M.; Hartwig, J. F. *J. Am. Chem. Soc.* **2009**, *131*, 8971; (d). Niu, J.-L.; Chen, Q.-T.; Hao, X.-Q.; Zhao, Q.-X.; Gong, J.-F.; Song, M.-P. *Organometallics* **2010**, *29*, 2148.

[39] (a). Osswald, T.; Rüegger, H.; Mezzetti, A. *Chem. Eur. J.* **2010**, *16*, 1388; (b). Osswald, T.; Mikhel, I. S.; Rüegger, H.; Butti, P.; Mezzetti, A. *Inorg. Chim. Acta* **2010**, *363*, 474.

[40] (a). Enthaler, S.; Erre, G.; Junge, K.; Schröder, K.; Addis, D.; Michalik, D.; Hapke, M.; Redkin, D.; Beller, M. *Eur. J. Org. Chem.* **2008**, 3352; (b). Yu, L.; Wang, Z.; Wu, J.; Tu, S.; Ding, K. *Angew. Chem. Int. Ed.* **2010**, *49*, 3627.

[41] Teller, H.; Flügge, S.; Goddard, R.; Fürstner, A. *Angew. Chem. Int. Ed.* **2010**, *49*, 1949.

[42] González, A. Z.; Toste, F. D. *Org. Lett.* **2010**, *12*, 200.

[43] (a). Pamies, O.; Dieguez, M. *Chem. Eur. J.* **2008**, *14*, 944; (b). Spiess, S.; Raskatov, J. A.; Gnamm, C.; Brödner, K.; Helmchen, G. *Chem. Eur. J.* **2009**, *15*, 11087.

[44] (a). Mariz, R.; Briceño, A.; Dorta, R.; Dorta, R. *Organometallics* **2008**, *27*, 6605; (b). Hashmi, A. S. K.; Hamzić, M.; Rominger, F.; Bats, J. W. *Chem. Eur. J.* **2009**, *15*, 13318; (c). Dalton, D. M.; Oberg, K. M.; Yu, R. T.; Lee, E. E.; Perreault, S.; Oinen, M. E.; Pease, M. L.; Malik, G.; Rovis, T. *J. Am. Chem. Soc.* **2009**, *131*, 15717; (d). Cavarzan, A.; Vianchini, G.; Sgarbossa, P.; Lefort, L.; Gladiali, S.; Scarso, A.; Strukul, G. *Chem. Eur. J.* **2009**, *15*, 7930.

Synthesis and reactivity studies of η^6-arene piano-stool complexes

2.1. Aim

Piano-stool type ruthenium complexes bearing phosphine ligands can be used to activate propargylic alcohols catalytically. To this end, I was interested in determining if phosphoramidite ligands might help increase the activity of ruthenium based catalysts. As such, I sought to make complexes of the type [$RuCl_2(\eta^6$-arene)(phosphoramidite)] and test their activity in the catalytic activation of propargylic alcohols via potential allenylidene intermediates.

2.2. Introduction

2.2.1. β-oxo esters ($R^1CO_2CR_2C(O)Me$)

Piano-stool type complexes of ruthenium typically fall into one of three basic categories: η^6-arene complexes, η^5-cyclopentadienyl complexes and η^5-indenyl complexes. Of these, η^6-arene complexes of the type [$RuCl_2(\eta^6$-arene)(L)] are particularly versatile because of the ability to tune these complexes via the arene ligand.[1] η^6-Arene complexes of the type [$RuCl(\mu$-Cl)(η^6-arene)]$_2$ react with monodentate ligands (L) to give the complexes [$RuCl_2(\eta^6$-arene)(L)], where L is a phosphine[2], phosphoramidite[3], phosphite[4], N-heterocyclic carbene (NHC)[5] or others.[6] Half sandwich complexes of this type are known to be catalytically active in a variety of reactions including transfer hydrogenation[7], ring-closing metathesis[5], atom-transfer radical addition[8] and synthesis of β-oxo esters from carboxylic acids and propargylic alcohols.[2] The latter reaction has also been adapted to allow reactions to take place in water.[9]

β-Oxo esters represent an important subclass of organic compounds. Certain β-oxo esters including steroidal derivatives show biological activity.[10] They also are potential intermediates in the synthesis of natural products, including the potent antibiotics daunorubicin and carminomycin.[11] They have also been reported as efficient photolabile protecting groups for carboxylic acids,[12] and they have been shown to be effective acylating agents.[13]

Several methods for the synthesis of this functionality are known. They can be obtained by esterification of α-hydroxy ketones with an appropriate acid chloride or anhydride.[14] Substitutions of α-halides by carboxylate salts have also been reported.[15] There is also an example of a palladium/copper cocatalyzed cross coupling between α-acyloxy stannanes and acyl chlorides.[16] With the availability of a large number of propargylic alcohols (made by addition of acetylide to an aldehyde/ketone), a synthetic route utilizing these starting materials is of potential use. As such, two step hydration/esterification procedures have been developed.[17] The first catalytic synthetic method utilizing propargylic alcohols was reported by Watanabe et al. in 1986.[18] Watanabe's catalytic system consists of bis(η^5-cyclooctadiene)ruthenium(II) / 2 PBu_3 / maleic anhydride and is capable of combining propargylic alcohols and acetic acid to form the corresponding β-oxo esters in moderate yields (Scheme 2.1).

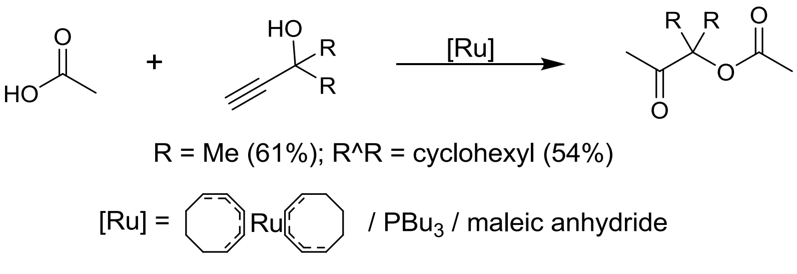
O
HO
+
HO
R
R
[Ru]
R R O
O
O
R = Me (61%); R^R = cyclohexyl (54%)
[Ru] =
Ru
/ PBu3 / maleic anhydride

Scheme 2.1. Watanabe's catalyst system for β-oxo ester formation.[18]

The following year Dixneuf et al. discovered alternate catalysts of the general formula [$RuCl_2(PR_3)(\eta^6$-arene)] for this conversion.[19a] Dixneuf's catalyst gives β-oxo esters from propargylic alcohols and a variety of carboxylic acids in low to high yields (30-92%). Dixneuf et al. also reported that the dimer [$Ru_2(\mu\text{-}O_2CH)_2(CO)_4(PPh_3)_2$] is active in the title reaction.[9,19b] High yields were obtained for sterically hindered substrates but the reaction requires an excess of the nucleophile and prolonged reaction times (15 h at 90 °C).

The above reported catalysts for β-oxo ester formation show high activity but the yields are substrate dependent and in some cases an excess of the nucleophile is required. With these systems enantioselectivity is not possible as the catalysts are achiral. However, Dixneuf reported that the complexes gave the products with retention of configuration when optically active propargylic alcohols were used.[9,19b]

2.3. Results

2.3.1. Synthesis of η^6-arene complexes

As the known phosphoramidite ligand **41a**[20] is readily available via a one-step reaction, I began my investigation with this ligand. The ligand reacts with the chloro-bridged dimer [RuCl(μ-Cl)(*p*-cymene)]$_2$ (**42**) in CH_2Cl_2 at room temperature to give the complex [$RuCl_2$(*p*-cymene)(**41a**)][21] (**43a**) in 96% yield (Scheme 2.2). The coordination of the phosphoramidite ligand is best shown by the desymmetrization of the η^6-arene protons in the ^1H NMR. In the complex, the chemically equivalent protons are diastereotopic, giving four distinct signals. The methyl groups of the ligand are also diastereotopic, giving two singlets in the ^1H NMR at 2.66 and 2.63 ppm. In the ^{31}P

NMR, very little shift is observed for the phosphorus signal upon coordination of the ligand to the metal (150.6 to 151.5 ppm). HRMS and IR are in accordance with the assigned structure. The complex was also unambiguously characterized by single-crystal X-ray crystallography (Figure 2.1). Selected bond lengths and angles are listed below (Figure 3.1). The bond angles about ruthenium range from 84.08(3)° for P(1)-Ru(1)-Cl(1) to 94.30(11)° for Cl(2)-Ru(1)-C(2). Thus, the geometry is best described as a slightly distorted octahedron.

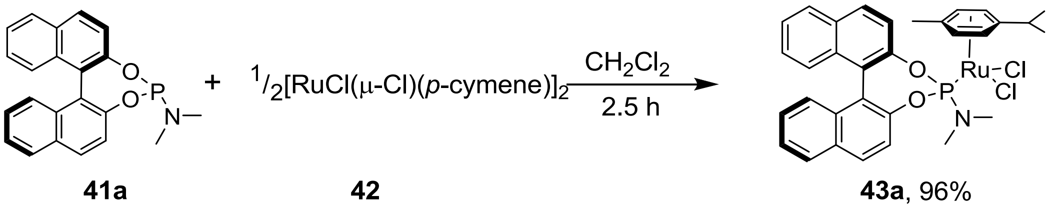
O
O
P
N
+
$^1/_2$[RuCl(μ-Cl)(*p*-cymene)]$_2$
CH_2Cl_2
2.5 h
O
O
P
Ru
Cl
Cl
N
41a
42
43a, 96%

Scheme 2.2. Phosphoramidite complex synthesis.

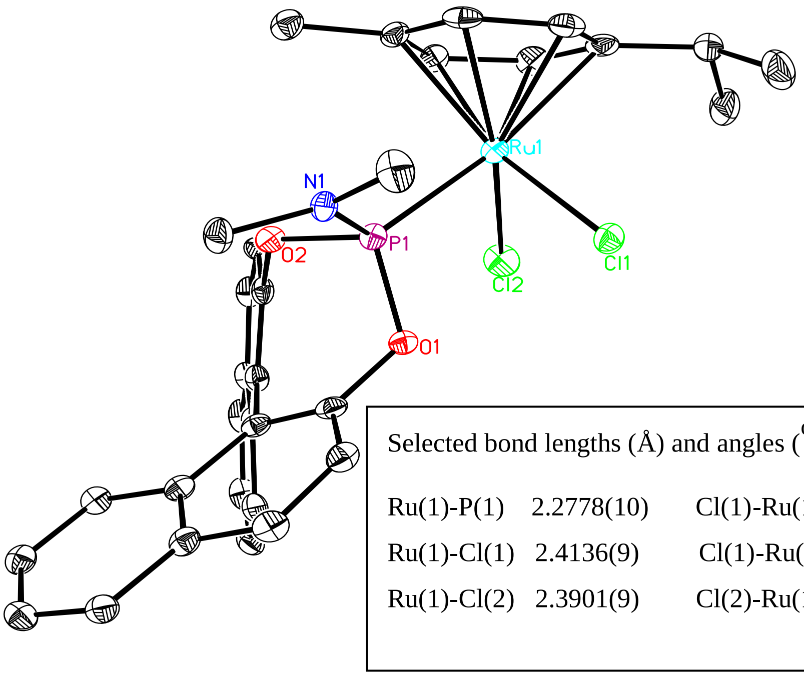
Ru1
N1
P1
O2
Cl2
Cl1
O1

Selected bond lengths (Å) and angles (°):

Ru(1)-P(1)	2.2778(10)	Cl(1)-Ru(1)-Cl(2)	88.85(3)
Ru(1)-Cl(1)	2.4136(9)	Cl(1)-Ru(1)-P(1)	84.08(3)
Ru(1)-Cl(2)	2.3901(9)	Cl(2)-Ru(1)-P(1)	85.15(3)

Figure 2.1. Crystal structure of **43a**.

2.3.2. Catalytic activation of propargylic alcohols

The complex **43a** was tested for activity in substitution reactions of propargylic alcohols using various nucleophiles such as alcohols, amines, and carboxylic acids. The best results were obtained with carboxylic acid nucleophiles, giving complete consumption of the propargylic alcohol after 18 h at 90 ^{o}C. The expected propargylic esters were not formed, however. Instead, it was found that complex **43a** gave β-oxo esters as the major product. The reaction gives broad substrate generality, although high temperature and prolonged reaction times are required. Various solvents were screened for the reaction and cyclohexane was found to be optimal. Reactions run in THF or 1,2-dichloroethane (DCE) were incomplete or suffered from excessive side products. The reaction does not proceed at lower temperature. The major side product of the reactions was found to be an unsaturated hydrocarbon. As illustrated in Scheme 2.3, this product is likely formed by the attack of water on an allenylidene intermediate. Accordingly, when 1,1-diphenyl-2-propyn-1-ol (**5a**) is heated to 90 ^{o}C in cyclohexane with 1.5 mol% **43a**, two products are formed in approximately a 1:1 ratio as observed by GC/MS (Scheme 2.3). This type of reactivity has been reported previously.[22]

Using the optimized conditions (1.5 mol% catalyst, cyclohexane, 18 h, 90 ^{o}C) primary, secondary, and tertiary aliphatic and aromatic propargylic alcohols could be used with aliphatic and aromatic carboxylic acids in all possible combinations. Cyclic as well as acyclic propargylic alcohols can be employed. In the case of the internal alkyne 2-methyl-3-hexyn-2-ol, however, no reaction occurs. The terminal alkyne functionality seems to be necessary for the activation of the propargylic alcohol. The reaction proceeds with moderate yields (15-57%) (Tables 2.1, 2.2).

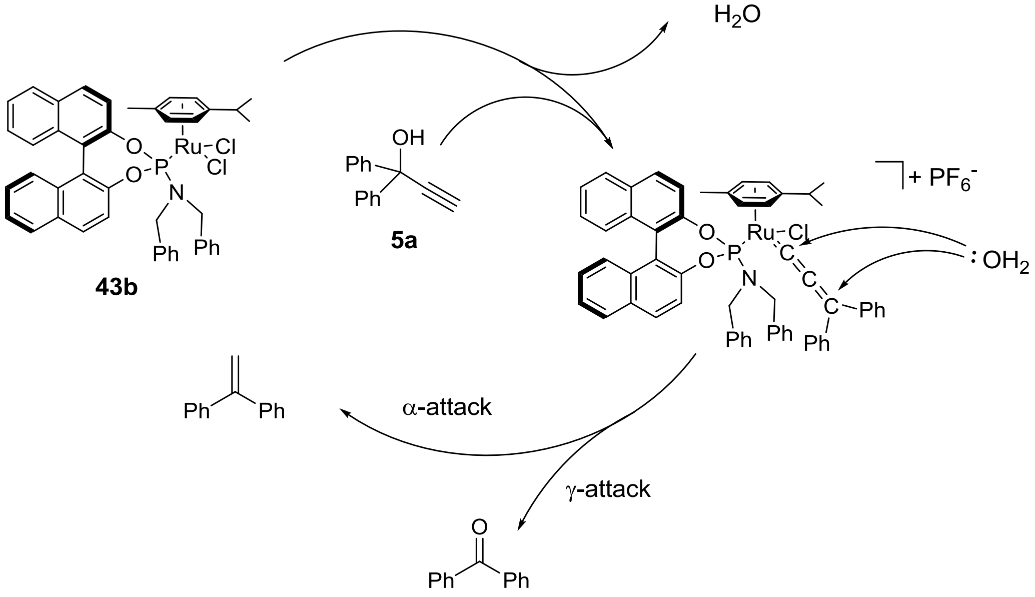

Scheme 2.3. Allenylidene cleavage by attack of H_2O.

Table 2.1. β-Oxo ester formation.

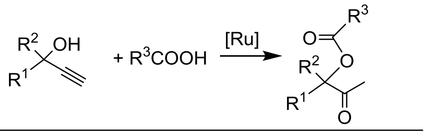

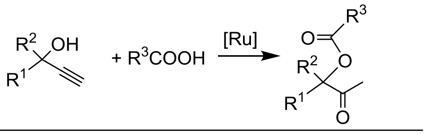

Entry	Substrates	Product	Yield[a]
1	$R^1=R^2=H$, $R^3=Ph$	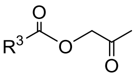	67% (41%)[b]
2	$R^1=R^2=H$ R^3=2-bromophenyl		77% (38%)[b]
3	$R^1=Ph$, $R^2= H$, $R^3=CH_3$	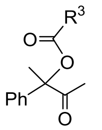	47% (31%)[b]
4	$R^1=R^3=Ph$, $R^2=H$		74% (53%)[b]
5	$R^1=Ph$, $R^2=H$ R^3=2-bromophenyl		78% (50%)[b]
6	R^1=*n*-pentyl, $R^2=H$ $R^3=Ph$	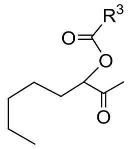	56% (40%)[b]
7	R^1=*n*-pentyl, $R^2=H$ R^3=2-bromophenyl		61% (46%)[b]
8	$R^1=R^2=Ph$, $R^3=CH_3$	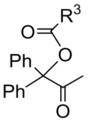	55% (41%)[b]
9	$R^1=R^2=R^3=Ph$		68% (39%)[b]
10	$R^1=R^2=Ph$ R^3=2-bromophenyl		54%
11	$R^1=Ph$, $R^2=R^3=CH_3$	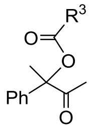	71% (57%)[b]
12	$R^1=R^3=Ph$, $R^2=CH_3$		82% (44%)[b]
13	$R^1=Ph$, $R^2=CH_3$, R^3=2-bromophenyl		84% (52%)[b]
14	R^1=*iso*-Bu, $R^2=CH_3$ $R^3=Ph$	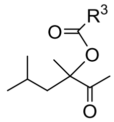	71% (36%)[b]
15	R^1=*iso*-Bu, $R^2=CH_3$ R^3=2-bromophenyl		86% (47%)[b]

[a] Isolated yields after column chromatography. Conditions: propargylic alcohol (0.7 mmol), carboxylic acid (0.7 mmol), catalyst **43c** (0.012 mmol) 5 h in cyclohexane (3 mL) at 90 °C.
[b] Same conditions using **43a** as catalyst with 18 h reaction time.

Table 2.2. Cyclic β-oxo ester formation.

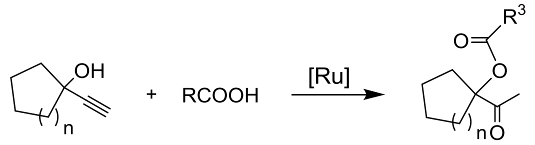

Entry	Substrates	Product	Yield[a]
1	n=1, R=Ph	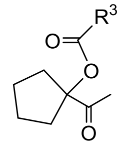	52% (15%)[b]
2	n=1, R=Ph		77% (40%)[b]
3	n=1, R=2-bromophenyl		86% (52%)[b]
4	n=2, R=CH_3	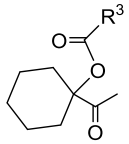	43% (16%)[b]
5	n=2, R=Ph		61% (42%)[b]
6	n=2, R=2-bromophenyl		87% (49%)[b]

[a] Isolated yields after column chromatography. Conditions: propargylic alcohol (0.7 mmol), carboxylic acid (0.7 mmol), catalyst **43c** (0.012 mmol) 5 h in cyclohexane (3 mL) at 90 °C. [b] Same conditions using **43a** as catalyst with 18 h reaction time.

2.3.3. Synthesis of sterically and electronically tuned complexes

In order to improve the activity of the system, various known and novel ligands were employed in the synthesis of the analogous complexes of the type [$RuCl_2$(*p*-cymene)(L)], where L is a phosphoramidite ligand. The ligands were chosen in an effort to obtain complexes exhibiting a range of steric and electronic properties. Nearly all of the ligands are based on the diol (R)-1,1'-binaphthyl-2,2'-diol ("(R)-BINOL") or its counterpart (R)-5,5',6,6',7,7',8,8'-octahydro-1,1'-binaphthyl-2,2'-diol ("(R)-octahydro BINOL"). These ligands are tuned sterically via substitution of the groups (R) on the nitrogen atom and electronically via substitution of the BINOL backbone (Figure 2.2). Most of the ligands are known and were synthesized by standard methods reported in the literature.[23] The new ligand **45b** was also synthesized in this manner. For comparison, a novel ligand not based on BINOL was also synthesized. (R)-5,5',6,6'-tetramethyl-3,3'-

di-*tert*-butyl-1,1'-biphenyl-2,2'-diol ("(R)-BIPHEN") (**46**) was reacted with hexamethylphoshorus triamide in toluene at 100 °C to form ligand **47** (Scheme 2.4). This diol was chosen because the two *t*-butyl groups on the phenyl rings should point directly at the metal in the complex.

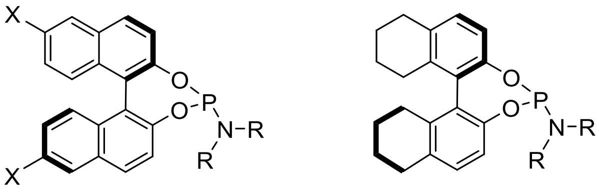

X = H, R = Me **41a**
X = H, R = ^{i}Pr **41b**
X = H, R = Bn **41c**
X = Br, R = Me **41d**

R = Me **45a**
R = Bn **45b**

Figure 2.2. Sterically and electronically tuned phosphoramidite ligands.[23]

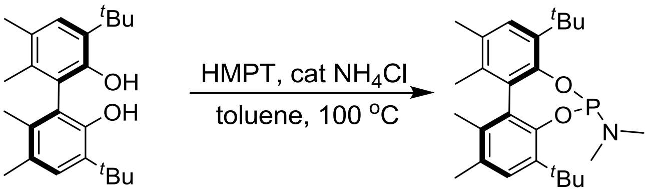

46

47, 60%

Scheme 2.4. Synthesis of a novel ligand based on R-BIPHEN.

The new ligands were all reacted with the dimer **42** under the standard conditions (CH_2Cl_2, rt, 16 h) and the resultant tuned complexes were obtained in high yield (Scheme 2.5). The sterically hindered ligand **47** is unreactive under these conditions and thus required more forcing conditions (DCE, 2.5 h, reflux) for the synthesis of the complex. Again the *p*-cymene protons in the complexes are rendered diastereotopic, giving four distinct doublets in the ^{1}H NMR spectra between 5.6 and 4.3 ppm. Likewise, six aromatic signals are observed for the *p*-cymene ligand in the ^{13}C NMR spectra (109-85 ppm). The complexes show a single peak in their ^{31}P NMR spectra typically in the range 141-143 ppm. The exceptions are complexes **48b** (136.8 ppm) and **49** (125.6 ppm). Interestingly, all of these signals are shifted considerably upfield from that of the parent complex **43a** (151.5 ppm). FAB MS shows small molecular ion peaks for all complexes as well as peaks corresponding to chloride loss. HRMS, IR and microanalysis are all in accordance with the assigned structures.

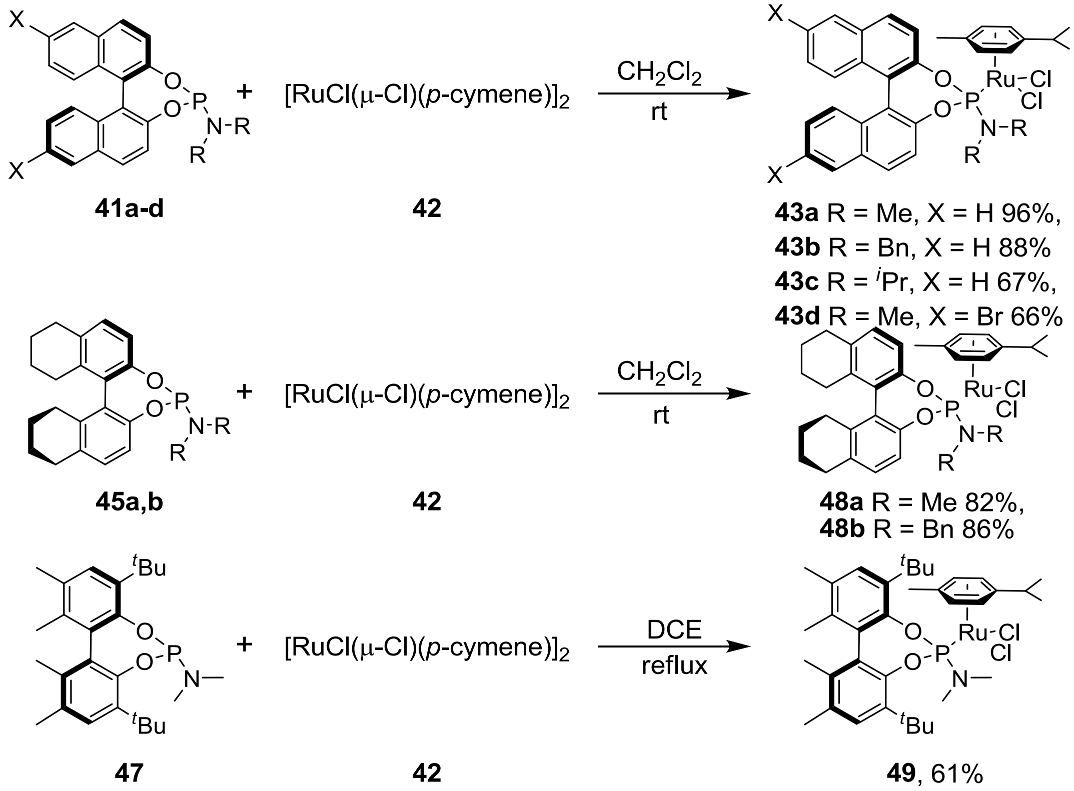

X
O
O
P
N-R
R
X
+
[RuCl(μ-Cl)(p-cymene)]2
CH2Cl2
rt
Ru-Cl
Cl
41a-d
42
43a R = Me, X = H 96%,
43b R = Bn, X = H 88%
43c R = iPr, X = H 67%,
43d R = Me, X = Br 66%
DCE
reflux
tBu
45a,b
48a R = Me 82%,
48b R = Bn 86%
47
49, 61%

Scheme 2.5. Synthesis of complexes [$RuCl_2$(*p*-cymene)(phosphoramidite)].

In order to get an accurate depiction of their relative reactivity, the various catalysts were then used in a test reaction under strictly comparable conditions. Aliquots were removed from the respective solutions after 2 and 4 h reaction times and filtered over silica to remove the catalyst. The samples were then analyzed by GC/MS. As shown in Table 2.3, several of the tuned catalysts out-performed the parent complex **43a**. Complex **43b**, bearing the *N*,*N*-dibenzyl substituent gave the best performance of all the catalysts. Using this complex, the reaction reached complete conversion in only four hours and showed less side product formation by GC/MS. The *N*,*N*-dibenzyl complex resulting from octahydro BINOL (**48b**) also showed nearly complete conversion in only four hours reaction time, suggesting that steric factors play a significant role in catalyst activity. Conversely, electronic tuning via substitution of the (R)-BINOL backbone showed little effect.

Table 2.3. Comparison of catalysts in β-oxo ester formation.

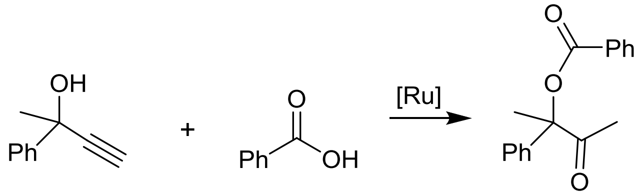

Catalyst[a]	%Conversion[b]		%Yield[b]	
	2 h	4 h	2 h	4 h
43a	25	61	20	49
	16[c]	35[c]	8[c]	15[c]
	22[d]	54[d]	21[d]	38[d]
43b	77	100	75	97
	66[c]	92[c]	64[c]	90[c]
43c	68	90	56	86
43d	12	52	12	45
48a	26	59	20	37
48b	75	98	73	95
51	20	73	15	63

[a] Conditions: 0.7 mmol 2-phenyl-3-butyn-2-ol, 0.7 mmol $PhCO_2H$, 0.012 mmol catalyst in 3 mL cyclohexane at 90 °C.

[b] Determined by GC/MS.

[c] Reaction run in toluene.

[d] Reaction run in cyclohexane/*p*-cymene 6:1.

2.4. Discussion

2.4.1. Comparison of tuned catalysts

The results from the comparison test indicate that the dibenzyl catalyst **43b** outperforms all others tested in the conversion of propargylic alcohols and carboxylic acids to β-oxo esters. As a result, this catalyst was then used for the same substrates as the parent complex **43a**. Not only is the second generation catalyst active for all of the same substrates, but it also gave consistently higher yields over a significantly shorter reaction time (5 h compared to 18 h for complex **43a**) (Tables 2.1 and 2.2). The yields increased between 14 and 38% for the reactions catalyzed by **43b**.

2.4.2. Reactions to further understand the mechanism

The reason for the increased activity of the second generation catalyst is not entirely clear. It cannot be explained by sterics alone as complex **43b** outperforms the complexes bearing the bulkier ligand **43c** (Table 2.3). The difference in activity must be related to a difference in the formation or reactivity of the catalytically active species. Thus the nature of the catalytically active species must be determined. Similar complexes bearing the *p*-cymene ligand have been reported to form the catalytically active species in situ by loss of *p*-cymene.[19b] In accordance with this proposed mechanism of activation, small amounts of *p*-cymene are observed in the GC/MS chromatograms of the crude products. In an effort to determine if *p*-cymene loss is involved in the activation of the catalyst, I sought to make a new complex for which arene loss is more difficult than in the corresponding *p*-cymene complexes.

Hexamethylbenzene (C_6Me_6) should be a more electron rich arene than *p*-cymene due to the six electron donating methyl groups attached to the ring as compared to the two alkyl groups present on *p*-cymene. The increased electron density of the arene ring should in turn lead to a stronger σ-bond between the π-electrons of the ring and the d-orbitals on the metal. This stronger metal-ligand bond should make formation of the proposed catalytically active species more difficult, leading to lower overall activity. Thus the ligand **41c** was reacted with the dimer $[RuCl(\mu\text{-}Cl)(C_6Me_6)]_2$ (**50**)[24] in CH_2Cl_2 at reflux for 6 h, giving complex **51** in 78% yield (Scheme 2.6). The complex bearing the dibenzyl ligand **42b** could not be isolated for comparison. If arene loss is necessary for activation, this catalyst should exhibit lower activity than the corresponding *p*-cymene complex. In fact, this is the case as shown in Table 2.1 (entries 4, 10). The hexamethylbenzene complex **51** gives only 73% conversion in the test reaction after four hours, compared to 90% for the corresponding *p*-cymene complex **43c**.

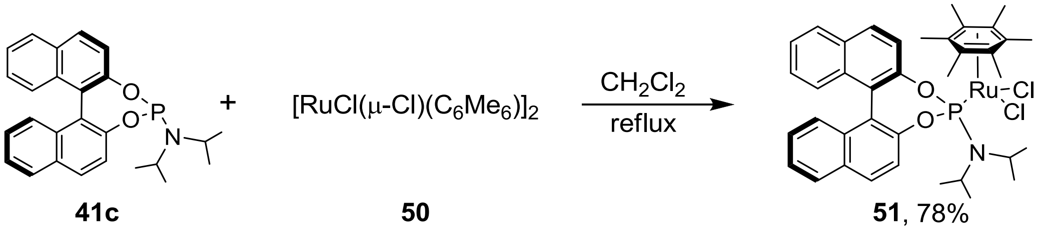

Scheme 2.6. Synthesis of a hexamethylbenzene (C_6Me_6) complex.

In an attempt to further support the notion that the active catalyst is formed by arene loss, I attempted the reaction in toluene as well as in the presence of an excess of *p*-cymene (Table 2.3, entries 2, 3). An excess of a coordinating arene ligand should significantly lower the reaction rate because the open coordination sites on the metal could be closed by coordination of the arene instead of activating the alkyne. In both cases a slight retardation of the rate is observed, but the decrease is relatively minor. These data suggest that arene loss is not involved in the formation of the active catalyst.

It cannot be ruled out, however, that the catalyst is activated via a ring slip (η^6-η^4 or η^6-η^2). Because it is not likely that the precatalyst is activated via *p*-cymene loss yet it is observed under the reaction conditions, I hypothesized that it may instead open decomposition pathways.

The unique feature of the dibenzyl complex **43b** compared to that of the others is the pendant phenyl rings. The phenyl rings may play a role in the complex's ability to stabilize the intermediate formed by *p*-cymene loss. In fact, Mezzetti et al. demonstrated that a similar complex bearing a phosphoramidite ligand would at elevated temperatures or after prolonged reaction times lose the *p*-cymene ligand[3] (Scheme 2.7). Upon arene dissociation, a pendant phenyl ring of the phosphoramidite ligand coordinates to the metal. In this way phosphoramidite ligands are shown to be potential two, four, six or eight electron donors.[3] If the dibenzyl phosphoramidite **43b** acts as an eight electron donor in the same manner, the catalyst lifetime could be increased, leading to increased activity.

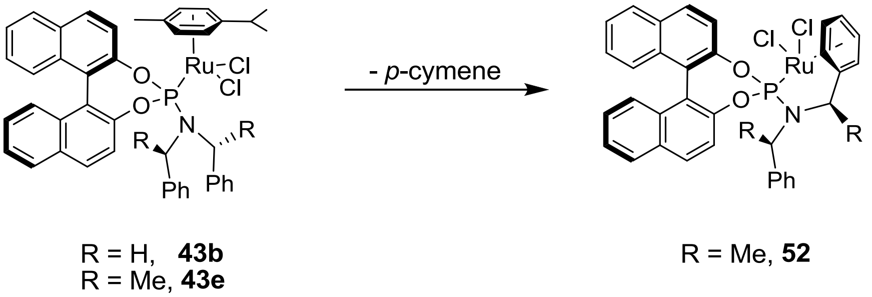

Scheme 2.7. Dissociation of the *p*-cymene ligand.[3]

To more conclusively determine the role of *p*-cymene loss in the reaction, compound **43b** was heated to 90 °C in cyclohexane in the absence of a propargylic alcohol. The result is a green solid with a complex ^{1}H NMR spectrum. Although this compound could not be isolated or well characterized, complete dissociation of the *p*-cymene ligand is evident by the disappearance of the coordinated arene protons in the ^{1}H NMR spectrum (normally present in the range 5.6-4.3 ppm). There is no evidence, however, that the pendant phenyl ring of the ligand coordinates to the metal. The mixture was then tested as catalyst in a standard reaction (2-phenyl-3-butyn-2-ol (**5b**) and benzoic acid) to see if the lack of *p*-cymene increased the activity. Although the mix is catalytically active, it is not active at lower temperatures nor does it appear to be more active than the precatalyst **43b**. Thus, in the case of complex **43b**, *p*-cymene dissociation likely does not lead to generation of the active catalyst, but it does not cause deactivation of the catalyst. In a final attempt to understand the observed differences in activity, the complexes **43a**, **43b** and **51** were used as catalysts in a test reaction and the conversion was followed over time. The known complex [RuCl$_2$(*p*-cymene)(PPh$_3$)] (**53**) was also used for comparison purposes (Figure 2.3).

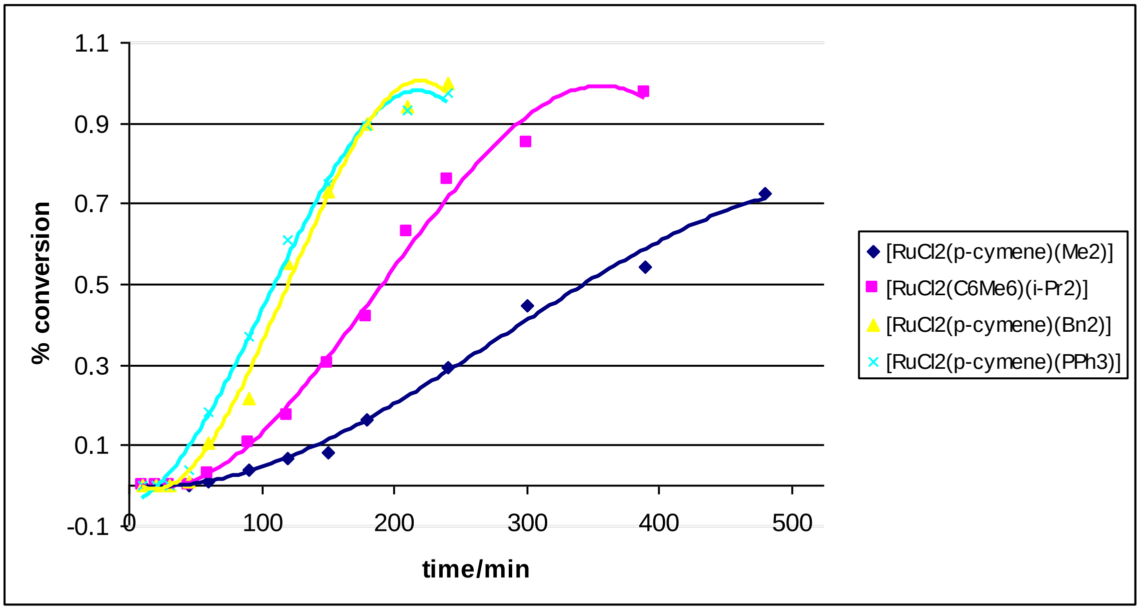

Figure 2.3. Kinetic comparison of catalysts.

For the kinetic test, the samples were prepared from a stock solution of the propargylic alcohol and benzoic acid.[25] The catalysts were added and the mixtures heated to 90 ^{o}C in a sealed screw cap vial. At appropriate time intervals the samples were removed from the heat source and aliquots were taken and filtered over silica to remove the catalyst. The samples were then analyzed by GC. The times shown on the corresponding data points correspond only to heating time and disregard the time the mixtures were not in the heat source (due to removal of aliquots). All of the complexes show an induction period of at least 30 minutes before any conversion is observed. This suggests that indeed the active catalyst is being formed in situ. The induction period is shortest for the dibenzyl complex **43b** and the phosphine complex **53**. Conversely, the hexamethylbenzene complex **51** shows an induction period of about 60 minutes, but the longest induction period and the slowest reaction rate are observed for the parent dimethyl complex **43a**.

2.4.3. Attempts at allenylidene synthesis

In order to determine the likelihood of the proposed allenylidene intermediate, I sought to test the ability of the catalyst to form a "stable" allenylidene that could be analyzed and spectroscopically characterized. When complex **43b** was reacted with 1,1-diphenyl-2-propyn-1-ol (**5a**) under Selegue's protocol (NH_4PF_6, MeOH, rt),[26] very little reaction was observed, potentially due to the poor solubility of the complex in the reaction medium. An alternative condition that has been employed involves the use of $AgPF_6$ in CH_2Cl_2 (Scheme 2.8). Complex **43b** reacts with $AgPF_6$ in CH_2Cl_2, giving AgCl as a precipitate. After filtration, 1,1-diphenyl-2-propyn-1-ol (**5b**) was added. The solution turns from orange to a very intense purple color in minutes. Over time (ca. 2 h), the solution slowly turns from purple to brown. Evaporation of the solvent and NMR analysis of the resulting residue shows a complex mixture. The primary peak in the ^{31}P NMR appears at 138.7 ppm, upfield of the starting material. Smaller peaks corresponding to impurities can be seen in the range 145-150 ppm. The ^{1}H NMR is less clear, showing many broad peaks, suggesting dynamic processes on the NMR time scale. Shorter reaction times (~1 h) do not significantly improve the quality of the crude product.

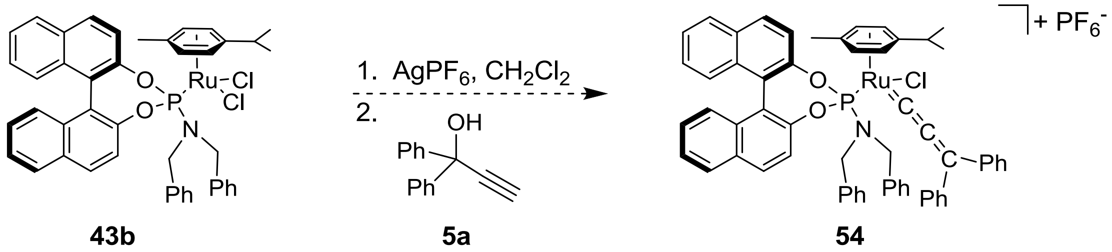

Scheme 2.8. Attempted synthesis of the allenylidene complex.

The observed color changes during the reaction suggest that perhaps the allenylidene is being formed *in situ* but is too reactive and would quickly react with solvent or the water formed during allenylidene formation. In addition to decomposition of an allenylidene species itself, decomposition of the reactive intermediate formed by chloride abstraction can occur, causing further degradation and leading to additional side products. One way to potentially stabilize this reactive intermediate is to use a coordinating solvent such as acetonitrile (MeCN) or THF. I hypothesized that solvent would coordinate to the metal temporarily occupying the coordination site and then dissociate in the presence of the propargylic alcohol. Abstraction of the chloride ligand from complex **43b** in MeCN results in the formation of the acetonitrile complex [RuCl(*p*-cymene)(**41b**)(MeCN)]PF_6 (**55**) (Scheme 2.9). ^{1}H NMR analysis shows the coordination of the solvent molecule by an upfield shift of the methyl protons (2.0-1.0 ppm). Upon addition of the propargylic alcohol **5a**, no reaction occurs even after several hours at elevated temperatures. This suggests that MeCN is too strongly coordinating, and does not dissociate from the metal easily to allow attack by the propargylic alcohol.

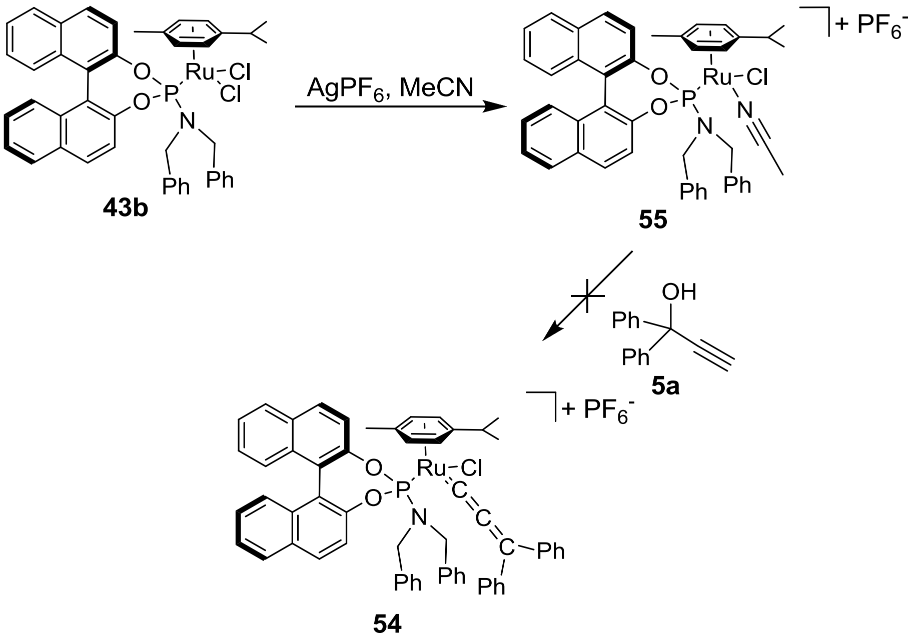

Scheme 2.9. Chloride abstraction in acetonitrile.

As THF is expected to be somewhat less coordinating, I next tested this solvent for the chloride abstraction. After filtration of the formed AgCl, **5a** was added and the solution quickly turned an intense purple color. After removal of the solvent the resulting residue was analyzed by NMR. The ^{1}H NMR shows an abundance of peaks, none of which is identifiable. The ^{31}P NMR also shows a number of peaks, all between 154 and 138 ppm. Thus, the complex is not an appropriate platform for stable allenylidene formation.

An alternative mechanism not involving an allenylidene intermediate has been reported previously by Watanabe[18] and Dixneuf[10] (Scheme 2.10). It involves activation of the alkyne by an η^2-coordination followed by attack of the carboxylate nucleophile. The η^1-alkenyl complex then undergoes an intramolecular transesterification. Finally, protonolysis yields the product and regenerates the active catalyst. It is important to note that the C-O bond of the propargylic alcohol is never broken in this cycle. This means that racemic propargylic alcohols must give racemic products. Likewise, optically active alcohols should show retention of configuration. This is what is reported by Dixneuf for both the *p*-cymene complex $[RuCl_2(PPh_3)(\eta^6\text{-}p\text{-cymene})]$ and the oxo-bridged dimer $[Ru_2(\mu\text{-}O_2CH)_2(CO)_4(PPh_3)_2]$. For both phosphoramidite catalysts **43a** and **43b**, no enantiomeric excesses were obtained when racemic propargylic alcohols were used. Conversely, when (R)-1-phenyl-2-propyn-1-ol was used with benzoic acid, the product was obtained without racemization as shown by chiral GC. As allenylidenes have an sp^2 hybridized carbon at the (formerly) propargylic position, the absolute configuration of the starting propargylic alcohol should have no effect on the absolute configuration of the product of a catalytic cycle involving an allenylidene intermediate. Thus the data obtained for the phosphoramidite complexes **43** are consistent with the previously reported mechanism.

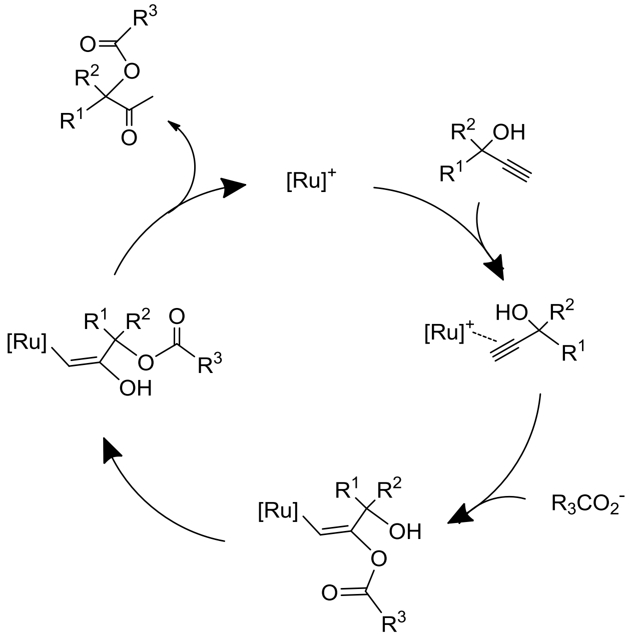

Scheme 2.10. Proposed mechanism of β-oxo ester formation.[10,18]

2.5. Summary and Prospective

A series of novel sterically and electronically tuned ruthenium piano-stool complexes of the type [$RuCl_2(\eta^6$-arene)(phosphoramidite)] have been synthesized and fully characterized. All of the complexes are active in the conversion of propargylic alcohols and carboxylic acids to β-oxo esters. Steric tuning of the catalyst shows a pronounced effect, but electronic tuning provided little difference in activity. Using one of these new complexes a small library of known and novel β-oxo esters were able to be synthesized in moderate to excellent yield (43-87%).

The reaction shows very broad substrate generality, tolerating aliphatic and aromatic primary, secondary and tertiary terminal propargylic alcohols with aliphatic and aromatic carboxylic acids. The reactants can be used in a 1:1 ratio with low catalyst loading (1.5 mol%) and without the addition of any cocatalysts or stoichiometric reagents. Thus, the broad substrate generality and mild reaction conditions compare well with previously reported catalysts.

The arene ligand was shown to be labile in the complexes, dissociating at elevated temperatures or after prolonged times in solution although the role of arene loss in the catalytic cycle remains unclear. The collective mechanistic data are consistent with the previously reported mechanism.

---

[1] Pike, R. D.; Sweigart, D. A. *Coord. Chem. Rev.* **1999**, *187*, 183.

[2] Devanne, D.; Ruppin, C.; Dixneuf, P. H. *J. Org. Chem.* **1988**, *53,* 926.

[3] (a). Huber, D.; Kumar, P. G. A.; Pregosin, P. S.; Mezzetti, A. *Organometallics* **2005**, *24*, 5221; (b). Mikhel, I. S.; Rüegger, H.; Butti, P.; Camponovo, F.; Huber, D.; Mezzetti, A. *Organometallics* **2008**, *27*, 2937.

[4] Merlic, C. A.; Pauly, M. E. *J. Am. Chem. Soc.* **1996**, *118*, 11319.

[5] Jafarpour, L.; Huang, J.; Stevens, E. D.; Nolan, S. P. *Organometallics* **1999**, *18*, 3761.

[6] Brunner, H.; Zwack, T.; Zabel, M.; Beck, W.; Böhm, A. *Organometallics* **2003**, *22*, 1743.

[7] Aydemir, M.; Baysal, A.; Meric, N.; Gümgüm, B. *J. Organomet. Chem.* **2009**, *694*, 2488.

[8] Diaz-Alvarex, A. E.; Crochet, P.; Zablocka, M.; Duhayon, C.; Cadierno, V.; Majoral, J.-P. *Eur. J. Inorg. Chem.* **2008**, 786.

[9] Cadierno, V.; Francos, J.; Gimeno, J. *Green Chem.* **2010**, *12*, 135.

[10] Darcel, C.; Bruneau, C.; Dixneuf, P. H.; Neef, G. *J. Chem. Soc., Chem. Commun.* **1994**, 333.

[11] Hansen, D. W. Jr.; Pappo, R.; Garland, R. B. *J. Org. Chem.* **1988**, *53,* 4244.

[12] (a). Ashraf, M. A.; Jones, M. A.; Kelly, N. E.; Mullaney, A.; Snaith, J. S.; Williams, I. W. *Tetrahedron Letters* **2003**, *44*, 3151; (b). Ashraf, M. A.; Russell, A. G.; Wharton, C. W.; Snaith, J. S. *Tetrahedron* **2007**, *63,* 586.

[13] Bruneau, C.; Kabouche, Z.; Neveux, M.; Sieller, B.; Dixneuf, P. H. *Inorg. Chim. Acta* **1994**, *222*, 154.

[14] Braoeff, E.; Ramírez, E.; Flores, E.; Valencia, N.; Sáncehz, M.; Heuze, I.; Cabeza, M. *Chem. Pharm. Bull.* **2003**, *51*, 1132.

[15] Scheid, G.; Kuit, W.; Ruijter, E.; Orru, R. V. A.; Henke, E.; Bornscheuer, U.; Wessjohann, L. A. *Eur. J. Org. Chem.* **2004**, 1063.

[16] Ye, J.; Bhatt, R. K.; Falck, J. R. *J. Am. Chem. Soc.* **1994**, *116*, 1.

[17] Yates, P.; Grewal, R. S.; Hayes, P. C.; Sawyer, J. F. *Can. J. Chem.* **1988**, *66*, 2805.

---

[18] Mitsudo, T.; Hori, Y.; Yamakawa, Y.; Watanabe, Y. *J. Org. Chem.* **1987**, 52, 2230.

[19] Bustelo, E. ; Dixneuf, P. H. *Adv. Synth. Catal.* **2007**, *349*, 933.

[20] Xu, Y.; Alcock, N. W.; Clarkson, G. J.; Docherty, G.; Woodward, G.; Wills, M. *Org. Lett.* **2004**, *6*, 4105.

[21] Costin, S.; Rath, N. P.; Bauer, E. B. *Adv. Synth. Catal.* **2008**, *350*, 2414.

[22] (a). Bianchini, C.; Peruzzini, M.; Zanobini, F.; Lopez, C.; de Los Rios, I.; Romerosa, A. *Chem. Commun.* **1999**, 443; (b). Wen, T. B.; Shou, Z. Y.; Lo, M. F.; Williams, I. D.; Jia, G. *Organometallics* **2003**, *22*, 5217; (c). Datta, S.; Chang, C.-H.; Yeh, K.-L.; Liu, R.-S. *J. Am. Chem. Soc.* **2003**, *125*, 9294.

[23] Duursma, A.; Boiteau, J.-G.; Lefort, L.; Boogers, J. A. F.; de Vries, A. H. M.; de Vries, J. G.; Minnaard, A. J.; Feringa, B. L. *J. Org. Chem.* **2004**, *69*, 8045.

[24] Bennett, M.; Smith, A.; *J. Chem. Soc. Dalton* **1974**, 233.

[25] The kinetic data was obtained with the assistance of undergraduate researcher Matthew J. Lenze.

[26] Selegue, J. P. *Organometallics* **1982**, *1*, 217.

Experimental Section

General. Chemicals were treated as follows: THF, toluene, diethyl ether, distilled from Na/benzophenone; CH_2Cl_2, distilled from CaH_2; isopropanol, simply distilled; 1,2-dichloroethane (DCE) and cyclohexane, used as received. [RuCl(μ-Cl)(*p*-cymene)]$_2$ (**42**, Strem), (R)-5,5’,6,6’-tetramethyl-3,3’-di-*t*-butyl-1,1’-biphenyl-2,2’-diol (**46**, Strem), hexamethylphosphorous triamide (Aldrich) all propargylic alcohols (Aldrich), Celite® (Aldrich), and other materials, used as received. “(R)-BINOL-*N,N*-dimethyl-phosphoramidite” **41a**,[1a] “(R)-BINOL-*N,N*-dibenzyl-phosphoramidite” **41b**[1b] and “(R)-BINOL-*N,N*-diisopropyl-phosphoramidite” **41c**[1b] were synthesized according to literature procedures.

NMR spectra were obtained at room temperature on a Bruker Avance 300 MHz or a Varian Unity Plus 300 MHz instrument and referenced to a residual solvent signal; all assignments are tentative. GC/MS spectra were recorded on a Hewlett Packard GC/MS System Model 5988A. Exact masses were obtained on a JEOL MStation [JMS-700] Mass Spectrometer. Melting points are uncorrected and were taken on an Electrothermal 9100 instrument. IR spectra were recorded on a Thermo Nicolet 360 FT-IR spectrometer.

“[((R)-BINOL-*N,N*-dimethyl-phosphoramidite)RuCl$_2$(*p*-cymene)]” (43a). To a Schlenk flask containing phosphoramidite **41a** (1.123 g, 3.125 mmol), CH_2Cl_2 (20 mL) was added followed by [RuCl(μ-Cl)(*p*-cymene)]$_2$ (**42**) (0.990 g, 1.62 mmol) to obtain a dark red solution. The solution was allowed to stir under nitrogen atmosphere at room temperature for 2.5 h, and then the solvent was removed by oil pump vacuum, yielding a red solid. Isopropanol (5 mL) was added and the solid was collected by filtration over a medium frit (10-15 M). It was then washed with isopropanol (2 × 1 mL) and dried under vacuum yielding **43a** as a red solid (1.988 g, 2.987 mmol, 96%), m.p. 201-202 °C dec. (capillary). Anal. calcd for $C_{32}H_{32}Cl_2NO_2PRu$: C, 57.75; H, 4.85. Found: C, 57.89; H, 4.87.

NMR (δ, $CDCl_3$) ^{1}H 7.95-7.86 (m, 5H, aromatic), 7.42-7.37 (m, 3H, aromatic), 7.27 (t, $^3J_{HH}$ = 7.8 Hz, 1H, aromatic), 7.21-7.19 (m, 3H, aromatic), 5.42 (d, $^3J_{HH}$ = 5.9 Hz, 1H, cymene), 5.40 (d, $^3J_{HH}$ = 5.9 Hz, 1H, cymene), 5.23 (d, $^3J_{HH}$ = 5.7 Hz, 1H, cymene), 4.59 (d, $^3J_{HH}$ = 5.7 Hz, 1H, cymene), 2.79 (sept, $^3J_{HH}$ = 6.9 Hz, 1H, $C\mathit{H}(CH_3)_2$ of cymene), 2.66 (s, 3H of $N(C\mathit{H}_3)_2$), 2.63 (s, 3H of $(NC\mathit{H}_3)_2$), 2.01 (s, 3H, $C\mathit{H}_3$ of cymene), 1.10 (d, $^3J_{HH}$ = 6.9 Hz, 3H, $CHC\mathit{H}_3$ of cymene), 1.03 (d, $^3J_{HH}$ = 6.9 Hz, 3H, $CHC\mathit{H}_3$ of cymene); $^{13}C\{^1H\}$ 150.2 (s, aromatic), 150.0 (s, aromatic), 148.6 (d, J_{CP} = 23.1 Hz, aromatic), 133.2 (d, J_{CP} = 7.5 Hz, aromatic), 132.9 (d, J_{CP} = 2.5 Hz, aromatic), 131.8 (s, aromatic), 131.7 (s, aromatic), 131.0 (s, aromatic), 130.3 (s, aromatic), 128.8 (d, J_{CP} = 12.6 Hz, aromatic), 127.4 (s, aromatic), 127.3 (s, aromatic), 127.0 (s, aromatic), 126.7 (s, aromatic), 125.9 (d, J_{CP} = 24.3 Hz, aromatic), 124.4 (d, J_{CP} = 12.6 Hz, aromatic), 123.5 (d, J_{CP} = 10.8 Hz, aromatic), 123.2 (d, J_{CP} = 8.7 Hz, aromatic), 121.0 (d, J_{CP} = 2.5 Hz, aromatic), 109.1 (s, cymene), 104.0 (s, cymene), 93.2 (d, J_{CP} = 20.4 Hz, cymene), 91.7 (d, J_{CP} = 40.5 Hz, cymene), 88.7 (d, J_{CP} = 19.5 Hz, cymene), 85.6 (d, J_{CP} = 11.7 Hz, cymene), 38.7 (d, $^2J_{CP}$ = 18.5 Hz, $N(\mathit{C}H_3)_2$), 30.7 (s), 22.8 (s), 22.3 (s), 18.8 (s); $^{31}P\{^1H\}$ 151.5.

HRMS calcd for $C_{32}H_{32}{}^{35}ClNO_2P^{102}Ru$ 630.0903, found 630.0885. IR (cm^{-1}, neat solid) 3045(w), 2966(w), 2924(w), 1588(w), 1505(w), 1462(m), 1227(s), 948(s).

"[((R)-BINOL-*N,N*-dibenzyl-phosphoramidite)RuCl$_2$(*p*-cymene)]" (43b). To a Schlenk flask containing **41b** (0.250 g, 0.489 mmol), CH_2Cl_2 (5 mL) was added followed by [RuCl(μ-Cl)(*p*-cymene)]$_2$ (0.150 g, 0.245 mmol) and the solution turned dark red. The solution was allowed to stir under nitrogen for 18 h. Solvent was removed by oil pump vacuum, yielding a red solid. The crude product was purified by flash filtration over 1 × 5 in. silica, using CH_2Cl_2/Et_2O 9:1 to pack/elute; red band was collected. Upon drying by oil pump vacuum, **43b** was obtained as a red solid (0.351 g, 0.429 mmol, 88%). Anal. calcd for $C_{44}H_{40}Cl_2NO_2PRu$: C, 64.63; H, 4.93. Found: C, 64.24; H, 4.99.

NMR (δ, $CDCl_3$) ^1H 8.04 (d, $^3J_{HH}$ = 8.8 Hz, 1H, aromatic), 7.99 (d, $^3J_{HH}$ = 8.1 Hz, 1H, aromatic), 7.95 (d, $^3J_{HH}$ = 8.8 Hz, 1H, aromatic), 7.89 (d, $^3J_{HH}$ = 8.1 Hz, 1H, aromatic), 7.79 (d, $^3J_{HH}$ = 8.8 Hz, 1H, aromatic), 7.49 (t, $^3J_{HH}$ = 7.3 Hz, 1H, aromatic), 7.43 (t, $^3J_{HH}$ = 7.3 Hz, 1H, aromatic), 7.34-7.15 (m, 15H, aromatic), 5.55 (d, $^3J_{HH}$ = 5.7 Hz, 1H, cymene), 5.40 (d, $^3J_{HH}$ = 5.7 Hz, 1H, cymene), 5.27 (d, $^3J_{HH}$ = 5.7 Hz, 1H, cymene), 5.01 (d, $^3J_{HH}$ = 5.7 Hz, 1H, cymene), 4.57 (d, $^3J_{HH}$ = 9.3 Hz, 1H, NC*H*H'Ph), 4.54 (d, $^2J_{HH}$ = 9.3 Hz, 1H, NC*H*H'Ph), 3.91 (d, $^2J_{HH}$ = 10.9 Hz, 1H, NCH*H*'Ph), 3.88 (d, $^2J_{HH}$ = 10.9 Hz, 1H, NCH*H*'Ph), 2.88 (sept, $^3J_{HH}$ = 6.8 Hz, 1H, C*H*(CH_3)$_2$ of cymene), 2.17 (s, 3H, C*H*$_3$ of cymene), 1.18 (d, $^3J_{HH}$ = 6.9 Hz, 3H, CHC*H*$_3$ of cymene), 1.15 (d, $^3J_{HH}$ = 6.9 Hz, 3H, CHC*H*$_3$ of cymene); $^{13}C\{^1H\}$ 149.7 (s, aromatic), 149.6 (s, aromatic), 148.6 (d, J_{CP} = 6.4 Hz, aromatic), 137.5 (d, J_{CP} = 2.3 Hz, aromatic), 132.6 (d, J_{CP} = 1.1 Hz, aromatic), 132.5 (s, aromatic), 131.1 (d, J_{CP} = 5.1 Hz, aromatic), 130.0 (d, J_{CP} = 0.8 Hz, aromatic), 128.8 (s, aromatic), 128.24 (s, aromatic), 128.17 (s, aromatic), 127.9 (s, aromatic), 127.0 (s, aromatic), 126.9 (s, aromatic), 126.4 (s, aromatic), 126.3 (s, aromatic), 125.4 (s, aromatic), 125.3 (s, aromatic), 124.0 (d, J_{CP} = 2.7 Hz, aromatic), 122.20 (d, J_{CP} = 2.7 Hz, aromatic), 122.17 (d, J_{CP} = 3.2 Hz, aromatic), 120.9 (s, aromatic), 110.3 (d, J_{CP} = 2.5 Hz, cymene), 104.3 (d, J_{CP} = 1.9 Hz, cymene), 90.2 (d, J_{CP} = 2.8 Hz, cymene), 89.3 (d, J_{CP} = 8.3 Hz, cymene), 89.1 (d, J_{CP} = 6.2 Hz, cymene), 87.2 (d, J_{CP} = 2.7 Hz, cymene), 50.1 (s, N*C*H_2), 50.0 (s, N*C*'H_2), 30.5 (s), 22.2 (s), 21.8 (s), 18.2 (s); $^{31}P\{^1H\}$ 142.2.

HRMS calcd for $C_{44}H_{40}{}^{35}Cl_2NO_2PNa^{102}Ru$ 840.1113, found 840.1116. IR (cm^{-1}, neat solid) 2953(w), 2917(w), 1591(m), 1461(m), 1226(s), 940(s).

"[((R)-BINOL-*N,N*-diisopropyl-phosphoramidite)RuCl$_2$(*p*-cymene)]" (43c). To a Schlenk flask containing **41c** (0.212 g, 0.510 mmol), CH_2Cl_2 (8 mL) was added followed by $[RuCl(\mu\text{-}Cl)(p\text{-cymene})]_2$ (**42**) (0149 g, 0.243 mmol) and the solution turned dark red. The solution was allowed to stir under nitrogen for 18 h. Solvent was removed by oil pump vacuum, yielding a red solid. The crude product was purified by flash chromatography (1 × 4.5 in. silica, CH_2Cl_2/diethyl ether, 49:1 v/v). Upon drying by oil pump vacuum, **43c** was obtained as a red solid (0.232 g, 0.326 mmol, 67%), m.p. 148-149 °C dec. (capillary). Anal. calcd for $C_{36}H_{40}Cl_2NO_2PRu$: C, 59.92; H, 5.59. Found: C, 60.26; H, 5.68.

NMR (δ, $CDCl_3$) ^{1}H 7.94-7.83 (m, 5H, aromatic), 7.45-7.34 (m, 3H, aromatic), 7.24-7.08 (m, 4H, aromatic), 5.30 (d, $^3J_{HH}$ = 6.0 Hz, 1H, cymene), 5.16 (d, $^3J_{HH}$ = 6.0 Hz, 1H, cymene), 5.01 (d, $^3J_{HH}$ = 5.7 Hz, 1H, cymene), 4.33 (d, $^3J_{HH}$ = 5.7 Hz, 1H, cymene), 3.71-3.64 (m, 2H, $NCH(CH_3)_2$), 2.76 (sept, $^3J_{HH}$ = 6.6 Hz, 1H, $CH(CH_3)_2$ of cymene), 2.01 (s, 3H, CH_3 of cymene), 1.13 (d, $^3J_{HH}$ = 6.5 Hz, 6H, $NCH(CH_3)_2$), 1.09 (t, $^3J_{HH}$ = 6.6 Hz, 6H, $NCH(CH_3)_2$), 0.69 (d, $^3J_{HH}$ = 6.9 Hz, 6H, $CH(CH_3)_2$ of cymene); $^{13}C\{^1H\}$ 150.3 (s, aromatic), 150.1 (s, aromatic), 148.3 (d, J_{CP} = 25.5 Hz, aromatic), 133.3 (s, aromatic), 133.1 (s, aromatic), 131.6 (s, aromatic), 131.5 (s, aromatic), 130.4 (s, aromatic), 130.2 (s, aromatic), 128.8 (d, J_{CP} = 15.3 Hz, aromatic), 127.4 (s, aromatic), 127.3 (s, aromatic), 126.9 (d, J_{CP} = 16.2 Hz, aromatic), 126.0 (s, aromatic), 125.7 (s, aromatic), 124.8 (s, aromatic), 123.4 (d, J_{CP} = 11.1 Hz, aromatic), 123.2 (s, aromatic), 122.2 (s, aromatic), 109.1 (s, cymene), 105.5 (d, J_{CP} = 12.0 Hz, cymene), 93.3 (s, cymene), 90.8 (d, J_{CP} = 45.6 Hz, cymene), 88.8 (d, J_{CP} = 16.5 Hz, cymene), 84.2 (s, cymene), 48.3 (d, $^2J_{CP}$ = 27.6 Hz, $NCH(CH_3)_2$), 31.0 (s), 24.8 (s), 23.6 (s), 23.0 (s), 22.6 (s), 18.9 (s); $^{31}P\{^1H\}$ 142.9 (s).

HRMS calcd for $C_{36}H_{40}{}^{35}Cl_2NO_2P^{102}Ru$ 721.1216, found 721.1215. IR (cm^{-1}, neat solid) 3052(w), 2964(m), 2925(m), 1589(w), 1464(m), 1230(m), 949(s).

"[((rac)-6,6'-dibromo-BINOL-*N,N*-dimethyl-phosphoramidite)RuCl$_2$(*p*-cymene)]" (43d). To a Schlenk flask containing **41d** (0.206 g, 0.398 mmol), CH_2Cl_2 (3 mL) was added followed by [RuCl(μ-Cl)(*p*-cymene)]$_2$ (**42**) (0.111 g, 0.181 mmol) to obtain a dark red solution. The solution was allowed to stir under nitrogen atmosphere at room temperature for 2.5 h, and then the solvent was removed by oil pump vacuum, yielding red solid. Diethyl ether (2 × 2.5 mL) was added and the resulting slurry was stirred and the solvent decanted. The solid was then dried under vacuum yielding **43d** as a red solid (0.198 g, 2.99 mmol, 66%). Anal. calcd for $C_{32}H_{30}Cl_2Br_2NO_2PRu$: C, 46.68; H, 3.67. Found: C, 46.49; H, 3.75.

NMR (δ, $CDCl_3$) ^{1}H 8.13 (s, 2H, aromatic), 8.02-7.91 (m, 3H, aromatic), 7.53 (d, $^3J_{HH}$ = 8.7 Hz, 1H, aromatic), 7.35 (d, $^3J_{HH}$ = 7.8 Hz, 2H, aromatic), 7.15 (d, $^3J_{HH}$ = 9.1 Hz, 2H, aromatic), 5.59-5.53 (m, 2H, cymene), 5.47 (d, $^3J_{HH}$ = 5.8 Hz, 1H, cymene), 4.93 (d, $^3J_{HH}$ = 5.9 Hz, 1H, cymene), 2.90-2.85 (m, 1H, $CH(CH_3)_2$ of cymene), 2.70 (s, 3H of $N(CH_3)_2$), 2.67 (s, 3H of $N(CH_3)_2$), 2.14 (s, 3H, CH_3 of cymene), 1.20 (d, $^3J_{HH}$ = 6.8 Hz, 3H, $CHCH_3$ of cymene), 1.08 (d, $^3J_{HH}$ = 6.8 Hz, 3H, $CHCH_3$ of cymene); ^{13}C{^{1}H}149.7 (s, aromatic), 149.5 (s, aromatic), 148.5 (d, J_{CP} = 6.0 Hz, aromatic), 132.2 (d, J_{CP} = 0.8 Hz, aromatic), 130.8 (d, J_{CP} = 1.6 Hz, aromatic), 130.5 (d, J_{CP} = 1.5 Hz, aromatic), 130.2 (d, J_{CP} = 7.4 Hz, aromatic), 129.9 (s, aromatic), 129.7 (s, aromatic), 129.5 (s, aromatic), 128.9 (s, aromatic), 128.1 (s, aromatic), 124.9 (d, J_{CP} = 3.0 Hz, aromatic), 122.6 (d, J_{CP} = 2.8 Hz, aromatic), 122.0 (d, J_{CP} = 2.1 Hz, aromatic), 121.8 (s, aromatic), 119.4 (s, aromatic), 119.3 (s, aromatic), 109.2 (d, J_{CP} = 2.4 Hz, cymene), 102.9 (d, J_{CP} = 1.6 Hz, cymene), 91.6 (d, J_{CP} = 4.9 Hz, cymene), 90.1 (d, J_{CP} = 7.4 Hz, cymene), 89.4 (d, J_{CP} = 5.8 Hz, cymene), 86.4 (d, J_{CP} = 4.1 Hz, cymene), 37.9 (s, NCH_3), 37.8 (s, NCH_3), 30.1 (s), 21.9 (s), 21.7 (s), 18.2 (s); ^{31}P{^{1}H} 152.0.

HRMS calcd for $C_{36}H_{52}{}^{35}Cl_2{}^{79}Br_2NO_2P^{102}Ru$ 820.8800, found 820.8773. IR (cm^{-1}, neat solid) 2917(w), 1582(m), 1492(m), 1322(m), 1227(m), 945(s).

"[((R)-BINOL(8H)-*N,N*-dimethyl-phosphoramidite)RuCl$_2$(*p*-cymene)]" (48a). To a Schlenk flask containing [RuCl(μ-Cl)(*p*-cymene)]$_2$ (**42**) (0.091 g, 0.149 mmol), a solution of **45a** (0.120 g, 0.327 mmol) in CH_2Cl_2 (5 mL) was added. The resulting red solution was stirred at room temperature for 5 h after which the solvent was removed under high vacuum. The red solid was then filtered over Celite® and washed with hexanes (20 mL) and the eluent discarded. The solid was then washed down using CH_2Cl_2 (20 mL) and the solution dried under high vacuum, yielding **48a** as a red solid (0.165 g, 0.245 mmol, 82%). Anal. calcd for $C_{32}H_{40}Cl_2NO_2PRu$: C, 57.06; H, 5.99. Found: C, 57.19; H, 5.95.

NMR (δ, $CDCl_3$) ^1H 7.36 (d, $^3J_{HH}$ = 8.2 Hz, 1H, aromatic), 7.07 (d, $^3J_{HH}$ = 9.6 Hz, 2H, aromatic), 6.93 (d, $^3J_{HH}$ = 8.2 Hz, 1H, aromatic), 5.42 (d, $^3J_{HH}$ = 6.2 Hz, 1H, cymene), 5.35 (d, $^3J_{HH}$ = 6.2 Hz, 1H, cymene), 5.09 (d, $^3J_{HH}$ = 5.8 Hz, 1H, cymene), 4.57 (d, $^3J_{HH}$ = 5.8 Hz, 1H, cymene), 2.85-2.73 (m, 7H, $3CH_2$ + $CH(CH_3)_2$), 2.66 (s, 3H, NCH_3), 2.63 (s, 3H, NCH_3), 2.32-2.17 (m, 2H, CH_2), 2.04 (s, 3H, CH_3 of cymene), 1.82-1.69 (m, 6H, 3 CH_2), 1.55-1.48 (m, 2H, CH_2), 1.15 (d, $^3J_{HH}$ = 6.9 Hz, 3H, $CHCH_3$ of cymene), 1.11 (d, $^3J_{HH}$ = 6.9 Hz, 3H, $CHCH_3$ of cymene); $^{13}C\{^1H\}$ 148.4 (s, aromatic), 148.2 (s, aromatic), 146.6 (d, J_{CP} = 5.5 Hz, aromatic), 138.4 (d, J_{CP} = 2.0 Hz, aromatic), 138.0 (d, J_{CP} = 1.7 Hz, aromatic), 134.7 (d, J_{CP} = 2.1 Hz, aromatic), 134.5 (d, J_{CP} = 2.2 Hz, aromatic), 129.3 (d, J_{CP} = 1.9 Hz, aromatic), 129.0 (d, J_{CP} = 0.8 Hz, aromatic), 127.7 (d, J_{CP} = 2.3 Hz, aromatic), 127.4 (d, J_{CP} = 2.2 Hz, aromatic), 121.2 (d, J_{CP} = 3.7 Hz, aromatic), 117.6 (d, J_{CP} = 2.3 Hz, cymene), 108.3 (d, J_{CP} = 2.0 Hz, cymene), 104.2 (d, J_{CP} = 2.8 Hz, cymene), 91.9 (d, J_{CP} = 4.6 Hz, cymene), 87.5 (d, J_{CP} = 4.8 Hz, cymene), 84.2 (d, J_{CP} = 2.4 Hz, cymene), 38.0 (s, NCH$_3$), 37.9 (s, NCH$_3$), 30.1 (s), 28.9 (s), 28.8 (s), 27.6 (s), 27.4 (s), 22.4 (s), 22.3 (s), 22.2 (s), 22.0 (s), 21.9 (s), 18.1 (s); ^{31}P{^{1}H} 145.5.

HRMS calcd for $C_{32}H_{40}{}^{35}Cl_2NO_2P^{102}Ru$ 673.1216, found 673.1185. IR (cm^{-1}, neat solid) 2932(s), 1467(s), 1220(s), 938(s).

"((R)-BINOL(8H)-*N,N*-dibenzyl-phosphoramidite)" (45b). To a Schlenk flask containing triethyl amine (0.25 mL, 1.9 mmol) and dibenzyl amine (0.36 mL, 1.9 mmol), toluene (10 mL) was added followed by phosphorous trichloride (0.15 mL, 1.7 mmol), which upon addition, yielded a white smoke. The white slurry was heated to 70 °C for 12 h upon which the color changed to yellow. After cooling to room temperature, triethyl amine was added (0.496 mL, 3.74 mmol) followed by 5,5',6,6',7,7',8,8'-octahydro-bi-2-naphthol (0.500 g, 1.70 mmol). An additional 4 mL toluene was added and the slurry stirred at room temperature for 24 h. Diethyl ether (5 mL) was added and the slurry was filtered over silica on 15 M frit and the filtrate was dried by oil pump vacuum, yielding a white solid. Solid was purified by flash filtration (1 × 4 in. silica) using CH_2Cl_2/hexanes 1:3 to pack/elute. Solution was then dried yielding **45b** as a white foam (0.570 g, 1.10 mmol, 65%). Calcd for $C_{34}H_{34}NO_2P$: C: 78.59; H: 6.60. Found: C: 77.88; H: 6.46.

NMR (δ, $CDCl_3$) ^{1}H 7.30-7.19 (m, 10H, aromatic), 7.05-7.02 (m, 2H, aromatic), 6.76 (d, $^3J_{HH}$ = 8.2 Hz, 1H, aromatic), 6.49 (d, $^3J_{HH}$ = 8.2 Hz, 1H, aromatic), 4.07 (d,

${}^2J_{HH}$ = 7.5 Hz, 1H, NC*H*H'Ph), 4.02 (d, ${}^2J_{HH}$ = 7.5 Hz, 1H, NC*H*H'Ph), 3.32 (d, ${}^2J_{HH}$ = 12.4 Hz, 1H, NCH*H*'Ph), 3.27 (d, ${}^2J_{HH}$ = 12.4 Hz, 1H, NCH*H*'Ph), 2.75-2.72 (m, 2H), 2.64-2.51 (m, 4H), 2.28-2.14 (m, 6H), 1.58-1.39 (m, 2H); ${}^{13}C\{{}^1H\}$ 148.5 (s, aromatic), 148.0 (d, J_{CP} = 3.8 Hz, aromatic), 138.3 (s, aromatic), 138.0 (s, aromatic), 137.3 (d, J_{CP} = 1.0 Hz, aromatic), 134.1 (s, aromatic), 133.0 (d, J_{CP} = 1.0 Hz, aromatic), 129.3 (s, aromatic), 128.9 (s, aromatic), 128.3 (s, aromatic), 128.1 (s, aromatic), 127.1 (s, aromatic), 118.8 (d, J_{CP} = 2.5 Hz, aromatic), 118.1 (s, aromatic), 48.2 (s, N*C*H_2Ph), 47.9 (s, N*C*H_2Ph), 29.2 (s), 29.0 (s), 27.7 (s), 22.69 (s), 22.67 (s), 22.6 (s), 22.5 (s); ${}^{31}P\{{}^1H\}$ 139.4.

HRMS calcd for $C_{36}H_{52}NO_2P$ 519.2327, found 519.2324. IR (cm^{-1}, neat solid) 3028(w), 2928(s), 2857(m), 1467(s), 1349(w), 1232(s), 931(s).

"[((R)-BINOL(8H)-*N,N*-dibenzyl-phosphoramidite)RuCl$_2$(*p*-cymene)]" (48b). To a Schlenk flask containing [RuCl(μ-Cl)(*p*-cymene)]$_2$ (**42**) (0.144 g, 0.235 mmol), a solution of **45b** (0.245 g, 0.471 mmol) in CH_2Cl_2 (6 mL) was added. The resulting red solution was stirred at room temperature for 16 h after which the solvent was removed under high vacuum. Hexanes (5 mL) was added and the slurry filtered over Celite® on silica gel (~1 cm). The solid was washed with hexanes (30 mL) and the eluent discarded. The product was then washed down using CH_2Cl_2/Et_2O 9:1 (25 mL) until the silica was no longer red. The solution was dried under high vacuum, yielding **48b** as a red solid (0.333 g, 0.403 mmol, 86%). Anal. calcd for $C_{44}H_{48}Cl_2NO_2PRu$, C, 63.99; H, 5.86. Found, C, 4.51; H, 6.31.

NMR (δ, $CDCl_3$) ^{1}H 7.34 (d, $^3J_{HH}$ = 8.1 Hz, 1H, aromatic), 7.20-7.13 (m, 11H, aromatic), 6.89 (d, $^3J_{HH}$ = 8.3 Hz, 1H, aromatic), 6.65 (d, $^3J_{HH}$ = 8.2 Hz, 1H, aromatic), 5.53 (d, $^3J_{HH}$ = 6.0 Hz, 1H, cymene), 5.38 (d, $^3J_{HH}$ = 5.9 Hz, 1H, cymene), 5.00 (d, $^3J_{HH}$ = 5.9 Hz, 1H, cymene), 4.93 (d, $^3J_{HH}$ = 6.0 Hz, 1H, cymene), 4.49 (d, $^2J_{HH}$ = 8.8 Hz, 1H, NC*H*H'Ph), 4.44 (d, $^2J_{HH}$ = 8.8 Hz, 1H, NC*H*H'Ph), 3.86 (d, $^2J_{HH}$ = 10.4 Hz, 1H, CH*H*'Ph), 3.80 (d, $^2J_{HH}$ = 10.4 Hz, 1H, NCH*H*'Ph), 2.85-2.54 (m, 7H), 2.36-2.29 (m, 1H), 2.22-2.19 (m, 1H), 2.15 (s, 3H, CH_3 of cymene), 1.88-1.74 (m, 6H), 1.57-1.44 (m, 2H), 1.21 (d, $^3J_{HH}$ = 6.9 Hz, 3H, CHCH_3 of cymene), 1.16 (d, $^3J_{HH}$ = 6.9 Hz, 3H, CHCH_3 of cymene); ^{13}C{^{1}H} 148.3 (s, aromatic), 148.1 (s, aromatic), 147.1 (d, J_{CP} = 5.9 Hz, aromatic), 138.2 (d, J_{CP} = 3.3 Hz, aromatic), 138.1 (d, J_{CP} = 1.8 Hz, aromatic), 137.7 (d, J_{CP} = 3.1 Hz, aromatic), 134.5 (d, J_{CP} = 1.9 Hz, aromatic), 134.4 (d, J_{CP} = 1.8 Hz, aromatic), 129.3 (d, J_{CP} = 1.8 Hz, aromatic), 128.9 (s, aromatic), 128.7 (s, aromatic), 127.4 (s, aromatic), 127.1 (d, J_{CP} = 2.1 Hz, aromatic), 126.8 (d, J_{CP} = 2.2 Hz, aromatic), 126.3 (s, aromatic), 120.7 (d, J_{CP} = 3.2 Hz, aromatic), 118.2 (d, J_{CP} = 2.3 Hz, aromatic), 109.2 (d, J_{CP} = 2.8 Hz, cymene), 105.6 (d, J_{CP} = 3.4 Hz, cymene), 99.2 (s), 90.3 (d, J_{CP} = 1.0 Hz, cymene), 89.4 (d, J_{CP} = 9.3 Hz, cymene), 87.6 (d, J_{CP} = 4.7 Hz, cymene), 85.3 (d, J_{CP} = 1.0 Hz, cymene), 49.8 (s, N*C*HH'Ph), 49.7 (s, N*C*HH'Ph), 30.6 (s), 30.3 (s), 28.7 (s), 28.6 (s), 27.5 (s), 27.1 (s), 22.4 (s), 22.2 (s), 22.1 (s), 21.2 (s), 18.0 (s); ^{31}P{^{1}H} 136.8.

HRMS calcd for $C_{44}H_{48}{}^{35}Cl_2NO_2P{}^{102}Ru$ 825.1842, found 825.1839. IR (cm^{-1}, neat solid) 2925(m), 2859(w), 1467(m), 1220(m), 938(s).

"(R)-BIPHEN-*N,N*-dimethyl-phosphoramidite" (47). To a Schlenk flask containing (R)-5,5',6,6'-tetramethyl-3,3'-di-t-butyl-1,1'-biphenyl-2,2'-diol ("(R)-BIPHEN", **46**) (0.217 g, 0.613 mmol), toluene (6 mL) was added followed by hexamethylphosphorous triamide (0.14 mL, 0.77 mmol) and NH_4Cl (0.10 g). The clear solution was heated at 100 °C for 12 h under nitrogen atmosphere. Upon cooling the solvent was removed and the solid was dried by oil pump vacuum. Diethyl ether (2 mL) was added to the white residue and the resulting suspension was cooled to –18 °C for 1 h and then filtered over a medium frit (10-15 M). The solid was washed with cold diethyl ether (2 × 1 mL). The filtrate was concentrated under vacuum to 1 mL and stored at –18 °C for 1 h. The suspension was filtered over medium frit again and both crops were dried by oil pump vacuum to give **47** as a white solid (0.160 g, 0.374 mmol, 61%), m.p. 150-152 °C (capillary).

NMR (δ, $CDCl_3$) ^{1}H 7.14 (s, 1H, Ph), 7.10 (s, 1H, Ph), 2.41 (br, 6H, 2CH_3), 2.27 (s, 3H, NCH_3), 2.26 (s, 3H, NCH_3), 1.89 (s, 3H, CH_3), 1.78 (s, 3H, CH_3), 1.46 (s, 9H, C(CH_3)$_3$), 1.41 (s, 9H, C(CH_3)$_3$); ^{13}C{^{1}H} 148.0 (s, Ph), 146.9 (d, J_{CP} = 20.1 Hz, Ph), 138.2 (d, J_{CP} = 12.3 Hz, Ph), 137.1 (s, Ph), 134.9 (s, Ph), 134.2 (s, Ph), 132.2 (d, J_{CP} = 18.9 Hz, Ph), 132.0 (s, Ph), 131.4 (d, J_{CP} = 9.6 Hz, Ph), 130.9 (s, Ph), 128.0 (s, Ph), 127.9 (s, Ph), 35.1 (s), 35.1 (d, J_{CP} = 14.1 Hz), 31.8 (d, J_{CP} = 21.3 Hz), 30.0 (s), 20.7 (d, J_{CP} = 22.4 Hz), 17.1 (s), 16.8 (s); ^{31}P{^{1}H} 140.6 (s).

HRMS calcd for $C_{26}H_{38}NO_2P$ 427.2640, found 427.2650. IR (cm^{-1}, neat solid) 2961(s), 2801(w), 1413(w), 1438(m), 1390(w), 1232(m), 979(s).

"[((R)-BIPHEN-*N,N*-dimethyl-phosphoramidite)RuCl$_2$(*p*-cymene)]" (49). To a Schlenk flask containing **48** (0.145 g, 0.339 mmol), DCE (5 mL) was added and the solid dissolved. [RuCl(μ-Cl)(*p*-cymene)]$_2$ (**42**, 0.099 g, 0.162 mmol) was then added and the resulting red solution was refluxed under nitrogen atmosphere for 2.5 h. The solvent was removed and the dark red solid was dried by oil pump vacuum and then extracted with diethyl ether (3 × 2 mL). The solvent was removed from the extracts and the product was dried by oil pump vacuum to give **49** as a purple solid (0.143 g, 0.195 mmol, 60%), m.p. 150-152 °C dec. (capillary). Anal. calcd for $C_{36}H_{52}Cl_2NO_2PRu$: C, 58.93; H, 7.14. Found: C, 58.22; H, 7.22.

NMR (δ, $CDCl_3$) ^1H 7.23 (s, 1H, Ph), 7.17 (s, 1H, Ph), 5.31 (d, $^3J_{HH}$ = 5.7 Hz, 1H, cymene), 5.03 (d, $^3J_{HH}$ = 5.7 Hz, 1H, cymene), 4.89 (br, 2H, cymene), 2.74 (sept, $^3J_{HH}$ = 6.9 Hz, 1H, $C\mathit{H}(CH_3)_2$ of cymene), 2.58 (s, 3H, $N(C\mathit{H}_3)_2$), 2.35 (s, 3H, $N(C\mathit{H}_3)_2$), 2.26 (s, 3H, $C\mathit{H}_3$), 1.94 (s, 3H, $C\mathit{H}_3$), 1.86 (s, 3H, $C\mathit{H}_3$), 1.70 (s, 3H, $C\mathit{H}_3$), 1.63 (s, 3H, $C\mathit{H}_3$), 1.43 (s, 18H, $C(C\mathit{H}_3)_3$), 1.15 (d, $^3J_{HH}$ = 6.9 Hz, 3H, $CHC\mathit{H}_3$ of cymene), 1.03 (d, $^3J_{HH}$ = 6.9 Hz, 3H, $CHC\mathit{H}_3$ of cymene); $^{13}C\{^1H\}$ 147.0 (d, J_{CP} = 61.5 Hz, Ph), 146.6 (d, J_{CP} = 22.2 Hz, Ph), 137.7 (d, J_{CP} = 15.6 Hz, Ph), 136.8 (d, J_{CP} = 8.7 Hz, Ph), 134.2 (s, Ph), 133.7 (d, J_{CP} = 7.8 Hz, Ph), 131.4 (s, Ph), 131.3 (d, J_{CP} = 6.6 Hz, Ph), 129.7 (d, J_{CP} = 12.6 Hz, Ph), 128.8 (d, J_{CP} = 10.2 Hz, Ph), 127.8 (s, Ph), 127.2 (s, Ph), 110.7 (s, cymene), 104.5 (s, cymene), 88.5 (s, cymene), 84.8 (s, cymene), 84.1 (d,

J_{CP} = 20.1 Hz, cymene), 84.0 (d, J_{CP} = 29.1 Hz, cymene), 39.6 (d, $^2J_{CP}$ = 14.6 Hz, N*C*H(CH$_3$)$_2$), 34.6 (s), 34.0 (s), 31.1 (s), 29.8 (s), 28.5 (s), 21.2 (s), 21.1 (s), 19.4 (s), 19.2 (s), 17.4 (s), 15.3 (s), 15.0 (s); $^{31}P\{^1H\}$ 125.6 (s).

HRMS calcd for $C_{36}H_{52}{}^{35}ClNO_2P^{102}Ru$ 698.2468, found 698.2465. IR (cm^{-1}, neat) 2955(s), 2917(s), 1420(m), 1228(m), 1175(m), 1026(s), 990(s).

"[((R)-BINOL-*N,N*-diisopropyl-phosphoramidite)RuCl$_2$(C$_6$Me$_6$)]" (51). To a Schlenk flask containing **41c** (0.100 g, 0.241 mmol), CH_2Cl_2 (5 mL) was added followed by $[RuCl(\mu\text{-}Cl)(C_6Me_6)]_2$ (**50**) (0.080 g, 0.120 mmol) and the solution turned dark red-brown. The solution was refluxed under nitrogen for 6 h. Solvent was removed by oil pump vacuum, yielding orange solid. The crude product was washed 2 × 4 mL dry Et_2O and the solvent decanted. Upon drying by oil pump vacuum, **51** was obtained as an orange solid (0.140 g, 0.187 mmol, 78%). Anal. calcd for $C_{38}H_{44}Cl_2NO_2PRu$, C, 60.88; H, 5.92. Found, C, 58.72; H, 5.95.

NMR (δ, $CDCl_3$) ^1H 8.43 (d, $^3J_{HH}$ = 8.9 Hz, 1H, aromatic), 7.96 (d, $^3J_{HH}$ = 4.4 Hz, 1H, aromatic), 7.93 (d, $^3J_{HH}$ = 5.4 Hz, 3H, aromatic), 7.56 (d, $^3J_{HH}$ = 4.9 Hz, 1H, aromatic), 7.37-7.39 (br, 2H, aromatic), 7.13-7.16 (m, 4H, aromatic), 3.57-3.64 (m, 2H, NC*H*(CH$_3$)$_2$), 1.75 (s, 18H, C$_6$(C*H*$_3$)$_6$), 1.16 (d, $^3J_{HH}$ = 6.3 Hz, 6H, NCH(C*H*$_3$)$_2$), 0.87 (d, $^3J_{HH}$ = 4.7 Hz, 6H, N-CH(C*H*$_3$)$_2$); $^{13}C\{^1H\}$ 149.1 (s, aromatic), 148.9 (s, aromatic), 148.1 (d, J_{CP} = 6.0 Hz, aromatic), 132.9 (d, J_{CP} = 2.1 Hz, aromatic), 132.4 (d, J_{CP} = 1.1 Hz, aromatic), 130.9 (d, J_{CP} = 0.7 Hz, aromatic), 129.1 (s, aromatic), 128.4 (s, aromatic), 127.8 (d, J_{CP} = 2.3 Hz, aromatic), 126.9 (s, aromatic), 126.5 (s, aromatic), 126.0 (s, aromatic), 125.73 (s, aromatic), 125.69 (d, J_{CP} = 1.0 Hz, aromatic), 125.6 (d, J_{CP} = 6.1 Hz, aromatic), 124.9 (s, aromatic), 124.8 (s, aromatic), 123.4 (d, J_{CP} = 3.2 Hz, aromatic), 122.2 (d, J_{CP} = 2.2 Hz, aromatic), 121.6 (d, J_{CP} = 1.0 Hz, aromatic), 99.0 (d, $^2J_{CP}$ = 4.2 Hz, $\mathit{C}_6(CH_3)_6$), 48.1 (s, NCH($CH_3)_2$), 48.0 (s, NCH($CH_3)_2$), 24.61 (s, NCH($\mathit{C}H_3)_2$), 24.57 (s, NCH($\mathit{C}H_3)_2$), 23.2 (br, NCH($\mathit{C}H_3)_2$), 15.6 (s, $C_6(\mathit{C}H_3)_6$); $^{31}P\{^1H\}$ 158.3.

HRMS calcd for $C_{38}H_{44}{}^{35}Cl_2NO_2P^{102}Ru$ 749.1529, found 749.1507. IR (cm^{-1}, neat solid) 2969(w), 2921(w), 1504(m), 1462(m), 1231(m), 1201(m), 944(s).

“[((R)-BINOL-*N,N*-dibenzyl-phosphoramidite)RuCl(*p*-cymene)(diphenylallenylidene)]” (54). To a Schlenk flask containing **43b** (0.075 g, 0.092 mmol), $AgPF_6$ (0.025 g, 0.099 mmol) was added as a solution in CH_2Cl_2 (3.5 mL). After 1 h stirring at rt, the orange slurry was filtered over Celite then 1,1-diphenyl-2-propyn-1-ol (**5a**) was added and the solution turned dark purple over the course of several minutes. After stirring 1 h at rt, the volatiles were removed under high vacuum, yielding **54** in ca. 70% spectroscopic purity.

NMR (δ, $CDCl_3$, partial) ^1H 5.69 (s, br, 1H, cymene), 5.25 (s, br, 1H, cymene), 4.78 (s, br, 1H, cymene), 4.30 (s, br, 1H, cymene), 2.22 (s, 3H, $C\mathit{H}_3$), 1.14 (d, $^3J_{HH}$ = 6.9 Hz, 6H, CH($C\mathit{H}_3)_2$); $^{31}P\{^1H\}$ 138.7.

General procedure for catalytic experiments. In a screw-capped vial the propargylic alcohol (0.7 mmol) and the carboxylic acid (0.7 mmol) were dissolved in cyclohexane (3 mL). The catalyst (0.012 mmol) was added and the sealed vial immersed in a heating mantle preheated to 90 °C. After 18 h for catalyst **43a** and 5 h for catalyst

43b, the sample was filtered through a short pad of silica gel and the filtrate analyzed by GC-MS. All volatiles were removed from the sample and the residue purified by flash chromatography (alumina, CH_2Cl_2/hexanes, 2:1 v/v) to obtain the products as yellow oils. In some cases, isolation of the products was compromised by difficulties in the visualization of product spots on the TLC (potentially lowering the overall yield).

X-ray Structure Determination for 43a: X-ray quality crystals of **43a** were obtained by slow diffusion of Et_2O into a solution of **43a** in CH_2Cl_2 at –18 °C.

Preliminary examination and X-ray data collection were performed using a Bruker Kappa Apex II single crystal X-Ray diffractometer equipped with an Oxford Cryostream LT device. Intensity data were collected by a combinations of ϖ and ϕ scans. Apex II, SAINT and SADABS software packages (Bruker Analytical X-Ray, Madison, WI, 2006) were used for data collection, integration and correction of systematic errors, respectively.

Crystal data and intensity data collection parameters are listed in Table 1. Structure solution and refinement were carried out using the SHELXTL- PLUS software package.[2] The structure was solved by direct methods and refined successfully in the space group, $P2_12_12_1$. The non-hydrogen atoms were refined anisotropically to convergence. All hydrogen atoms were treated using appropriate riding model (AFIX m3).

CCDC 689545 contains the supplementary crystallographic data for **43a**.

---

[1] (a). Hulst, R.; de Vries, N. K.; Feringa, B. L. *Tetrahedron: Asymmetry*, **1994**, *5*, 699; (b). Duursma, A.; Boiteau, J.-G.; Lefort, L.; Boogers, J. A. F.; de Vries, A. H. M.; de Vries, J. G.; Minnaard, A. J.; Feringa, B. L. *J. Org. Chem*. **2004**, *69*, 8045.

[2] Sheldrick, G. M. *Acta Cryst*. **2008**, *A64*, 112.

Synthesis and reactivity studies of η^5-cyclopentadienyl complexes

3.1. Aim

A mixed phosphine/phosphoramidite ruthenium complex bearing a Cp ligand should present a more stable platform for catalytic activation of propargylic alcohols compared to the complexes bearing a *p*-cymene ligand presented in the previous section. I proposed to synthesize new mixed phosphine/phosphoramidite complexes of ruthenium and test their ability to activate propargylic alcohols. The phosphoramidite ligand would again allow for efficient steric tuning of the complex. Both stoichiometric reactions intended to form stable, isolable allenylidenes as well as catalytic substitutions of propargylic alcohols are investigated.

3.2. Introduction

3.2.1. Ruthenium allenylidene complexes

Arene loss in piano-stool complexes opens multiple coordination sites and makes the complex electron deficient. I have all ready demonstrated in the previous section that complexes of the type [$RuCl_2(\eta^6$-arene)(phosphoramidite)] would easily lose the arene ligand at elevated temperatures or after prolonged times in solution. An allenylidene complex was shown to be formed by displacing a chloride ligand as opposed to the arene, although in the case of a phosphine complex, formation of an allenylidene via *p*-cymene substitution is known (Scheme 3.1).[1,2] In the interest of creating a more stable platform for the potential activation of propargylic alcohols, I envisioned replacing the η^6-*p*-cymene ligand with an η^5-cyclopentadienyl (Cp) ligand. The Cp ligand is anionic and thus should be less likely to dissociate as compared to a neutral η^6-arene ligand.

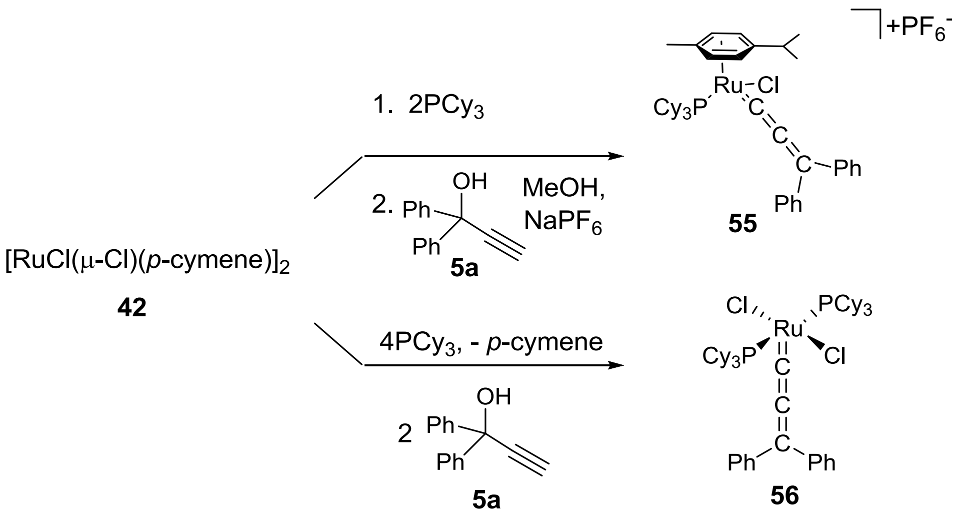

Scheme 3.1. Formation of allenylidenes from a *p*-cymene ruthenium complex.[1,2]

In order to have the new Cp complex be isoelectronic to the η^6-*p*-cymene complex, one of the anionic chloride ligands must be replaced by a neutral two electron donor ligand. The complex [CpRuCl(PPh_3)$_2$] (**68**) is commercially available and thus gives a good starting point for exploration of the activation of propargylic alcohols. Selective substitution of one or both of the PPh_3 ligands is possible at elevated temperatures.[3]

Various phosphine complexes of this type have been shown to be active in reactions with propargylic alcohols involving allenylidene and vinylvinylidene formation.[4] Selegue synthesized a series of vinylvinylidene complexes (**59**) from **58** utilizing strongly electron-donating trimethylphosphine ligands (Scheme 3.2).[4a] The complexes could be deprotonated by NaOMe to give η^1-alkynyl complexes (**60**). Interestingly, PPh_3 could not be used as a ligand in this reaction. An electronic preference for vinylvinylidene formation combined with a steric preference for allenylidene formation (particularly for the larger PPh_3 ligands) is suggested to explain the observed reactivity difference. The cationic fragment $[CpRu(PPh_3)_2]^+$ has been shown to form stable allenylidenes in reactions with propargylic alcohols without α-protons.[4a]

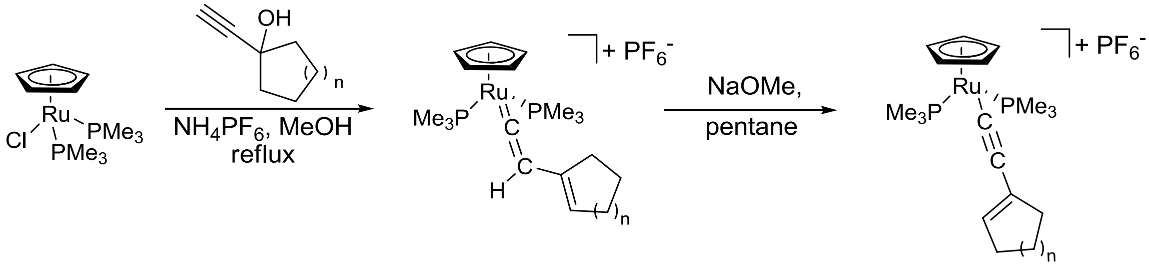
OH
n
NH4PF6, MeOH
reflux
Ru
Cl
PMe3
PMe3
+ PF6-
Ru
Me3P
PMe3
C
C
H
n
NaOMe,
pentane
+ PF6-
Ru
Me3P
PMe3
C
C
n

58 **59** **60**

Scheme 3.2. Formation of a vinylvinylidene complex.[4a]

Allenylidenes formed from cyclopentadienyl phosphine complexes undergo various types of reactions. The allyldiphenylphosphine derivative (**61**) undergoes a [2+2] cycloaddition reaction with the $C_\alpha=C_\beta$ double bond of the allenylidene chain to form the cyclobutylidene complex **62** (Scheme 3.3).[5] Allenylidenes of type **61a** are also known to add neutral nucleophiles such as amines, alcohols or phosphines at C_α to give Fisher type carbene complexes or at C_γ to give η^1-alkynyl complexes.[3] Anionic nucleophiles such as Grignard reagents typically add to C_γ (Scheme 3.4).[6]

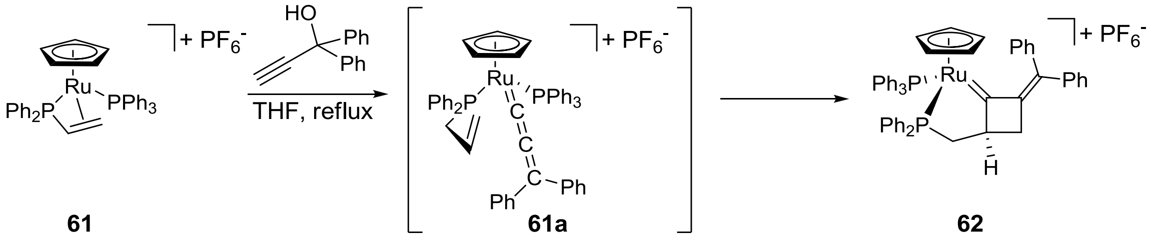
+ PF6-
Ru
Ph2P
PPh3
HO
Ph
Ph
THF, reflux
+ PF6-
Ru
Ph2P
PPh3
C
C
C
Ph
Ph
+ PF6-
Ph
Ph3P
Ru
Ph
Ph2P
H

61 **61a** **62**

Scheme 3.3. Formation of a cyclobutylidene complex.[5]

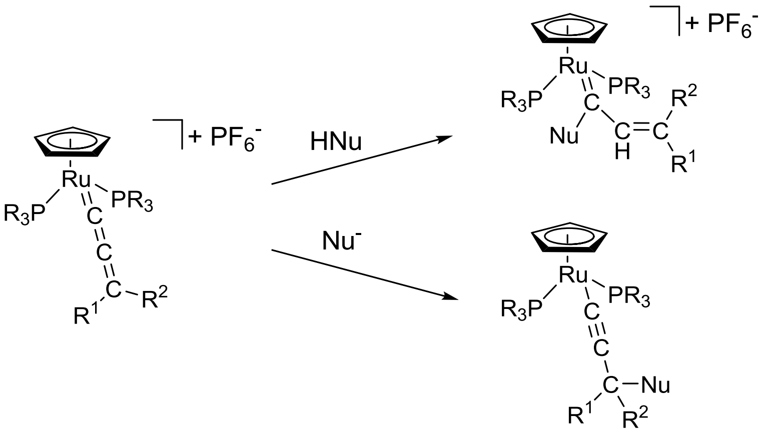

+ PF$_6^-$
HNu
Nu$^-$
Ru
R$_3$P
PR$_3$
C
R^1
R^2
Nu
H

Scheme 3.4. Nucleophilic attack on allenylidene complexes.[3,6]

Electron-rich allenylidenes are considerably more stable to nucleophilic attack than relatively electron-poor ones.[7] Instead, these allenylidenes can be protonated by strong acids such as HBF_4 to give alkenylcarbyne complexes. Alkenylcarbyne complexes such as **66** are shown to react with weak aprotic nucleophiles to give vinylidene complexes (Scheme 3.5). The precursor allenylidenes do not react with the same nucleophiles under similar conditions. This mode of reactivity represents an alternative path for a potential catalytic cycle involving allenylidene intermediates. Currently, the most widely accepted mechanism of propargylic substitution reactions involves direct nucleophilic attack of the allenylidene at C_γ.[8]

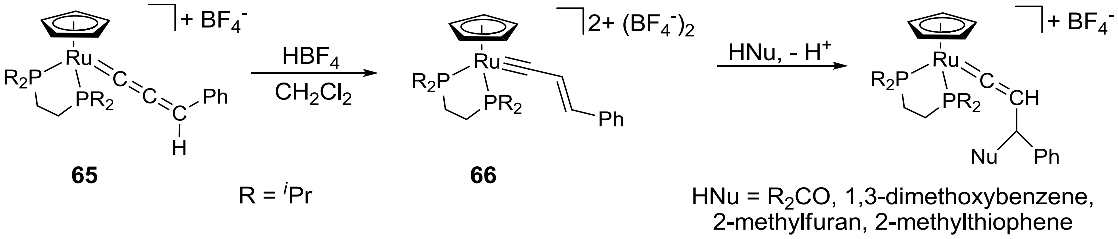

+ BF$_4^-$
HBF$_4$
CH$_2$Cl$_2$
2+ (BF$_4^-$)$_2$
HNu, - H$^+$
+ BF$_4^-$
Ru
R$_2$P
PR$_2$
Ph
H
CH
Nu
65
66
R = ^{i}Pr
HNu = R$_2$CO, 1,3-dimethoxybenzene, 2-methylfuran, 2-methylthiophene

Scheme 3.5. Protonation of an allenylidene complex.[7]

3.3. Results

3.3.1. Synthesis of novel mixed phosphine/phosphoramidite complexes

The ligand **41a** (Scheme 3.6) was used for the initial reaction because it was the easiest to access. At reflux in $CHCl_3$, selective substitution of one of the PPh_3 ligands of $[CpRuCl(PPh_3)_2]$ (**68**) occurs to give the mixed phosphine/phosphoramidite complex $[CpRuCl(PPh_3)($**41a**$)]$ (**69a**) in 64% yield as a 5:3 mixture of diastereomers (Scheme 3.6). A new stereocenter is formed at the metal center during the reaction, and thus is the origin of the two diastereomers in the product. The complex is purified by flash chromatography, giving the product in the same 5:3 mixture of diastereomers. Attempts to yield a single diastereomer by fractional recrystallization failed.

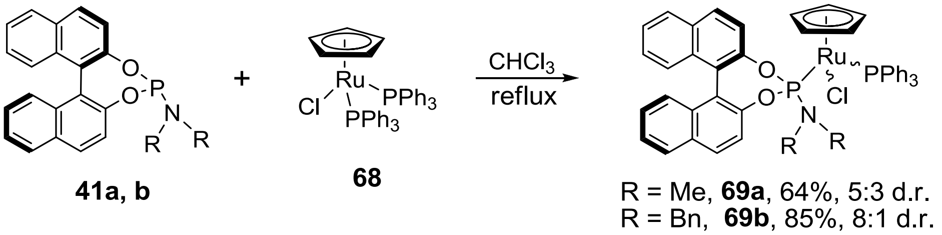

Scheme 3.6. Synthesis of new mixed phosphine/phosphoramidite complexes.

The effect of sterics on the diastereoselectivity was examined by changing the substituents on the nitrogen from the small methyl groups to the significantly larger benzyl substituents. The phosphoramidite ligand **41b**[9] bearing the *N*,*N*-dibenzyl substituent was reacted with complex **68** in $CHCl_3$ at reflux for 16 h. The product $[CpRuCl(PPh_3)($**41b**$)]$ (**69b**) was formed in an 8:1 mixture of diastereomers as determined by ^1H NMR spectroscopy of the crude product. After purification by flash chromatography, the major diastereomer could be isolated in a 74% yield by fractional crystallization from CH_2Cl_2/MeOH (Scheme 3.7).

For comparison purposes, the known ligand **45b**[10] with a partially hydrogenated backbone was also used in complex synthesis. The complex **70** was isolated in 59% yield after column chromatography in an 8:1 diastereomeric ratio, the same ratio as complex **69b** bearing the *N*,*N*-dibenzyl substituent. Fractional recrystallization yields the major diastereomer of **70** in 46% yield.

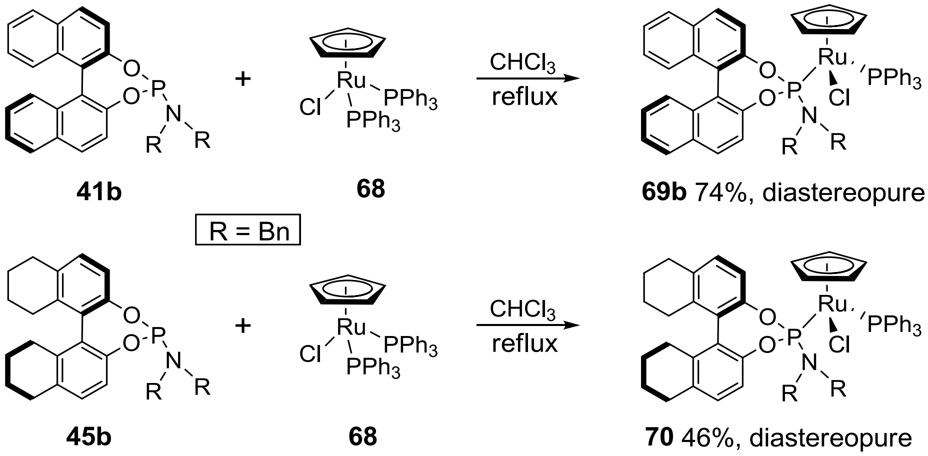

Scheme 3.7. Synthesis of diastereopure Cp ruthenium complexes.

All of the new complexes are fully characterized by NMR (^{1}H, ^{31}P, ^{13}C), IR HRMS and microanalysis. Coordination of the incoming ligand is best revealed by a downfield shift of the phosphoramidite signals in the ^{31}P NMR spectra. The free ligands show signals between 150 and 140 ppm in the ^{31}P NMR spectra while the complexes exhibit signals between 178 and 164 ppm. The signals are all doublets showing $^2J_{PP}$ couplings between 148 and 168 Hz. The PPh_3 ligands gave resonances in the range 48-45 ppm. In the ^{1}H NMR spectrum, the Cp signals appear between 4.7 and 4.5 ppm. For complexes **69b** and **70** the benzylic protons (α to the N atom) are rendered diastereotopic, giving four doublets between 4.9 and 3.3 ppm. IR spectra and HRMS are also in accordance with the assigned structures.

The structures of **69b** and **70** were unequivocally established by single-crystal X-ray crystallography (Figure 3.1). Selected bond lengths and angles are shown in Table 3.1. For comparison, data for [CpRuCl(PPh_3)$_2$] (**68**) was also added.[11] The angles about ruthenium range from 87.37 ° for Cl(1)-Ru-P(1) to 99.11 ° for P(1)-Ru-P(2), where P(1) is the phosphine and P(2) is the phosphoramidite. The angles are slightly perturbed from those observed in complex **68**, particulary the P(1)-R-P(2) bond angle, which is significantly smaller than that of **68** (103.99(4) °). Thus the geometry can be best described as octahedral with small distortions. The Ru-PPh_3 bond lengths are similar to those observed for **68** (2.34 Å), slightly longer than the corresponding Ru-P(2) distances for the phosphoramidite ligands (2.3294(8) and 2.3231(16) Å compared to 2.2426(8) and 2.2404(14) Å). The relative strength of these bonds may be due to increased backbonding for the phosphoramidite ligand compared to PPh_3, shortening the Ru-P bond length. The absolute configuration about the metal center is the same for both complexes.

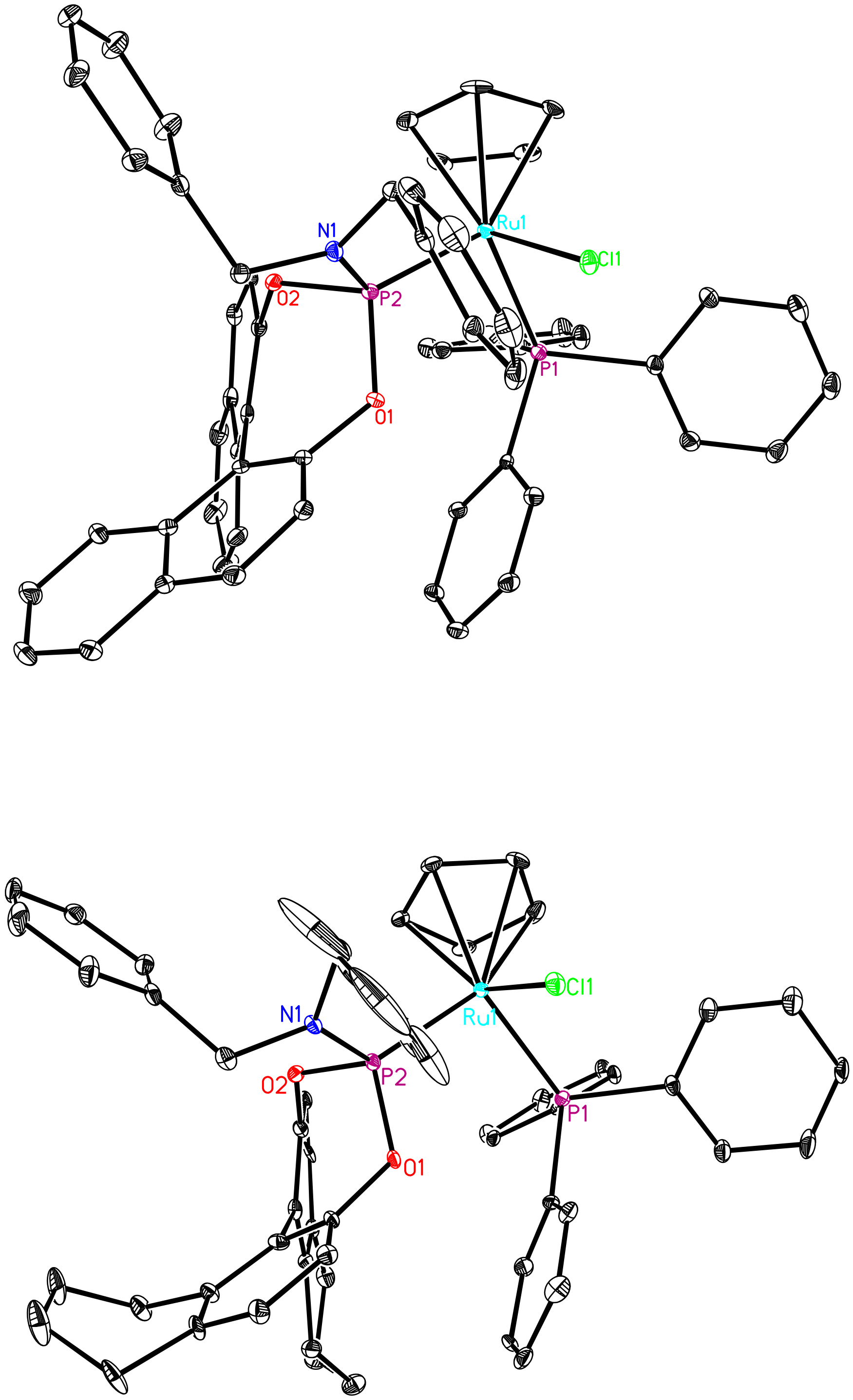

Ru1
N1
Cl1
O2
P2
P1
O1
Cl1
N1
Ru1
O2
P2
P1
O1

Figure 3.1. X-ray structures of **69b** (top) and **70** (bottom).

Table 3.1. Selected bond lengths and angles for complexes **69b** and **70**.[11]

Entry	Bond(s)	[CpRuCl (PPh_3)$_2$] (**68**)	[CpRuCl(PPh_3) (**41b**)] (**69b**)	[CpRuCl(PPh_3) (**45b**)] (**70**)
Bond Lengths (Å)[a]				
1	Ru-P(1)	2.337(1)	2.3294(8)	2.3231(16)
2	Ru-P(2)	2.335(1)	2.2426(8)	2.2404(14)
3	Ru-Cl	2.453(2)	2.4302(7)	2.4415(16)
Bond Angles (°)				
4	P(1)-Ru-P(2)	103.99(4)	99.11(3)	97.88(6)
5	Cl-Ru-P(1)	89.05(3)	87.37(3)	88.05(6)
6	Cl-Ru-P(2)	90.41(4)	92.28(3)	93.85(6)

[a] P(2) is the phosphoramidite ligand, P(1) is PPh_3, where appropriate.

3.4. Discussion

3.4.1. Stability tests

The new Cp complexes are designed to impart a greater degree of structural stability in comparison with the complexes bearing η^6-arene ligands, the hypothesis being that the anionic Cp ligand is less likely to dissociate than the corresponding neutral η^6-arene ligands. Thus, after forming the new complexes [CpRuCl(PPh_3)(L)] (L is a phosphoramidite ligand), I sought to determine their thermal stability, particularly in reference to the metal stereocenter and ligand dissociation reactions. Complex **69b** was dissolved in $CDCl_3$ and heated to 45 ^oC (care was not taken to exclude moisture or air) and the sample was analyzed by NMR (^1H, ^{31}P) after 2.5 h, 6 h and 60 h. Under these conditions some decomposition (<20%) does occur, with new signals appearing in the ^{31}P NMR spectrum corresponding to the oxidation products of the ligands (29.5 ppm for $O=PPh_3$ and 14.5 ppm for the oxide of **41b**), but the majority of the starting material remains and no signals corresponding to a second diastereomer could be found. The new oxide peaks are formed in a 1:1 ratio (assessed by ^{31}P NMR), suggesting that there is no preference for oxidation of one of the ligands selectively. No evidence for the dissociation of Cp is seen in the ^{1}H or ^{31}P NMR spectra. Similar data are obtained at 90 ^{o}C, although at this temperature the decomposition reaction is much faster, giving complete oxidation in only 6 h.

The possibility of substituting both PPh_3 ligands for phosphoramidites is also of interest as it would alleviate the necessity of separating diastereomers. When complex **68** was heated to reflux in $CDCl_3$ in the presence of 2.5 equivalents of ligand **41b**, both monosubstitution and disubstitution products were observed after 24 h. The doubly substituted product gave two very broad signals in the ^{31}P NMR spectrum at 179.9 and 171.5 ppm (the two ligands are diastereotopic), possibly due to dynamic processes on the NMR time scale. FAB MS analysis of the crude mixture also showed molecular ions for both the mono- and disubstituted products. The bis(phosphoramidite) complex was not isolated.

3.4.2. Allenylidene formation

After determining that the new complexes were likely configurationally stable and not especially prone to decomposition, I sought to determine whether stable allenylidenes could be formed as well. Reacting compound **69b** under Selegue's conditions[4a] with slight modifications ($NaPF_6$, MeOH, rt) only modest conversion was observed after 24 h (< 40%, ^{1}H NMR), possibly due to the low solubility of the compound in the reaction medium. Warming the mixture to 40 ^{o}C and/or significantly increasing the reaction time (up to 6 days) did not greatly improve the results. After prolonged reaction times (6 days), the mixture also showed two new sets of doublets in approximately a 1:1 ratio (167.9, 49.1 ppm and 165.8, 46.9 ppm) in the ^{31}P NMR spectrum. These new doublets likely represent the two possible diastereomers of the expected allenylidene product. The presence of the intended product was able to be confirmed by FAB MS (M^+ at 1130) and IR via the diagnostic allenylidene $Ru=C=C=CR_2$ stretch at 1934 cm^{-1}.[7]

The lack of cosolubility of the complex (**69b**) and the activator ($NaPF_6$) prompted me to use a solvent mixture (Scheme 3.8). Complex **69b** was dissolved in freshly distilled THF to which a solution of $NaPF_6$ in MeOH was added. The propargylic alcohol was then added to the homogeneous yellow solution. The solution gradually darkened, becoming an intense purple. Removal of the solvent followed by ^1H and ^{31}P NMR analysis revealed only ca. 50% conversion after a 24 h period. Complex **69a** also reacts under similar conditions to give a purple compound. However, even after extended reaction times at 40 ^oC (> 24 h) the conversion does not exceed 50% and significant side product formation is evident. Under identical reaction conditions, compound **70** does not give allenylidene formation.

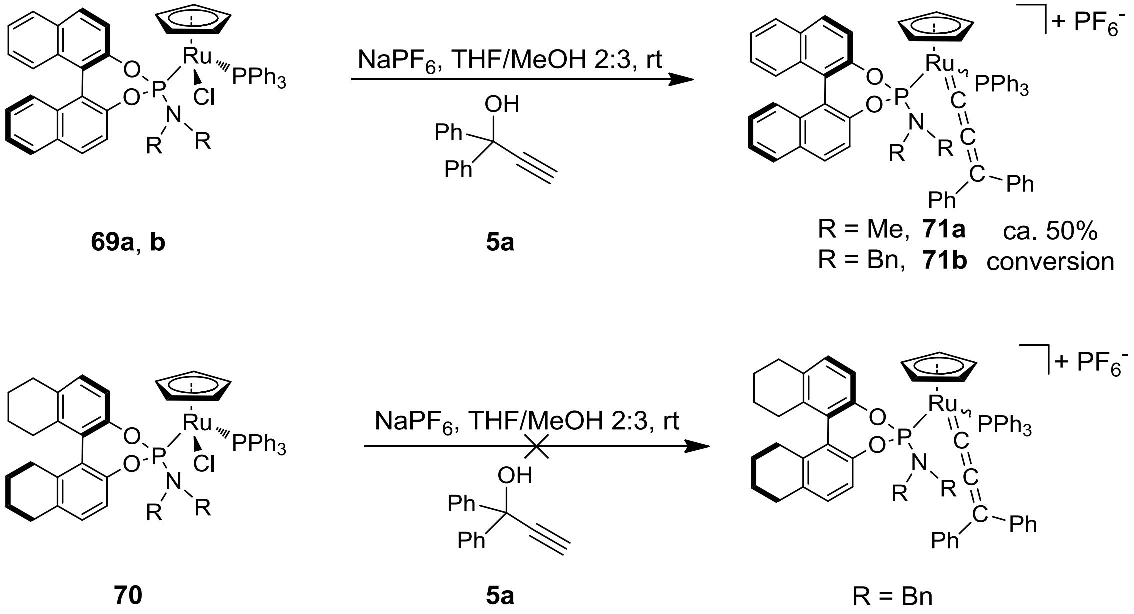

Scheme 3.8. Synthesis of allenylidene complexes.

Allenylidene formation appears to be possible, although the mild activation conditions are causing a very slow reaction rate and there are competing side reactions. More forcing conditions can allow for complete activation (via chloride abstraction) and potentially give a cleaner reaction. Activation of the complex via a dissociative mechanism wherein the chloride ligand is first removed creates a Lewis acidic complex capable of coordinating a propargylic alcohol via the alkyne. In the case of complexes **69**, the use of a more reactive chloride abstracting agent such as $AgPF_6$ is necessary to facilitate the dissociation step. Addition of $AgPF_6$ to a solution of **69b** in CH_2Cl_2 resulted in the formation of a precipitate (AgCl) and a darkening of the solution from yellow to a dark orange color. After removing the AgCl by filtration, the propargylic alcohol 1,1-diphenyl-2-propyn-1-ol (**5a**) was added and the solution immediately turned an intense purple color. After a 4 h reaction time the solvent was removed in vacuo and the crude sample was analyzed by NMR (^{1}H, ^{31}P and ^{13}C). Complete consumption of **69b** was observed and the allenylidene **71b** was the major product (Scheme 3.9). The diastereoselectivity of allenylidene formation is independent of the configuration of the metal center of **69b** as the product (**71b**) is formed in an 8:1 ratio of diastereomers regardless of whether **69b** was used as a single diastereomer or as an 8:1 d.r. Dynamic processes in the chloride abstracted species **72** are a likely explanation of the observed diastereoselectivity (Scheme 3.10).

The ^{31}P NMR again reveals doublets at 167.9 and 49.1 ppm, 165.8 and 46.9 ppm with $^{2}J_{PP}$ coupling constants of 39 Hz and 49 Hz respectively. In this case, however, the major product (167.9, 49.1 ppm) is considerably larger than the minor one. The methylene protons of the benzyl substituents are diastereotopic (as in the starting complex **69b**), giving multiplets in the ^{1}H NMR between 4.4 and 3.2 ppm. In the ^{13}C NMR the diagnostic peaks of the allenylidene can be seen at 293 (C_α), 199 (C_β) and 163 ppm (C_γ).[8] The FAB MS shows a molecular ion peak at 1130 amu corresponding to the cationic portion of **71b** and the IR spectrum again shows the allenylidene ($Ru=C=C=CR_2$) stretch at 1934 cm^{-1} in accordance with the assigned structure.

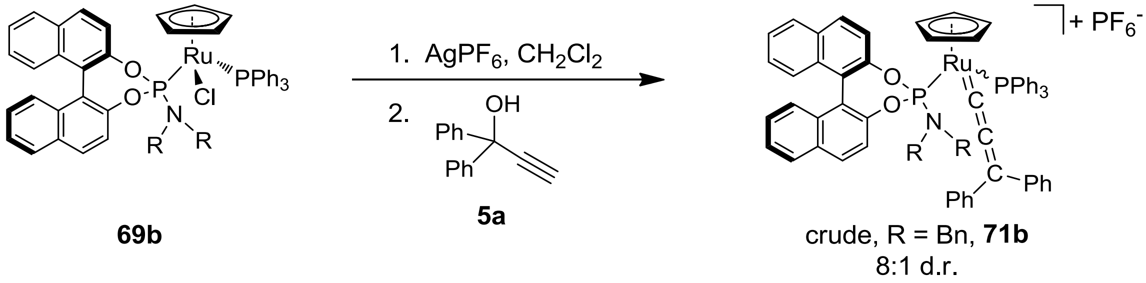

Scheme 3.9. Synthesis of a Cp allenylidene complex via activation with $AgPF_6$

When **69a** bearing the *N*,*N*-dimethyl substituent in place of the *N*,*N*-dibenzyl substituent was subjected to similar activation conditions ($AgPF_6$ in CH_2Cl_2), the solution turned green instead of the expected dark orange color. Addition of the propargylic alcohol after filtration then caused the solution to turn a red-brown color. NMR analysis of this mixture revealed a number of unidentifiable products with no indication of formation of the desired allenylidene **71a**.

The importance of the benzyl substituents on the phosphoramidite ligands may be attributed to their potential to stabilize an electron-deficient intermediate. This type of secondary interaction has been shown previously and is hypothesized as a cause of the increased activity of the catalyst in the reaction outlined in Chapter 2.[12] By this reasoning, complex **70** bearing the *N*,*N*-dibenzyl substituent on the phosphoramidite ligand would be expected to show similar reactivity to that of **69b**. Upon activation of **70** with $AgPF_6$ in CH_2Cl_2, the solution again turns dark orange and forms a precipitate (Scheme 3.10). After filtration of the formed AgCl, the propargylic alcohol (**5a**) was added and the solution turned dark purple. NMR analysis revealed a complex mixture containing many different compounds. Somehow the partially hydrogenated backbone of this ligand causes an unpredictable reaction pattern or cannot stabilize the reactive intermediate.

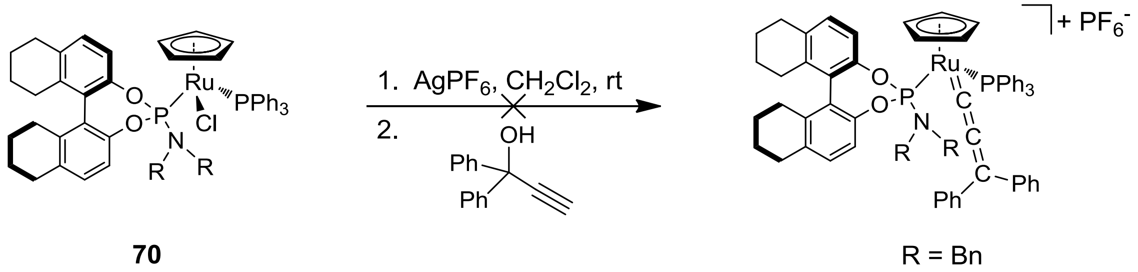

Scheme 3.10. Attempted allenylidene formation from complex **70**.

With the nature of the intermediate formed by chloride abstraction remaining unknown, the role of the *N,N*-dibenzyl substituent in the reactivity of the complexes cannot be determined. The next step then was to analyze the intermediate as to clues that might better explain its behavior. After chloride abstraction from **69b** with $AgPF_6$ in $CDCl_3$ or CD_2Cl_2 (Scheme 3.10), the ^{31}P NMR shows two new broad doublets at 186 and 47 ppm ($^2J_{PP}$ = 62 Hz). The ^1H NMR also reveals very broad signals suggesting dynamic processes occurring on the NMR time scale. A FAB MS reveals complete consumption of starting material, showing no molecular ion peak for **69b** but showing instead a peak for $[CpRu(PPh_3)($**41b**$)]^+$ (**72**) (Scheme 3.11).

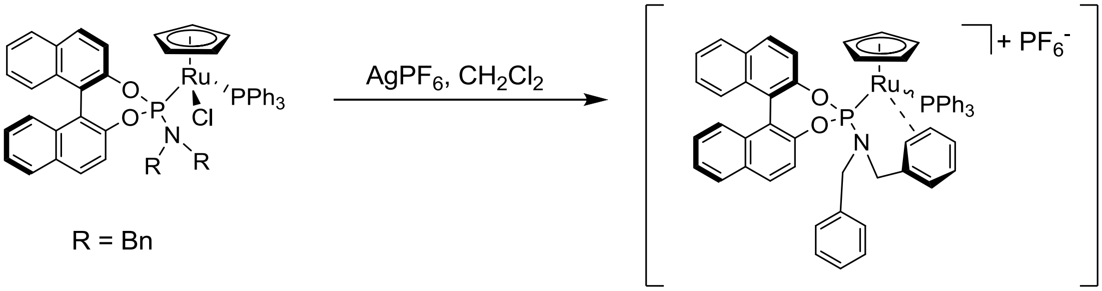

69b **72**

Scheme 3.11. Formation of a reactive intermediate by chloride abstraction.

Allenylidene formation utilizing $AgPF_6$ as activator (Scheme 3.9) sometimes gave inconsistent results, likely due to changes in humidity or photodecomposition of the activator (all chloride abstraction experiments were done in the absence of light). As such, other activators were tested in this reaction. Chloride removal from **69b** was tested with $TlPF_6$[13] in CH_2Cl_2 and THF and was found to be inefficient as complete activation was never observed. $(Et_3O)PF_6$[14] in CH_2Cl_2 works well as an activator and can be used in allenylidene formation as well. However, the allenylidene complex **71b** was never able to be isolated after repeated attempts at recrystallization. The high level of solubility of the complex in a variety of organic solvents makes precipitation of the complex difficult and ultimately led to the failure of the recrystallization attempts.

3.4.3. Catalytic activation of propargylic alcohols

The complex **69b** is clearly able to activate propargylic alcohols via formation of allenylidenes in stoichiometric reactions. Because the allenylidene could not be isolated, I then tested the ability of the complex to activate propargylic alcohols catalytically. Nucleophiles such as alcohols, amines, thiols and β-dicarbonyls were tested in reactions with 2-phenyl-3-butyn-2-ol (**5b**) and 1,1-diphenyl-2-propyn-1-ol (**5a**). In all cases the propargylic alcohol is first mixed with a solution of the activated catalyst in CH_2Cl_2

($AgPF_6$ or $(Et_3O)PF_6$ was used as activator). The nucleophile is then added and the solutions are stirred at room temperature overnight. No reaction is observed regardless of the propargylic alcohol or nucleophile that is used. A likely explanation is that the catalytic cycle is interrupted by formation of a stable intermediate. This could be the allenylidene itself or it could also be an intermediate formed by attack of the nucleophile on the allenylidene (Scheme 3.12).

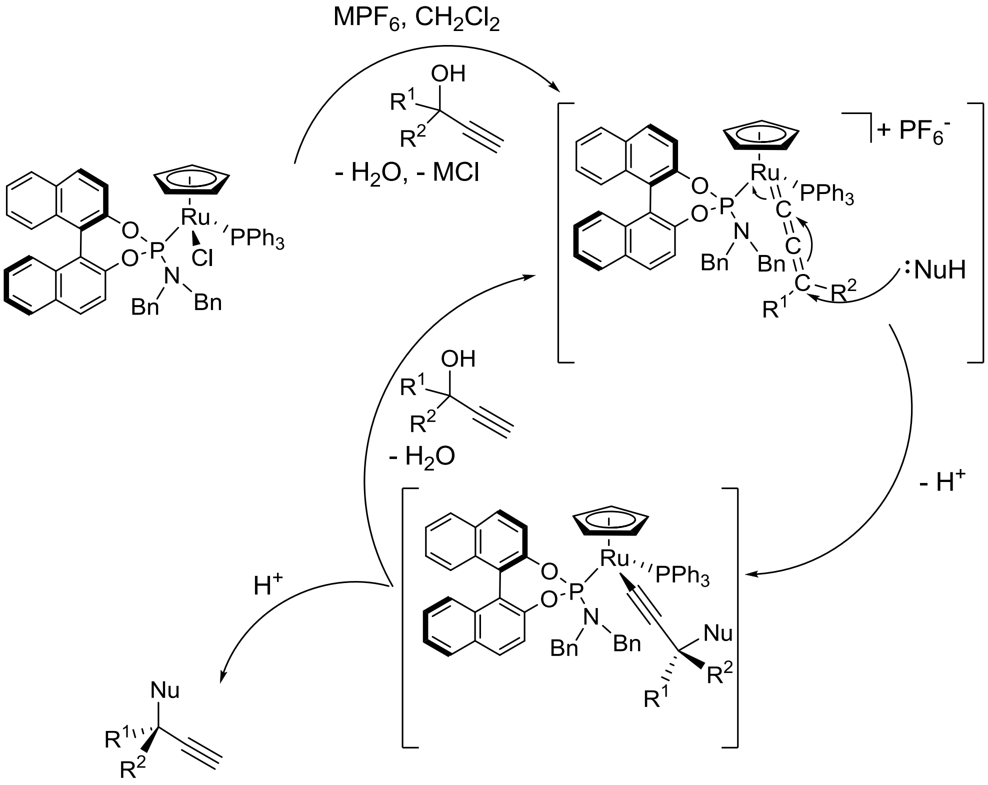

Scheme 3.12. A potential catalytic cycle for propargylic substitution.

3.4.4. Catalytic C-C bond formation

Due to the fact that complex **69b** is inactive in catalytic reactions of propargylic alcohols, I hypothesized that it could instead be used as a chiral platform for Lewis acid catalysis. Reactions to create new C-C bonds are especially important in organic chemistry and the Mukaiyama aldol reaction is of particular interest. The Mukaiyama aldol reaction is known to be catalyzed by a variety of Lewis acids, and asymmetric versions of the reaction are also known.[15]

The catalyst (**69b**) was preactivated using $(Et_3O)PF_6$ in CH_2Cl_2 then added to a solution of 1-*t*-butyldimethylsilyloxy-1-methoxyethene (**73**) and the corresponding aromatic aldehyde/ketone in CH_2Cl_2 (Table 3.2). After 24 h the solutions were analyzed by GC/MS and the resulting chromatograms revealed some starting aldehyde/ketone (**74**) and a significant product peak. Complete consumption of **73** was confirmed by NMR. The resulting β-silyloxy esters **75** were isolated by flash chromatography in 31-53% yield.

Table 3.2. Catalytic results of the Mukaiyama aldol reaction.

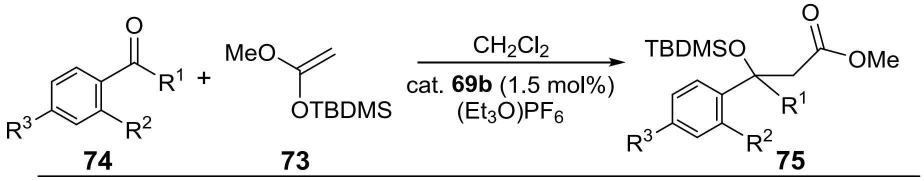

Entry [a]	Substrate	Product	Yield [b]	ee
1	R^1=R^2=R^3=H	R^1=R^2=R^3=H, R^4=$OSiMe_2{}^tBu$	53%	3% [c]
2	R^1=CH_3, R^2=R^3=H	R^1=CH_3, R^2=R^3=H, R^4=$OSiMe_2{}^tBu$	48%	5% [d]
3	R^1=R^2=H R^3=OMe	R^1=R^2=H, R^3=OMe, R^4=$OSiMe_2{}^tBu$	50%	-[e]
4	R^1=R^3=H R^2=Cl	R^1=R^3=H, R^2=Cl, R^4=H	31%	2% [c]

[a] Conditions: Catalyst **69b** (0.007 mmol) was preactivated with $(Et_3O)PF_6$ in CH_2Cl_2 and after 2 h added to the substrates **73** and **74** (0.472 mmol each). The resulting solution was maintained at room temperature for 24 h.
[b] Isolated yield after chromatography. [c] Determined by chiral GC.
[d] Determined by ^1H NMR with a chiral shift reagent. [e] Determination of the enantiomeric excess was not possible.

Virtually no enantiomeric excesses (ee's) were found for the products as determined by chiral GC or ^1H NMR with a chiral shift reagent. There are several possible reasons that stereoinduction is not possible in this reaction. The structural motif itself may not allow for stereodifferentiation, leaving attack of the substrate from both sides equally likely. Another possibility to consider is the relative effect of the two stereocenters on the molecule. Stereodifferentiation based on catalysts with multiple stereocenters can vary by the relative configuration of the stereocenters.[16] Specifically, the absolute configuration at one stereocenter can have significantly greater impact on the stereochemical outcome of the reaction relative to the effect of the other stereocenter. In cases where the absolute configuration at two stereocenters both have significant impact, the relative stereochemistry can have a cooperative or inhibitive effect, potentially resulting in very high or very low ee's, respectively.

Preactivation of catalyst **69b** creates a reactive intermediate **72** (Scheme 3.11). As discussed previously, this intermediate shows evidence of dynamic behavior in the ^{1}H and ^{31}P NMR spectra. It is likely that this intermediate is not configurationally stable at the metal center, although formation of allenylidene **71b** has been shown to occur with a high diastereomeric excess (8:1 d.r., Scheme 3.9). Thus coordination of the carbonyl may occur at one of two potential open coordination sites, leading to two different diastereomers. If the diastereomers are not dissimilar in energy the formation of both could lead to a loss of stereodifferentiation in the attack of the incoming nucleophile.

3.5. Summary and Prospective

A set of new mixed phosphine/phosphoramidite complexes has been synthesized and fully characterized. The substituents on the N atom of the phosphoramidite ligand have a profound impact on the diastereoselectivity of the metal complex formation. In the case of the ligands bearing the *N*,*N*-dibenzyl substituent the complexes are formed in an 8:1 diastereomeric ratio. Complexes **69a**, **b** were shown to form stable allenylidenes that were able to be characterized by NMR (^{1}H, ^{31}P, ^{13}C), IR and FAB MS. Activation under mild conditions ($NaPF_6$ in MeOH/THF 2:3, room temperature) is possible but low conversions are observed. In the case of complex **69b**, stronger activation conditions could be utilized ($AgPF_6$ or $(Et_3O)PF_6$ in CH_2Cl_2) and in these cases complete conversion is observed, giving primarily the expected product **71b**.

The precatalyst **69b** can be activated using $AgPF_6$ or $(Et_3O)PF_6$ and the resulting species **72** is catalytically active in the Mukaiyama-aldol reaction between 1-*t*-butyl-dimethylsilyloxy-1-methoxyethene and various aromatic aldehydes and ketones. The product β-silyloxy esters were obtained in moderate yields but virtually no ee's were obtained as analyzed by chiral GC and ^{1}H NMR. Configurational instability at the metal stereocenter of the active catalyst may be the cause as dynamic processes are evident in the ^{1}H NMR of this species.

---

[1] Semeril, D.; Bruneau, C.; Dixneuf, P. H. *Organometallics* **2003**, *22*, 4459.

[2] Schanz, H.-J.; Jafarpour, L.; Stevens, E. D.; Nolan, S. P. *Organometallics* **1999**, *18*, 5187.

[3] Pavik, S.; Mereiter, K.; Puchberger, M.; Kirchner, K. *Organometallics* **2005**, *24*, 3561.

[4] (a). Selegue, J. P.; Young, B. A.; Logan, S. L. *Organometallics* **1991**, *10*, 1972; (b). Chang, S.-H.; Tsai, W.-R.; Ma, H.-, W.; Lin, Y.-C.; Huang, S.-L.; Liu, Y.-H.; Wang, Y. *Organometallics* **2009**, *28*, 1863; (c). Lui, M-C.; Chung, C.-P.; Chang, W.-C.; Lin, Y.-C.; Wang, Y.; Liu, Y.-H. *Organometallics* **2009**, *28*, 5204.

[5] Díez, J.; Gamasa, M. P.; Gimeno, J.; Lastra, E.; Villar, A. *Organometallics* **2005**, *24*, 1410.

[6] Cadierno, V.; Gamasa, M. P.; Gimeno, J.; Gonzalez,-Bernardo, C. *J. Organomet. Chem*. **1994**, *474*, C27.

[7] (a). Bustelo, E.; Jiménez-Tenorio, M.; Puerta, M. C.; Valerga, P. *Organometallics* **2006**, *25*, 4019; (b). Bustelo, E.; Jiménez-Tenorio, M.; Puerta, M. C.; Valerga, P. *Organometallics* **2007**,

---

26, 4300; (c). Pino-Chamorro, J. A.; Bustelo, E.; Puerta, M. C.; Valerga, P. *Organometallics* **2009**, *28*, 1546.

[8] (a). Nishibayashi, Y.; Imajima, H.; Onodera, G.; Uemura, S. *Organometallics* **2005**, *24*, 4106; (b). Inada, Y.; Nishibayashi, Y.; Uemura, S. *Angew. Chem. Int. Ed.* **2005**, *44*, 7715; (c). Matsuzawa, H.; Miyake, Y.; Nishibayashi, Y. *Angew. Chem. Int. Ed.* **2007**, *46*, 6488; (d). Matsuzawa, H.; Kanao, K.; Miyake, Y.; Nishibayashi, Y. *Org. Lett.* **2007**, *26*, 5561; (e). Daini, M.; Yoshikawa, M.; Inada, Y.; Uemura, S.; Sakata, K.; Kanao, K.; Miyake, Y.; Nishibayashi, Y. *Organometallics* **2008**, *27*, 2046; (f). Yada, Y.; Miyake, Y.; Nishibayashi, Y. *Organometallics* **2008**, *27*, 3614; (g). Fukamizu, K.; Miyahe, Y.; Nishibayashi, Y. *J. Am. Chem. Soc.* **2008**, *130*, 10498; (h). Yamauchi, Y.; Miyake, Y.; Nishibayashi, Y. *Organometallics* **2009**, *28*, 48; (i). Tanabe, Y.; Kanao, K.; Miyake, Y.; Nishibayashi, Y. *Organometallics* **2009**, *28*, 1138; (j). Kanao, K.; Miyake, Y.; Nishibayashi, Y. *Organometallics* **2009**, *28*, 2920; (k). Inada, Y.; Nishibayashi, Y.; Hidai, M.; Uemura, S. *J. Am. Chem. Soc.* **2002**, *124*, 15172.

[9] Hulst, R.; de Vries, N. K.; Feringa, B. L. *Tetrahedron: Asymmetry* **1994**, *5*, 699.

[10] Costin, S.; Rath, N. P.; Bauer, E. B. *Adv. Synth. Catal.* **2008**, *350*, 2414.

[11] Bruce, M. I.; Wong, F. S.; Skelton, B. W.; White, A. H. *J. Chem. Soc. Dalton Trans.* **1981**, 1398.

[12] (a). Huber, D.; Kumar, P. G. A.; Pregosin, P. S.; Mezzetti, A. *Organometallics* **2005**, *24*, 5221; (b). Mikhel, I. S.; Rüegger, H.; Butti, P.; Camponovo, F.; Huber, D.; Mezzetti, A. *Organometallics* **2008**, *27*, 2937.

[13] Forniés, J.; Fortuño, C.; Ibáñez, S.; Martín, A. *Inorg. Chem.* **2008**, *47*, 5978.

[14] Santoro, F.; Althaus, M.; Bonaccorsi, C.; Gischig, S.; Mezzetti, A. *Organometallics* **2008**, *27*, 3866.

[15] Carreira, E. M. *Comprehensive Asymmetric Catalysis I-III*, **1999**, *3*, 997.

[16] Doyle, M. P.; Morgan, J. P.; Fettinger, J. C.; Zavalij, P. Y.; Colyer, J. T.; Timmons, D. J.; Carducci, M. D. *J. Org. Chem.* **2005**, *70*, 5291.

Experimental Section

General. Chemicals were treated as follows: THF, toluene, diethyl ether (Et_2O), distilled from Na/benzophenone; CH_2Cl_2, MeOH, distilled from CaH_2. (R)-1,1'-binaphthyl-2,2'-diol ((R)-BINOL) (Strem), phosphorus trichloride (PCl_3), *N*-methyl-2-pyrrolidinone (NMP) (Acros), 1,1-diphenyl-2-propyn-1-ol (**5a**) (Aldrich), $AgPF_6$ (Aldrich), $(Et_3O)PF_6$ (Aldrich), $[CpRuCl(PPh_3)_2]$ (**68**, Cp = cyclopentadienyl anion, Strem) and other materials used as received. "(R)-BINOL-*N,N*-dimethyl-phosphoramidite" **41a**,[1a] and "(R)-BINOL-*N,N*-dibenzyl-phosphoramidite" **41b**[1b] were synthesized according to literature procedures.

NMR spectra were obtained at room temperature on a Bruker Avance 300 MHz or a Varian Unity Plus 300 MHz instrument and referenced to a residual solvent signal; all assignments are tentative. Exact masses were obtained on a JEOL MStation [JMS-700] Mass Spectrometer. Melting points are uncorrected and were taken on an Electrothermal 9100 instrument. IR spectra were recorded on a Thermo Nicolet 360 FT-IR spectrometer. Elemental Analyses were performed by Atlantic Microlab Inc., Norcross, GA, USA.

"[CpRuCl(PPh$_3$)((R)-BINOL-*N,N*-dimethylphosphoramidite)]" (69a). To a Schlenk flask containing phosphoramidite **41a** (0.400 g, 1.11 mmol) and $[CpRu(PPh_3)_2Cl]$ (**68**) (0.735 g, 1.01 mmol), $CHCl_3$ (15 mL) was added and the solids dissolved. The orange solution was then heated to reflux for 8 h. Upon cooling, the solvent was removed under vacuum, giving an orange solid. The solid was purified by flash chromatography (2.5 × 17 cm Florisil®, CH_2Cl_2/Et_2O 49:1 v/v) to obtain **69a** as a yellow solid as mixture of diastereomers (5:3, ^1H NMR) (0.535 g, 0.650 mmol, 64%), m.p. 202–203 °C dec. (capillary). Anal. Calcd. for $C_{45}H_{38}ClNO_2P_2Ru$: C, 65.65; H, 4.65. Found: C, 65.27; H, 4.77%.

NMR (δ, $CDCl_3$) ^1H 7.86 (d, $^3J_{HH}$ = 8.6 Hz, 2H, binaphthyl), 7.82 (d, $^3J_{HH}$ = 4.5 Hz, 0.6H, binaphthyl*), 7.80 (d, $^3J_{HH}$ = 3.5 Hz, 1H, binaphthyl), 7.77 (d, $^3J_{HH}$ = 2.9 Hz, 1H, binaphthyl), 7.06 (d, $^3J_{HH}$ = 8.2 Hz, 0.6H, binaphthyl*) 7.63–7.53 (m, 3H, aromatic), 7.40–7.35 (m, 4H, aromatic), 7.34–7.21 (m, 10H, aromatic), 7.19–7.08 (m, 10H, aromatic), 7.06 (d, $^3J_{HH}$ = 1.7 Hz, 1.6H, aromatic), 7.03 (d, $^3J_{HH}$ = 1.6 Hz, 1.6H, aromatic), 7.02–6.95 (m, 7H, aromatic), 4.48 (s, 5H, Cp), 4.39 (s, 3H, Cp*), 2.42 (s, 3H, CH_3), 2.39 (s, 3H, CH_3), 2.30 (s, 1.8H, CH_3*), 2.27 (s, 1.8H, CH_3*); $^{13}C\{^1H\}$ (partial) 82.9 (s, Cp), 81.9 (s, Cp*), 39.04 (s, CH_3), 38.96 (s, CH_3), 38.4 (s, CH_3*), 38.3 (s, CH_3*); $^{31}P\{^1H\}$ 177.8 (d, $^2J_{PP}$ = 68.0 Hz, phosphoramidite) 176.0 (d, $^2J_{PP}$ = 64.8 Hz, phosphoramidite*), 48.7 (d, $^2J_{PP}$ = 68.0 Hz, PPh_3), 46.9 (d, $^2J_{PP}$ = 64.8 Hz, PPh_3*).

HRMS calcd for $C_{45}H_{38}{}^{35}ClNO_2P_2{}^{102}Ru$ 823.1109, found 823.1094. MS (FAB): 823 (**69a**$^+$, 95%), 788 ([**69a**–Cl]$^+$, 60%), 526 ([**69a**–PPh_3–Cl]$^+$, 30%), 429 ([$CpRuPPh_3$]$^+$, 100%). IR (cm^{-1}, neat solid) 3050 (w), 2840 (w), 2796 (w), 1617 (w), 1589 (m), 1463 (m), 1432 (m), 1229 (s).

"[CpRuCl (PPh_3)((R)-BINOL-*N,N*-dibenzylphosphoramidite)]" (69b). To a Schlenk flask containing phosphoramidite **41b** (0.299 g, 0.568 mmol) and [$CpRu(PPh_3)_2Cl$] (**68**) (0.387 g, 0.533 mmol), $CHCl_3$ (8 mL) was added and the solids dissolved. The orange solution was then heated to reflux for 16 h. Upon cooling, the solvent was removed under vacuum, giving an orange solid. The solid was purified by flash chromatography (2 ×17 cm silica, CH_2Cl_2/diethyl ether 49:1 v/v) to obtain **69b** as an orange solid as a mixture of diastereomers (>8:1, ^{1}H NMR) (0.444 g, 0.455 mmol, 85%). The compound was recrystallized from CH_2Cl_2/MeOH to obtain **69b** as a single diastereomer (0.386 g, 0.395 mmol, 74%), m.p. 189–190 °C dec. (capillary). Anal. Calcd. for $C_{57}H_{46}ClNO_2P_2Ru$: C, 70.18; H, 4.75. Found: C, 69.89; H, 4.72.

NMR (δ, $CDCl_3$) ^{1}H 8.06 (d, $^3J_{HH}$ = 4.9 Hz, 1H, binaphthyl), 8.01 (d, $^3J_{HH}$ = 5.3 Hz, 1H, binaphthyl), 7.74 (d, $^3J_{HH}$ = 4.9 Hz, 1H, binaphthyl), 7.55 (t, $^3J_{HH}$ = 4.3 Hz, 1H, binaphthyl), 7.47 (d, $^3J_{HH}$ = 5.3 Hz, 1H, binaphthyl), 7.42–7.32 (m, 11H, aromatic), 7.31–7.27 (m, 6H, aromatic), 7.15–7.09 (m, 7H, aromatic), 7.08–6.92 (m, 7H, br, aromatic), 6.73 (d, $^3J_{HH}$ = 5.3 Hz, 1H, binaphthyl), 4.92 (d, $^2J_{HH}$ = 6.8 Hz, 1H, NC*H*H'), 4.89 (d, $^2J_{HH}$ = 6.8 Hz, 1H, NCH*H'*), 4.71 (s, 5H, Cp), 3.83 (d, $^2J_{HH}$ = 6.1 Hz, 1H, NC*H*H'), 3.79 (d, $^2J_{HH}$ = 6.8 Hz, 1H, NCH*H'*); ^{13}C{^{1}H} 151.1 (t, J_{CP} = 24.1 Hz, aromatic), 149.3 (s, br, aromatic), 139.6 (s, br, aromatic), 137.9 (s, br, aromatic), 137.6 (s, br, aromatic), 135.0 (s, br, aromatic), 133.8 (d, J_{CP} = 16.5 Hz, aromatic), 132.8 (d, J_{CP} = 17.4 Hz, aromatic), 131.5 (s, br, aromatic), 131.1 (s, br, aromatic), 130.6 (d, J_{CP} = 12.0 Hz, aromatic), 130.4 (d, J_{CP} = 12.0 Hz, aromatic), 129.7 (s, br, aromatic), 129.3 (d, J_{CP} = 12.0 Hz, aromatic), 129.1 (d, J_{CP} = 15.3 Hz, aromatic), 128.4 (s, br, aromatic), 128.2 (s, br, aromatic), 127.8 (d, J_{CP} = 16.2 Hz, aromatic), 127.1 (d, J_{CP} = 18.0 Hz, aromatic), 126.9 (s, br, aromatic), 126.7 (s, br, aromatic), 126.5 (t, J_{CP} = 14.5 Hz, aromatic), 125.8 (d, J_{CP} = 14.3 Hz, aromatic), 125.6 (d, J_{CP} = 14.7 Hz, aromatic), 125.5 (d, J_{CP} = 14.7 Hz, aromatic), 125.0 (d, J_{CP} = 14.8 Hz, aromatic), 123.6 (s, aromatic), 123.4 (s, aromatic), 122.8 (s, aromatic), 122.3 (s, aromatic), 121.5 (s, aromatic), 81.6 (d, $^2J_{CP}$ = 44.3 Hz, br, Cp), 51.2 (d, $^2J_{CP}$ =25.7 Hz, br, N*C*H_2), 50.1 (d, $^2J_{CP}$ = 82.6 Hz, br, N*C*H_2); $^{31}P\{^1H\}$ 171.8 (d, $^2J_{PP}$ = 61.6 Hz, phosphoramidite), 45.2 (d, $^2J_{PP}$ = 61.6 Hz, *P*Ph_3).

HRMS calcd for $C_{57}H_{46}{}^{35}ClNO_2P_2{}^{102}Ru$ 975.1735, found 975.1702. MS (FAB) 975 (**69b**$^+$, 90%), 940 ([**69b**–Cl]$^+$, 45%), 678 ([**69b**–PPh_3–Cl]$^+$, 92%), 429 ([$CpRuPPh_3$]$^+$, 100%). IR (cm^{-1}, neat solid) 3052 (m), 1617 (w), 1591 (w), 1460 (w), 1432 (m), 1229 (s).

“CpRuCl(PPh_3)((R)-BINOL(8H)-*N,N*-dibenzylphosphoramidite)” (70). To a Schlenk flask containing phosphoramidite **45b** (0.200 g, 0.385 mmol) and [CpRu(PPh_3)$_2$Cl] (**68**) (0.225 g, 0.310 mmol), $CHCl_3$ (8 mL) was added and the solids dissolved. The orange solution was then heated to reflux for 16 h. Upon cooling, the solvent was removed under vacuum, giving an orange solid. The solid was purified by flash chromatography (2 × 10 cm silica, CH_2Cl_2/Et_2O 49:1 v/v) to obtain **70** as an orange solid as a mixture of diastereomers (8:1, ^1H NMR) (0.181 g, 0.184 mmol, 59%). The compound was recrystallized from CH_2Cl_2/MeOH to obtain **70** as a single diastereomer

(0.141 g, 0.143 mmol, 46%), m.p. 218–219 °C dec. (capillary). Anal. Calcd. for $C_{57}H_{54}ClNO_2P_2Ru$: C, 69.61; H, 5.53. Found: C, 69.54; H, 5.68%.

NMR (δ, $CDCl_3$) ^{1}H 7.37–7.25 (m, 10H, aromatic), 7.24–7.09 (m, 16H, aromatic), 6.80 (d, $^3J_{HH}$ = 8.2 Hz, 1H, binaphthyl), 6.57 (d, $^3J_{HH}$ = 8.2 Hz, 1H, binaphthyl), 6.21 (d, $^3J_{HH}$ = 8.0 Hz, 1H, binaphthyl), 4.91 (d, $^2J_{HH}$ = 10.0 Hz, 1H, NC*H*H'), 4.85 (d, $^2J_{HH}$ = 10.0 Hz, 1H, NCH*H'*), 4.60 (s, 5H, Cp), 3.41 (d, $^2J_{HH}$ = 10.8 Hz, 1H, NC*H*H'), 3.35 (d, $^2J_{HH}$ = 10.8 Hz, 1H, NCH*H'*), 2.96 (t, $^3J_{HH}$ = 6.0 Hz, 2H, CH_2), 2.72–2.38 (m, 4H, 2CH_2), 2.11–1.95 (m, 2H, CH_2), 1.92–1.71 (m, 3H, alkyl), 1.70–1.55 (m, 4H, 2CH_2), 1.40–1.25 (m, 1H, alkyl); ^{13}C{^{1}H} 149.3 (d, J_{CP} = 60.0 Hz, aromatic), 148.6 (d, J_{CP} = 24.0 Hz, aromatic), 139.8 (d, J_{CP} = 7.8 Hz, aromatic), 139.1 (s, aromatic), 138.2 (s, aromatic), 137.8 (s, aromatic), 137.6 (s, aromatic), 134.4 (s, br, aromatic), 133.5 (s, aromatic), 133.4 (s, aromatic), 129.3 (s, aromatic), 129.2 (s, aromatic), 129.0 (s, aromatic), 128.4 (s, aromatic), 128.1 (s, aromatic), 127.7 (s, aromatic), 127.6 (s, aromatic), 127.4 (d, J_{CP} = 36.0 Hz, aromatic), 127.1 (d, J_{CP} = 9.1 Hz, aromatic), 126.9 (s, aromatic), 81.0 (s, Cp), 50.1 (s, N*C*H$_2$), 50.0 (s, N*C*H$_2$), 29.7 (s, *C*H$_2$), 29.2 (s, *C*H$_2$), 28.2 (s, *C*H$_2$), 27.6 (s, *C*H$_2$), 23.1 (s, *C*H$_2$), 23.0 (s, *C*H$_2$), 22.9 (s, *C*H$_2$), 22.8 (s, *C*H$_2$); ^{31}P{^{1}H} 163.8 (d, $^2J_{PP}$ = 60.1 Hz, phosphoramidite), 46.0 (d, $^2J_{PP}$ = 60.1 Hz, *P*Ph$_3$).

HRMS calcd for $C_{57}H_{54}{}^{35}ClNO_2P_2{}^{102}Ru$ 983.2361, found 983.2329. MS (FAB): 983 (**70**$^+$, 45%), 948 ([**70**–Cl]$^+$, 15%), 686 ([**70**–PPh$_3$–Cl]$^+$, 100%), 429 ([CpRuPPh$_3$]$^+$, 95%). IR (cm^{-1}, neat solid) 3052 (m), 3022 (m), 2929 (s), 2858 (m), 1582 (w), 1469 (s), 1433 (s).

"[CpRu(PPh$_3$)((R)-BINOL-*N,N*-dimethylphosphoramidite)(diphenylallenylidene)][PF$_6$]" (**71a**). To a Schlenk flask containing **69a** (0.051 g, 0.062 mmol) and 1,1-diphenyl-2-propyn-1-ol (**5a**) (0.014 g, 0.069 mmol), THF (2 mL) was added and the solids dissolved. NaPF$_6$ was added as a solution in MeOH (3 mL) and the solution turned red. After heating to 40 °C for 26 h, the solution was allowed to cool to RT and the volatiles were removed under high vacuum. The resulting solid was dissolved in CH_2Cl_2 and filtered over Celite to remove any insoluble material. After removal of all volatiles, ca. 50% conversion to **71a** is observed by ^{1}H NMR.

NMR (δ, $CDCl_3$) ^{1}H (partial) 5.43 (s, 5H, Cp), 5.34 (s, 2.5H, Cp*), 2.40 (s, 3H, CH3), 2.36 (s, 3H, CH3), 2.21 (s, 1.5H, CH3*), 2.15 (s, 1.5H, CH3*); ^{31}P{^{1}H} 169.5 (d, $^2J_{PP}$ = 41.9 Hz, phosphoramidite) 168.7 (d, $^2J_{PP}$ = 40.7 Hz, phosphoramidite*), 47.6 (d, $^2J_{PP}$ = 41.9 Hz, *P*Ph$_3$), 46.9 (d, $^2J_{PP}$ = 40.7 Hz, *P*Ph$_3$*).

FAB MS 978 (**71a**$^+$ 100%), 788 (**71a**–Ph$_2$ allenylidene, 10%), 716 (**71a**–PPh$_3$$^+$ 10%). IR (cm^{-1}, neat solid) 3057 (w), 1946 (s, C=C=CPh$_2$), 1434 (s), 1224 (s), 835 (s).

"[CpRu(PPh$_3$)((R)-BINOL-*N,N*-dibenzylphosphoramidite)(diphenylallenylidene)][PF$_6$]" (**71b**). To a Schlenk flask containing **69b** (0.083 g, 0.085 mmol), AgPF$_6$ (0.023 g, 0.091 mmol) was added as a solution in CH_2Cl_2 (3 mL) and the solid dissolved. After 1 h, the dark orange solution was filtered over Celite to remove AgCl and 1,1-diphenyl-2-propyn-1-ol (**5a**) (0.022 g, 0.107 mmol) was added. The solution immediately turns purple. After 1 h stirring at rt, volatiles were removed under high vacuum, giving **71b** in ca. 80% spectroscopic purity.

NMR (δ, $CDCl_3$) ^{1}H (partial) 5.41 (s, 5H, Cp), 4.40–4.31 (m, 2H, CH_2), 3.28–3.18 (m, 2H, CH_2); ^{13}C{^{1}H}293.2 (s, C_α), 190.0 (s, C_β), 162.9 (s, C_γ), 90.5 (s, Cp), 49.5 (s, CH_2), 49.4 (s, CH_2); ^{31}P{^{1}H} 167.7 (d, $^2J_{PP}$ = 38.6 Hz, phosphoramidite), 46.0 (d, $^2J_{PP}$ = 49.0 Hz, PPh_3).

FAB MS 1130 (**71b**$^+$ 100%), 868 (**71b**–PPh_3^+ 15%), 678 (**71b**–PPh_3–Ph_2 allenylidene, 20%). IR (cm^{-1}, neat solid) 3058 (m), 1934 (s, C=C=CPh_2), 1432 (s), 1232 (s), 826 (s).

X-ray Structure Determination for 69b and 70: X-ray quality crystals of **69b** were obtained by addition of hexanes to a solution of **69b** in THF, which was stored at rt for several days. X-ray quality crystals of **70** were obtained by slow diffusion of MeOH into a solution of **70** in $CHCl_3$ at –18 °C.

Preliminary examination and X-ray data collection were performed using a Bruker Kappa Apex II single crystal X-Ray diffractometer equipped with an Oxford Cryostream LT device. Intensity data were collected by a combinations of ϖ and ϕ scans. Apex II, SAINT and SADABS software packages (Bruker Analytical X-Ray, Madison, WI, 2008) were used for data collection, integration and correction of systematic errors, respectively.

Structure solution and refinement were carried out using the SHELXTL- PLUS software package.[2] The structures were solved by direct methods and refined successfully in the space groups $P2_12_12_1$ (**69b**), $P2_1$ (**70**). The non-hydrogen atoms were refined anisotropically to convergence. All hydrogen atoms were treated using appropriate riding model (AFIX m3). Disorder in the solvent molecule ($CHCl_3$) in case of **70** and the 2 THF molecules in case of **69b** were resolved with partial occupancy atoms.

CCDC 694648 and 694647 contain the supplementary crystallographic data for **69b** and **70**.

---

[1] (a). Hulst, R.; de Vries, N. K.; Feringa, B. L. *Tetrahedron: Asymmetry*, **1994**, *5*, 699; (b). Duursma, A.; Boiteau, J.-G.; Lefort, L.; Boogers, J. A. F.; de Vries, A. H. M.; de Vries, J. G.; Minnaard, A. J.; Feringa, B. L. *J. Org. Chem*. **2004**, *69*, 8045.

[2] Sheldrick, G. M. *Acta Cryst*. **2008**, *A64*, 112.

Synthesis and coordination chemistry of a new P-donor ligand class

4.1. Aim

Electronic tuning of ruthenium complexes via the phosphoramidite ligands has shown little effect. By changing the oxygen atoms of the phosphoramidite ligands to sulfur atoms, the σ-donating ability of the phosphorus atom can be altered. I set out to form new stable dithiaphosphoramidite ligands and test their utility as ligands in catalytic activation of propargylic alcohols.

4.2. Introduction

4.2.1. Dithiaphosphoramidites

Steric tuning of phosphoramidite ligands in ruthenium complexes has been shown to have a profound impact on the reactivity and diastereoselectivity of the complexes. Electronic tuning via alteration of the binaphthyl backbone of the phosphoramidite ligand, on the other hand, has had little impact on the reactivity. For example, in the formation of β-oxo esters described in Chapter 2, comparable results were obtained for the "electronically tuned" ligands compared to their counterparts that are not tuned electronically (Scheme 4.1).[1] Addition of electron-withdrawing bromo- substituents (**43a, d**) or partial hydrogenation of the BINOL backbone (**43b**, **45b**) showed little effect on the activity of the catalysts. I hypothesized that electronic tuning closer to the phosphorus donor atom would show a greater impact on the reactivity of the complexes. To this end, I envisioned replacing the oxygen atoms next to the phosphorus with sulfur atoms. The sulfur atoms are less electronegative, thus potentially giving a ligand with greater electron density on the phosphorus atom, in turn leading to a better σ-donor.

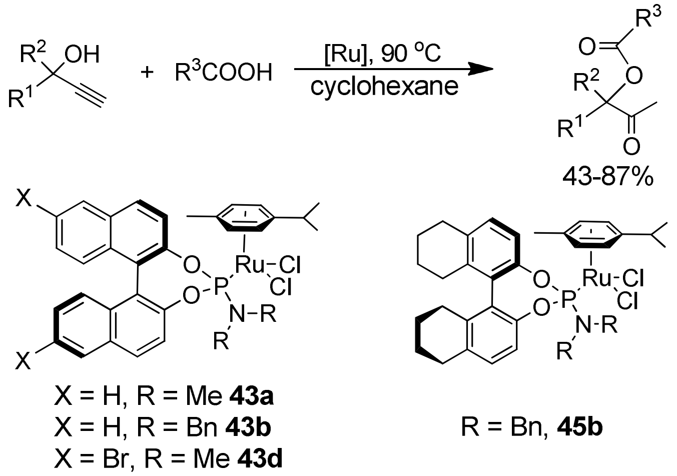

Scheme 4.1. Attempted electronic tuning via phosphoramidite ligands.

This type of structure has been reported previously, the first appearing in 1982 (**83** in Scheme 4.2).[2] Later, similar structures were used as phosphorylating agents in the synthesis of oligo(deoxyribonucleoside phosphorothioate)s.[3] In these compounds the P-N bond is shown to be easily cleaved. The lability of the P-N bond in these structures is used to orchestrate the phosphorylation reaction. The first example of these structures (herewith after referred to as dithiaphosphoramidites) as ligands for transition metal complexes was reported in 2009 by our laboratory.[4]

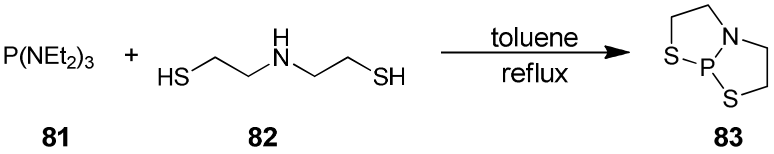

Scheme 4.2. Synthesis of the first dithiaphosphoramidite.[2]

4.3. Results

4.3.1. Synthesis of dithiaphosphoramidite ligands and ruthenium complexes thereof

The previously synthesized dithiaphosphoramidites were shown to have limited stability towards P-N and/or P-S bond cleavage.[2] All of these previously reported compounds are based on alkyl thiols/amines.[2,3] I proposed that if aryl thiols and/or amines are used, the compounds would show increased stability. The majority of phosphoramidite ligands are based on the commercially available diol 1,1-binapthyl-2,2’-diol (BINOL)[5] so the sulfur analog 1,1’-binaphthyl-2,2’-dithiol (thioBINOL) (**88**) is a logical starting point for the synthesis of this new ligand class (Scheme 4.3).

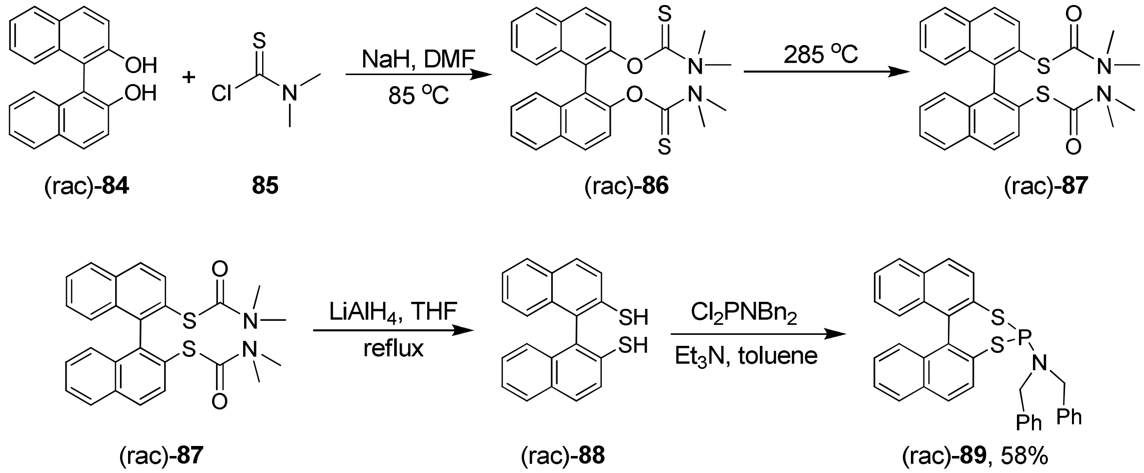
OH
OH
+
S
Cl
N
NaH, DMF
85 °C
S
O
N
O
N
S
285 °C
O
S
N
S
N
O
(rac)-84
85
(rac)-86
(rac)-87
O
S
N
S
N
O
LiAlH4, THF
reflux
SH
SH
Cl2PNBn2
Et3N, toluene
S
P
S
N
Ph
Ph
(rac)-87
(rac)-88
(rac)-89, 58%

Scheme 4.3. Synthesis of the new dithiaphosphoramidite ligand (rac)-**89**.[6]

Beginning from racemic (rac)-BINOL ((rac)-**84**), (rac)-thioBINOL ((rac)-**88**) can be synthesized in a 3-step procedure as outlined in Scheme 4.3.[6] First the diol is reacted with *N,N*-dimethylthiocarbamoyl chloride (**85**) to give the thiocarbamate **86**. Thermally induced isomerization under neat conditions (Newman-Kwart rearrangement) followed by reduction with $LiAlH_4$ gives the dithiol **88**. Reaction with the *in situ* generated *N,N*-dibenzyl-1,1-dichlorophosphinamine (Cl_2PBn_2) gives the new ligand (rac)-**89** in 58% yield after chromatographic workup.

The new ligand (**88**) shows similar spectroscopic properties to that of the structurally related phosphoramidite **43b**.[7] In the ^1H NMR spectrum, the methylene (CH_2) protons are diastereotopic, giving a complex splitting pattern in the range 3.99-3.81 ppm. This is in contrast to the phosphoramidite **43b** which gives four distinct doublets between 4.29 and 3.47 ppm. The chemical shift of 159.8 ppm for the signal in the ^{31}P NMR spectrum is also significantly downfield of that of **43b** (144.7 ppm). The HRMS of **88** shows an accurate molecular ion for **88**·H$^+$. The IR spectrum is also in accordance with the assigned structure.

To begin testing the coordination chemistry of this new ligand class, I sought complexes of the type [RuCl$_2$(*p*-cymene)(L)] where L is a dithiaphosphoramidite ligand. Analogous phosphoramidite complexes have been synthesized previously and were shown to be active in the conversion of propargylic alcohols to β-oxo esters (Chapter 2).[1] In this way the tuning effect of the ligand can be determined by comparison against the previously reported phosphoramidite complex **43b** (Chapter 2). Using standard conditions developed for the phosphoramidite complexes (CH$_2$Cl$_2$ solvent, room temperature, 6 h), the ligand (rac)-**89** was reacted with the dimer [RuCl(μ-Cl)(*p*-cymene)]$_2$ (**42**) to give [RuCl$_2$(*p*-cymene)((rac)-**89**)] ((rac)-**90**), isolated in 67% yield as a tan solid after recrystallization.

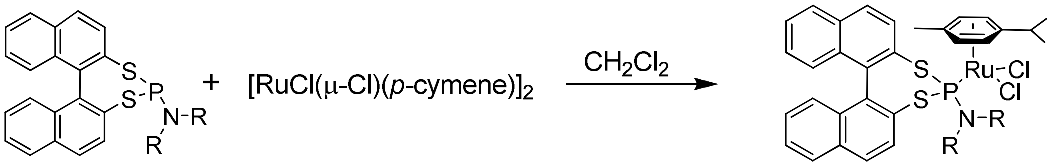

(rac)-**89**

R = Bn, **90**, 67%

Scheme 4.4. Synthesis of the first dithiaphosphoramidite ruthenium complex **90**.

The new complex is characterized spectroscopically by NMR (^{1}H, ^{13}C, ^{31}P), IR and HRMS. Coordination of the dithiaphosphoramidite ligand is clearly shown by a shift of the ^{31}P NMR signal from 155.8 ppm to 163.6 ppm, significantly downfield of that of **43b** (142.2 ppm). Again, the arene protons of the *p*-cymene ligand are rendered diastereotopic, showing four doublets in the ^{1}H NMR spectrum between 5.6 and 5.4 ppm and six signals in the ^{13}C NMR spectrum (110.6 ppm-80.0 ppm), similar to that of **43b**. IR and HRMS are in accordance with the assigned structure, but an accurate elemental analysis was not obtained, possibly due to ongoing decomposition.

4.3.2. Catalytic activation of propargylic alcohols

As described in Chapter 2 the phosphoramidite complexes [RuCl$_2$(*p*-cymene)(L)] (where L is a phosphoramidite) are catalytically active in activation of propargylic alcohols. Accordingly, I tested complex **90** as catalyst in substitution reactions of propargylic alcohols as well (Scheme 4.5). Simple alcohols were chosen as nucleophiles for initial experiments as they have been shown to be effective nucleophiles for ruthenium catalyzed propargylic substitutions.[8] The tertiary propargylic alcohols 1,1-diphenyl-2-propyn-1-ol (**5a**) and 2-phenyl-3-butyn-2-ol (**5b**) react with methanol or ethanol at 90 °C in the presence of 1.5 mol% **90** to give the corresponding propargylic ethers in 40-85% isolated yield. The propargylic ethers showed limited stability, cleaving on silica gel during chromatography. The stability of the products on basic alumina was greater, but it cannot be ruled out that the yields were adversely affected due to cleavage of the ethers during purification.

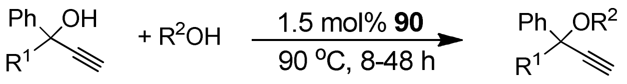

R^1 = Ph, R^2 = Me, 58%
R^1 = Me, R^2 = Me, 85%
R^1 = Me, R^2 = Et, 40%

Scheme 4.5. Etherification of propargylic alcohols using (rac)-**90**.

4.4. Discussion

4.4.1. Synthesis and reactivity of new complexes

Despite the fact that several literature procedures exist for the synthesis of thioBINOL (**88**),[6] the reaction turned out to be difficult, recrystallization of the thiocarbamate **86** being the limiting factor. The high temperatures required for the thermal rearrangement to obtain **87** make it necessary to have the starting material (**86**) with purity in excess of 99%. Acceptable conditions for recrystallization of the racemic thiocarbamate (**86**) were found by dissolving the material in a minimum of CH_2Cl_2 followed by addition of hexanes to give about a 1:1 ratio. Slow evaporation of this mixture gave crystals of the desired (rac)-**86** in high purity. Interestingly, under identical conditions the (R)-thiocarbamate ((R)-**86**) does not give crystalline material. Instead the product oils out of solution, failing to significantly improve the purity of (R)-**86**. Thus the following experiments were all performed using racemic material.

As shown in Scheme 4.2, hexaethylphosphorus triamide (**81**) can react with dithiols in a reaction analogous to the synthesis of the phosphoramidites **41a** and **47** (Scheme 2.2, Chapter 2) to form dithiaphosphoramidites. However, under similar reaction conditions thioBINOL (**88**) and hexamethylphosphorus triamide do not react to form the desired *N,N*-dimethyl dithiaphosphoramidite. The reaction instead gives a multitude of products without an identifiable major product (^{1}H, ^{31}P NMR). Beginning from PCl_3 and dibenzylamine (as applied in the synthesis of **41b**), the *N,N*-dibenzyl dithiaphosphoramidite **89** is obtained as the major product (Schemes 4.3, 4.4). In all cases, a small amount of thioBINOL (**88**) remains at the end of the reaction so special care must be taken to separate the dithiol from the product. Synthesis of the complex

[$RuCl_2$(*p*-cymene)(**89**)] (**90**) proceeds in 6 h in CH_2Cl_2 at ambient temperature, similar to the conditions applied for the analogous phosphoramidite complex **43b**.

For the catalytic etherification of propargylic alcohols, various conditions were applied including variations in temperature and solvent. After optimization, the best results were obtained by using the alcohol nucleophile as solvent at 90 °C. Under these conditions, complete conversion to the corresponding propargylic ethers was observed by GC/MS after 8-48 h. Both methanol and ethanol could be used as nucleophiles but the bulkier isopropanol is unreactive under similar conditions. In all cases a single product peak is observed by GC/MS after the reported reaction time. The reaction of 1,1-diphenyl-2-propyn-1-ol (**5a**) with methanol is by far the fastest reaction, giving complete consumption of **5a** in only an 8 h reaction time. In fact, if this reaction is allowed to proceed longer, a second addition of methanol occurs (as observed by GC/MS), adding across the C≡C triple bond in an anti-Markovnikov fashion. This product proved to be highly unstable and all attempts to isolate it yielded only 3,3-diphenyl-2-propenal (**92**) (Scheme 4.6). The aldehyde is a structural isomer of the starting propargylic alcohol and has been reported as the product of a reaction with a similar piano-stool complex ([$Ru(OSO_2CF_3)$(*p*-cymene)(PCy_3)(CO)], Cy ≡ cyclohexyl) as catalyst.[9]

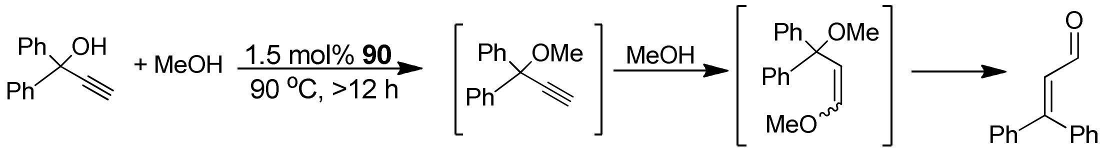

5a **92**

Scheme 4.6. Double addition of methanol.

4.4.2. Stability tests

After running this reaction a number of times a trend developed in which it became apparent that the catalyst performed better when it was freshly made (<48 h previously). In the case of the analogous phosphoramidite complex **43b**, the catalyst retained complete activity after extended time frames (>1 month) so I hypothesized that **90** was unstable in air at room temperature even in the solid state on the scale of weeks. Phosphoramidite complexes **43** were shown to have lability in the *p*-cymene ligand in solution and dithiaphosphoramidites such as **83** have unstable P-N bonds, so multiple decomposition pathways are available. It seems that the decomposition products are inactive or at least less active than the precatalyst **90**.

When attempting to obtain X-ray quality crystals of complex **90** using various solvents for slow diffusion or slow evaporation methods, dibenzylamine hydrochloride was instead obtained in several cases (shown by ^{1}H NMR). This suggests significant lability in the dithiaphosphoramidite P-N bond, similar to the reactivity of the previously reported dithiaphosphoramidites.[6] Subsequently, hydrolytic stability tests were performed on both the ligand and the metal complex (Scheme 4.7). First samples of the ligand **89** and the complex **90** were dissolved in $CDCl_3$ and NMR spectra (^{1}H, ^{31}P) were obtained to confirm the purity of the compounds. Next a drop of water was added to the samples and they were shaken briefly. The ^{1}H and ^{31}P NMR spectra of the samples taken after addition of water confirm significant decomposition, with several new signals appearing near 0 ppm in the ^{31}P NMR, suggesting formation of various phosphorous acid products such as **93**.

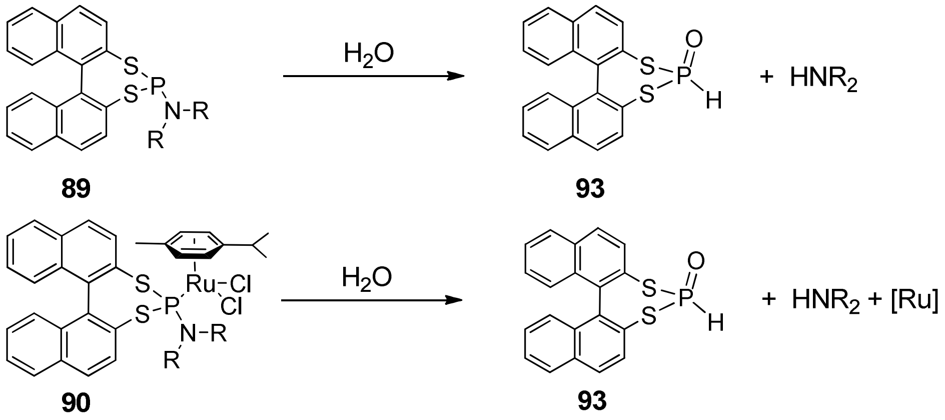

Scheme 4.7. Hydrolysis of **89** and **90**.

Considering the instability of the complex in the presence of water, it is unlikely that the active catalyst in the etherification reaction contains the dithiaphosphoramidite ligand as it appears in the precatalyst. Destruction of the ligand may be occurring to open a coordination site at ruthenium and allow activation of the propargylic alcohol. The observed differences in reaction rate in the order 1,1-diphenyl-2-propyn-1-ol (**5a**)/methanol > 2-phenyl-3-butyn-2-ol (**5b**)/methanol > 2-phenyl-3-butyn-2-ol (**5b**)/ethanol suggests the reaction may go through a propargylic carbocation intermediate, instead of the desired allenylidene.

4.5. Summary and Prospective

The first complex bearing a dithiaphosphoramidite ligand has been synthesized and characterized spectoscopically. This new complex is active in the etherification of aromatic tertiary propargylic alcohols. It is likely that the reaction proceeds via a propargylic carbocation intermediate. The catalytically active species may be formed by decomposition of the dithiaphosphoramidite ligand as it has been shown to have poor stability in the presence of water. Overall, a new ligand class has been established, but the factors affecting the stability of these ligands must be further explored in order to obtain more stable ligands and complexes.

---

[1] Costin, S.; Rath, N. P.; Bauer, E. B. *Adv. Synth. Catal.* **2008**, *350*, 2414.

[2] Jurkschat, K.; Mügge, C.; Rzschach, A.; Uhlig, W.; Zschunke A. *Terahedron. Lett.* **1982**, *23*, 1345.

[3] (a). Okruszek, A.; Sierzchala, A.; Sochacki, M.; Stec, W. J. *Tetrahedron Lett.* **1992**, *33*, 7585; (b). Okruszek, A.; Sierzchala, A.; Fearon, K. L.; Stec, W. J. *J. Org. Chem.* **1995**, *60*, 6998; (c). Miller, G. P.; Siverman, A. P.; Kool, E. T. *Bioorg. Med. Chem.* **2008**, *16*, 56; (d). Olesiak, M.; Okruszek, A. *Phosphorus, Sulfur, and Silicon* **2009**, *184*, 1548.

[4] Costin, S.; Sedinkin, S. L; Bauer, E. B. *Tetrahedron Lett.* **2009**, *50*, 922.

[5] Duursma, A.; Boiteau, J.-G.; Lefort, L.; Boogers, J. A. F.; de Vries, A. H. M.; de Vries, J. G.; Minnaard, A. J.; Feringa, B. L. *J. Org. Chem.* **2004**, *69*, 8045.

[6] (a). Fabbri, D.; Delogu, G.; De Lucchi, O. *J. Org. Chem.* **1993**, *58*, 1748; (b). Bandarage, U. K.; Simpson, J.; Smith, R. A. J.; Weavers, R. T. *Tetrahedron* **1994**, *11*, 3463; (c). Hatano, M.; Maki, T.; Moriyama, K.; Arinobe, M.; Ishihara, K. *J. Am. Chem. Soc.* **2008**, *130*, 16858.

[7] Arnold, L. A.; Imbos, R.; Mandoli, A.; de Vries, A. H. M.; Naasz, R.; Feringa, B. L. *Tetrahedron* **2000**, *56*, 2865.

[8] Tanabe, Y.; Kanao, K.; Miyake, Y.; Nishibayashi, Y. *Organometallics* **2009**, *28*, 1138.

[9] Bustelo, E.; Dixneuf, P. H. *Adv. Synth. Catal.* **2007**, *349*, 933.

Experimental Section

General. Chemicals were treated as follows: THF, toluene, diethyl ether, distilled from Na/benzophenone; CH_2Cl_2, distilled from CaH_2. [RuCl(μ-Cl)(*p*-cymene)]$_2$ (**42**) (Strem), all propargylic alcohols (Aldrich), and other materials, used as received. (rac)-1,1'-binaphthyl-2,2'-dithiol "(rac)-thioBINOL" **88**[1] was synthesized according to literature procedures. All reactions were carried out under an atmosphere of nitrogen applying Schlenk techniques.

NMR spectra were obtained at room temperature on a Bruker Avance 300 MHz or a Varian Unity Plus 300 MHz instrument and referenced to a residual solvent signal; all assignments are tentatively. GC/MS spectra were recorded on a Hewlett Packard GC/MS System Model 5988A. Exact masses were obtained on a JEOL MStation [JMS-700] Mass Spectrometer. Melting points are uncorrected and were taken on an Electrothermal 9100 instrument. IR spectra were recorded on a Thermo Nicolet 360 FT-IR spectrometer. Elemental analyses were performed by Atlantic Microlab.

"(rac)-thioBINOL-*N,N*-dibenzyl-phosphoramidite" (89). To a Schlenk flask containing triethyl amine (0.55 mL, 4.2 mmol) and dibenzyl amine (0.27 mL, 1.4 mmol), toluene (5 mL) was added followed by phosphorus trichloride (0.12 mL, 1.3 mmol), which upon addition, yielded a white smoke. The white slurry was heated to 70 °C for 8 h upon which the color changed to yellow. After cooling to room temperature, (rac)-thioBINOL (0.401 g, 1.26 mmol, **88**) was added. An additional 4 mL toluene was then added and the slurry stirred at room temperature for 24 h. The slurry was filtered over silica and the filtrate was dried by oil pump vacuum, yielding a white solid. The solid was purified by flash chromatography (1 × 6 in. silica) using CH_2Cl_2/hexanes (1:5 v/v). The solvent was removed and the solid dried under high vacuum yielding **89** as a white foam (0.397g, 1.10 mmol, 58%), m.p. 194-196 °C dec. (capillary).

NMR (δ, $CDCl_3$) ^{1}H 7.99-7.84 (m, 5H, aromatic), 7.76 (d, $^3J_{HH}$ = 8.5 Hz, 1H, aromatic), 7.62 (d, $^3J_{HH}$ = 8.7 Hz, 1H, aromatic), 7.49-7.41 (m, 2H, aromatic), 7.36-7.28 (m, 5H, aromatic), 7.25-7.18 (m, 6H, aromatic), 7.11 (d, $^3J_{HH}$ = 8.4 Hz, 1H, aromatic), 7.01 (d, $^3J_{HH}$ = 8.2 Hz, 1H, aromatic), 3.99-3.81 (m, 4H, 2CH_2); $^{13}C\{^1H\}$141.8 (s, aromatic), 141.7 (s, aromatic), 137.7 (s, aromatic), 134.2 (s, aromatic), 132.3 (s, aromatic), 133.2 (s, aromatic), 132.9 (s, aromatic), 132.7 (s, aromatic), 132.5 (d, J_{CP} = 8.1 Hz, aromatic), 132.1 (s, aromatic), 131.7 (s, aromatic), 130.2 (s, aromatic), 129.4 (s, aromatic), 129.3 (s, aromatic), 128.8 (s, aromatic), 128.7 (s, aromatic), 128.6 (s, aromatic), 128.4 (d, J_{CP} = 8.1 Hz, aromatic), 127.7 (s, aromatic), 127.6 (s, aromatic), 127.5 (s, aromatic), 126.8 (s, aromatic), 126.5 (s, aromatic), 125.8 (s, aromatic), 125.2 (s, aromatic), 53.5 (s, CH$_2$), 53.3 (s, CH$_2$); $^{31}P\{^1H\}$ 159.8 (s).

HRMS calcd for $C_{34}H_{27}NPS_2$ (**89**·H$^+$) 544.1323, found 544.1313. IR (cm^{-1}, neat solid) 3023(w), 2882(w), 1574(m), 1490(m), 1443(m), 1049(m).

"[RuCl$_2$((rac)-thioBINOL-*N,N*-dibenzyl-phosphoramidite)(*p*-cymene)]" (90). To a Schlenk flask containing thiophosphoramidite **89** (0.198 g, 0.365 mmol), [RuCl(μ-Cl)(*p*-cymene)]$_2$ (0.112 g, 0.182 mmol, **42**) was added followed by CH_2Cl_2 (6 mL) to obtain a dark red solution. The solution was allowed to stir under nitrogen atmosphere at room temperature for 6 h, and then the solvent was removed by oil pump vacuum, yielding a brown solid. The solid was recrystallized using a mixture of CH_2Cl_2 and Et_2O at -18 °C, yielding **90** as a brown solid (0.208 g, 0.245 mmol, 67%), m.p. 163.5-164.5 °C dec. (capillary). Anal. calcd for $C_{44}H_{40}Cl_2NS_2PRu$: C, 62.18; H, 4.74. Found: C, 59.56; H, 4.83.

NMR (δ, $CDCl_3$) ^1H 8.03 (d, $^3J_{HH}$ = 8.6 Hz, 1H, aromatic), 7.84 (d, $^3J_{HH}$ = 6.0 Hz, 1H, aromatic), 7.81 (d, $^3J_{HH}$ = 5.4 Hz, 1H, aromatic), 7.76 (d, $^3J_{HH}$ = 8.3 Hz, 1H, aromatic), 7.60 (d, $^3J_{HH}$ = 8.7 Hz, 1H, aromatic), 7.40-7.31 (m, 4H, aromatic), 7.30-7.20 (m, 12H, aromatic), 7.13-7.03 (m, 4H, aromatic), 6.87 (d, $^3J_{HH}$ = 8.5 Hz, 1H, aromatic), 6.75 (d, $^3J_{HH}$ = 8.5 Hz, 1H, aromatic), 5.56-5.55 (m, 2H, cymene), 5.50 (d, $^3J_{HH}$ = 5.8 Hz, 1H, cymene), 5.39 (d, $^3J_{HH}$ = 5.8 Hz, 1H, cymene), 4.57 (d, $^2J_{HH}$ = 10.2 Hz, 1H, C*H*H'), 4.52 (d, $^2J_{HH}$ = 10.2 Hz, 1H, C*H*H'), 3.54-3.43 (m, 2H, CH_2), 2.95 (sept, $^3J_{HH}$ = 6.8 Hz, 1H, $CH(CH_3)_2$), 2.08 (s, 3H, Me), 1.19 (d, $^3J_{HH}$ = 6.8 Hz, 3H, $CH(CH_3)_2$), 1.08 (d, $^3J_{HH}$ = 6.8 Hz, 3H, $CH(CH_3)_2$); $^{13}C\{^1H\}$ 146.1 (s, aromatic), 141.3 (s, aromatic), 137.9 (s, aromatic), 134.5 (d, J_{CP} = 8.0 Hz, aromatic), 134.1 (s, aromatic), 133.8 (s, aromatic), 133.0 (s, aromatic), 132.1 (s, aromatic), 130.8 (s, aromatic), 130.3 (s, aromatic), 129.5-127.1 (m, unresolved), 126.5 (d, J_{CP} = 13.2 Hz, aromatic), 126.2 (s, aromatic), 125.5 (s, aromatic), 125.1 (s, aromatic), 121.1 (s, aromatic), 110.6 (s, cymene), 97.8 (s, cymene), 94.0 (s, cymene), 90.3 (s, cymene), 81.9 (s, cymene), 80.0 (s, cymene), 52.8 (NCH_2); $^{31}P\{^1H\}$ 163.6 (s).

HRMS calcd for $C_{44}H_{40}{}^{35}ClNS_2P^{102}Ru$ (**90**–Cl) 814.1072, found 814.1051. IR (cm^{-1}, neat solid) 2958(w), 1574(m), 1494(m), 1454(m), 1425(m), 744(s).

General procedure for catalytic experiments. In a screw-capped vial the propargylic alcohol **5b** (0.073 g, 0.50 mmol) was dissolved in methanol (3 mL). The catalyst (0.008 mmol) was added and the sealed vial immersed in a heating mantle preheated to 90 °C. After 24 h, the sample was filtered through a short pad of silica gel and the filtrate analyzed by GC/MS. All volatiles were removed from the sample and the residue purified by flash chromatography (silica, CH_2Cl_2/hexanes, 1:1 v/v) to obtain the product as an orange oil.

NMR (δ, $CDCl_3$) ^1H 7.53–7.50 (m, 1H, Ph), 7.28–7.21 (m, 4H, Ph), 3.13 (s, 3H, $OC\mathit{H}_3$), 2.63 (s, 1H, $C{\equiv}C\mathit{H}$), 1.65 (s, 3H, $C\mathit{H}_3$); $^{13}C\{^1H\}$142.6 (s, Ph), 128.7 (s, Ph), 128.3 (s, Ph), 126.4 (s, Ph), 84.1 (s, $\mathit{C}{\equiv}CH$), 76.8 (s, $C{\equiv}\mathit{C}H$), 75.0 (s, $\mathit{C}OCH_3$), 52.9 ($O\mathit{C}H_3$), 33.0 ($\mathit{C}H_3$).

---

[1] (a). Fabbri, D.; Delogu, G.; De Lucchi, O. *J. Org. Chem.* **1993**, *58*, 1748; (b). Bandarage, U. K.; Simpson, J. ; Smith, R. A. J.; Weavers, R. T. *Tetrahedron* **1994**, *11*, 3463; (c). Hatano, M.; Maki, T.; Moriyama, K.; Arinobe, M.; Ishihara, K. *J. Am. Chem. Soc.* **2008**, *130*, 16858.

Activation of propargylic alcohols by η^5-indenyl ruthenium complexes

5.1. Aim

Piano-stool complexes bearing an η^5-indenyl ligand show increased reactivity in substitution reactions relative to the corresponding η^5-cyclopentadienyl complexes. Mixed phosphine/phosphoramidite piano-stool complexes bearing η^5-indenyl ligands (analogous to the complexes described in Chapter 3) are likely to show enhanced reactivity relative to the corresponding Cp complexes. I aimed to synthesize new indenyl phosphoramidite complexes and test their reactivity with propargylic alcohols in catalytic and stoichiometric experiments.

5.2. Introduction

5.2.1. Activation of propargylic alcohols by η^5-piano-stool ruthenium complexes

The stability of piano-stool type ruthenium complexes bearing phosphoramidite ligands has been shown to be dependent on the type of arene. Those complexes bearing an η^5-cyclopentadienyl (Cp) ligand have shown much greater stability than the corresponding η^6-*p*-cymene derivatives (Chapters 2, 3). As described in Chapter 3, complex **69b** was shown to form a stable (although not isolable) allenylidene complex when reacted with 1,1-diphenyl-2-propyn-1-ol (**5a**) after chloride abstraction with $AgPF_6$ (Scheme 5.1).[13]

However, catalytic substitution reactions with 1,1-diphenyl-2-propyn-1-ol (**5a**) or other propargylic alcohols and various nucleophiles such as amines and alcohols all failed, potentially due to stability of an intermediate in a potential catalytic cycle. Complexes bearing an η^5-indenyl (Ind) ligand have been shown to have enhanced reactivity relative to their Cp counterparts, a phenomenon known as the "indenyl effect".[1] This enhanced reactivity allows faster rates in substitution reactions[2] and could possibly lead to increased reactivity of allenylidene complexes.

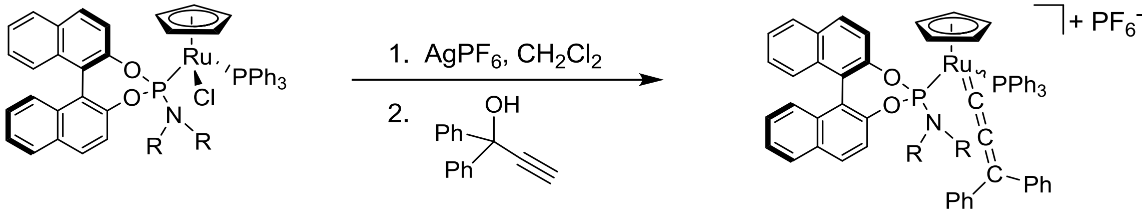

69b **5a** R = Bn, **71b**

Scheme 5.1. Synthesis of an allenylidene complex.[13]

Bis(phosphine) complexes such as [(Ind)RuCl$(PPh_3)_2$] (**110**) react with various propargylic alcohols to form allenylidene complexes analogous to the cyclopentadienyl complexes reported in Chapter 3.[3] Nucleophiles tend to add to C_γ of the allenylidene chain to give neutral η^1-alkynyl complexes as shown in Scheme 5.2. For certain nucleophiles (such as NaOMe), the reaction is reversible, giving the starting allenylidene upon addition of HBF_4. For most nucleophiles, however, protonation with HBF_4 gives the substituted vinylidene complex. Demetalation of the vinylidenes in refluxing acetonitrile (MeCN) gives the propargylic substitution product and the solvato complex [(Ind)Ru$(PR_3)_2$(MeCN)]$^+$.[4] Unique reactivity is observed in the case of a phosphine nucleophile as isomerization to an η^1-allenyl complex occurs after extended times in solution.[3]

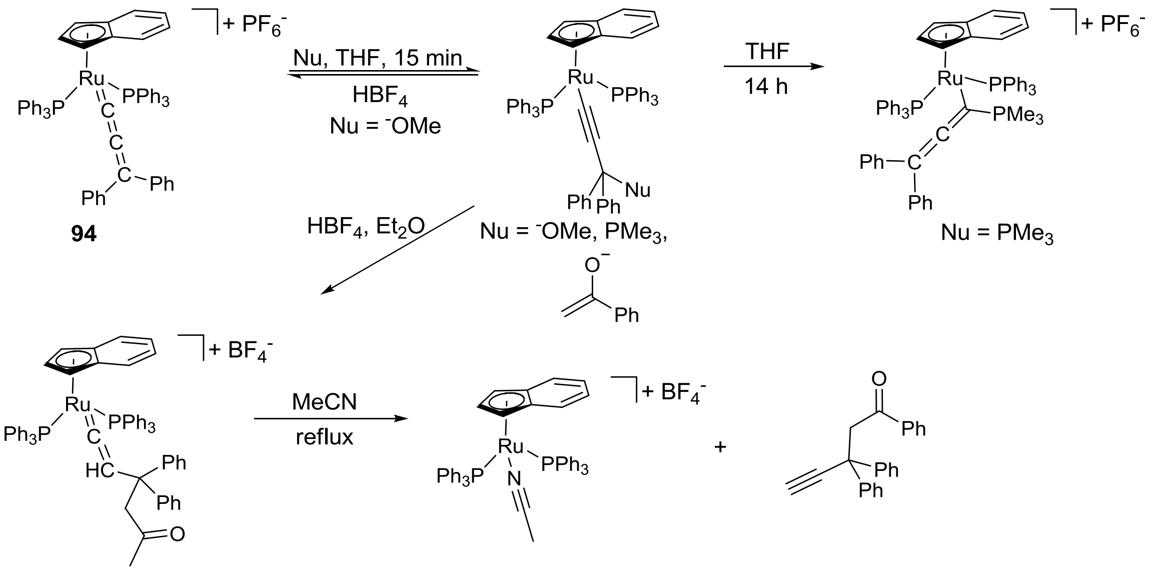

Ru
PPh3
Ph3P
C
C
C
Ph
Ph
+ PF6-
94
Nu, THF, 15 min
HBF4
Nu = -OMe
Ru
PPh3
Ph3P
Ph
Ph
Nu
Nu = -OMe, PMe3,
O-
Ph
THF
14 h
Ru
PPh3
Ph3P
PMe3
C
C
Ph
Ph
+ PF6-
Nu = PMe3
HBF4, Et2O
Ru
PPh3
Ph3P
C
HC
Ph
Ph
O
+ BF4-
MeCN
reflux
Ru
PPh3
Ph3P
N
+ BF4-
+
O
Ph
Ph
Ph

Scheme 5.2. Addition of nucleophiles to an allenylidene complex.[3]

5.2.2. Allenylidene versus vinylvinylidene formation

In the case of propargylic alcohols having protons on a carbon α- to the hydroxy group, vinylvinylidenes such as **96** in Scheme 5.4 are often formed preferentially.[5] Vinylvinylidenes show a unique reactivity relative to their allenylidene counterparts. They can add nucleophiles at C_β to form η^1-alkenyl complexes (Scheme 5.3).[6] This is contrary to allenylidene complexes, for which C_β is nucleophilic and can be protonated.[7] In this way, an allenylidene-vinylvinylidene tautomerization is shown to occur (Scheme 5.4). Formation of an allenylidene complex (derived from **95**) in the presence of PPh_3 gives the η^1-alkynyl complex **99** resulting from addition of the phosphine to C_γ. Conversely, in the absence of PPh_3, vinylvinylidenes (**96**) are formed. The vinylvinylidenes can then add PPh_3 selectively to C_β (via attack on the isomeric η^2-alkynyl complex).[6]

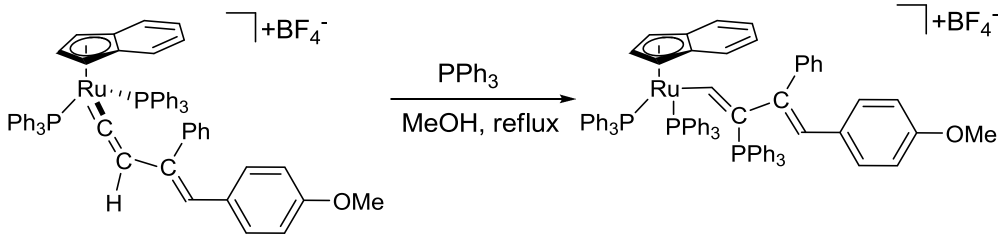
+BF$_4^-$
Ru
PPh$_3$
Ph$_3$P
C
C
H
C
Ph
OMe
PPh$_3$
MeOH, reflux
+BF$_4^-$
Ru
Ph$_3$P
PPh$_3$
C
PPh$_3$
C
Ph
OMe

Scheme 5.3. Unique reactivity of vinylvinylidene complexes.[6]

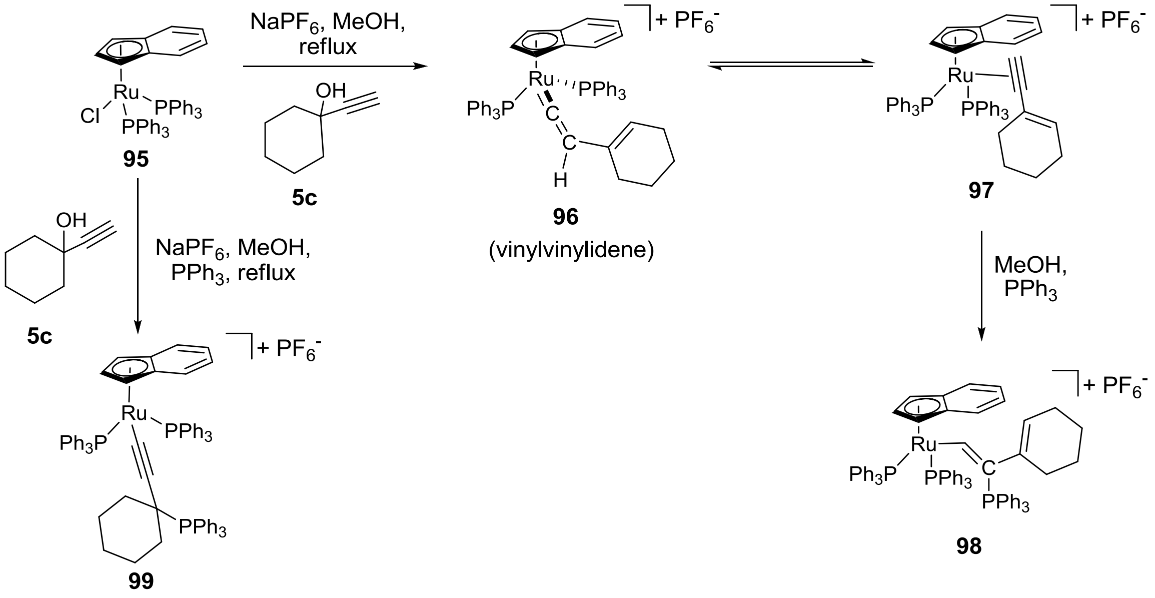
Ru
Cl
PPh$_3$
PPh$_3$
95
NaPF$_6$, MeOH, reflux
OH
5c
+ PF$_6^-$
Ru
PPh$_3$
Ph$_3$P
C
C
H
96
(vinylvinylidene)
+ PF$_6^-$
Ru
Ph$_3$P
PPh$_3$
97
MeOH, PPh$_3$
+ PF$_6^-$
Ru
Ph$_3$P
PPh$_3$
C
PPh$_3$
98
OH
5c
NaPF$_6$, MeOH, PPh$_3$, reflux
+ PF$_6^-$
Ru
Ph$_3$P
PPh$_3$
PPh$_3$
99

Scheme 5.4. Evidence for an allenylidene-vinylvinylidene tautomerization.[6]

Stoichiometric activation of propargylic alcohols via indenyl ruthenium complexes typically occurs via allenylidene or vinylvinylidene intermediates. The vinylvinylidene complex **96** reacts with a second equivalent of the propargylic alcohol **5c** to give a bicyclic allenylidene complex **100** (Scheme 5.5).[8] However, the most broadly applied method for stoichiometric activation of propargylic alcohols involves direct attack of nucleophiles at C_γ of an allenylidene.[4] This method can be applied for multi-step asymmetric substitution of propargylic alcohols, giving in some cases high enantioselectivity in the products (Scheme 5.6).[4d]

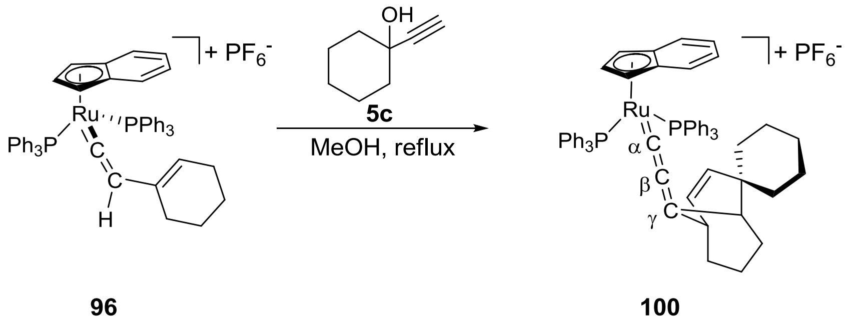
+ PF6-
Ru
PPh3
Ph3P
C
C
H
OH
5c
MeOH, reflux
+ PF6-
Ru
PPh3
Ph3P
α C
β C
γ C
96
100

Scheme 5.5. Formation of a bicyclic allenylidene complex.[8]

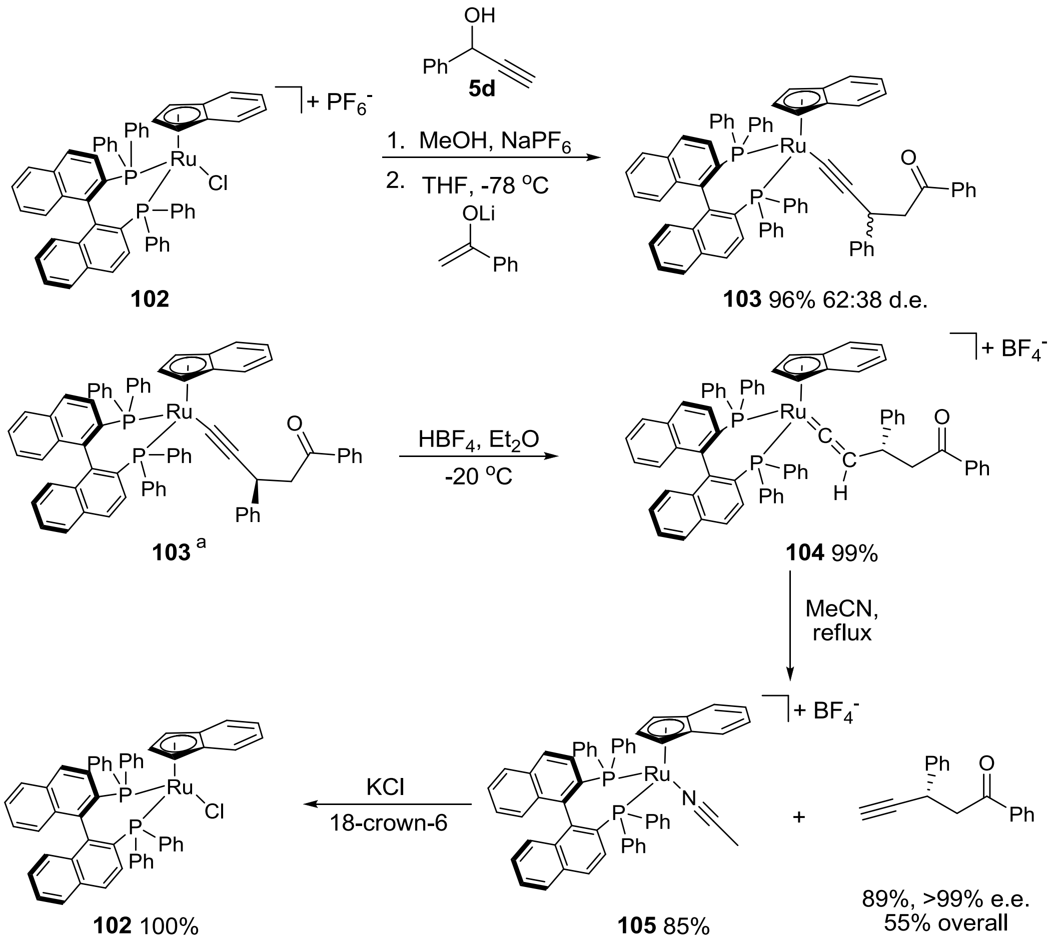
OH
Ph
5d
+ PF6-
Ph
Ph
P
Ru
Cl
P–Ph
Ph
1. MeOH, NaPF6
2. THF, -78 °C
OLi
Ph
Ph Ph
P
Ru
O
Ph
P–Ph
Ph
Ph
102
103 96% 62:38 d.e.
HBF4, Et2O
-20 °C
+ BF4-
C
C
H
104 99%
103 a
MeCN,
reflux
+ BF4-
N
KCl
18-crown-6
+
Ph
O
Ph
102 100%
105 85%
89%, >99% e.e.
55% overall

[a] The diastereomers were separated by column chromatography

Scheme 5.6. Stoichiometric enantioselective substitution of propargylic alcohols.[4d]

5.2.3. Ruthenium hydride complexes

In all cases shown above the metal precursors are activated by loss of chloride from a ruthenium chloride complex. Substitution of the chloride in these reactions by a hydride gives the resulting complex (**106**) which exhibits a unique reactivity with alkynes and propargylic alcohols in particular.[9] The hydride complexes are obtained from the corresponding ruthenium chlorides by substitution with NaOMe followed by β-elimination of the alkoxide. 1,2-insertion of the alkyne into the Ru–H bond of **106** gives an η^1-hydroxy alkenyl complex that spontaneously dehydrates to give an unsaturated alkenyl complex (**107**). Protonation with HBF_4 occurs at C_δ to give a vinylalkylidene complex (**108**) (Scheme 5.7).

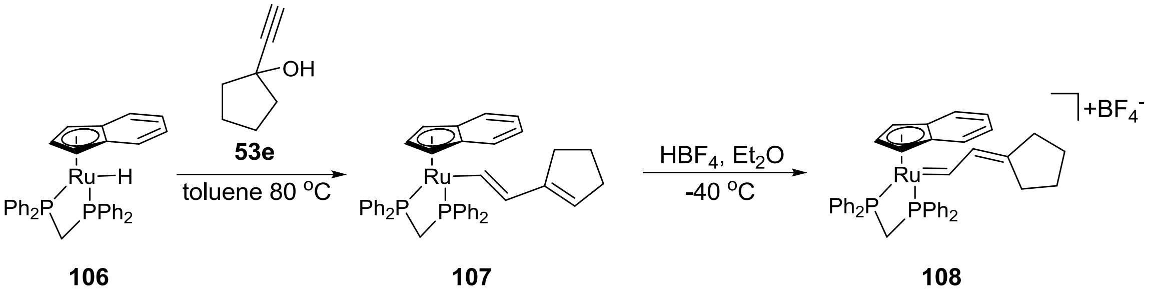

Scheme 5.7. Synthesis of a vinylalkylidene complex.[9]

Piano-stool ruthenium complexes bearing indenyl ligands are often employed in allenylidene chemistry.[4] Many of the requisite precursor complexes utilize phosphine ligands such as PPh_3 or 1,1'-binaphthyl-2,2'-bis(diphenylphosphine) (BINAP) (Schemes 5.2, 5.6). Tunable allenylidenes are desirable because catalytic substitution of propargylic alcohols via allenylidene intermediates requires that the intermediates be stable enough to be formed but reactive enough to not inhibit a catalytic cycle.

Phosphoramidite ligands represent a useful alternative to phosphines for the synthesis of tunable metal complexes and allenylidene complexes in particular.

5.3. Results

5.3.1. Synthesis of mixed phosphine/phosphoramidite indenyl ruthenium complexes

As described in Chapter 3, complexes of the type [CpRuCl(PPh_3)(L)] (where L is a phosphoramidite ligand) can be synthesized by thermal ligand exchange from the complex [CpRuCl(PPh_3)$_2$] (**68**) with the corresponding phosphoramidite ligand. I accessed indenyl complexes of the type [(Ind)RuCl(PPh_3)(phosphoramidite)] in a similar manner from the known complex [(Ind)RuCl(PPh_3)$_2$] (**110**).[10] The previously applied ligands **41a** and **41b** were again used in the substitution reaction. Refluxing ligand **41b** in THF with one equivalent of [(Ind)RuCl(PPh_3)$_2$] (**110**) gives [(Ind)RuCl(PPh_3)(**41b**)] (**111b**) in 87% isolated yield after chromatographic work up (Scheme 5.8). As for complexes **69** bearing the Cp ligand, the new complex **111b** contains stereocenters both on the ligand and on the metal center itself. Unlike complex **69b**, however, complex **111b** is formed as a single diastereomer as determined by ^{1}H and ^{31}P NMR spectroscopy. The complex [(Ind)RuCl(PPh_3)(**41a**)] (**111a**) was synthesized in a similar manner, giving the new complex in 79% yield as a 2:1 mixture of diastereomers (determined by ^{1}H NMR spectroscopy). Toluene was used as solvent in place of THF because the latter tended to elute along with **111a** during column chromatography.

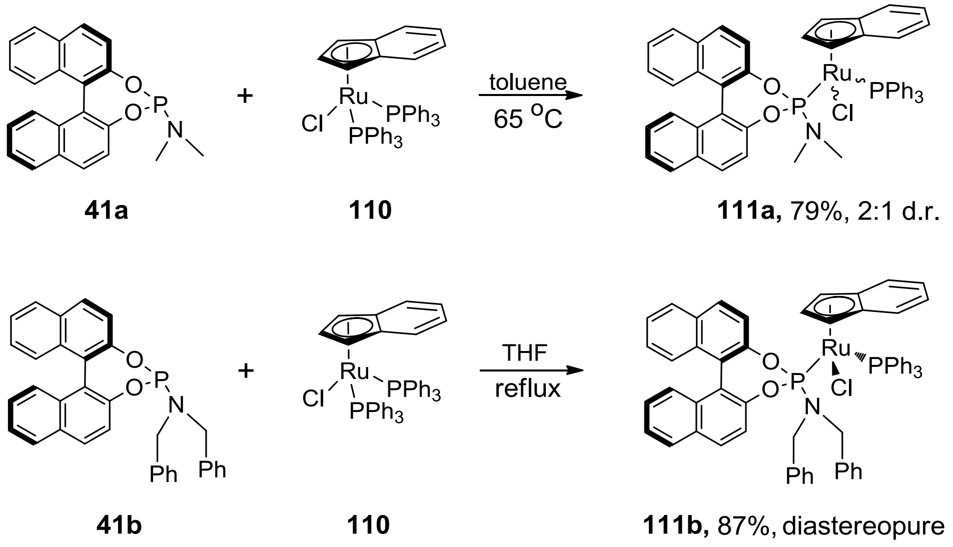

41a **110** **111a,** 79%, 2:1 d.r.

41b **110** **111b,** 87%, diastereopure

Scheme 5.8. Synthesis of new indenyl phosphoramidite complexes of ruthenium.

Again the diastereoselectivity appears to be heavily dependent on the substituents on the N atom of the phosphoramidite ligand. I was interested in determining whether changing the center of chirality would have an impact on the diastereoselectivity of metal complex formation. An alternative ligand **114** bearing a chiral center on the amine portion was synthesized by previously applied methods (Scheme 5.9).[11] The new ligand **114** gives a singlet at 145.0 ppm in the ^{31}P NMR spectrum, similar to the shifts of the other free phosphoramidite ligands. Additionally, ligand **41e** was synthesized according to literature procedures.[12] Ligands **41e** and **114** substitute a single phosphine ligand of [(Ind)RuCl(PPh$_3$)$_2$] (**110**) to give the complexes [(Ind)RuCl(PPh$_3$)(phosphoramidite)] (**111c**, **d**) in 67% and 80% isolated yields, respectively (Scheme 5.10). The complex (**111d**) based on BINOL once again showed very high diastereoselectivity, as only one diastereomer was detected by NMR spectroscopy (^{1}H, ^{31}P). The catechol based ligand (**114**) showed no diastereoselectivity upon complex formation, giving the product in a 1:1 mixture of diastereomers.

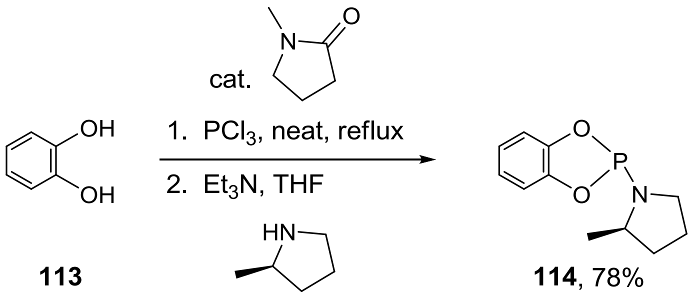
cat.
1. PCl3, neat, reflux
2. Et3N, THF
OH
OH
HN
O
N
P
113
114, 78%

Scheme 5.9. New phosphoramidite ligand synthesis.[11]

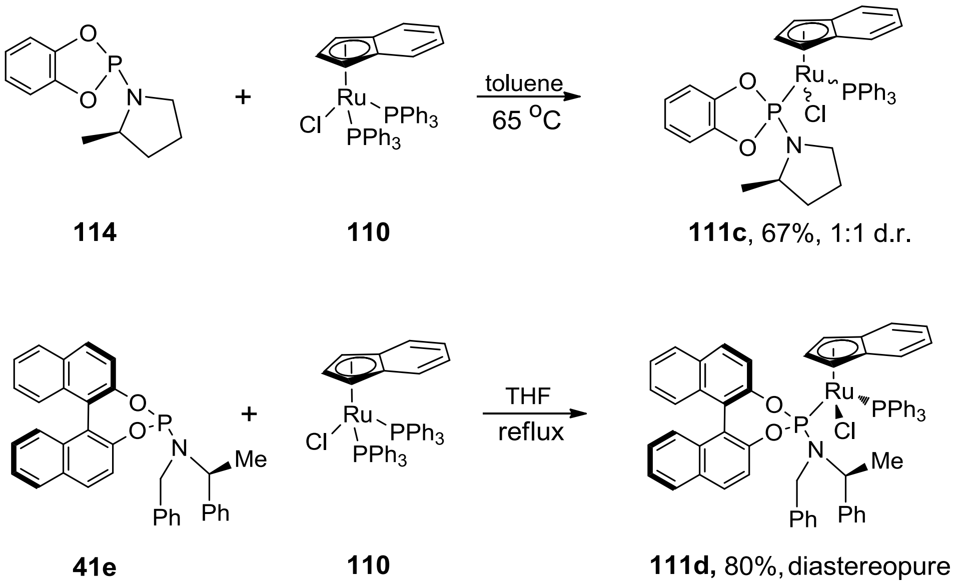
+
toluene
65 °C
Ru
Cl
PPh3
PPh3
114
110
111c, 67%, 1:1 d.r.
THF
reflux
Me
Ph
Ph
41e
110
111d, 80%, diastereopure

Scheme 5.10. Synthesis of new chiral complexes.

In all cases, coordination of the phosphoramidite ligand results in a downfield shift of the ^{31}P NMR signal. The free ligands show resonances in the range 141-152 ppm and in the complexes, the signals are doublets in the range 180-176 ppm, giving coupling constants $^{2}J_{PP}$ from 58-77 Hz. The PPh_3 signals fall in the range 62-46 ppm, typical for other ruthenium complexes bearing a PPh_3 ligand.[13] In the ^{1}H NMR, the chirality of the phosphoramidite renders the protons of the indenyl ligand diastereotopic, showing three distinct signals for the three protons on the five-membered ring between 6.56 and 3.71 ppm. The FAB MS shows a strong molecular ion peak as well as peaks corresponding to loss of chloride, PPh_3 and the phosphoramidite. IR, HRMS and in most cases microanalysis are in accordance with the assigned structures.

Complex **111b** bearing the *N*,*N*-dibenzyl substituent was characterized structurally by X-ray crystallography. Not surprisingly, **111b** has the same configuration about the metal as the Cp analog with the same ligand. The bond angles about the metal are also similar for the two complexes (**111b** and **69b**) (Table 5.1). The metal ligand bond lengths for **111b** show a greater discrepancy between Ru-P(1) and Ru-P(2) relative to **69b** (2.196 and 2.350 Å). The angles about ruthenium range from 87.37^{o} to 99.11^{o}, demonstrating the pseudooctahedral geometry about ruthenium.

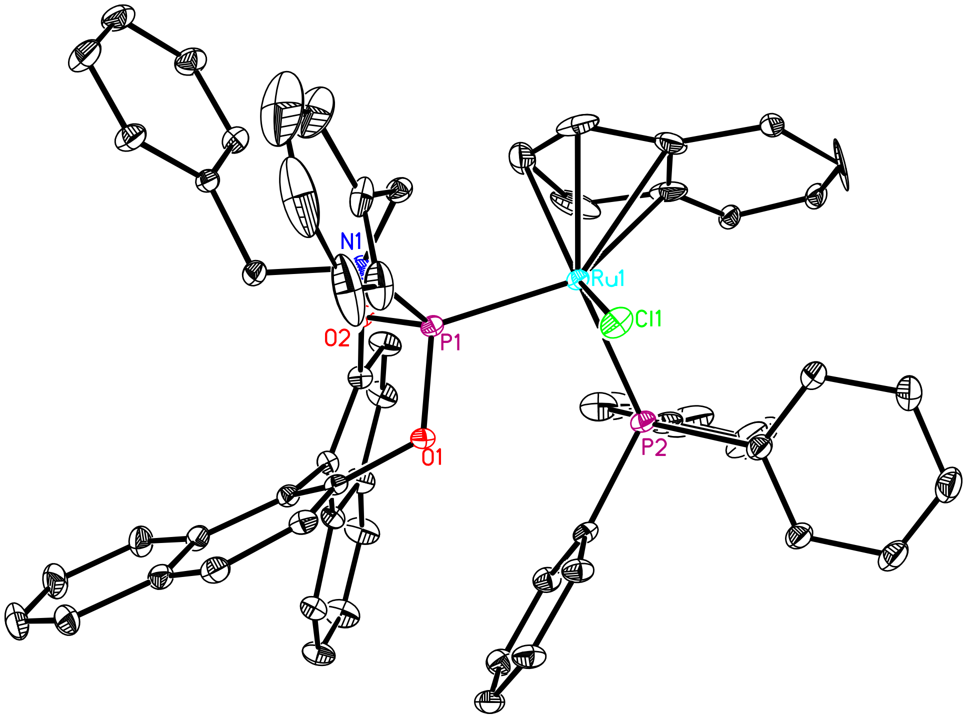

Figure 5.1. Crystal structure of **111b**.

Table 5.1. Selected bond lengths and angles for complex **111b**.

Entry	Bond(s)	[(Ind)RuCl(PPh$_3$) (**41b**)] (**111b**)	[CpRuCl(PPh$_3$) (**41b**)] (**69b**)
Bond Lengths (Å)			
1	Ru-P(1)	2.1961(7)	2.2426(8)
2	Ru-P(2)	2.3504(8)	2.3294(8)
3	Ru-Cl	2.4439(7)	2.4302(7)
Bond Angles (°)			
4	P(1)-Ru-P(2)	98.87(3)	99.11(3)
5	Cl-Ru-P(1)	89.28(3)	92.28(3)
6	Cl-Ru-P(2)	86.99(3)	87.37(3)

[a] P(1) is the phosphoramidite ligand, P(2) is PR$_3$.

5.3.2. Synthesis of allenylidene complexes

Gimeno reported previously that the phosphine complex [(Ind)RuCl(PPh$_3$)$_2$] (**110**) reacts with 1,1-diphenyl-2-propyn-1-ol (**5a**) in the presence of NaPF$_6$ in refluxing methanol to give the cationic allenylidene complex [(Ind)Ru(PPh$_3$)$_2$(=C=C=CPh$_2$)]PF$_6$ (**94**).[3] Under similar conditions complex **111b** shows little activity, giving low conversion (~10%) and a 1:1 diastereomeric ratio in the product after 5 h reaction time. However, if **111b** is preactivated by chloride abstraction using AgPF$_6$ or (Et$_3$O)PF$_6$, the resulting cationic fragment reacts with 1,1-diphenyl-2-propyn-1-ol (**5a**) to give allenylidene **116a** as a single diastereomer as seen by ^{1}H NMR (Scheme 5.11). The substrate generality of the reaction was then tested by employing a number of different propargylic alcohols. Under conditions identical to those employed for the synthesis **116a**, tertiary propargylic alcohols bearing electron-rich as well as electron-poor aromatic substituents give stable, isolable allenylidenes (**116b-e**, Figure 5.2). The new allenylidene complexes were all isolated by recrystallization as purple crystals with yields in the range 66-94%.

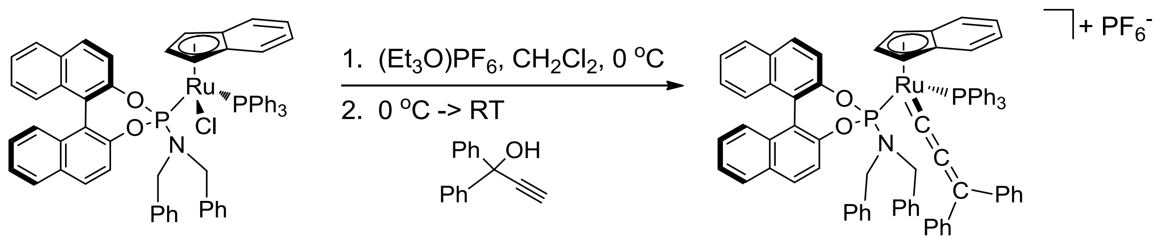

111b **5a** **116a**, 85%, diastereopure

Scheme 5.11. Synthesis of the first phosphoramidite allenylidene complex.

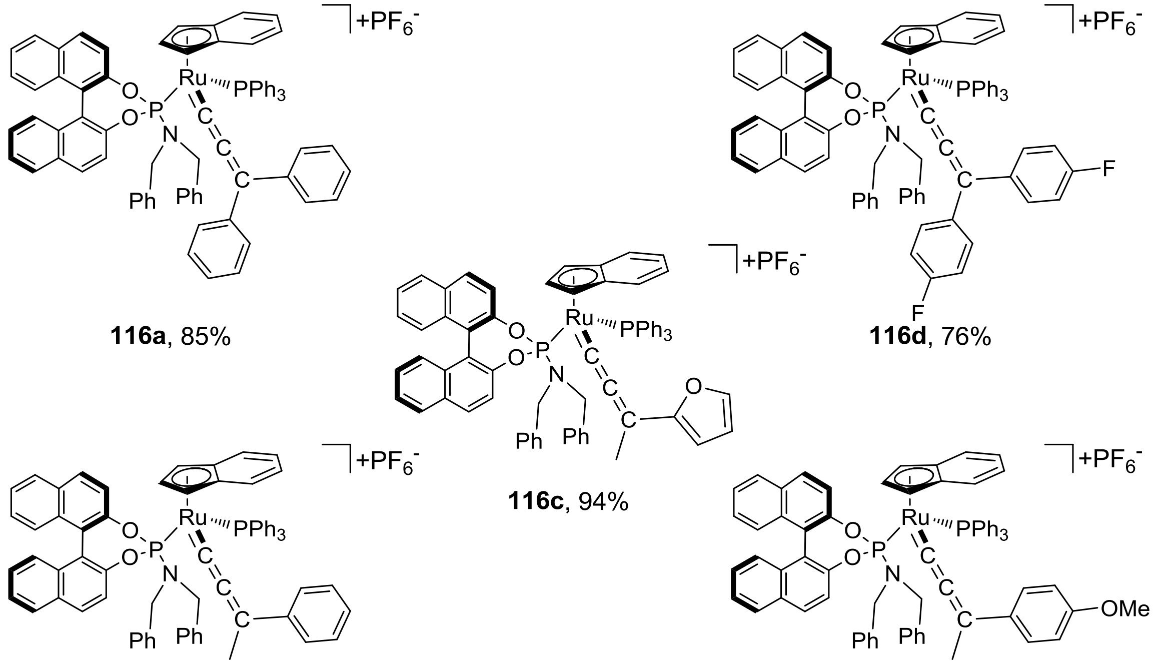

116a, 85% **116d**, 76% **116c**, 94% **116b**, 66% **116e**, 66%

Figure 5.2. Allenylidenes bearing electron-donating and electron-withdrawing groups.

The new allenylidene complexes are all characterized by NMR (^{1}H, ^{13}C, ^{31}P), IR and HRMS. The best evidence for their formation is seen in the ^{13}C NMR. The allenic carbon atoms exhibit characteristic signals far downfield in the ^{13}C NMR. In particular, the C_α (299.4-293.8 ppm) and C_β (199.7-185.2 ppm) resonances are diagnostic.[7] The C_α resonances also show coupling to the phosphorus atoms on ruthenium ($^2J_{CP}$ = 21-24 Hz).

The allenylidene formation is further confirmed by IR; the characteristic allenylidene stretch ($C=C=CR_2$) appears as an intense band between 1949 and 1935 cm^{-1}.[7]

Two of the complexes have also been characterized structurally (Figures 5.3, 5.4). X-ray quality crystals of **116a, b** were obtained by slow diffusion of Et_2O into a solution of **116a, b** in CH_2Cl_2 at -10 °C. The absolute configuration at the metal center is the same as for the starting complex **111b**, effectively replacing the chloro ligand with the allenylidene with overall retention of configuration. Again, the Ru-P bond for the phosphoramidite ligand is shorter than the Ru-PPh_3 bond, suggesting greater π-acidity of the phosphoramidite ligand. The bond angles about ruthenium range from 85.82(7) °/84.81(6) ° for C(10)-Ru-P(2) to 100.13(2) °/100.416(17) ° for P(1)-Ru-P(2), confirming the pseudooctahedral geometry about the metal. For the allenylidene chain, the bond angles for C(10)-C(11)-C(12) are 177.6(3) ° and 174.9(2) ° for **116a, b**, respectively. A slight perturbation from linearity is common for complexes of this type.[3] The bond lengths of the allenic chain are not equal; the $C_\alpha=C_\beta$ bond is significantly shorter than the $C_\beta=C_\gamma$ bond (1.250(3)/1.250(4) vs. 1.348(3)/1.357(4) Å) for complexes **116a, b**. This difference in bond lengths is the result of the alkynyl carbocation resonance contributor shown in Equation 5.1 and this phenomenon has been reported previously.[3]

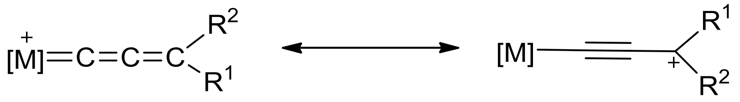

(5.1)

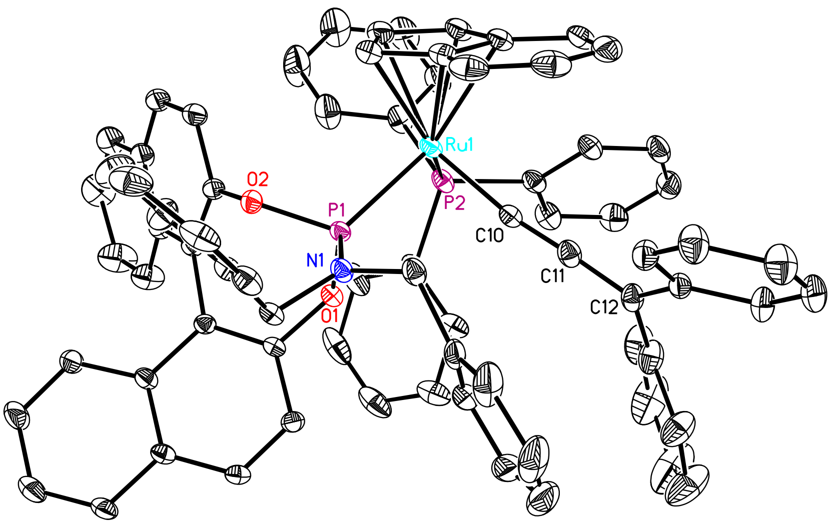
Ru1
O2
P1
P2
C10
N1
C11
O1
C12

Figure 5.3. Crystal structure of allenylidene complex **116a**.*

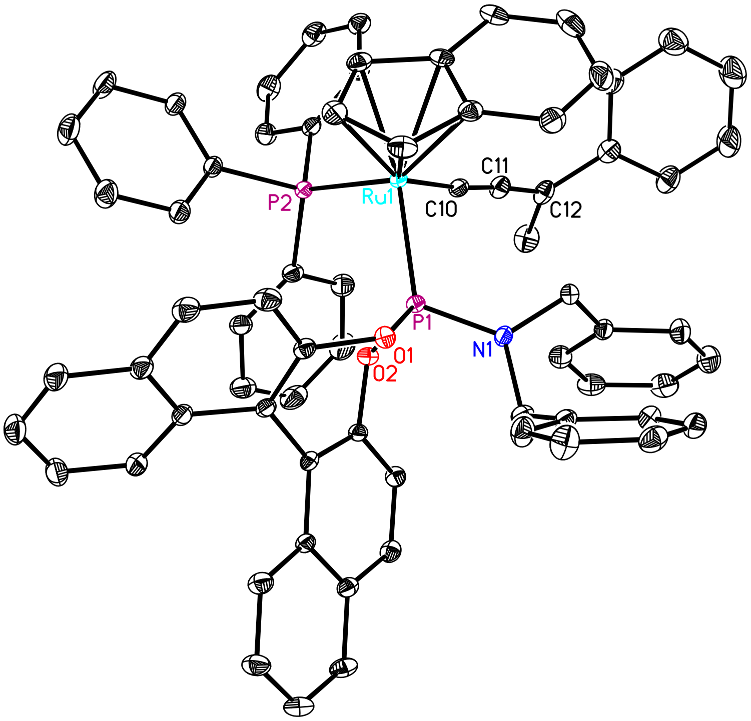
C11
P2
Ru1
C10
C12
P1
O1
N1
O2

Figure 5.4. Crystal structure of allenylidene **116b**.*

(*Counter ions and solvents are omitted for clarity)

Table 5.2. Selected bond lengths and angles for complexes **116a, b**.

Entry	Bond(s)	**116a**·CH_2Cl_2	**116b**·$2CH_2Cl_2$
Bond Lengths (Å)			
1	Ru-P(1)	2.2730(6)	2.2729(5)
2	Ru-P(2)	2.3131(7)	2.3037(5)
3	Ru=C(10)	1.887(2)	1.8937(19)
4	C(10)=C(11)	1.250(4)	1.250(3)
5	C(11)=C(12)	1.357(4)	1.348(3)
Bond Angles (°)			
6	P(1)-Ru-P(2)	100.13(2)	100.416(17)
7	C(10)-Ru-P(1)	92.73(7)	92.39(6)
8	C(10)-Ru-P(2)	85.82(7)	84.81(6)
9	C(10)-C(11)-C(12)	177.6(3)	174.9(2)

Also of note is the fact that the benzo- portion of the indenyl ligand is oriented along the allenylidene chain. This conformational preference could have an impact on the direction of attack by potential nucleophiles. If the top face of the allenylidene is better shielded, a potential nucleophile may have to approach from the lower side of the complex, closer to the position of the P-donor ligands. As seen in a space-filled model for the crystal structure of complex **116b** (the phosphoramidite ligand is on the left of the allenylidene, the phosphine on the right), there is a significant difference in the closest contact between the allenylidene and the P-donor ligands (Figure 5.5). Not surprisingly, the larger phosphoramidite ligand appears to more effectively mask one side of the allenylidene. The distance between C_γ of the allenylidene and the centroid of the closest phenyl ring of PPh_3 is 5.0 Å compared to only 3.8 Å to the centroid of the closest phenyl ring of the phosphoramidite (calculated with Mercury 1.4.2 software).

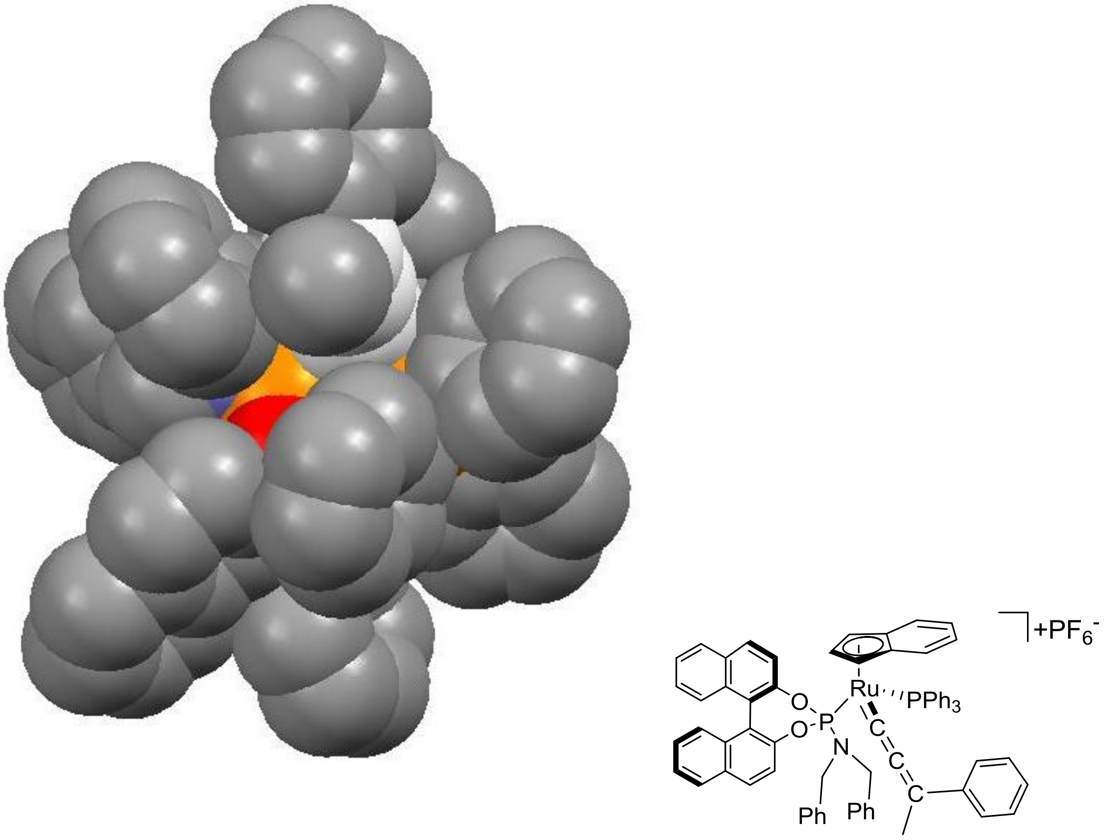

Figure 5.5. A space-filled model of complex **116b**.

For the allenylidene complexes with protons on C_δ, in no case was the formation of vinylvinylidenes observed. Often allenylidenes with protons on C_δ are formed in competition with vinylvinylidenes (**118** in Scheme 5.12).[5] Dehydration of the intermediate hydroxy vinylidene species can occur via loss of the vinylidene proton (to give the allenylidene **116b**) or the δ-proton (to give the vinylvinylidene **118**). Vinylvinylidenes are disfavored for sterically very hindered complexes as the bent geometry of the ligand creates a greater disfavorable steric interaction relative to the linear geometry of the allenylidene.[5]

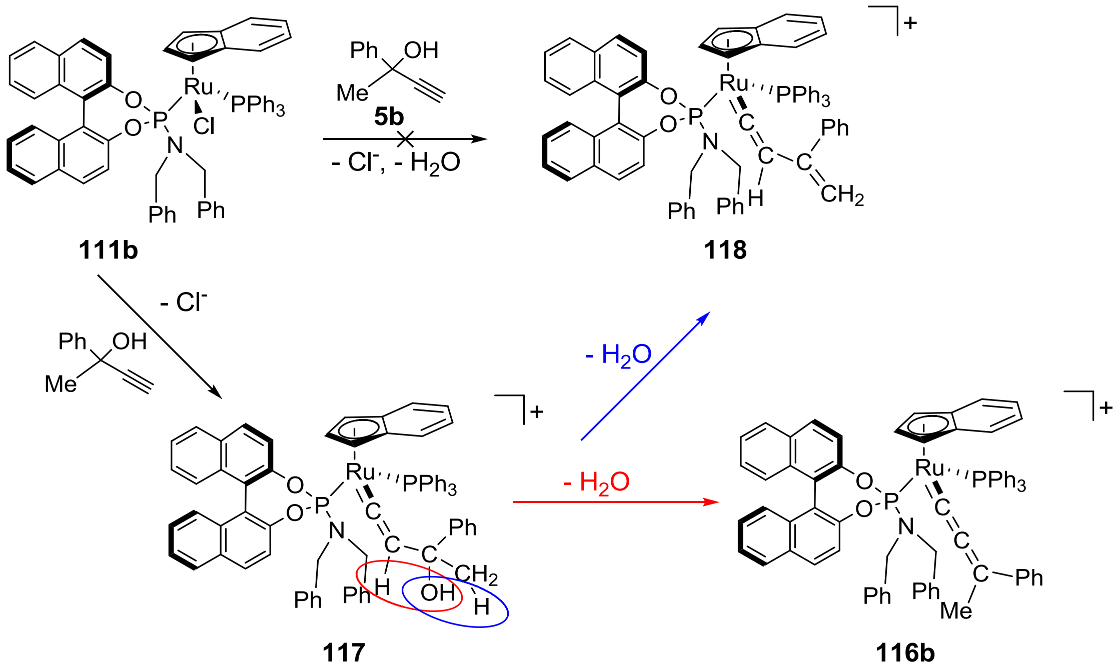

Scheme 5.12. Allenylidene versus vinylvinylidene formation.

Although the allenylidene formation proceeded without formation of vinylvinylidenes for a variety of aryl methyl propargylic alcohols, the reaction failed for aliphatic propargylic alcohols. When aliphatic propargylic alcohols such as 1-ethynyl-1-cyclohexanol (**5c**) or 3,5-dimethyl-1-hexyn-3-ol (**5f**) were reacted with **111b** under the standard conditions shown in Scheme 5.11, no single major product was formed (Scheme 5.13). Instead, numerous unidentifiable signals were observed in the ^{31}P and ^{1}H NMR spectra. It is clear that the aryl substituent on the allenylidene must have some sort of stabilizing effect.

As a way of testing the stabilizing effect of the aryl substituent, the secondary propargylic alcohol 1-phenyl-2-propyn-1-ol (**5d**) was employed in allenylidene synthesis (Scheme 5.14). Although this reaction does not give a wide range of products similar to that observed in reactions of aliphatic propargylic alcohols (Scheme 5.13), it does not proceed so cleanly as the reactions of the tertiary aromatic propargylic alcohols (observed by ^{31}P NMR). Two major products are clearly visible in the ^{31}P NMR (170.9, 51.1 ppm and 168.6, 48.3 ppm). It is possible that these products are diastereomers (**119**), likely differing in the configuration on the allenylidene chain (i.e. the orientation of the phenyl ring). Only tertiary aromatic propargylic alcohols are capable of forming allenylidenes in high yield as single diastereomers.

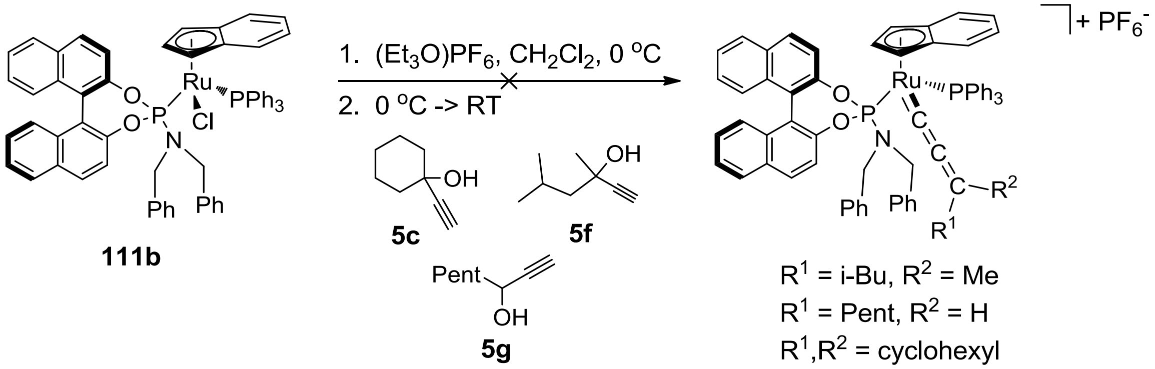
111b
1. (Et3O)PF6, CH2Cl2, 0 °C
2. 0 °C -> RT
5c
5f
5g
Pent
OH
R1 = i-Bu, R2 = Me
R1 = Pent, R2 = H
R1,R2 = cyclohexyl
+ PF6-
PPh3
Cl
Ph
Ph

Scheme 5.13. Attempted synthesis of aliphatic allenylidenes.

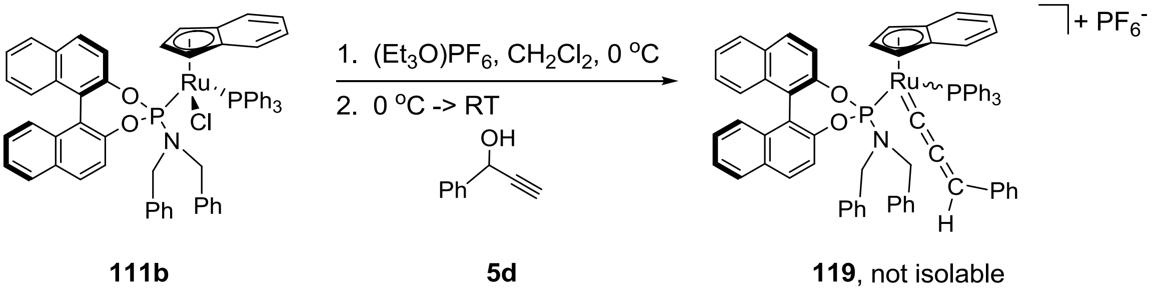
1. (Et3O)PF6, CH2Cl2, 0 °C
2. 0 °C -> RT
111b
5d
119, not isolable
+ PF6-
PPh3
Cl
Ph
Ph
OH
H

Scheme 5.14. Synthesis of a secondary allenylidene.

After establishing the stability rules for allenylidenes derived from complex **111b**, complexes **111a, c-d** were tested for their ability to form allenylidenes as well with the results for **111d** shown in Scheme 5.15. In the case of complexes **111a**, **c** the reaction proceeded only very slowly and side product formation was evident in the ^{1}H and ^{31}P NMR spectra of the crude reaction mixtures. Better results were obtained for complex **111d**. After activation with $(Et_3O)PF_6$ in CH_2Cl_2, 1,1-diphenyl-2-propyn-1-ol (**53a**) reacts with the cationic fragment [(Ind)Ru(PPh_3)(**41e**)]PF_6 to give allenylidene **120a**.

Similarly, allenylidenes **120b, c** can be obtained from the corresponding propargylic alcohols.

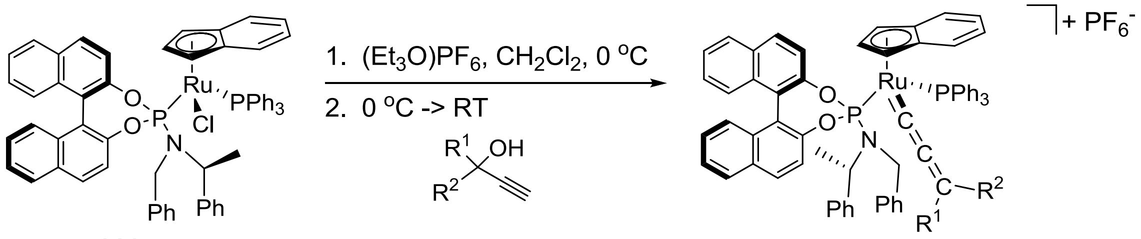

111d

$R^1 = R^2 = Ph$ **120a**
$R^1 = Ph, R^2 = Me$ **120b**
$R^1 = 2\text{-furyl}, R^2 = Me$ **120c**

Scheme 5.15. Synthesis of allenylidenes **120**.

The new allenylidenes **120** are not as easily recrystallized as their counterparts **116**. The excess propargylic alcohol can be removed by washing the solids with Et_2O, giving **120** as purple solids in ca. 90% spectroscopic purity. The new allenylidenes are only moderately stable in solution, showing significant decomposition (^1H, ^{31}P NMR) after 6-12 h time.

5.3.3. Catalytic activation of propargylic alcohols

Because it was shown that **111b** is able to form stable allenylidenes, the chloride abstracted species $[(Ind)Ru(PPh_3)($**41b**$)]^+$ was also tested for activity in a variety of catalytic propargylic substitution reactions. The propargylic alcohols 1,1-diphenyl-2-propyn-1-ol (**5a**) and 2-phenyl-3-butyn-2-ol (**5b**), 1-phenyl-2-propyn-1-ol (**5d**) and 1-octyn-3-ol (**5g**) were all used in test reactions with nucleophiles such as *t*-butyl amine, diethyl amine, *N*-methylbenzyl amine, methanol, 1,2-ethanedithiol and 1,3-pentanedione. THF and CH_2Cl_2 were used as solvent. When performed at ambient temperature all reactions failed. Additives such as DBU (1,8-diazabicyclo[5.4.0]-undec-7-ene), NaOMe or NH_4PF_6 do not improve the results.

Because it has been shown that the activated complex $[(Ind)Ru(PPh_3)(\mathbf{41b})]^+$ forms stable allenylidenes upon reaction with at least some of the tested propargylic alcohols, it is possible that the catalytic cycle is simply halted at this or another intermediate. Thus the reactions were performed at elevated temperatures in an attempt to drive the reaction forward. At 80 ^{o}C, the reaction of various amines with propargylic alcohols still does not proceed. Reaction of 1,1-diphenyl-2-propyn-1-ol (**5a**) or 2-phenyl-3-butyn-2-ol (**5b**) with methanol at 80 ^{o}C in 1,2-dichloroethane (DCE) or THF does proceed to some extent. Using 1 mol% catalyst and one equivalent of methanol at 80 ^{o}C, 30-40% conversion is achieved after 20 h (determined by ^{1}H NMR). The reaction does not work for 1-phenyl-2-propyn-1-ol (**5d**) or 1-octyn-3-ol (**5g**), suggesting that perhaps propargylic cations are involved as intermediates in place of allenylidenes. Excess methanol or addition of catalytic base (DBU or NaOMe) retard or completely inhibit the reaction.

The lack of reactivity observed in the case of amine nucleophiles and the decrease in rate observed for alcohol nucleophiles in the presence of base indicates that metal coordination of the nucleophile is a problem. This means that for optimal reactivity a non-coordinating nucleophile is necessary. Electron-rich aromatic compounds such as 1,3-dimethoxybenzene can undergo a Friedel-Crafts type alkylation with an allenylidene as the electrophile.[14] Secondary propargylic alcohols have been shown to be most active in this type of reaction for previously reported catalysts.[14]

When 1-phenyl-2-propyn-1-ol (**5d**) was reacted with electron rich compounds at 85 ^{o}C in DCE in the presence of catalytic (1 mol%) [(Ind)Ru(PPh$_3$)(**41b**)]PF$_6$ and 10 mol% NH$_4$PF$_6$, the corresponding propargylated aromatic compounds are obtained (Scheme 5.16). Various solvents were screened for the reaction including DCE, THF, toluene and chlorobenzene. Among these, chlorobenzene and DCE performed the best followed by toluene. THF is not a suitable solvent for this reaction. The reaction was also run at a variety of different temperatures. Not surprisingly, the reaction does not occur at ambient temperature. Unexpectedly, however, the reaction runs best at 50 ^{o}C and slows down at higher temperatures (50 ^{o}C > 65 ^{o}C > 85 ^{o}C). A probable reason for the observed reactivity is decomposition of the catalyst. At elevated temperatures, the rate of decomposition is likely higher, effectively decreasing the catalyst load. The addition of catalytic amounts (~10 mol%) of NH$_4$PF$_6$ is necessary for the reaction.

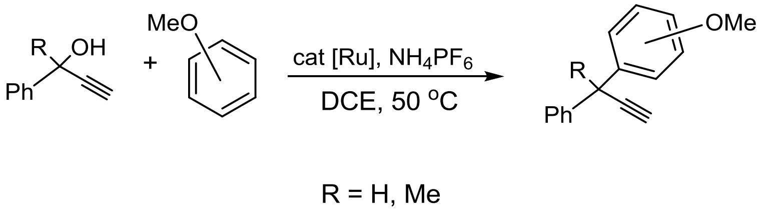

Scheme 5.16. Catalytic propargylic substitution with electron-rich aromatics.

Using the optimized conditions (chlorobenzene or DCE as solvent, 50 ^{o}C, 1 mol% catalyst, 10 mol% NH$_4$PF$_6$, 24 h), the conversion still does not exceed 70% for a number of dimethoxybenzene derivatives (Table 5.3). Isolation of the products proved difficult, and none of the products were isolated in greater than 50% yield in 90+% spectroscopic purity. Addition of an excess of the dimethoxybenzene, increased catalyst loading or increased reaction times do not significantly improve the results (Table 5.3, entries 3, 4).

In most cases, a mixture of regioisomers is also observed in the products. Overall, the activity of the catalyst appears to be too low to give satisfactory results.

Table 5.3. Substitution of propargylic alcohols by electron-rich aromatics.

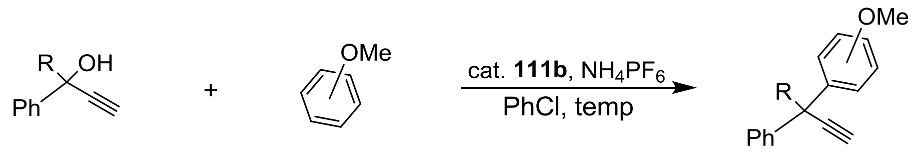

Entry	Substrates	Temperature/°C	Yield[a]
1	R = H, Ar = 1,3-dimethoxybenzene	85	45%
2	R = H, Ar = 1,3-dimethoxybenzene	85	49%[b]
3	R = H, Ar = 1,3-dimethoxybenzene	85	51%[c]
4	R = H, Ar = 1,3-dimethoxybenzene	85	60%[d]
5	R = H, Ar = 1,3-dimethoxybenzene	65	63%
6	R = H, Ar = 1,3-dimethoxybenzene	50	70%
7	R = Me, Ar = 1,3-dimethoxybenzene	85	29%[d]
8	R = H, Ar = 1,2-dimethoxybenzene	85	56%
9	R = H, Ar = 1,4-dimethoxybenzene	85	34%
10	R = H, Ar = 2,3-dimethoxytoluene	85	45%[e]

[a] Yields determined by GC/MS. Conditions: propargylic alcohol (0.5 mmol), aromatic (0.5 mmol), catalyst **111b** (0.005 mmol), catalytic NH_4PF_6 (0.05 mmol) 24 h in chlorobenzene (2 mL) at 85 °C.
[b] 2 Equivalents 1,3-dimethoxybenzene were used. [c] 0.010 mmol **111b**.
[d] 48 h reaction time. [e] Determined by ^1H NMR.

A possible catalytic cycle for substitution reactions of propargylic alcohols catalyzed by [(Ind)Ru(PPh_3)(**41b**)]$^+$ is depicted in Scheme 5.17. Formation of an allenylidene intermediate is hypothesized, but instead of immediate attack of the nucleophile at C_γ of the allenylidene (commonly hypothesized for similar reactions),[14] protonation of C_β by NH_4^+ is proposed. The resulting alkenylcarbyne is more electrophilic and thus able to react with weaker nucleophiles such as aromatic compounds. Attack at C_γ now gives the vinylidene which, upon demetalation, gives the product and regenerates the active catalyst. This type of mechanism has been proposed previously, and stoichiometric experiments verify its plausibility.[7]

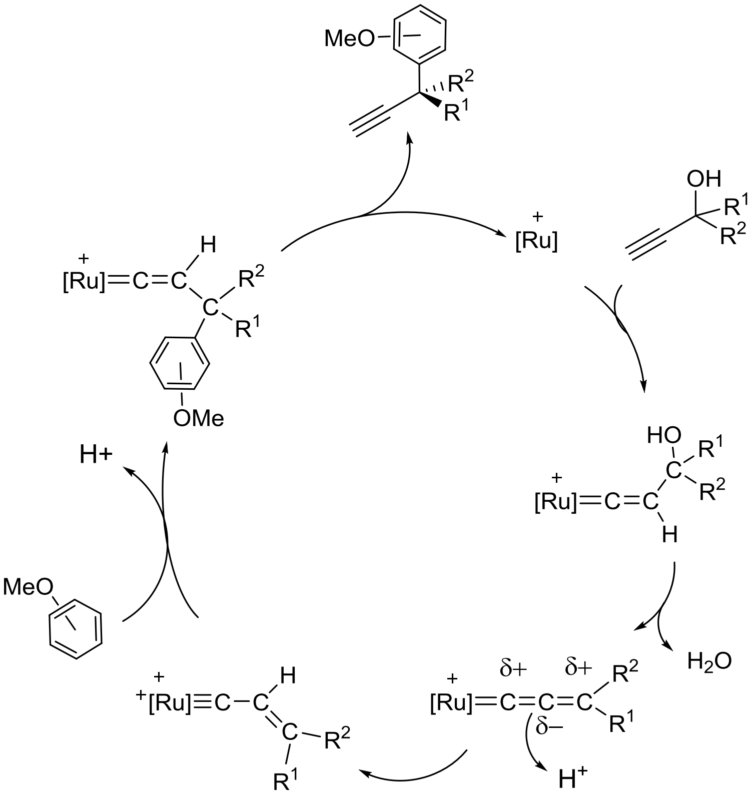

Scheme 5.17. Proposed catalytic cycle for propargylic substitution.[7]

5.4. Discussion

5.4.1. Ligand substitution in indenyl ruthenium phosphine complexes

Substitution reactions of the precursor [(Ind)RuCl(PPh_3)$_2$] (**110**), exchanging one phosphine for a phosphoramidite ligand occurs much more quickly than in the case of the corresponding Cp complex [CpRuCl(PPh_3)$_2$] (**68**) (4 h vs. 15 h at 60 °C). This enhanced reactivity can be correlated to the indenyl effect as described above (Scheme 5.16). It is unlikely that for this reaction the indenyl effect is solely the result of a more facile η^5-η^3 ring slip. Gimeno et al. reported that this same precursor complex undergoes exchange of PPh_3 by secondary phosphines (HPR_2) via a dissociative mechanism.[15] He in turn argues that the observed rate increase for the indenyl complex relative to the cyclopentadienyl one is the result of an increase in the metal-arene bond strength of the 16 electron intermediate relative to the stable 18 electron reactant and product. Gimeno claims that this difference in relative bond strengths is greater for the indenyl complex, thus enhancing the rate of the reaction. It is likely that substitution of the complex $[(Ind)RuCl(PPh_3)_2]$ (**110**) by phosphoramidite ligands **41a-b, e**, **114** occurs by the same mechanism (Scheme 5.18).

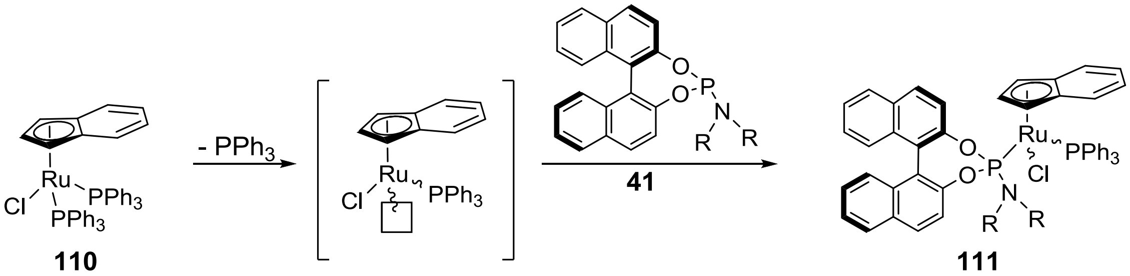

Scheme 5.18. Proposed mechanism of substitution.

Worth mention is also the fact that a significant increase in diastereoselectivity for the substitution reaction is observed in changing from the cyclopentadienyl complexes $[CpRuCl(PPh_3)(\mathbf{41})]$ (**69**) to the indenyl complexes $[(Ind)RuCl(PPh_3)(\mathbf{41})]$ (**111**). Two phosphoramidite ligands **41a, b** were used in the synthesis of both the Cp complexes $[CpRuCl(PPh_3)(\mathbf{41})]$ (**69**) and the indenyl complexes $[(Ind)RuCl(PPh_3)(\mathbf{41})]$ (**111**). The diastereoselectivity of the complexes bearing **41a** increased from 30% to 33%

diastereomeric excess (d.e.), a minor improvement. A much more marked improvement was observed for the complex bearing **41b** moving from 78% d.e. to >98% d.e. (a second diastereomer is never observed in the ^{1}H or ^{31}P NMR spectra). The complete lack of diastereoselectivity for complex **111c** and the formation of a single diastereomer of complex **111d** together suggest that size alone, and not the position of the stereocenter relative to the metal, controls diastereoselectivity.

5.4.2. Allenylidene formation

Activation of complex **111b** by chloride abstraction using $(Et_3O)PF_6$ or $AgPF_6$ results in a reactive intermediate $[(Ind)Ru(PPh_3)($**41b**$)]PF_6$. Formation of this intermediate in a CH_2Cl_2 solution results in a slight darkening of the solution from orange to red. In the absence of a nucleophile this red color will persist for at least 2 h. Indeed, addition of 1,1-diphenyl-2-propyn-1-ol (**5a**) to a solution containing the reactive intermediate 2 h after activation gives the expected allenylidene complex **116a** without significant signs of decomposition (the chloride abstraction reaction was complete within 1 h at 0 ^{o}C) (Scheme 5.11). This observation is important because in the case of the analogous Cp complex $[CpRuCl(PPh_3)($**41b**$)]$ (**69b**), activation by chloride abstraction seems to more readily lead to decomposition pathways (Chapter 3).

The decomposition of the chloride abstracted species $[CpRuCl(PPh_3)($**41b**$)]^+$ could be seen visually in many cases, the solution turning from red to brown or green. Always in these cases reaction with 1,1-diphenyl-2-propyn-1-ol (**5a**) resulted in some product formation, but decomposition was always evident and a mixture of products was obtained. One possible explanation for the increased stability of

$[(\text{Ind})\text{RuCl}(\text{PPh}_3)(\mathbf{41b})]^+$ relative to $[\text{CpRuCl}(\text{PPh}_3)(\mathbf{41b})]^+$ is increased metal-arene bond strength. The same explanation given by Gimeno to explain the indenyl effect in phosphine substitution applies to this phenomenon.[15] Again the intermediate is a 16 electron complex; the difference being that this one is cationic (Schemes 5.18, 5.19). The increased stability of the intermediate was used to explain the observed rate increase in the substitution reaction, but in the case of chloride abstraction the reaction is done under more forcing conditions. Thus instead of a measurable rate increase, a lack of decomposition reactions is observed.

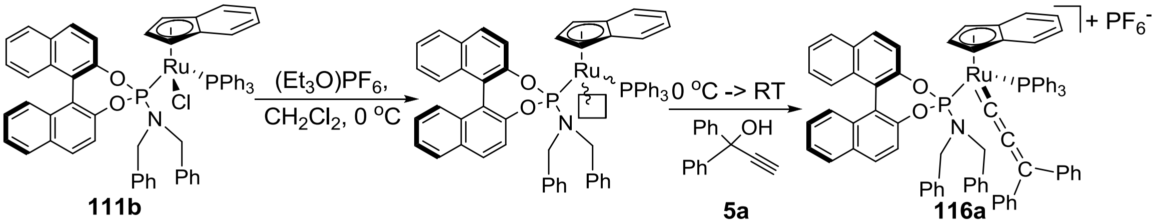

Scheme 5.19. The indenyl effect in allenylidene formation.

A significant difference in stability of the chloride abstracted species of **111b** and **111d** is also observed. Upon chloride abstraction from **111b** or **111d**, the resulting complexes both react with propargylic alcohols **5** to form allenylidenes (**116**, **120** respectively). In the case of **111d** the results proved to be inconsistent when attempts to reproduce them were undertaken, although the cause could not be determined. In some cases the reaction to obtain **120** proceeds cleanly after activating for 30 min or for 60 min but in other cases significant side products are formed after similar activation times. It cannot be ruled out that trace amounts of water or oxygen somehow disturbs the reaction but the former is formed in an equimolar amount during allenylidene formation so it is improbable that this is the cause of the observed inconsistencies.

The allenylidenes **120a-c** also show considerably less stability than the analogous **116a-c**. For complexes **120b, c** suitable ^{13}C NMR spectra were unobtainable due to ongoing decomposition. C_{α} appears very weakly in all the allenylidene ^{13}C NMR spectra and in most cases it is additionally coupled. Thus in the time required for data collection, the complexes **120b, c** were undergoing decomposition and additional peaks become visible. Also in the ^{1}H NMR of the allenylidenes the integration of the protons in the aromatic region (6.5-8.0 ppm) is consistently above expected, despite the fact that no additional peaks can be seen elsewhere. Combustion analysis of the allenylidenes gives a wt% carbon below expected, suggesting hydrolytic or oxidative decomposition of the complexes (Experimental).

5.4.3. Nucleophilic addition to allenylidenes

The above described allenylidenes are susceptible to nucleophilic attack by strong nucleophiles. For example, the diphenyl allenylidene (**116a**) was reacted with MeLi in THF at 0 ^{O}C. Upon addition of MeLi, the solution immediately turned from dark purple to orange. FAB MS of the crude reaction mixture confirmed the addition of the methyl group. In the IR, the allenylidene stretch at 1935 cm^{-1} disappeared as expected. However, the new complex was could not be isolated. Although γ-attack by the incoming nucleophile is likely,[3,4] the data did not firmly distinguish α- vs. γ- attack.

Other nucleophiles such as amines, thiols and alkoxides also react with the new allenylidene complexes as evidenced by an immediate color change. Reaction of complexes **116a, b** with *t*-butyl amine, diethyl amine, 1,2-ethanedithiol or sodium methoxide results in a color change from purple to orange (Scheme 5.20). NMR analysis

(^{1}H, ^{31}P) does not clearly reveal the nature of the products. FAB MS of the crude reaction mixtures in no case reveals a molecular ion peak, showing instead only a peak corresponding to the starting allenylidene, consistent with loss of the nucleophile. Reaction with weak nucleophiles such as H_2O or methanol does not occur after prolonged times (>24 h) at ambient temperature.

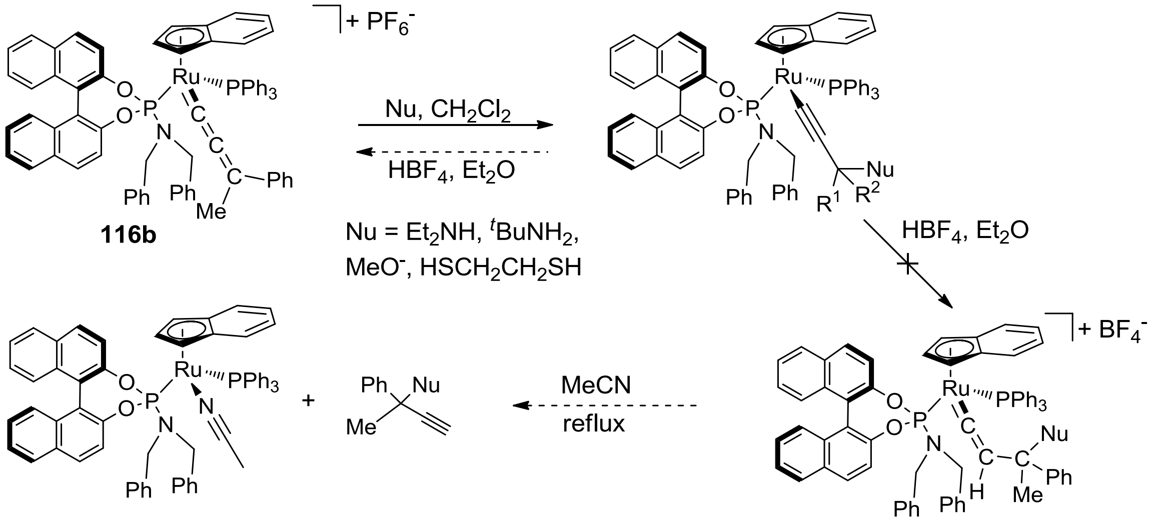
+ PF6-
Ru
PPh3
O
P
N
C
C
C
Ph
Ph
Ph
Me
116b
Nu, CH2Cl2
HBF4, Et2O
Nu = Et2NH, tBuNH2,
MeO-, HSCH2CH2SH
Nu
R1
R2
HBF4, Et2O
+ BF4-
H
Me
MeCN
reflux
+
Ph
Nu
Me

Scheme 5.20. Nucleophilic attack on allenylidene **116b**.

Stoichiometric multi-step substitution reactions of propargylic alcohols have been reported previously.[4,7] After nucleophilic attack to give the η^1-alkynyl complex, protonation with HBF_4 gives the vinylidene. Subsequent demetalation in refluxing acetonitrile liberates the substituted alkyne (Scheme 5.6). This sequence was attempted for complex **116b**, but the expected products were not obtained (Scheme 5.20). It is possible that protonation with HBF_4 does not give the desired vinylvinylidene but instead gives back the starting allenylidene as reverse reactions of this type have been reported previously (Scheme 5.2).[3]

5.5. Summary and Prospective

New mixed phosphine/phosphoramidite indenyl complexes of ruthenium have been synthesized. Like the cyclopentadienyl complexes, the indenyl complexes show a pronounced steric effect in diastereoselectivity in complex formation. The most sterically encumbered ligands give the corresponding complexes with complete diastereoselectivity. Smaller ligands showed little or no preference for one stereoisomer (≤ 2:1 d.r.). X-ray crystallography reveals that the indenyl complex has the same absolute configuration about ruthenium as for the analogous cyclopentadienyl complex (Chapter 3).

One of these new complexes has been converted to the first phosphoramidite allenylidene complexes by employing a variety of propargylic alcohols. They are all isolated in high yield as purple solids and are fully characterized. The complexes are formed as single diastereomers, beginning from diastereopure precursor complexes. The absolute configuration of the precursor complexes and the allenylidenes is the same, giving overall retention of configuration. Electron-rich as well as electron-poor propargylic alcohols can be used in the synthesis, but only tertiary propargylic alcohols bearing at least one aromatic substituent at C_γ form stable, isolable allenylidenes. Allenylidenes with δ-protons do not form vinylvinylidenes, contrary to many previously reported complexes.

The complex formed by chloride abstraction from one of the indenyl complexes is catalytically active in substitution of propargylic alcohols be electron-rich aromatics. 1-phenyl-2-propyn-1-ol shows the highest reactivity, but 2-phenyl-3-butyn-2-ol shows activity as well. Aliphatic propargylic alcohols do not undergo the desired reaction.

Even after optimization of the reaction conditions, low conversions are observed (~50%). The catalytic cycle is hypothesized to proceed via an allenylidene intermediate.

---

[1] Calhorda, M. J.; Ramao, C. C.; Veiros, M. C. *Chem. Eur. J.* **2002**, *8*, 868.

[2] Basolo, F. *Coord. Chem. Rev.* **1982**, *43*, 7.

[3] Cadierno, V.; Gamasa, M. P.; Gimeno, J.; Lastra, E. *J. Organomet. Chem.* **1994**, *474*, C27.

[4] (a). Cadierno, V.; Conejero, S.; Gamasa, M. P.; Gimeno, J.; Pérez-Carreño, E.; García-Granda, S. *Organometallics* **2001**, *20*, 3175; (b). Cadierno, V.; Conejero, S.; Gamasa, M. P.; Gimeno, J.; Rodriguez, M. A. *Organometallics* **2002**, *21*, 203; (c). Cadierno, V.; Conejero, S.; Gamasa, M. P.; Gimeno, J. *Dalton Trans.* **2003**, 3060; (d). Nishibayashi, Y.; Imajima, H.; Onodera, G.; Uemura, S. *Organometallics* **2005**, *24*, 4109.

[5] Selegue, J. P.; Young, B. A.; Logan, S. L. *Organometallics* **1991**, *10*, 1972.

[6] (a). Cadierno, V.; Gamasa, M. P.; Gimeno, J.; González-Bernardo, C. *Organometallics* **2001**, *20*, 5177; (b). Cadierno, V.; Gamasa, M. P.; Gimeno, J.; Borge, J.; Garcia-Granda, S. *Organometallics* **1997**, *16*, 3178.

[7] (a). Bustelo, E.; Jiménez-Tenorio, M.; Puerta, M. C. ; Valerga, P. *Organometallics* **2006**, *25*, 4019; (b). Bustelo, E.; Jiménez-Tenorio, M.; Puerta, M. C. ; Valerga, P. *Organometallics* **2007**, *26*, 4300; (c). Pino-Chamorro, J. A.; Bustelo, E.; Puerta, M. C. ; Valerga, P. *Organometallics* **2009**, *28*, 1546.

[8] Cadierno, V.; Gamasa, M. P.; Gimeno, J.; Lastra, E.; Borge, J.; Garcia-Granda, S. *Organometallics* **1994**, *13*, 745.

[9] (a). Gamasa, M. P.; Gimeno, J.; Martín-Vaca; B. M. *Organometallics* **1998**, *17*, 3707; (b). Bieger, K.; Díez, J.; Gamasa, M. P.; Gimeno, J.; Pavlišta, M.; Rodríguez–Alvarez, Y.; García–Granda, S.; Santiago–García, R. *Eur. J. Inorg. Chem.* **2002**, 1647.

[10] Costin, S.; Rath, N. P.; Bauer, E. B. *Tetrahedron Lett.* **2009**, *50*, 5485.

[11] (a). Hulst, R.; de Vries, N. K.; Feringa, B. L. *Tetrahedron: Asymmetry* **1994**, *5*, 699; (b). Rimkus, A.; Sewald, N. *Org. Lett.* **2003**, *5*, 79.

[12] Smith, C. R.; Mans, D. J.; RajanBabu, T. V. *Organic Syntheses* **2008**, *85*, 238.

[13] Costin, S.; Rath, N. P.; Bauer, E. B. *Inorg. Chim. Acta* **2009**, *362*, 1935.

[14] (a). Inada, Y.; Nishibayashi, Y.; Uemura, S. *Angew. Chem. Int. Ed.* **2005**, *44*, 7715; (b). Matsuzawa, H.; Miyake, Y.; Nishibayashi, Y. *Angew. Chem. Int. Ed.* **2007**, *46*, 6488; (c). Matsuzawa, H.; Kanao, K.; Miyake, Y.; Nishibayashi, Y. *Org. Lett.* **2007**, *9*, 5561; (d). Daini, M.

Yoshikawa, M.; Inada, Y.; Uemura, S.; Sakata, K.; Kanao, K.; Miyake, Y.; Nishibayashi, Y. *Organometallics* **2008**, *27*, 2046.

[15] Gamasa, M. P.; Gimeno, J.; Gonzalez–Bernardo, C.; Martín-Vaca; B. M. *Organometallics* **1996**, *15*, 302.

Experimental Section

General. Chemicals were treated as follows: THF, toluene, diethyl ether (Et_2O), distilled from Na/benzophenone; CH_2Cl_2, distilled from CaH_2. (R)-1,1'-binaphthyl-2,2'-diol ((R)-BINOL) (Strem), catechol (**113**) (Fisher), phosphorus trichloride (PCl_3), *N*-methyl-2-pyrrolidinone (Acros), (R)-2-methylpyrrolidine (Aldrich),1,1-diphenyl-2-propyn-1-ol (**5a**) (Aldrich), 2-phenyl-3-butyn-2-ol (**5b**) (Aldrich), $(Et_3O)PF_6$ (Aldrich), Celite® (Aldrich), *t*-butylmethyl ether (Aldrich) and other materials, used as received. "(R)-BINOL-*N,N*-dimethyl-phosphoramidite" **41a**,[1a] "(R)-BINOL-*N,N*-dibenzyl-phosphoramidite" **41b**,[1b] "(R)-BINOL-*N*-dibenzyl-*N*-α-methylbenzyl-phosphoramidite" **41e**[1c] and $[RuCl(Ind)(PPh_3)_2]$ (**110**, Ind = indenyl anion)[2] were synthesized according to literature procedures.

NMR spectra were obtained at room temperature on a Bruker Avance 300 MHz or a Varian Unity Plus 300 MHz instrument and referenced to a residual solvent signal; all assignments are tentative. Exact masses were obtained on a JEOL MStation [JMS-700] Mass Spectrometer. Melting points are uncorrected and were taken on an Electrothermal 9100 instrument. IR spectra were recorded on a Thermo Nicolet 360 FT-IR spectrometer. Elemental Analyses were performed by Atlantic Microlab Inc., Norcross, GA, USA.

"**(R)-catechol-2-methyl-pyrrolidine-phosphoramidite**", (R)-**114**. To a Schlenk flask containing catechol (0.402 g, 3.65 mmol), phosphorus trichloride (PCl_3) was added (2.0 mL, 23 mmol) followed by *N*-methyl-2-pyrrolidinone (0.01 mL, 0.1 mmol). The resulting slurry was heated to reflux for 30 min. Excess PCl_3 was removed by oil pump vacuum, yielding a yellow liquid. Et_2O (5.0 mL) was added and removed under vacuum twice to remove remaining PCl_3. The liquid was dissolved in THF (12 mL) and triethyl amine was added (0.83 mL, 6.3 mmol) followed by (R)-2-methylpyrrolidine (0.32 mL, 3.2 mmol). After stirring for 1 h at RT, the resulting slurry was filtered over Celite® and the solvent removed under vacuum. The yellow liquid was dissolved in CH_2Cl_2 (30 mL), and extracted with 2 × 30 mL saturated $NaHCO_3$ (aq). The organic layer was dried over Na_2SO_4, filtered, and the volatiles removed by oil pump vacuum, yielding (R)-**114** as a yellow oil. (0.569 g, 2.55 mmol, 78%). Found: C, 58.90; H, 6.31. Calc. for $C_{11}H_{14}NO_2P$: C, 59.19; H, 6.32.

NMR (δ, $CDCl_3$) ^{1}H 6.92-6.84 (m, 2H, Ph), 6.82-6.75 (m, 2H, Ph), 3.79-3.63 (m, 1H, NC*H*CH_3), 2.92-2.73 (m, 2H, NCH_2), 1.90-1.78 (m, 1H, C*H*H’), 1.77-1.52 (m, 2H, CH_2), 1.41-1.29 (m, 1H, CH*H*’), 1.11 (d, $^3J_{HH}$ = 6.4 Hz, 3H, CH_3); $^{13}C\{^1H\}$ 146.8 (d, $^2J_{CP}$ = 8.1 Hz, *C*O), 146.6 (d, $^2J_{CP}$ = 8.1 Hz, *C*’O), 122.0 (s, Ph), 111.5 (s, Ph), 54.5 (d, $^2J_{CP}$ = 22.2 Hz, N*C*H), 44.3 (d, $^2J_{CP}$ = 4.1 Hz, N*C*H_2), 34.6 (d, $^3J_{CP}$ = 3.5 Hz, *C*H_2), 24.9 (d, $^3J_{CP}$ = 1.6 Hz, *C*H_2), 24.0 (d, $^3J_{CP}$ = 8.3 Hz, *C*H_3); $^{31}P\{^1H\}$ 145.0 (s).

HRMS calcd for $C_{11}H_{14}NO_2P$ 223.0762, found 223.0755. IR (neat solid, cm^{-1}) 3061(m) , 2966(s), 2871(s), 1604(m), 1483(s), 1335(s), 1240(s), 859(s), 745(s).

“**[(Ind)RuCl (PPh_3)((R)-catechol-2-methylpyrrolidine-phosphoramidite)**” (**111c**). To a Schlenk flask containing [RuCl(Ind)$(PPh_3)_2$] (**110**) (0.109 g, 0.141 mmol), phosphoramidite (R)-**114** (0.032 g, 0.14 mmol) was added as a solution in toluene (3 mL). The mixture was heated to 65 °C for 2 h after which the solvent was removed by oil pump vacuum. The resulting red solid was purified by flash chromatography, employing 1 × 11 cm silica. The remaining ligand and PPh_3 were eluted using CH_2Cl_2, then the complex was eluted using CH_2Cl_2/*t*-butylmethyl ether 9:1 (v/v), collecting the red band. The solvent was removed by oil pump vacuum, giving complex **111c** as an orange solid in a 1:1 diastereomeric mixture (0.069 g, 0.094 mmol, 67%), m.p. 99–100 °C dec. (capillary). Found: C, 61.07; H, 4.96. Calc. for $C_{38}H_{36}NO_2P_2ClRu$: C, 61.91; H, 4.92.

NMR (δ, $CDCl_3$)[3] ^1H 7.74–7.57 (m, 2H, aromatic), 7.33–6.94 (m, 34H, aromatic), 6.90–6.73 (m, 3H, aromatic), 6.73–6.57 (m, 3H, aromatic), 6.51–6.37 (m, 2H, aromatic), 6.00–5.85 (m, 2H, aromatic), 5.09 (s, br, 1H, indenyl), 4.92 (s, br, 2H, indenyl), 4.69 (s, br, 1H, indenyl), 4.31 (s, br, 1H, indenyl), 4.01 (s, br, 1H, indenyl), 3.89–3.79 (m, 1H, $NCHCH_3$), 3.79–3.69 (m, 1H, $NCHCH_3$*), 3.45–3.32 (m, 1H, NC*H*H'), 3.21–3.08 (m, 1H, NC*H*H'*), 2.91–2.80 (m, 1H, NCH*H*'), 2.78–2.65 (m, 1H, NCH*H*'*), 1.89–1.57 (m, 5H, $2CH_2$, C*H*H'), 1.57–1.44 (m, 1H, C*H*H'*), 1.37–1.23 (m, 2H, 2CH*H*'), 0.96 (d, $^3J_{HH}$ = 6.4 Hz, 3H, CH_3), 0.81 (d, $^3J_{HH}$ = 6.4 Hz, 3H, CH_3*); $^{13}C\{^1H\}$ 148.2 (d, J_{CP} = 5.6 Hz, aromatic), 147.6 (d, J_{CP} = 6.9 Hz, aromatic), 147.0 (d, J_{CP} = 5.0 Hz, aromatic), 146.1 (d, J_{CP} = 5.6 Hz, aromatic), 136.8 (s, aromatic), 136.5 (s, aromatic), 136.1 (s, aromatic), 135.9 (s, aromatic), 134.2 (d, J_{CP} = 2.7 Hz, aromatic), 134.1 (d, J_{CP} = 2.1 Hz, aromatic), 129.5 (d, J_{CP} = 2.2 Hz, aromatic), 129.4 (d, J_{CP} = 2.2 Hz , aromatic), 128.4 (s, aromatic), 128.3 (s, aromatic), 127.7 (d, J_{CP} = 7.1 Hz, aromatic), 127.6 (d, J_{CP} = 6.7 Hz, aromatic), 127.2 (s, aromatic), 126.5 (d, J_{CP} = 5.2 Hz, aromatic), 125.7 (s, aromatic), 123.9 (s, aromatic), 121.3 (d, J_{CP} = 4.0 Hz, aromatic), 121.0 (d, J_{CP} = 2.0 Hz, aromatic), 115.2 (d, $^2J_{CP}$ = 3.8 Hz, indenyl), 114.1 (s, br, indenyl), 111.3 (d, $^2J_{CP}$ = 7.7 Hz, indenyl*), 110.9 (d, $^2J_{CP}$ = 7.0 Hz, indenyl*), 110.7 (d, J_{CP} = 4.5 Hz, aromatic), 109.9 (d, J_{CP} = 7.7 Hz, aromatic), 109.7 (d, J_{CP} = 7.0 Hz, aromatic), 108.4 (s, br, aromatic), 91.4 (s, indenyl), 90.7 (s, indenyl*), 69.8 (d, $^2J_{CP}$ = 14.3 Hz, indenyl), 68.4 (d, $^2J_{CP}$ = 8.5 Hz, indenyl), 66.7 (d, $^2J_{CP}$ = 5.9 Hz, indenyl*), 64.3 (d, $^2J_{CP}$ = 2.6 Hz, indenyl*), 54.8 (s, N*C*H), 54.4 (s, N*C*H*), 47.2 (d, $^2J_{CP}$ = 10.7 Hz, N*C*H$_2$), 47.0 (d, $^2J_{CP}$ = 9.2 Hz, N*C*H$_2$*), 34.7 (d, J_{CP} = 3.8 Hz, *C*H$_2$), 34.5 (d, J_{CP} = 4.9 Hz, *C*H$_2$*), 25.4 (d, J_{CP} = 5.8 Hz, *C*H$_2$), 25.1 (d, J_{CP} = 6.0 Hz, *C*H$_2$*), 23.1 (s, br, *C*H$_3$), 22.7 (s, br, *C*H$_3$*); ^{31}P{^{1}H} 180.2 (d, $^2J_{PP}$ = 77.0 Hz, phosphoramidite), 176.8 (d, $^2J_{PP}$ = 72.8 Hz, phosphoramidite*), 61.9 (d, $^2J_{PP}$ = 77.0 Hz, *P*Ph$_3$), 55.6 (d, $^2J_{PP}$ = 72.8 Hz, *P*Ph$_3$*).

HRMS calcd for $C_{38}H_{36}NO_2P_2{}^{35}Cl^{102}Ru$ 737.0952, found 737.0950. IR (neat solid, cm^{-1}) 3051(w), 2964(w), 1479(m), 1235(m), 1090(m), 818(m).

"[(Ind)RuCl(PPh$_3$)((R)-BINOL-*N,N*-dimethyl-phosphoramidite)]" (**111a**). To a Schlenk flask containing [RuCl(Ind)(PPh$_3$)$_2$] (0.218 g, 0.281 mmol) and phosphoramidite **41a** (0.101 g, 0.281 mmol), toluene (5 mL) was added and the mixture was heated to 65 °C for 2 h. The solvent was removed under vacuum, and the resulting solid was purified by flash chromatography, employing 2 × 15 cm silica. The remaining ligand and PPh$_3$ were eluted using CH$_2$Cl$_2$, then the complex was eluted using CH$_2$Cl$_2$/*t*-butylmethyl ether 9:1 (v/v), collecting the red band. The solvent was removed under vacuum, giving **111a** as an orange solid in a 2:1 diastereomeric mixture (0.195 g, 0.223 mmol, 79%), m.p. 148–149 °C dec. (capillary).

NMR (δ, $CDCl_3$)[3] ^1H 7.90–7.66 (m, 6H, aromatic), 7.52 (d, $^3J_{HH}$ = 4.3 Hz, 2H, aromatic), 7.45–7.08 (m, 18H, aromatic), 7.06–6.95 (m, 5H, aromatic), 6.92–6.80 (m, 14H, aromatic), 6.73 (t, $^3J_{HH}$ = 7.2 Hz, 1H, aromatic), 6.55 (d, $^3J_{HH}$ = 8.3 Hz, 1H, aromatic), 5.47–5.40 (m, 1H, indenyl), 5.28 (s, br, 1H, indenyl), 4.97 (s, br, 0.5H, indenyl*), 4.63 (s, br, 0.5H, indenyl*), 4.18 (s, br, 1H, indenyl), 3.71 (s, br, 0.5H, indenyl*), 2.47 (s, 3H, CH_3), 2.43 (s, 3H, CH_3’), 1.92 (s, br, 1.5H, CH_3*), 1.89 (s, br, 1.5H, CH_3’*); $^{13}C\{^1H\}$ (major diastereomer)[4] 153.2 (s, aromatic), 150.9 (d, J_{CP} = 14.7 Hz, aromatic), 149.6 (d, J_{CP} = 8.0 Hz, aromatic), 136.7 (s, aromatic), 136.1 (s, aromatic), 134.6 (d, J_{CP} = 10.5 Hz, aromatic), 134.2 (d, J_{CP} = 10.0 Hz, aromatic), 133.4 (s, aromatic), 133.1 (s, aromatic), 131.3 (s, aromatic), 131.2 (d, J_{CP} = 3.7 Hz, aromatic), 130.2 (s, aromatic), 129.8 (s, aromatic), 129.4 (s, br, aromatic), 128.8 (s, aromatic), 128.6 (d, J_{CP} = 3.3 Hz, aromatic), 128.4 (s, aromatic), 128.3 (s, aromatic), 128.2 (s, aromatic), 128.1 (s, aromatic), 127.8 (s, aromatic), 127.7 (s, aromatic), 127.6 (s, aromatic), 127.4 (s, aromatic), 127.2 (s, aromatic), 127.1 (s, aromatic), 126.2 (s, aromatic), 126.0 (s, aromatic), 125.2 (d, J_{CP} = 4.2 Hz, aromatic), 125.0 (s, aromatic), 124.8 (s, aromatic), 124.0 (s, aromatic), 123.9 (s, aromatic), 123.0 (d, J_{CP} = 3.3 Hz, aromatic), 122.0 (s, aromatic), 118.3 (s, aromatic), 113.0 (d, J_{CP} = 5.5 Hz, indenyl), 112.2 (d, J_{CP} = 5.9 Hz, indenyl), 91.4 (s, indenyl), 66.9 (d, J_{CP} = 9.7 Hz, indenyl), 63.3 (s, indenyl), 39.5 (s,

CH_3), 39.4 (CH_3'); $^{31}P\{^1H\}$ 177.5 (s, br, phosphoramidite*), 176.3 (d, $^2J_{PP}$ = 65.1 Hz, phosphoramidite), 52.1 (s, br, *P*Ph$_3$*), 49.2 (d, $^2J_{PP}$ = 65.1 Hz, *P*Ph$_3$).

HRMS calcd for $C_{49}H_{40}NO_2P_2{}^{35}Cl^{102}Ru$ 873.1265, found 873.1284. IR (neat solid, cm^{-1}) 3047(w), 2917(w), 1586(w), 1432(m), 1223(m), 945(m), 693(m).

"[(Ind)RuCl(PPh$_3$)((R)-BINOL-*N,N*-dibenzyl-phosphoramidite)]" (**111b**). To a Schlenk flask containing [RuCl(Ind)(PPh$_3$)$_2$] (0.303 g, 0.390 mmol) and phosphoramidite **41b** (0.200 g, 0.391 mmol), THF (8 mL) was added, and the solids dissolved. The red solution was heated to reflux for 1 h. The solvent was removed under vacuum, and the resulting solid was purified by flash chromatography, employing 2.5 × 15 cm silica. The remaining ligand and PPh$_3$ were eluted using CH_2Cl_2 then the complex was eluted using CH_2Cl_2/Et_2O 99:1 (v/v), collecting the red band. The solvent was removed under vacuum, giving **111b** as a single diastereomer (0.347 g, 0.338 mmol, 87%), m.p. 176–177 °C dec. (capillary). Found: C, 71.44; H, 4.66. Calc. for $C_{61}H_{48}NO_2P_2ClRu$: C, 71.44; H, 4.72.

NMR (δ, $CDCl_3$) ^1H 8.11 (t, $^3J_{HH}$ = 8.3 Hz, 2H, aromatic), 7.70 (d, $^3J_{HH}$ = 8.1 Hz, 1H, aromatic), 7.62 (d, $^3J_{HH}$ = 8.4 Hz, 1H, aromatic), 7.54 (t, $^3J_{HH}$ = 7.1 Hz, 1H, aromatic), 7.52-7.44 (m, 2H, aromatic), 7.35-7.20 (m, 14H, aromatic), 7.15-6.84 (m, 12H, aromatic), 6.75 (d, $^3J_{HH}$ = 8.8 Hz, 3H, aromatic), 6.50-6.35 (m, 5H, aromatic), 5.71 (s, br, 1H, indenyl), 5.36 (s, br, 1H, indenyl), 5.00 (d, $^2J_{HH}$ = 10.6 Hz, 1H, NC*H*H'), 4.95 (d, $^2J_{HH}$ = 10.6 Hz, 1H, NCH*H*'), 4.05 (s, br, 1H, indenyl), 3.54 (d, $^2J_{HH}$ = 15.1 Hz, 1H, NC*H*H'), 3.49 (d, $^2J_{HH}$ = 15.1 Hz, 1H, NCH*H*'); $^{13}C\{^1H\}$ 151.3 (s, aromatic), 151.1 (s, aromatic), 149.2 (s, aromatic), 148.5 (s, aromatic), 139.4 (s, aromatic), 134.3 (s, br, aromatic), 133.8 (s, aromatic), 132.7 (s, aromatic), 131.5 (s, aromatic), 131.1 (s, aromatic), 130.2 (s, aromatic), 130.0 (s, aromatic), 129.5 (s, aromatic), 128.6 (s, aromatic), 128.4 (s, aromatic), 127.2 (s, aromatic), 126.2 (s, aromatic), 125.8 (s, aromatic), 125.5 (s, aromatic), 125.0 (s, aromatic), 124.4 (s, aromatic), 123.3 (s, aromatic), 122.8 (s, aromatic), 122.0 (s, aromatic), 121.4 (s, aromatic), 113.6-113.5 (m, indenyl), 111.8-111.7 (m, indenyl), 90.4 (s, indenyl), 67.1 (d, $^2J_{CP}$ = 10.8 Hz, indenyl), 62.0 (s, indenyl), 50.6 (s, N*C*H$_2$), 50.5 (s, N*C*H$_2$); ^{31}P{^{1}H} 172.8 (d, $^2J_{PP}$ = 58.5 Hz, phosphoramidite), 46.8 (d, $^2J_{PP}$ = 58.5 Hz, *P*Ph$_3$).

HRMS calcd for $C_{61}H_{48}NO_2P_2{}^{35}Cl^{102}Ru$ 1025.1892, found 1025.1924. IR (neat solid, cm^{-1}) 3050(w), 1586(w), 1223(m), 940(m), 741(m), 692(m).

“[(Ind)RuCl(PPh$_3$)((R)-BINOL-*N*-benzyl-*N*-α-methylbenzyl-phosphoramidite)]” (**111d**). To a Schlenk flask containing [RuCl(Ind)(PPh$_3$)$_2$] (0.442 g, 0.569 mmol) and phosphoramidite **41e** (0.299 g, 0.570 mmol), THF (10 mL) was added, and the solids dissolved. The red solution was heated to reflux for 3 h. The solvent was removed under vacuum, and the resulting solid was purified by flash chromatography, employing 2 × 16 cm silica. The remaining ligand and PPh$_3$ were eluted using CH_2Cl_2 then the complex was eluted using CH_2Cl_2/Et_2O 99:1 (v/v), collecting the red band. The solvent was removed under vacuum, giving **111d** as a single diastereomer (0.471 g, 0.453 mmol, 80%), m.p. 162–164 °C dec. (capillary). Found: C, 71.04; H, 4.84. Calc. for $C_{62}H_{50}NO_2P_2ClRu$: C, 71.63; H, 4.85.

NMR (δ, $CDCl_3$) ^{1}H 7.98 (d, $^3J_{HH}$ = 8.9 Hz, 2H, aromatic), 7.62–7.55 (m, 4H, aromatic), 7.43 (t, $^3J_{HH}$ = 7.2 Hz, 1H, aromatic), 7.35–7.29 (m, 5H, aromatic), 7.27–7.25 (m, 2H, aromatic), 7.20–7.01 (m, 9H, aromatic), 7.00–6.85 (m, 7H, aromatic), 6.80–6.72 (m, 4H, aromatic), 6.62–6.58 (m, br, 2H, aromatic), 6.44 (d, $^3J_{HH}$ = 8.9 Hz, 1H, aromatic), 6.33–6.22 (m, br, 4H, aromatic), 6.19 (d, $^3J_{HH}$ = 8.4 Hz, 1H, aromatic), 5.81–5.79 (m, 1H, indenyl), 5.57 (s, br, 1H, indenyl), 3.98 (s, br, 1H, indenyl), 3.90–3.81 (m, 1H, C*H*H'), 3.22–3.13 (m, 1H, CH*H*'), 1.07 (d, $^3J_{HH}$ = 7.2 Hz, 3H, CH_3);[5] ^{13}C{^{1}H} 151.4 (s, aromatic), 151.2 (s, aromatic), 143.2 (d, J_{CP} = 8.1 Hz, aromatic), 142.8 (s, aromatic), 137.9 (s, aromatic), 137.5 (s, aromatic), 137.4 (s, aromatic), 137.0 (s, aromatic), 135.7 (d, J_{CP} = 39.9 Hz, aromatic), 134.2 (s, aromatic), 133.7 (s, aromatic), 133.2 (s, aromatic), 133.1 (s, aromatic), 132.7 (s, aromatic), 131.4 (s, aromatic), 131.0 (s, aromatic), 130.1 (s, aromatic), 129.7 (s, aromatic), 129.2 (s, aromatic), 128.7 (s, aromatic), 128.5 (d, J_{CP} = 24.0 Hz, aromatic), 128.3 (d, J_{CP} = 18.0 Hz, aromatic), 128.1 (s, aromatic), 128.0 (s, aromatic), 127.2 (s, aromatic), 127.1 (s, aromatic), 126.5 (s, aromatic), 126.3 (s, aromatic), 126.0 (s, aromatic), 125.7 (d, J_{CP} = 26.1 Hz, aromatic), 124.9 (s, aromatic), 123.9 (s, aromatic), 122.9 (s, aromatic), 122.7 (s, aromatic), 122.0 (s, aromatic), 121.3 (s, aromatic), 114.3 (d, $^2J_{CP}$ = 18.0 Hz, indenyl), 113.0 (d, $^2J_{CP}$ = 24.0 Hz, indenyl), 90.4 (s, indenyl), 68.3 (d, $^2J_{CP}$ = 48.0 Hz, indenyl), 59.1 (s, indenyl), 54.9 (d, $^2J_{CP}$ = 68.1 Hz, N*C*), 49.0 (s, N*C*'), 21.7 (d, $^3J_{CP}$ = 21.9 Hz, *C*H_3); ^{31}P{^{1}H}172.0 (d, $^2J_{PP}$ = 58.6 Hz, phosphoramidite), 45.9 (d, $^2J_{PP}$ = 58.6 Hz, *P*Ph_3).

HRMS calcd for $C_{62}H_{50}NO_2P_2{}^{35}Cl\ {}^{102}Ru$ 1039.2048, found 1039.2004. IR (neat solid, cm^{-1}) 3051(w), 2927(w), 1584(w), 1430(m), 1221(m), 949(s).

“[(Ind)Ru(PPh$_3$)((R)-BINOL-*N*,*N*-dibenzylphosphoramidite) (diphenylallenylidene)][PF$_6$]” (**116a**). In a typical procedure, to a Schlenk flask containing complex **111b** (0.149 g, 0.145 mmol), CH_2Cl_2 (3 mL) was added, and the orange solution was cooled to 0 °C. $(Et_3O)PF_6$ (0.036 g, 0.147 mmol) was added as solution in CH_2Cl_2 (3 mL). The solution darkened slightly over 1 h, then 1,1-diphenyl-2-propyn-1-ol (**5a**, 0.037 g, 0.177 mmol, 1.2 equiv) was added. The solution quickly turned dark purple. After 30 min, the cold bath was removed and the solution was allowed to warm to rt for 30 min. The solvent was removed by oil pump vacuum and the purple solid washed 4 × 3 mL Et_2O and dried under vacuum, giving **116a** as a single diastereomer (0.163 g, 0.123 mmol, 85%), m.p. 173 °C dec. (capillary). Found: C, 67.02; H, 4.55. Calc. for $C_{76}H_{58}F_6NO_2P_3Ru\cdot(CH_2Cl_2)_{0.5}$: C, 67.18; H, 4.35.[6]

NMR (δ, $CDCl_3$) ^1H 8.25 (d, $^3J_{HH}$ = 8.8 Hz, 1H, aromatic), 8.09 (d, $^3J_{HH}$ = 8.2 Hz, 1H, aromatic), 7.80 (d, $^3J_{HH}$ = 8.8 Hz, 1H, aromatic), 7.65 (d, $^3J_{HH}$ = 8.1 Hz, 1H, aromatic), 7.60-7.47 (m, 4H, aromatic), 7.34 (d, $^3J_{HH}$ = 8.5 Hz, 1H, aromatic), 7.28 (t, $^3J_{HH}$ = 7.0 Hz, 3H, aromatic), 7.22-6.70 (m, 37H, aromatic), 6.62 (d, $^3J_{HH}$ = 4.8 Hz, 2H, aromatic), 6.49 (s, br, 1H, indenyl), 5.51 (s, br, 1H, indenyl), 5.28 (s, br, 1H, indenyl), 5.23 (s, $C\mathit{H}_2Cl_2$), 4.10 (d, $^2J_{HH}$ = 10.4 Hz, 1H, NC*H*H’), 4.05 (d, $^2J_{HH}$ = 10.4 Hz, 1H, NCH*H*’), 3.06 (d, $^2J_{HH}$ = 14.3 Hz, 1H, NC*H*H’), 3.02 (d, $^2J_{HH}$ = 14.3 Hz, 1H, NCH*H*’); $^{13}C\{^1H\}$ 293.8 (d, $^2J_{CP}$ = 21.9 Hz, C_α), 199.2 (s, C_β), 160.3 (s, C_γ), 149.4 (d, J_{CP} = 16.1

Hz, aromatic), 147.9 (d, J_{CP} = 7.2 Hz, aromatic), 143.0 (s, aromatic), 136.6 (d, J_{CP} = 2.6 Hz, aromatic), 135.0-133.0 (m, aromatic), 132.6 (s, aromatic), 132.5 (s, aromatic), 131.8 (d, J_{CP} = 2.8 Hz, aromatic), 131.5 (s, aromatic), 131.4 (s, aromatic), 130.9 (s, aromatic), 130.1 (s, aromatic), 129.4 (s, aromatic), 129.3 (s, aromatic), 129.2 (d, J_{CP} = 2.8 Hz, aromatic), 128.9 (s, aromatic), 128.8 (s, aromatic), 128.7 (s, aromatic), 128.6 (s, aromatic), 128.5-128.1 (m, aromatic), 128.0 (s, aromatic), 127.7 (s, aromatic), 127.1 (s, aromatic), 126.9 (s, aromatic), 126.4 (s, aromatic), 125.8 (s, aromatic), 124.6 (s, aromatic), 123.4 (s, aromatic), 122.5 (d, J_{CP} = 2.2 Hz, aromatic), 122.1 (d, J_{CP} = 3.3 Hz, aromatic), 121.6 (d, J_{CP} = 2.7 Hz, aromatic), 120.2 (s, aromatic), 112.3 (d, J_{CP} = 4.1 Hz, indenyl), 108.1 (s, indenyl), 94.1 (s, indenyl), 85.3 (s, indenyl), 84.2 (d, $^2J_{CP}$ = 7.0 Hz, indenyl), 50.4 (s, CH$_2$), 50.3 (s, CH$_2$'); ^{31}P{^{1}H} 169.5 (d, $^2J_{PP}$ = 34.0 Hz, phosphoramidite), 52.3 (d, $^2J_{PP}$ = 34.0 Hz, PPh$_3$), –143.4 (septet, $^1J_{PF}$ = 711 Hz, PF$_6$).

HRMS calcd for $C_{76}H_{58}NO_2P_2{}^{102}Ru$ 1180.2985, found 1180.2981. IR (neat solid, cm^{-1}) 3056(w), 2918(w), 1935(s, =C=C=C), 1586(w), 1223(m), 1058(s), 1028(s).

"[(Ind)Ru(PPh$_3$)((R)-BINOL-*N,N*-dibenzyl-phosphoramidite) (methylphenylallenylidene)][PF$_6$]" (116b).[6] 0.082 g (0.064 mmol, 66%) from 0.100 g (0.0977 mmol) **111b** and 0.017 g (0.116 mmol) **5b**, m.p. 173 °C dec. (capillary). Found: C, 67.28; H, 4.48. Calc. for $C_{71}H_{52}NO_2P_3F_6Ru\cdot(Et_2O)_{0.25}$: C, 67.47; H, 4.60.

NMR (δ, CDCl$_3$) ^{1}H 8.30 (d, $^3J_{HH}$ = 8.7 Hz, 1H, aromatic), 8.16 (d, $^3J_{HH}$ = 8.1 Hz, 1H, aromatic), 7.87 (d, $^3J_{HH}$ = 8.4 Hz, 1H, aromatic), 7.79 (t, $^3J_{HH}$ = 7.8 Hz, 2H, aromatic), 7.72–7.54 (m, 5H, aromatic), 7.48 (d, $^3J_{HH}$ = 8.4 Hz, 1H, aromatic), 7.40–6.80

(m, 35H, aromatic), 6.56 (s, br, 1H, indenyl), 5.38 (s, br, 2H, indenyl), 4.01 (d, ${}^2J_{HH}$ = 10.8 Hz, 1H, C*H*H'), 3.96 (d, ${}^2J_{HH}$ = 10.8 Hz, 1H, CH*H*'), 3.42 (q, ${}^3J_{HH}$ = 7.2 Hz, 1H, C*H*$_2$, Et$_2$O), 3.15 (d, ${}^2J_{HH}$ = 13.8 Hz, 1H, C*H*H'), 3.10 (d, ${}^2J_{HH}$ = 13.8 Hz, 1H, CH*H*'), 1.64 (s, 3H, C*H*$_3$), 1.13 (d, ${}^3J_{HH}$ = 6.9 Hz, 1.5H, C*H*$_3$, Et$_2$O); ^{13}C{^{1}H} 297.5 (dd, ${}^2J_{CP}$ = 23.5 Hz, ${}^2J_{CP}$ = 20.7 Hz, C_α), 195.5 (d, ${}^3J_{CP}$ = 13.8 Hz, C_β), 162.8 (s, C_γ), 149.7 (s, aromatic), 149.5 (s, aromatic), 147.9 (d, J_{CP} = 27.6 Hz, aromatic), 141.6 (s, aromatic), 136.7 (d, J_{CP} = 10.8 Hz, aromatic), 134.0 (s, aromatic), 133.5–133.3 (m, aromatic), 132.7 (s, aromatic), 131.9 (s, aromatic), 131.6 (s, aromatic), 131.4 (s, aromatic), 131.1 (s, aromatic), 130.6 (s, aromatic), 129.6–127.8 (m, aromatic), 127.6 (d, J_{CP} = 24.6 Hz, aromatic), 127.1 (s, aromatic), 126.8 (s, aromatic), 126.4 (s, aromatic), 125.9 (s, aromatic), 124.6 (s, aromatic), 123.7 (s, aromatic), 122.4 (s, aromatic), 121.9–121.7 (m, aromatic), 120.3 (s, aromatic), 112.4 (s, indenyl), 108.2 (d, ${}^2J_{CP}$ = 16.2 Hz, indenyl), 95.1 (s, indenyl), 83.7 (d, ${}^2J_{CP}$ = 30.3 Hz, indenyl), 82.7 (s, indenyl), 65.9 (s, C*H*$_2$, Et$_2$O), 50.3 (s, *C*H$_2$), 50.2 (s, *C*H$_2$), 30.3 (s, *C*H$_3$), 15.4 (s, *C*H$_3$, Et$_2$O); ^{31}P{^{1}H} 171.4 (d, ${}^2J_{PP}$ = 37.6 Hz, phosphoramidite), 53.4 (d, ${}^2J_{CP}$ = 37.6 Hz, *P*Ph$_3$), –143.4 (septet, ${}^1J_{PF}$ = 711 Hz, *P*F$_6$).

HRMS calcd for $C_{71}H_{56}NO_2P_2{}^{102}Ru$ 1118.2828, found 1118.2827. IR (neat solid, cm^{-1}) 3052(w), 1942(s, =C=C=C), 1585(w), 1224(m), 1066(w), 828(s).

“[(Ind)Ru(PPh$_3$)((R)-BINOL-*N*,*N*-dibenzylphosphoramidite)((2-furyl)methylallenylidene)][PF$_6$]“ (**116c**). 0.116 g (0.0913 mmol, 94%) from 0.100 g

(0.0976 mmol) **111b**, 0.014 g (0.117 mmol) 2-(2-furyl)-3-butyn-2-ol, m.p. 188–190 °C dec. (capillary). Found: C, 64.93; H, 4.30. Calc. for $C_{69}H_{54}NO_3P_3F_6Ru{\cdot}(H_2O)$: C, 65.20; H, 4.44.

NMR (δ, CD_2Cl_2) ^1H 8.23 (d, $^3J_{HH}$ = 8.8 Hz, 1H, aromatic), 8.10 (d, $^3J_{HH}$ = 8.4 Hz, 1H, aromatic), 7.89 (s, 1H, aromatic), 7.78 (d, $^3J_{HH}$ = 8.8 Hz, 1H, aromatic), 7.72–7.67 (m, 2H, aromatic), 7.57–7.51 (m, 1H, aromatic), 7.37 (d, $^3J_{HH}$ = 8.3 Hz, 1H, aromatic), 7.27–7.23 (m, 8H, aromatic), 7.17–7.12 (m, 6H, aromatic), 7.11–7.00 (m, 8H, aromatic), 7.00–6.85 (m, 13H, aromatic), 6.61–6.59 (m, 1H, aromatic), 6.37 (s, br, indenyl), 5.20 (s, br, indenyl), 5.11 (s, br, indenyl), 3.90 (d, $^2J_{HH}$ = 11.0 Hz, 1H, C*H*H’), 3.84 (d, $^2J_{HH}$ = 11.0 Hz, 1H, CH*H*’), 3.01 (d, $^2J_{HH}$ = 13.4 Hz, 1H, C*H*H’), 2.95 (d, $^2J_{HH}$ = 13.4 Hz, 1H, CH*H*’), 1.50 (s, H_2O), 1.46 (s, 3H, CH_3); $^{13}C\{^1H\}$ 282.7–281.6 (m, C_α), 185.2 (s, C_β), 160.9 (s, C_γ), 151.5 (s, aromatic), 150.0 (d, J_{CP} = 16.1 Hz, aromatic), 148.4 (d, J_{CP} = 7.3 Hz, aromatic), 145.3 (s, aromatic), 142.4 (s, aromatic), 139.7 (s, aromatic), 137.4 (s, br, aromatic), 136.7 (d, J_{CP} = 10.4 Hz, aromatic), 133.8 (s, br, aromatic), 133.0 (s, aromatic), 132.3 (s, aromatic), 131.8 (s, aromatic), 131.4 (d, J_{CP} = 8.4 Hz, aromatic), 130.7 (s, br, aromatic), 129.8 (s, aromatic), 129.2 (d, J_{CP} = 4.4 Hz, aromatic), 128.9 (s, aromatic), 128.7 (s, aromatic), 128.4 (s, aromatic), 128.2 (s, aromatic), 128.0 (s, aromatic), 127.7 (d, J_{CP} = 4.4 Hz, aromatic), 127.3 (d, J_{CP} = 6.2 Hz, aromatic), 127.1 (s, aromatic), 126.6 (s, aromatic), 126.0 (s, aromatic), 124.9 (s, aromatic), 124.0 (s, aromatic), 122.9 (s, aromatic), 122.3–121.9 (m, aromatic), 120.7 (s, aromatic), 116.2 (s, aromatic), 112.2 (s, indenyl), 107.6 (s, indenyl), 95.5 (s, indenyl), 82.7 (s, indenyl), 81.7

(s, indenyl), 50.4 (s, CH_2), 50.3 (s, CH_2), 28.2 (s, CH_3); $^{31}P\{^1H\}$ 174.3 (d, $^2J_{PP}$ = 38.2 Hz, phosphoramidite), 55.9 (d, $^2J_{PP}$ = 38.2 Hz, PPh_3), –143.4 (septet, $^1J_{PF}$ = 711 Hz, PF_6).

HRMS calcd for $C_{69}H_{54}NO_3P_2{}^{102}Ru$ 1108.2622, found 1108.2654. IR (neat solid, cm^{-1}) 3267(m, H_2O), 3051(w), 2923(w), 1949(s, =C=C=C), 1546(w), 1430(m), 1221(m), 940(s).

“[(Ind)Ru(PPh$_3$)((R)-BINOL-*N*,*N*-dibenzylphosphoramidite) (di(4-fluorophenyl)allenylidene)][PF$_6$]” (**116d**). 0.135 g (0.0992 mmol, 76%) from 0.102 g (0.0995 mmol) **111b**, 0.029 g (0.119 mmol) 3,3-di(4-flurorophenyl)-2-propyn-1-ol, m.p. 196–198 °C dec. (capillary). Found: C, 66.60; H, 3.97. Calc. For $C_{76}H_{56}NO_2P_3F_8Ru$: C, 67.06; H, 4.15.

NMR (δ, $CDCl_3$) ^1H 8.25 (d, $^3J_{HH}$ = 8.8 Hz, 1H, aromatic), 8.10 (d, $^3J_{HH}$ = 8.1 Hz, 1H, aromatic), 7.81 (d, $^3J_{HH}$ = 9.0 Hz, 1H, aromatic), 7.66 (d, $^3J_{HH}$ = 8.0 Hz, 1H, aromatic), 7.55–7.50 (m, 2H, aromatic), 7.37 (d, $^3J_{HH}$ = 8.4 Hz, 1H, aromatic), 7.26 (t, $^3J_{HH}$ = 7.6 Hz, 3H, aromatic), 7.19–7.02 (m, 16H, aromatic), 7.00–6.96 (m, 6H, aromatic), 6.95–6.90 (m, 5H, aromatic), 6.86–6.82 (m, 11H, aromatic), 6.66 (d, $^3J_{HH}$ = 8.9 Hz, 1H, aromatic), 6.56 (s, br, 1H, indenyl), 5.53 (s, br, 1H, indenyl), 5.22 (s, br, 1H, indenyl), 4.07 (d, $^2J_{HH}$ = 10.5 Hz, 1H, C*H*H’), 4.02 (d, $^2J_{HH}$ = 10.5 Hz, 1H, CH*H*’), 3.04 (d, $^2J_{HH}$ = 14.2 Hz, 1H, C*H*H’), 2.99 (d, $^2J_{HH}$ = 14.2 Hz, 1H, CH*H*’); $^{13}C\{^1H\}$ 291.9–291.3 (m, C_α), 198.5 (s, C_β), 166.9 (s, C_γ), 163.5 (s, aromatic), 155.5 (s, aromatic), 149.3

(d, J_{CF} = 61.5 Hz, aromatic), 147.8 (d, J_{CP} = 28.8 Hz, aromatic), 139.2 (s, aromatic), 136.6 (s, aromatic), 133.7 (s, aromatic), 133.6 (s, aromatic), 133.2 (s, aromatic), 132.4 (s, aromatic), 131.7 (s, aromatic), 131.3 (s, aromatic), 130.8 (s, br, aromatic), 130.0 (s, aromatic), 129.2 (s, aromatic), 128.8 (s, aromatic), 128.6 (s, aromatic), 128.5 (s, aromatic), 128.3 (s, br, aromatic), 128.0 (s, aromatic), 127.6 (s, aromatic), 127.1 (d, J_{CP} = 18.3 Hz, aromatic), 126.9 (s, aromatic), 126.4 (s, aromatic), 125.9 (s, aromatic), 124.8 (s, aromatic), 123.5 (s, aromatic), 122.4 (s, aromatic), 122.0 (s, aromatic), 121.6 (s, aromatic), 120.0 (s, aromatic), 116.4 (s, aromatic), 116.1 (s, aromatic), 112.4 (s, aromatic), 107.6 (s, indenyl), 94.3 (s, indenyl), 85.7 (s, indenyl), 83.9 (d, $^2J_{CP}$ = 28.8 Hz, indenyl), 66.0 (s, indenyl), 50.3 (s, N*C*H_2), 50.1 (s, N*C*H_2'); ^{31}P{^{1}H} 169.8 (d, $^2J_{PP}$ = 35.2 Hz, phosphoramidite), 52.8 (d, $^2J_{PP}$ = 35.2 Hz, *P*Ph_3), –143.5 (septet, $^1J_{PF}$ = 711 Hz, *P*F_6).

HRMS calcd for $C_{76}H_{56}NO_2P_2F_2{}^{102}Ru$ 1216.2797, found 1216.2761. IR (neat solid, cm^{-1}) 3053 (w), 1938 (s, =C=C=C), 1592 (m), 1502 (w), 1226 (m), 952 (m), 831 (s).

"[(Ind)Ru(PPh$_3$)((R)-BINOL-*N,N*-dibenzylphosphoramidite) (methyl(4-methoxyphenyl)allenylidene)][PF$_6$]" (**116e**). 0.083 g (0.064 mmol, 66%) from 0.100 g (0.0979 mmol) **111b**, 0.021 g (0.119 mmol) 2-(4-methoxylphenyl)-3-butyn-2-ol, m.p. 150–152 ^{o}C dec. (capillary). Found: C, 66.58; H, 4.58. Calc. For $C_{72}H_{58}NO_3P_3F_6Ru$: C, 66.87; H, 4.52.

NMR (δ, $CDCl_3$) ^1H 8.21 (d, $^3J_{HH}$ = 8.8 Hz, 1H, aromatic), 8.07 (d, $^3J_{HH}$ = 8.1 Hz, 1H, aromatic), 7.79 (d, $^3J_{HH}$ = 8.8 Hz, 1H, aromatic), 7.71–7.65 (m, 2H, aromatic), 7.53–7.49 (m, 3H, aromatic), 7.39 (d, $^3J_{HH}$ = 8.51 Hz, 1H, aromatic), 7.30–7.19 (m, 3H, aromatic), 7.18–7.10 (m, 10H, aromatic), 7.08–6.80 (m, 19H, aromatic), 6.76–6.60 (m, 4H, aromatic), 6.31 (s, br, 1H, indenyl), 5.22 (s, br, 2H, indenyl), 3.97 (d, $^2J_{HH}$ = 10.6 Hz, 1H, C*H*H'), 3.92 (d, $^2J_{HH}$ = 10.6 Hz, 1H, CH*H*'), 3.87 (s, 3H, OCH_3), 3.02 (d, $^2J_{HH}$ = 13.0 Hz, 1H, C*H*H'), 2.97 (d, $^2J_{HH}$ =13.0 Hz, 1H, CH*H*'), 1.59 (s, 3H, CH_3); $^{13}C\{^1H\}$ 282.0 (dd, $^2J_{CP}$ = 23.5 Hz, $^2J_{CP}$ = 21.3 Hz, C_α), 181.9 (s, C_β), 166.0 (s, C_γ), 163.6 (s, aromatic), 149.8 (d, J_{CP} = 15.5 Hz, aromatic), 148.0 (d, J_{CP} = 7.5 Hz, aromatic), 136.9 (d, J_{CP} = 2.3 Hz, aromatic), 135.8 (s, aromatic), 133.3 (s, br, aromatic), 132.6 (s, aromatic), 131.8 (s, aromatic), 131.3 (s, aromatic), 131.1 (s, aromatic), 130.4 (s, br, aromatic), 128.9 (d, J_{CP} = 2.3 Hz, aromatic), 128.7 (s, aromatic), 128.6 (s, aromatic), 128.5 (s, aromatic), 128.2 (s, aromatic), 128.0 (s, aromatic), 127.9 (s, aromatic), 127.8 (s, aromatic), 127.2 (s, aromatic), 126.9 (s, aromatic), 126.2 (s, aromatic), 125.8 (s, aromatic), 124.6 (s, aromatic), 123.9 (s, aromatic), 122.4 (d, J_{CP} = 2.3 Hz, aromatic), 122.0 (d, J_{CP} = 3.5 Hz, aromatic), 121.8 (d, J_{CP} = 2.9 Hz, aromatic), 120.4 (s, aromatic), 115.2 (s, aromatic), 111.7 (s, aromatic), 107.9 (d, $^2J_{CP}$ = 4.6 Hz, indenyl), 95.4 (s, indenyl), 81.8 (d, $^2J_{CP}$ = 7.7 Hz, indenyl), 80.2 (s, indenyl), 66.1 (s, indenyl), 56.5 (s, OCH_3), 50.1 (s, NCH_2), 50.0 (s, NCH_2'), 29.3 (s, CH_3); $^{31}P\{^1H\}$ 173.1 (d, $^2J_{PP}$ = 38.8

Hz, phosphoramidite), 54.6 (d, $^2J_{PP}$ = 38.8 Hz, *P*Ph$_3$), –143.5 (septet, $^1J_{PF}$ = 711 Hz, *P*F$_6$).

HRMS calcd for $C_{72}H_{58}NO_3P_2{}^{102}Ru$ 1148.2935, found 1148.2966. IR (neat solid, cm^{-1}) 3053(w), 1941(s, =C=C=C), 1587(s), 1225(w), 1172(m), 832(m).

"[Ru(Ind)(PPh$_3$)((R)-BINOL-N-benzyl-N-α-methylbenzyl-phosphoramidite)(diphenylallenylidene)][PF$_6$]" (120a). 0.121 g (0.0880 mmol, 91%) from 0.100 g (0.0966 mmol) **111d**, 0.022 g (0.106 mmol) **5a**, m.p. 168–169 °C dec. (capillary). Found: C, 67.14; H, 4.41. Calc. for $C_{77}H_{60}NO_2P_3F_6Ru(H_2O)_2$: C, 67.24; H, 4.69.

NMR (δ, CDCl$_3$) ^{1}H 8.26 (d, $^3J_{HH}$ = 8.8 Hz, 1H, aromatic), 8.13 (d, $^3J_{HH}$ = 8.2 Hz, 1H, aromatic), 7.73 (d, $^3J_{HH}$ = 8.8 Hz, 1H, aromatic), 7.66 (d, $^3J_{HH}$ = 8.1 Hz, 1H, aromatic), 7.60–7.46 (m, 6H, aromatic), 7.33–7.10 (m, 10H, aromatic), 7.09–6.96 (m, 13H, aromatic), 6.90–6.81 (m, 16H, aromatic), 6.59–6.55 (m, 3H, aromatic), 5.39 (s, br, 1H, indenyl), 5.13 (s, br, 1H, indenyl), 4.84–4.79 (m, 1H, C*H*CH$_3$), 3.96–3.85 (m, 1H, C*H*H'), 3.52–3.40 (m, 1H, CH*H*'), 1.52 (s, H$_2$O), 0.54 (d, $^3J_{HH}$ = 7.1 Hz, 3H, C*H*$_3$); ^{13}C{^{1}H} 295.1–294.6 (m, C_α), 199.7–199.6 (m, C_β), 159.9 (s, C_γ), 149.3 (d, J_{CP} = 15.8 Hz, aromatic), 147.8 (d, J_{CP} = 7.5 Hz, aromatic), 143.0 (s, aromatic), 141.0 (s, aromatic), 140.5 (s, aromatic), 133.5 (s, aromatic), 132.5 (s, br, aromatic), 131.9 (s, aromatic), 131.7 (s, br, aromatic), 131.4 (s, aromatic), 130.5 (d, J_{CP} = 7.4 Hz, aromatic), 129.4 (s, aromatic), 128.8 (s, br, aromatic), 128.6 (s, aromatic), 128.5 (s, aromatic), 128.2 (s, aromatic), 127.8 (s, aromatic), 127.5 (s, aromatic), 127.3 (s, aromatic), 127.1 (s, aromatic), 126.8 (s, aromatic), 126.5 (s, aromatic), 125.8 (s, aromatic), 124.8 (s, aromatic), 123.0 (s, aromatic), 122.4 (s, aromatic), 121.8 (s, aromatic), 121.5 (s, aromatic), 120.5 (s, aromatic), 112.7 (s, indenyl), 107.8 (s, indenyl), 94.0 (s, indenyl), 85.0 (s, indenyl), 82.7 (s, indenyl), 57.0 (d, $^2J_{CP}$ = 1.7 Hz, N*C*), 48.8 (d, $^2J_{CP}$ = 12.7 Hz, N*C*'), 20.8 (s, *C*H$_3$); ^{31}P{^{1}H} 172.2 (d, $^2J_{PP}$ = 35.2 Hz, phosphoramidite), 53.1 (d, $^2J_{PP}$ = 35.2 Hz, *P*Ph$_3$), –143.4 (septet, $^1J_{PF}$ = 711 Hz, *P*F$_6$).

HRMS calcd for $C_{77}H_{60}NO_2P_2{}^{102}Ru$ 1194.3142, found 1194.3121. IR (neat solid, cm^{-1}) 3267(m, H$_2$O), 2916(w), 1929(s, =C=C=C), 1584(w), 1430(m), 1217(m), 948(s).

"[Ru(Ind)(PPh$_3$)((R)-BINOL-N-benzyl-N-α-methylbenzyl-phosphoramidite)(methylphenylallenylidene)][PF$_6$]" (**120b**). 0.092 g (0.072 mmol, 72%) from 0.101 g (0.0967 mmol) **111d**, 0.017 g (0.116 mmol) **5b**, m.p. 169–171 °C dec. (capillary). Found: C, 66.72; H, 4.50. Calc. for $C_{72}H_{58}NO_2P_3F_6Ru(H_2O)$: C, 66.77; H, 4.67.

NMR (δ, CDCl$_3$) ^{1}H 8.24 (d, $^3J_{HH}$ = 8.8 Hz, 1H, aromatic), 8.09 (d, $^3J_{HH}$ = 8.0 Hz, 1H, aromatic), 7.77 (d, $^3J_{HH}$ = 8.9 Hz, 1H, aromatic), 7.72 (d, $^3J_{HH}$ = 4.3 Hz, 1H, aromatic), 7.70 (d, $^3J_{HH}$ = 2.2 Hz, 1H, aromatic), 7.58–7.50 (m, 3H, aromatic), 7.37 (d, $^3J_{HH}$ = 7.6 Hz, 4H, aromatic), 7.31–7.22 (m, 7H, aromatic), 7.21–7.12 (m, 12H, aromatic), 7.10–7.02 (m, 4H, aromatic), 7.00–6.93 (m, 4H, aromatic), 6.90–6.82 (m, 5H, aromatic), 6.79–6.66 (m, 3H, aromatic), 6.48 (s, br, 1H, indenyl), 5.25 (s, br, 1H, indenyl), 5.23 (s, br, 1H, indenyl), 3.71–3.61 (m, 1H, C*H*H'), 3.49–3.36 (m, 1H, CH*H*'), 1.74 (s, *H*$_2$O), 1.50 (s, 3H, C*H*$_3$), 0.47 (d, $^3J_{HH}$ = 7.2 Hz, 3H, CHC*H*$_3$); ^{13}C{^{1}H}[7] (partial) 299.4 (m, C_α), 196.0 (s, C_β), 162.2 (s, C_γ), 151–118 (aromatic), 95.3 (s, indenyl), 88.8 (s, indenyl), 87.1 (s, indenyl), 56.0 (s, N*C*), 54.0 (s, N*C*), 30.3 (s, *C*H_3), 20.7 (s, *C*H_3); $^{31}P\{^1H\}$ 175.0 (d, $^2J_{PP}$ = 37.5 Hz, phosphoramidite), 54.1 (d, $^2J_{PP}$ = 37.5 Hz, *P*Ph_3), –143.4 (septet, $^1J_{PF}$ = 711 Hz, *P*F_6).

HRMS calcd for $C_{72}H_{58}NO_2P_2{}^{102}Ru$ 1132.2986, found 1132.2975. IR (neat solid, cm^{-1}) 3267(w, H_2O), 3058(w), 1935(s, =C=C=C), 1584(w), 1433(m), 1224(m), 948(m).

“[Ru(Ind)(PPh_3)((R)-BINOL-N-benzyl-N-α-methylbenzyl-phosphoramidite) ((2-furyl)methylallenylidene)][PF_6]” (120c). 0.115 g (0.0895 mmol, 93%) from 0.100 g (0.0963 mmol) **111d**, 0.016 g (0.118 mmol) 2-(2-furyl)-3-butyn-2-ol, m.p. 185–187 °C dec. (capillary). Found: C, 64.80; H, 4.46. Calc. for $C_{70}H_{56}NO_3P_3F_6Ru(H_2O)$: C, 65.42; H, 4.55.

NMR (δ, $CDCl_3$) ^1H 8.21 (d, $^3J_{HH}$ = 8.7 Hz, 1H, aromatic), 8.09 (d, $^3J_{HH}$ = 7.9 Hz, 1H, aromatic), 7.86 (s, 1H, aromatic), 7.74–7.69 (m, 4H, aromatic), 7.54–7.50 (m, 1H, aromatic), 7.34–7.14 (m, 18H, aromatic), 7.10–6.93 (m, 14H, aromatic), 6.81–6.74 (m, 2H, aromatic), 6.57–6.56 (m, 2H, aromatic), 6.35 (s, br, 1H, indenyl), 5.12 (s, br, 2H, indenyl), 4.76–4.70 (m, 1H, C*H*CH_3), 3.64–3.53 (m, 1H, C*H*H’), 3.48–3.36 (m, 1H, CH*H*’), 1.60 (s, H_2O), 1.44 (s, 3H, CH_3), 0.48 (d, $^3J_{HH}$ = 7.2 Hz, 3H, CHCH_3); $^{13}C\{^1H\}$160.6 (C_γ), 156.2 (s, aromatic), 151.1 (s, br, aromatic), 149.5 (d, J_{CP} = 14.9 Hz, aromatic), 147.9 (d, J_{CP} = 8.4 Hz, aromatic), 141.5 (d, J_{CP} = 2.8 Hz, aromatic), 140.6 (s, aromatic), 133.8 (d, J_{CP} = 9.2 Hz, aromatic), 133.5 (s, aromatic), 132.8 (d, J_{CP} = 2.2 Hz, aromatic), 132.4 (d, J_{CP} = 10.3 Hz, aromatic), 131.9 (s, aromatic), 131.4 (s, aromatic), 131.3 (s, aromatic), 130.7 (s, aromatic), 129.2 (s, aromatic), 128.9 (s, aromatic), 128.7 (s, br, aromatic), 128.6 (s, aromatic), 128.4 (s, aromatic), 128.1 (s, aromatic), 128.0 (s, br, aromatic), 127.4 (s, aromatic), 127.2 (s, br, aromatic), 127.1 (s, aromatic), 126.9 (d, J_{CP} = 2.2 Hz, aromatic), 126.8 (s, aromatic), 126.3 (s, aromatic), 125.8 (s, aromatic), 124.4 (s, aromatic), 123.6 (s, aromatic), 122.3 (d, J_{CP} = 2.4 Hz, aromatic), 122.0 (s, aromatic), 121.9–121.7 (m, aromatic), 120.8 (s, br, aromatic), 116.1 (s, indenyl), 111.9 (s, indenyl), 108.7 (s, indenyl), 95.1 (s, indenyl), 80.6 (s, indenyl), 57.2 (s, br, N*C*), 27.8 (s, CH_3), 20.6 (s, CH_3); $^{31}P\{^1H\}$ 175.7 (d, $^2J_{PP}$ = 37.7 Hz, phosphoramidite), 54.5 (d, $^2J_{PP}$ = 37.7 Hz, PPh_3), –143.4 (septet, $^1J_{PF}$ = 711 Hz, PF_6).

HRMS calcd for $C_{70}H_{56}NO_3P_2{}^{102}Ru$ 1122.2778, found 1122.2787. IR (neat solid, cm^{-1}) 3267(m, H_2O), 2919(w), 1949(s, =C=C=C), 1430(m), 1221(m), 943(m).

X-ray Structure Determination for 111b and 116a, b, d: X-ray quality crystals of **111b** were obtained by addition of Et_2O to a solution of **111b** in CH_2Cl_2, which was stored at –10 °C for several days. X-ray quality crystals of **116a, b, d** were obtained by slow diffusion of Et_2O into a solution of **116a, b, d** in CH_2Cl_2 at –10 °C.

Preliminary examination and X-ray data collection were performed using a Bruker Kappa Apex II single crystal X-Ray diffractometer equipped with an Oxford Cryostream LT device. Intensity data were collected by a combinations of ϖ and ϕ scans. Apex II, SAINT and SADABS software packages (Bruker Analytical X-Ray, Madison, WI, 2008) were used for data collection, integration and correction of systematic errors, respectively.

Crystal data and intensity data collection parameters are listed in Table 1. Structure solution and refinement were carried out using the SHELXTL- PLUS software package.[8] The structures were solved by direct methods and refined successfully in the space groups $P2_1$ (**111b**), P1 (**116a**) and P1 (**116b**). The non-hydrogen atoms were refined anisotropically to convergence. All hydrogen atoms were treated using appropriate riding model (AFIX m3). The structure of **111b** shows disorder in the ligand as well as in the solvent. The structure of **116a** shows disorder in the solvent. The disorders have been modeled with partial occupancy atoms.

CCDC 726745, 726746 and 730038 contain the supplementary crystallographic data for **111b**, **116a** and **116b**.

---

[1] (a). Hulst, R.; de Vries, N. K.; Feringa, B. L. *Tetrahedron: Asymmetry*, **1994**, *5*, 699; (b). Duursma, A.; Boiteau, J.-G.; Lefort, L.; Boogers, J. A. F.; de Vries, A. H. M.; de Vries, J. G.; Minnaard, A. J.; Feringa, B. L. *J. Org. Chem*. **2004**, *69*, 8045; (c). Smith, C. R.; Mans, D. J.; RajanBabu, T. V. *Organic Syntheses* **2008**, *85*, 238.

[2] Oro, L. A.; Ciriano, M. A.; Campo, M. *J. Organomet. Chem*., **1985**, *289*, 117.

[3] The star sign (*) denotes the second (minor) diastereomer.

[4] Very few peaks corresponding to the minor diastereomer are observed and thus are not reported.

[5] The methine proton is not visible and is assumed to be overlapped with aromatic protons.

[6] Allenylidenes **116b-d** were synthesized as for complex **116a**.

[7] The ^{13}C NMR reported is partial due to ongoing decomposition of the sample during data collection. The indenyl and aliphatic peak assignments were made by analogy to the related complexes; all assignments are tentative.

[8] Sheldrick, G. M. *Acta Cryst*. **2008**, *A64*, 112.

Electronic tuning of η^5-indenyl complexes via ligand substitution

6.1. Aim

Using the sterically tuned complex [(Ind)RuCl(PPh$_3$)(**41b**)] (**111b**, Scheme 5.8, Chapter 5) as a guide, new electronically tuned complexes that can form allenylidenes are targeted. The new complexes to be synthesized were tested for their ability to form stable allenylidenes as well as for catalytic activity in reactions of propargylic alcohols with various carbon and heteroatom centered nucleophiles.

6.2. Introduction

6.2.1. Electronic tuning via indene substitution

I showed in the previous chapter that the indenyl complex [(Ind)RuCl(PPh$_3$)(**41b**)] (**111b**) was shown to form stable allenylidenes in reactions with tertiary aromatic propargylic alcohols after preactivation by chloride abstraction.[1] Catalytic activation of propargylic alcohols is also possible using electron-rich aromatic compounds as nucleophiles, but the reaction gives low conversions (~50%) even after optimization of the reaction conditions (Scheme 5.19, Chapter 5). Coordinating nucleophiles such as amines show no reactivity under similar conditions. It is clear that additional catalyst tuning is necessary to fine-tune the reactivity for a more broadly applicable catalyst.

Thus far steric tuning has shown a significant impact on the diastereoselectivity of complex formation and has had a significant influence on the stability of the allenylidenes. The sterics of the complex have been fine-tuned to allow allenylidene formation and prevent vinylvinylidene formation (Scheme 5.12, Chapter 5). Electronic tuning has proven to be more difficult, however, but it is still of interest as a way to effectively alter allenylidene stability and create a better catalyst. There are several positions on [(Ind)RuCl(PR_3)(phosphoramidite)] that allow for electronic tuning. The phosphoramidite ligand is not the optimal choice as previous electronic tuning efforts via this ligand have shown little effect (Chapters 2, 3).[2] Instead, orthogonal steric and electronic tuning of mixed phosphine/phosphoramidite piano-stool complexes of ruthenium bearing an η^5-indenyl ligand should be possible by changing the substituents R on the N atom of the phosphoramidite, X on the indenyl ligand and R’ on the phosphine ligand (Figure 6.1).

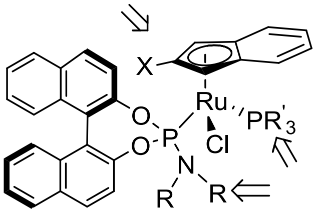

Figure 6.1. Steric and electronic tuning sites in indenyl complexes.

Electronic tuning via the indenyl ligand is of particular interest because by substituting one or more protons on indene with an electron-donating or electron-withdrawing group, the tuning effect takes place on an atom directly attached to the metal with little effect on the sterics. Indene derivatives with strongly electron-donating or electron withdrawing groups have not been used in ruthenium piano-stool complexes, but

1,2,3-trimethylindenyl ruthenium complexes have been synthesized previously (Figure 6.2).[3]

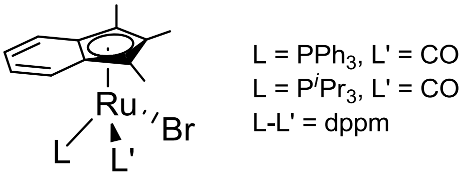

Figure 6.2. Trimethylindenyl phosphine ruthenium complexes.[3]

6.2.2. Electronic tuning via phosphine substitution

Electronic tuning via the phosphine ligand can be achieved by an appropriate choice of the precursor complex. The phosphines of the bis(triphenylphosphine) complex [(Ind)RuCl(PPh_3)$_2$] (**110**) can in some cases be substituted by bidentate phosphines (or other P-donor ligands) to give complexes of the type [(Ind)RuCl(P-P)] (P-P is a chelating P-donor ligand, Scheme 6.1).[4] Substitution of both PPh_3 ligands by monodentate ligands or by ligands with N-donor atoms does not reliably give the neutral complexes, however. Attempts to isolate neutral complexes of the type [(Ind)RuCl(PR_3)$_2$], [(Ind)RuCl(P-N)], [(Ind)RuCl(N-N)] (P-N and N-N are bidentate ligands) by heating the corresponding ligands with the bis(phosphine) complex **110** in toluene can give instead the corresponding cationic complexes resulting from chloride substitution (Scheme 6.2).[5]

Electronic tuning via substitution of PPh_3 potentially could lead to a wide range of electronically tuned ruthenium complexes. However, because both phosphine ligands cannot be reliably substituted by a number of different ligands, a reaction path that allows circumvention of the phosphine substitution reactions would simplify the problem and potentially allow for the synthesis of a wider range of substituted products. The previously reported complex [(Ind)RuCl(cod)][6] (**125**) (cod = 1,5-cyclooctadiene) has been shown to allow facile substitution of the diene ligand with mono- or bidentate ligands. In this way, mixed complexes of the type [(Ind)RuCl(PR_3)(L)] have been synthesized, even those which cannot be formed by double phosphine substitution.[5,6a]

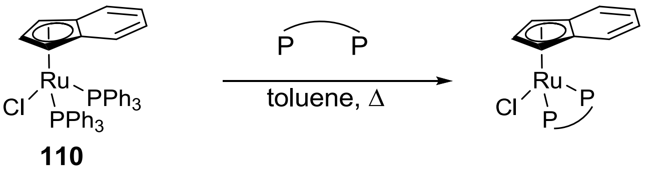
Ru
Cl
PPh3
PPh3
110
P P
toluene, Δ
Ru
Cl
P
P

Scheme 6.1. Substitution of PPh_3 by a chelating bis(phosphine) ligand.[4]

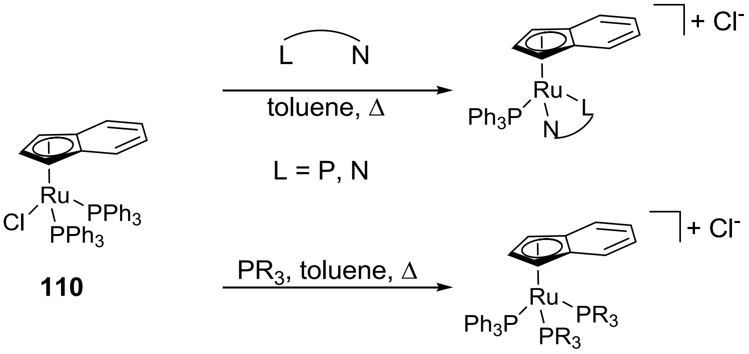
L N
toluene, Δ
L = P, N
+ Cl-
Ru
Ph3P
L
N
Ru
Cl
PPh3
PPh3
110
PR3, toluene, Δ
+ Cl-
Ru
Ph3P
PR3
PR3

Scheme 6.2. Synthesis of cationic complexes.[5]

Phosphine substitution can also be circumvented by the use of complexes of the type [(Ind)RuX$(CO)_2$] (X = Cl, Br, I).[3] These complexes are available by reaction of the carbonyl bridged dimer $[(Ind)Ru(CO)(\mu\text{-}CO)]_2$ (**128**) with a halogen (X_2). Oxidative removal of one of the carbonyl ligands allows for substitution by a neutral two electron donor such as a phosphine (Scheme 6.3). I was inspired by the above mentioned literature examples and thus set out to apply related tuning efforts in my chemistry.

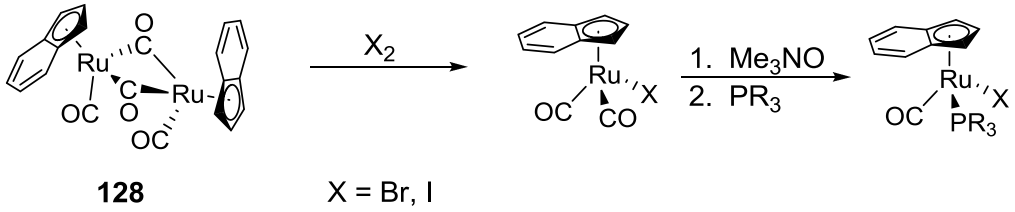

Scheme 6.3. Synthesis of mixed carbonyl phosphine complexes.[3]

6.3. Results

6.3.1. Attempts at coordination of indene derivatives

Various electronically tuned indene derivatives have been reported previously, such as 2-nitroindene,[7] 2-(*p*-toluenesulfonyl)indene[8] and 2-bromoindene (**131**).[9] Of these, 2-bromoindene (**131**) is especially interesting because although it is not strongly electronically tuned, the bromo- substituent can potentially be substituted for more strongly electronically tuned substituents such as –C≡N via a Cu(I) mediated reaction.[10] In this way a whole range of tuned indenes are potentially available. 2-Bromoindene[9] (**131a**) and 2-(*p*-toluenesulfonyl)indene[8] (**131b**) were synthesized according to literature methods (Scheme 6.4) to test the applicability of indene derivatives in metal complex synthesis.

When the new derivatives were reacted under conditions identical to those used for the synthesis of the known [(Ind)RuCl(PPh_3)$_2$] (**110**),[11] coordination of the new indene derivatives is not observed (Scheme 6.5). Under these conditions the indene derivatives are unreactive. Using a stronger base such as NaH in THF can ensure that the deprotonation reaction is not a limiting factor. Under these conditions coordination of the arene fails again. It is possible that electron-poor indene derivatives simply lack the donating capabilities necessary to form piano-stool complexes.

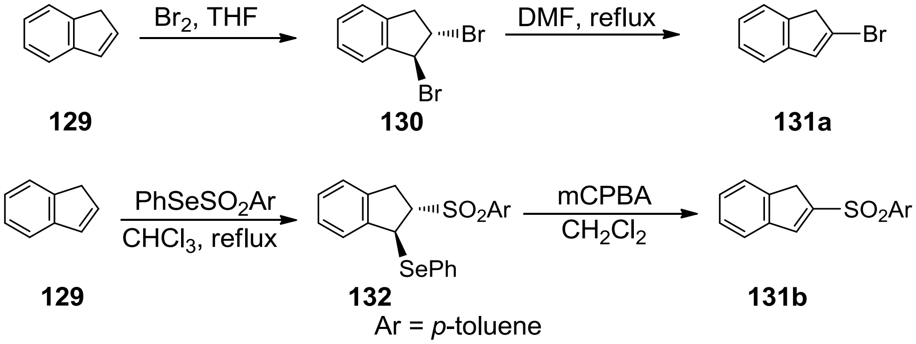
Br2, THF
Br
Br
DMF, reflux
Br
129
130
131a
PhSeSO2Ar
CHCl3, reflux
SO2Ar
SePh
mCPBA
CH2Cl2
SO2Ar
129
132
131b
Ar = p-toluene

Scheme 6.4. Synthesis of indene derivatives.[8,9]

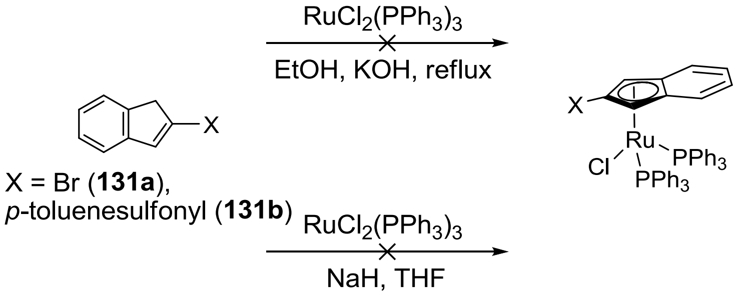
RuCl2(PPh3)3
EtOH, KOH, reflux
X
X
Ru
Cl
PPh3
PPh3
X = Br (131a),
p-toluenesulfonyl (131b)
RuCl2(PPh3)3
NaH, THF

Scheme 6.5. Attempted synthesis of new indenyl ruthenium complexes.

6.3.2. Synthesis and reactivity of a ruthenium diene complex

The synthesis of [(Ind)RuCl(cod)] (**125**) is accomplished in two steps beginning from $RuCl_3$•xH_2O.[4] In the first step $RuCl_3$•xH_2O is reacted with an excess of 1,5-cyclooctadiene in refluxing ethanol to give the polymer $[RuCl_2(cod)]_n$ (**126**). The polymer is then reacted with potassium indenide (KInd) to give the product

[(Ind)RuCl(cod)] (**125**). Because the literature is unclear as to the base used to yield KInd,[6] several variations were tested. KO^{t}Bu in THF showed poor solubility, giving no reaction. A suspension of KH in mineral oil in THF gives the indenide and addition of this solution to a suspension of $[RuCl_2(cod)]_n$ (**126**) in THF gave [(Ind)Ru(η^3,η^2-cod)] (**127**) (formed by deprotonation of [(Ind)RuCl(cod)] (**126**)) instead of the expected [(Ind)RuCl(cod)] (**125**) (Scheme 6.6). KInd generated by reduction of indene using potassium metal gave similar results. According to Gimeno, when NaInd was used in place of KInd [(Ind)Ru(η^3,η^2-cod)] (**127**) was obtained.[4] The desired [(Ind)RuCl(cod)] (**125**) is then synthesized by addition of HCl. Protonation of the obtained [(Ind)Ru(η^3,η^2-cod)] (**127**) does indeed give the desired [(Ind)RuCl(cod)] (**125**), but the yields are low and highly variable (10-40% for two steps). In an attempt to improve the reproducibility of the reaction NaH deprotonation was employed. Under these conditions, however, the expected product (**127**) was not obtained at all. Use of LiInd by deprotonation of indene with BuLi did not improve the results.

The small amounts of **125** obtained in this reaction were tested in reactions with phosphoramidites. Reaction of **125** with **41b** in THF at reflux gives the double substitution product **111f** exclusively, even with only one equivalent **41b** (Scheme 6.7). Attempts to trap the monosubstituted product with MeCN or triphenylphosphite ($P(OPh)_3$) failed. Although the doubly substituted product is not uninteresting, due to the ongoing problems with the synthesis of **125**, alternative precursors were examined.

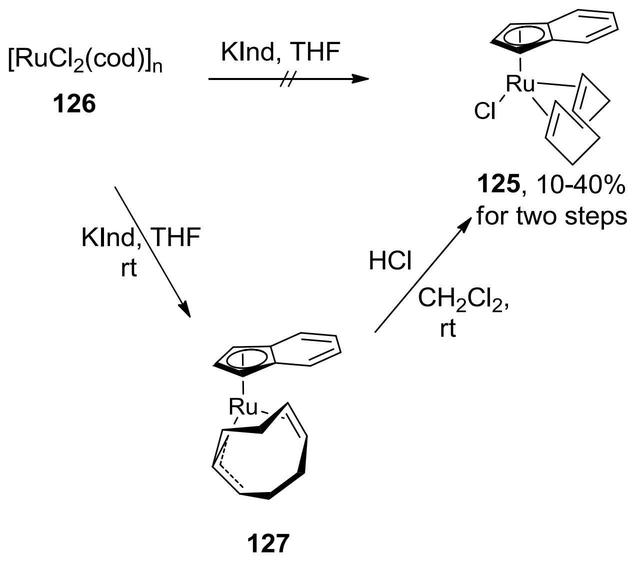
[RuCl2(cod)]n
126
KInd, THF
125, 10-40%
for two steps
KInd, THF
rt
HCl
CH2Cl2,
rt
Ru
Cl
127

Scheme 6.6. Synthesis of [(Ind)RuCl(cod)] (**125**).[4]

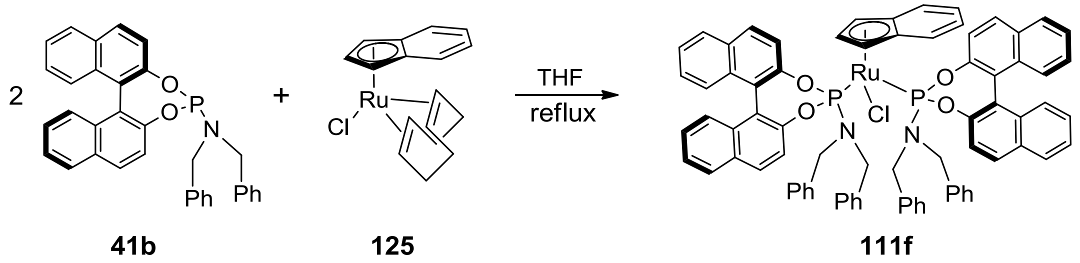
2
+
THF
reflux
O
P
N
Ph
Ru
Cl
41b
125
111f

Scheme 6.7. Synthesis of a bis(phosphoramidite) complex.

6.3.3. Synthesis of a tripyrrolylphosphine complex

In pursuing electronic tuning via substitution of PPh_3 it is important to create a pronounced electronic effect on the new ligand (relative to PPh_3) while disturbing the sterics as little as possible. Incremental substitution of the phenyl groups on PPh_3 by pyrrole decreases the σ-donating ability of the ligands while enhancing the π-acidity. Tripyrrolylphosphine ($PPyr_3$) in particular has been shown to have a significantly greater

π-acidity than PPh_3.[12] Reaction of [(Ind)RuCl(PPh_3)$_2$] (**110**) with phosphoramidite **41b** and $PPyr_3$ in refluxing toluene gives [(Ind RuCl($PPyr_3$)(**41b**)] (**133**) in 59% yield as a single diastereomer after chromatographic work up (Scheme 6.8). As for complexes **111**, coordination of the ligand **41b** creates a new stereocenter at the metal center, giving the possibility of two diastereomers. Again, the complex **133** forms as a single diastereomer (^{1}H, ^{31}P NMR), similar to **111b** reported in Chapter 5. Conversely, dipyrrolylphenylphosphine and pyrrolyldiphenylphosphine do not give satisfactory results in one or two step substitutions of this type due to low conversion coupled with excessive side products as seen by ^{31}P NMR.

As expected, the new complex **132** shows two doublets in the ^{31}P NMR. The phosphoramidite signal appears at 170.7 ppm, similar to the corresponding complex bearing PPh_3 (172.8 ppm). The $PPyr_3$ phosphorus signal appears at 124.8 ppm, significantly downfield of the free ligand (79.6 ppm). The $^2J_{PP}$ coupling (77.6 Hz) is similar to that of the related PPh_3 complexes (Chapter 5). In the ^{1}H NMR the methylene (NCH_2) protons are diastereotopic, giving four doublets in the range 4.5-3.1 ppm. IR and HRMS data are consistent with the assigned structure. X-ray quality crystals of **132** were obtained by slow diffusion of methanol into a solution of **132** in CH_2Cl_2 (Figure 6.3).

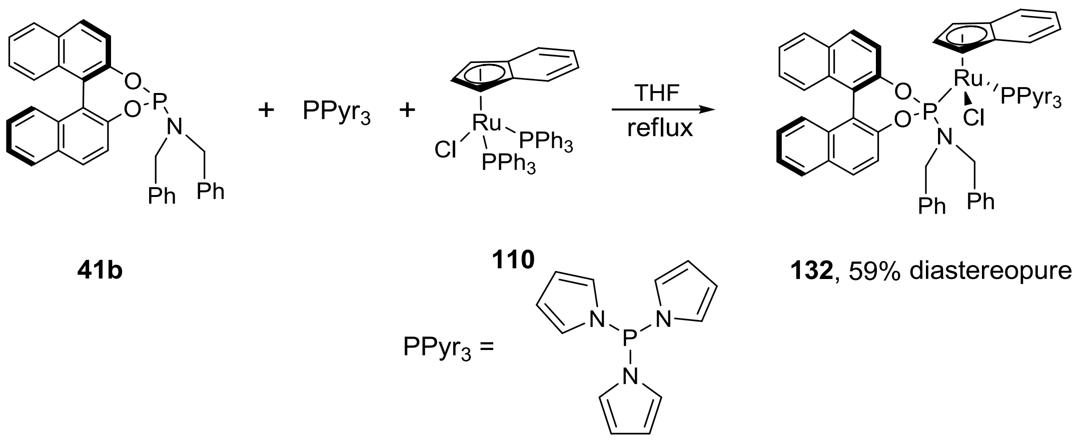

41b

110

132, 59% diastereopure

Scheme 6.8. Synthesis of a tripyrrolylphosphine complex **132**.

The Ru-P(2) bond (2.21 Å, where P(2) is $PPyr_3$) is significantly shorter than the Ru-P(1) bond (2.28 Å, P(1) is the phosphoramidite), showing the impact of the π-acidity of the tripyrrolylphosphine (Table 6.1). The bond angles about ruthenium range from 86.91^o for P(2)-Ru-Cl to 103.87^o for P(1)-Ru-Cl, confirming the pseudooctahedral geometry. It is worth noting that the largest bond angle about the metal is the P(1)-Ru-Cl angle and not the P(1)-Ru-P(2) angle as would be expected given that P(1) and P(2) are the most sterically demanding ligands. The absolute configuration about the metal is as for the related piano-stool complexes [(Ind)RuCl(PPh_3)(**41b**)] (**111b**) and [CpRuCl(PPh_3)(**41b**)] (**69b**). Key structural data are compiled in Table 6.1; [(Ind)RuCl(PPh_3)(**41b**)] (**111b**) and [CpRuCl(PPh_3)(**41b**)] (**69b**) are included for comparison. Crystallographic parameters are listed in Table 6.2.

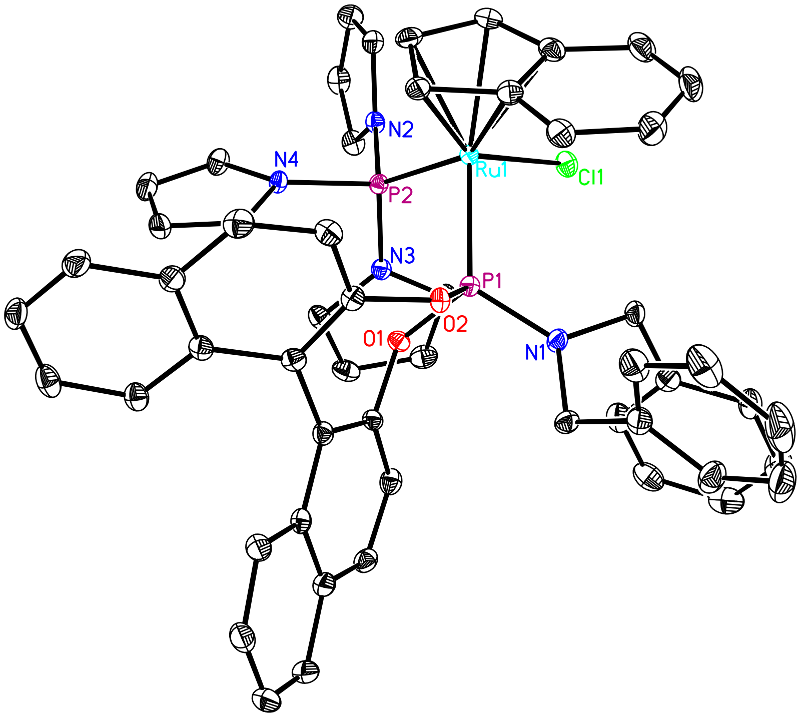

Figure 6.3. Crystal structure of **132**.

Table 6.1. Selected bond lengths and angles of **132**.

Entry	Bond(s)	**132**	[(Ind)RuCl(PPh_3)(**41b**)] (**111b**)	[CpRuCl(PPh_3)(**41b**)] (**69b**)
Bond Lengths (Å)				
1	Ru-P(1)	2.2801(5)	2.1961(7)	2.2426(8)
2	Ru-P(2)	2.2051(5)	2.3504(8)	2.3294(8)
3	Ru-Cl	2.4464(5)	2.4439(7)	2.4302(7)
Bond Angles (°)				
4	P(1)-Ru-P(2)	94.71(2)	98.87(3)	99.11(3)
5	Cl-Ru-P(1)	103.874(16)	89.28(3)	92.28(3)
6	Cl-Ru-P(2)	86.906(19)	86.99(3)	87.37(3)

Table 6.2. Crystallographic parameters for **132**.

Empirical formula	$C_{55}H_{45}ClN_4O_2P_2Ru$
Formula weight	992.41
Temperature / Wavelength	100(2) K / 0.71073 Å
Crystal system	Orthorhombic
Space group	$P2_12_12_1$
Unit cell dimensions	a = 10.3517(7) Å
	b = 11.6479(8) Å
	c = 36.510(2) Å
	α = 90°.
	β = 90°.
	γ = 90°.
Volume / Z	4402.2(5) $Å^3$ / 4
Density (calculated)	1.497 Mg/m^3
Absorption coefficient	0.540 mm^{-1}
F(000)	2040
Crystal size / mm^3	0.25 x 0.18 x 0.13
Theta range for data collection	1.84 to 27.59°.
Index ranges	-13<=h<=13, -15<=k<=15, -46<=l<=47
Reflections collected	128242
Independent reflections	10178 [R(int) = 0.0509]
Absorption correction	Semi-empirical from equivalents
Max. and min. transmission	0.9341 and 0.8791
Data / restraints / parameters	10178 / 0 / 586
Goodness-of-fit on F^2	1.058
Final R indices [I>2sigma(I)]	R1 = 0.0243, wR2 = 0.0542
R indices (all data)	R1 = 0.0278, wR2 = 0.0556
Largest diff. peak and hole	0.354 and -0.408 e.$Å^{-3}$
Absolute structure parameter	-0.020(15)

6.3.4. Synthesis and reactivity of new bidentate P,N-phosphoramidite ligands

The failure of the ligands Ph_2PPyr and $PhPPyr_2$ to yield viable complexes leaves this method of electronic tuning incomplete at best. Ideally a series of electronically tuned ligands could be synthesized by the same general procedure while meeting minimum requirements of yield and giving high diastereoselectivity in complex formation. Attempts at substitution of both PPh_3 ligands of $[(Ind)RuCl(PPh_3)_2]$ (**110**) by one bidentate or two monodentate P-donor ligands (such as phosphines, phosphites and phosphoramidites) fail in most cases. Thus N-donor ligands represent an interesting alternative. Pyridine and its derivatives are known to form coordination bonds to ruthenium, giving stable complexes.[13] In addition, many derivatives of pyridine that vary greatly in steric and electronic properties are commercially available.[14] When $[(Ind)RuCl(PPh_3)($**41b**$)]$ (**111b**) is heated to reflux with pyridine as solvent, the desired substitution does not occur (Scheme 6.9). Slow decomposition of **111b** can be seen by the appearance of new peaks in the ^1H NMR spectrum, but the desired $[(Ind)RuCl(py)($**41b**$)]$ (py = pyridine) is not obtained. Substitution of the second PPh_3 ligand (beginning from $[(Ind)RuCl(PPh_3)_2]$ (**110**)) is clearly difficult. Increasing the entropic favorability of the reaction by utilizing a chelating ligand may help to drive the reaction forward.

P, N chelating phosphoramidite ligands are extremely rare, especially in the case of phosphoramidites with a dangling pyridyl group.[15] The first ligand bearing the *N*-(2-pyridyl)methyl substituent[16] (**135a**) was synthesized in 80% yield by previously applied methods (Scheme 6.10).[17] The *N*-benzyl substituent was specifically chosen because this new ligand is nearly identical to the *N*,*N*-dibenzyl ligand that has consistently shown the highest activity and greatest stability in the corresponding metal complexes. When **135a** is combined with [(Ind)RuCl(PPh_3)$_2$] (**110**) and heated to reflux in toluene for 15 h, double substitution of PPh_3 takes place and [(Ind)RuCl(**135a**)] (**136a**) is obtained in 60% yield after chromatographic work up (Scheme 6.11).

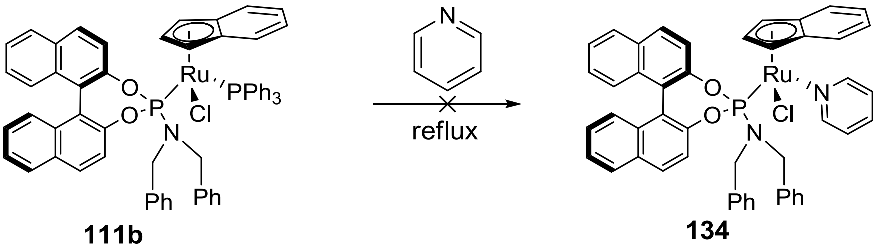

Scheme 6.9. Attempted synthesis of a pyridyl complex.

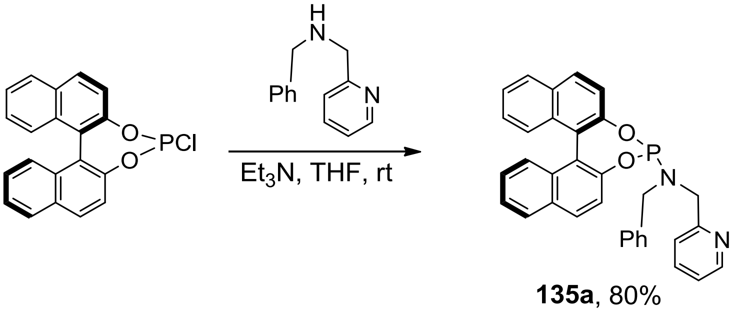

Scheme 6.10. Synthesis of a new P,N-chelating phosphoramidite.

Complex **136a** shows a single peak in the ^{31}P NMR, confirming that both PPh_3 ligands are displaced in the product. In the ^{1}H NMR the indenyl peaks fall in the range 4.78-4.34 ppm, similar to the mixed phosphine/phosphoramidite complexes described in

Chapter 5. The methylene protons show coupling to the P atom, giving a complex, non-first order splitting pattern.

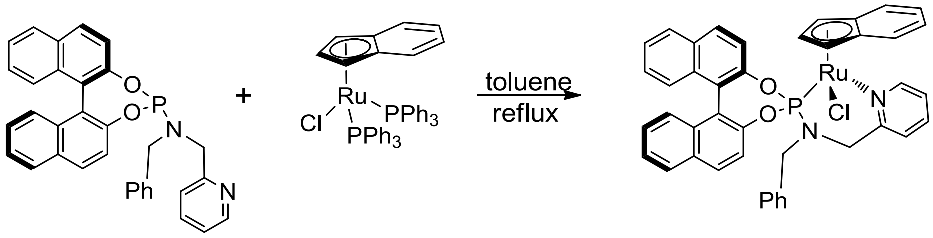

135a **110** **136a**, 60%

Scheme 6.11. Synthesis of a new P,N-phosphoramidite complex.

The bidentate P, N-coordinating phosphoramidite ligand **135a** gives a basis for future tuning efforts via substitution of the pyridyl ring. A general, high-yielding synthesis is necessary to create a small library of new electronically tuned ligands. Concurrent steric and electronic tuning was envisioned by beginning with the commercially available 2-bromo-6-methoxypyridine (**137**). Halogen-lithium exchange in THF followed by formylation using DMF (*N*,*N*-dimethylformamide) gives 6-methoxy-2-pyridinecarboxaldehyde (**138**) in 71% yield (Scheme 6.12). Combining the aldehyde with benzyl amine in methanol with 3 Å molecular sieves gives the corresponding *N*-benzylimine after stirring overnight (15 h). Subsequent reduction with $NaBH_4$ yields the secondary amine (**139**) in 84% yield after chromatographic workup. It is important to ensure that the imine formation is complete before addition of $NaBH_4$ because the alcohol (resulting from reduction of the aldehyde) reacts with the chlorophosphite intermediate in a similar manner as the amine to form a phosphite. Separation of the phosphite and phosphoramidite is a difficult task and thus avoiding formation of the alcohol is crucial. Allowing the imine formation to run for 15 h then removing all volatiles under vacuum gives the imine with no sign of the aldehyde (shown by ^{1}H NMR). The reduction then proceeds smoothly and the amine is converted to the phosphoramidite **135b** in 67% yield using standard conditions (Scheme 6.12).[17]

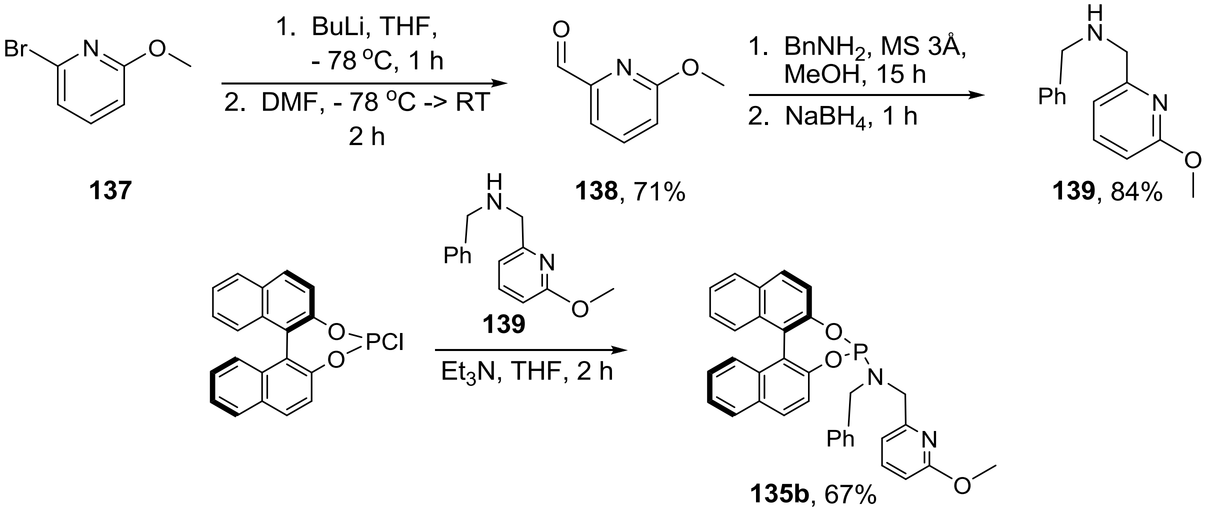
Br
N
O
1. BuLi, THF,
- 78 °C, 1 h
2. DMF, - 78 °C -> RT
2 h
137
O
N
O
138, 71%
1. BnNH2, MS 3Å,
MeOH, 15 h
2. NaBH4, 1 h
H
N
Ph
N
O
139, 84%
O
O
PCl
H
N
Ph
N
O
139
Et3N, THF, 2 h
O
O
P
N
Ph
N
O
135b, 67%

Scheme 6.12. Synthesis of an electronically tuned P,N-phosphoramidite ligand.

The reaction between the new phosphoramidite **135b** and [(Ind)RuCl(PPh$_3$)$_2$] (**110**) in reluxing toluene does not give the expected complex derived from double substitution of PPh$_3$ ([(Ind)RuCl(**135b**)] (**136b**)), but instead only a single substitution to give **140** is observed (Scheme 6.13). Complex **140** could not be isolated, possibly due to ongoing decomposition (seen by the appearance of new peaks in the ^{31}P NMR spectrum). As the 6-methoxy substituted pyridyl ring can be expected to be more electron donating than its unsubstituted analog, the reason for this unexpected difference in reactivity is likely sterics. The 6-methoxy group would presumably point directly toward the metal in the intended product with a bidentate coordination mode. This steric interaction is likely the reason for the observed monodentate coordination.

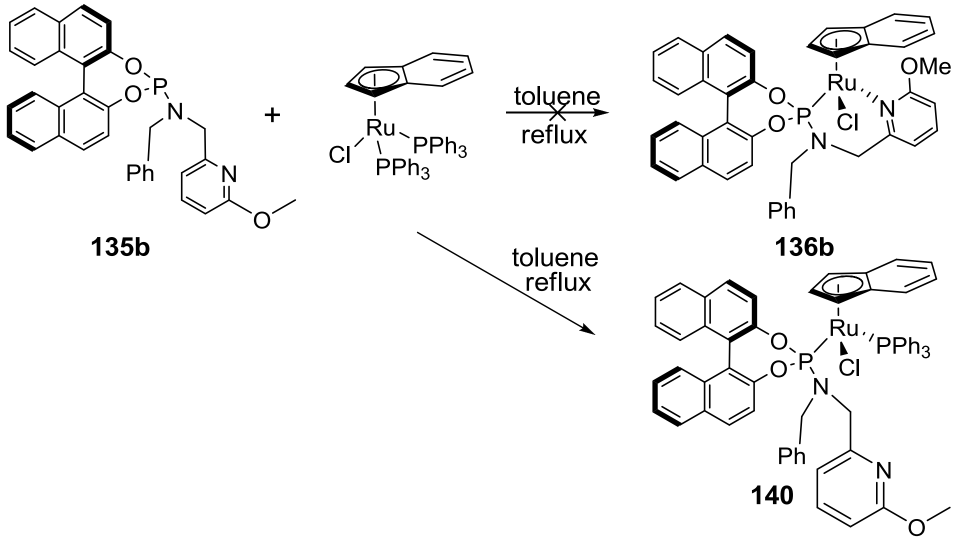

Scheme 6.13. Unexpected reactivity of the new bidentate ligand.

Formation of the mixed complex is best seen by the presence of two doublets in the ^{31}P NMR. The phosphoramidite signal appears at 175.3 ppm with a coupling constant of 36.9 Hz, in the range of the other mixed phosphine/phosphoramidite complexes reported in Chapter 5. In the ^{1}H NMR, the methylene protons of the ligand are diastereotopic, giving multiplets in the range 7.8-3.7 ppm. The methoxy protons appear as a singlet at 3.71 ppm. There does not appear to be a second diastereomer in the ^{1}H NMR of the crude reaction mixture, but the ^{31}P NMR reveals a second set of doublets (~10%) that may correspond to a diastereomer.

6.3.5. Decomposition of bidentate phosphoramidite ligands

Interestingly, the ligands **135a, b** show an inherent lability toward hydrolysis. Attempting to purify **135a** or **135b** by flash chromatography on silica gel (the method used to purify **41b**) results in complete hydrolysis. Under these conditions the BINOL is isolated at ~70% recovery. The ligands are not only sensitive in the presence of silica, however. Over the course of several days to weeks the ligands will hydrolyze even in the solid state. The solids will slowly change color from white to yellow, signifying ongoing decomposition. Evidence for the hydrolysis of the ligands can also be seen in the ^{31}P NMR. After several days of exposure to air, the singlet at 145.8, 146.0 ppm (**135a, b** respectively) is replaced by a number of peaks in the range 5-0 ppm. No peaks are visible in the range 15-12 ppm, confirming that decomposition is due to hydrolysis and not oxidation (phosphoramidite oxides are typically seen in this range).[18]

The reason for the hydrolysis lability of these ligands is not entirely clear. The dibenzyl ligand **41b** (differing only in the 2-position of the aromatic ring) shows remarkable stability to hydrolysis in the solid state. Indeed, after more than 30 days exposure to open atmosphere, no hydrolysis peaks are observed in the ^{31}P NMR. The N atom of the pyridyl ring clearly plays a role in the hydrolysis of the ligand. It is possible that the addition of an electronegative heteroatom simply makes ligands **135a, b** more hygroscopic than the corresponding monodentate ligands **41a-d**. An increased attraction to water would make the ligands have greater contact with water thus increasing the likelihood of hydrolysis.

An alternative explanation would be that the N-atom of the pyridyl ring is somehow involved in the transition state of the hydrolysis reaction (Figure 6.4).

Coordination of the ligand (**135a**) to ruthenium in a bidentate fashion dramatically increases the stability of the ligand; the complex does not show moisture sensitivity in the solid state, as evidenced by ^{1}H and ^{31}P NMR after storage for several weeks. This corroborates the idea that the N atom is involved in the transition state of the hydrolysis reaction. Once the lone pair of N is sequestered in a coordination bond to ruthenium, it is no longer able to form a hydrogen bond to water, thus leaving the ligands no more moisture sensitive than their monodentate counterparts (not containing a coordinating N atom). Ultimately, the consequence of the hydrolysis lability of the ligand means that it must be reacted with an appropriate metal precursor shortly after synthesis (≤ 24 h) for optimal results.

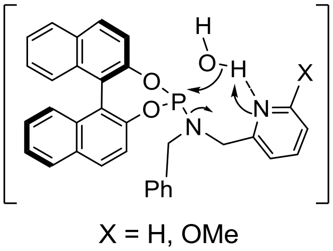

Figure 6.4. Hydrolysis of the P,N-bidentate phosphoramidite ligands.

By analogy to ligand **135a**, I hypothesized that **135b** might show greater stability toward hydrolysis once coordinated to a metal in a bidentate fashion. Because the ligand is unable to substitute both phosphine ligands of [(Ind)RuCl(PPh$_3$)$_2$] (**110**), the cationic complex [(Ind)Ru(PPh$_3$)(**135b**)]X$^-$ was targeted. Reaction of the monosubstituted complex **140** with AgBF$_4$ in THF gives [(Ind)Ru(PPh$_3$)(**135b**)]BF$_4$ (**141a**, Scheme 6.14). The complex shows significant spectroscopic differences from its neutral counterpart. In the ^{1}H NMR, the indenyl proton signals shift from 5.6, 5.2 and 4.0 ppm in **140** to 5.2, 5.1 and 3.4 ppm in **141a**. In the ^{31}P NMR, the phosphoramidite signal shifts 1 ppm upfield relative to that in **140** (175.4-174.5 ppm). The cationic complex can also be synthesized by refluxing **135b** with [(Ind)RuCl(PPh_3)] (**110**) and $NaPF_6$ in methanol to give [(Ind)Ru(PPh_3)(**135b**)]PF_6 (**141b**). The spectroscopic properties of **141b** are the same as those reported for **141a**. Recrystallization of **141a, b** fails to give pure product.

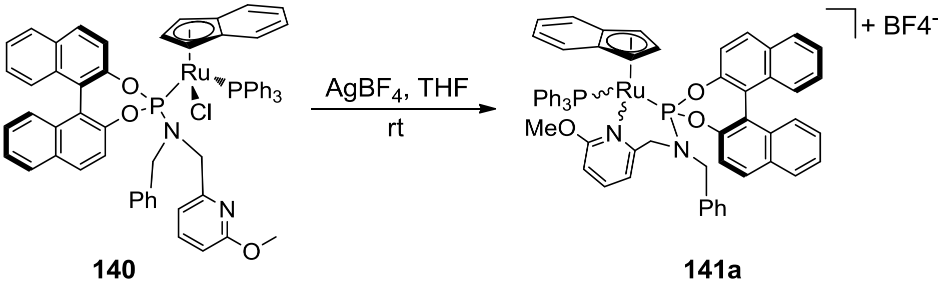

140   **141a**

Scheme 6.14. Synthesis of a cationic complex **141a**.

6.4. Discussion

6.4.1. Attempts at electronic tuning via indene substitution

Electronic tuning of piano-stool ruthenium complexes bearing phosphoramidite ligands is a nontrivial task. Attempts at electronic tuning via the phosphoramidite ligands themselves showed little effect (Chapters 2, 3). Alteration of indene with electron-withdrawing or electron-donating substituents is a potential way of tuning the molecule electronically while not affecting the sterics. However, the indene derivatives 2-bromoindene (**131**) and 2-(*p*-toluenesulfonyl)indene do not coordinate to ruthenium under the conditions used to form the parent precursor [(Ind)RuCl($(PPh_3)_2$] (**110**). Thus the only remaining option for complex tuning is replacement of the phosphine by another neutral two electron donor.

6.4.2. Electronic tuning via phosphine substitution

Substituting PPh_3 by tripyrrolylphosphine ($PPyr_3$) is possible and the new complex [(Ind)RuCl($PPyr_3$)(**41b**)] (**132**) was synthesized in 59% yield in one step beginning from [(Ind)RuCl($(PPh_3)_2$] (**110**). The new complex again forms as a single diastereomer. Substitution of both PPh_3 ligands in this reaction requires high temperatures (110 ^{o}C) and an excess of $PPyr_3$ (3 equivalents). Because the phosphines $PhPPyr_2$ and Ph_2PPyr could not be converted to viable mixed phosphine/phosphoramidite complexes, a broad range of tuned complexes is unavailable. In order to properly ascertain the effect of electronic tuning a small library of tuned complexes must be synthesized and tested for activity in reactions with propargylic alcohols. The sensitivity of the complexes to steric effects, seen both in the diastereoselectivity of complex formation as well as the reactivity of the complexes (Chapter 5), means that steric factors need to be considered when targeting electronically tuned complexes.

6.4.3. Reactivity of bidentate phosphoramidite complexes

Bidentate ligands are a good choice for substitution of both PPh_3 ligands on [(Ind)RuCl($(PPh_3)_2$] (**110**) because the entropic favorability of the reaction can help push the reaction towards completion. Using the chelate effect to an advantage allows tuning via ligand classes that may not coordinate in a monodentate form. This is clearly seen in the new class of bidentate phosphoramidite ligands containing a pendant pyridyl moiety. Even in the presence of a large excess of pyridine at high temperatures, the complex [(Ind)RuCl(PPh_3)(**41b**)] (**111b**) is inert to substitution of PPh_3 by pyridine. On the other hand the bidentate ligand **135a** can substitute both PPh_3 ligands of [(Ind)RuCl($(PPh_3)_2$] (**110**) in refluxing toluene to give [(Ind)RuCl(**135a**)] (**136a**) as a single diastereomer.

The difference in the electronic properties of the ligands **41a, b** is not outwardly apparent due to the difference in their mode of reactivity with [(Ind)RuCl($(PPh_3)_2$] (**110**). Whereas the parent ligand **135a** gives the expected double phosphine substitution, **135b** yields the monosubstituted product. This steric difference leaves the two complexes not easy to compare as they should be expected to show considerably different reactivity based on their coordination mode and not on their electronic differences.

6.4.4. Catalytic activation of propargylic alcohols

All of the new complexes have been tested in stoichiometric and catalytic experiments involving propargylic alcohols. Activation of [(Ind)RuCl($PPyr_3$)(**41b**)] (**132**) or [(Ind)RuCl(**135a**)] (**136a**) by (Et_3O)PF_6 in CH_2Cl_2 (as performed in Chapters 3, 5) gives the reactive species [(Ind)Ru($PPyr_3$)(**41b**)]PF_6 or [(Ind)Ru(**135a**)]PF_6, respectively. Addition of 1,1-diphenyl-2-propyn-1-ol (**5a**) causes the solution to turn from orange to dark purple, as expected for allenylidene formation. NMR analysis (^{1}H, ^{31}P) reveals a mixture of products. The instability of the intermediate cation is likely the cause of the observed formation of many products instead of only the expected allenylidenes. $PPyr_3$ in particular was chosen specifically for its relative electron deficiency (compared to PPh_3). Because [(Ind)RuCl(PPh_3)(**135b**)] (**140**) cannot be isolated cleanly, it was not tested for activity in reactions with propargylic alcohols.

The complexes **132** and **136a** were also tested for catalytic activity in propargylic substitution reactions. Propargylic amination, etherification and Friedel-Crafts reactions were all tested on propargylic alcohols 1,1-diphenyl-2-propyn-1-ol (**5a**), 2-phenyl-3-butyn-2-ol (**5b**) and 2-propyn-1-ol (**5d**). The reactions were run at temperatures between rt and 50 ^{o}C in CH_2Cl_2, THF or 1,2-dichloroethane (DCE). In all cases no conversion is observed. Chloride abstraction from **132**, **136a** perhaps leaves the resultant species too reactive toward decomposition reactions, instead of turning over in a catalytic cycle.

6.5. Summary and Prospective

New sterically and electronically tuned phosphoramidite ruthenium complexes have been synthesized. All of these complexes have been isolated in diastereomeric purity. The new complexes do not form stable, isolable allenylidenes, potentially due to the high reactivity of the intermediate species.

A new P, N-bidentate phosphoramidite ligand class has been developed. A general synthetic sequence beginning from 2-bromopyridine derivatives has been created. The availability of pyridine derivatives of this type makes this synthetic strategy applicable for the synthesis of a wide range of electronically tuned ligands.

6.6. Conclusions

Piano-stool ruthenium complexes can activate propargylic alcohols both in stoichiometric as well as catalytic reactions. In the case of η^6-*p*-cymene complexes, the catalytic activity of the complexes is clearly related, in part, to the steric effects of the ligands with the more hindered complexes outperforming their less sterically crowded counterparts. Although it is not the biggest ligand, the complex with ligand **41b** (the ligand bearing the *N*,*N*-dibenzyl substituent) outperforms all other complexes. The arene ligand of these complexes has been shown to be labile, dissociating at elevated temperatures or after prolonged times in solution (CH_2Cl_2, cyclohexane) or in the solid state. Although arene dissociation appears to be less likely in coordinating solvents such as THF or acetonitrile, allenylidene formation in these solvents gives excessive side product formation or no reaction at all. The complexes overall were shown to be inactive in reactions involving allenylidene intermediates.

Mixed phosphine/phosphoramidite complexes of ruthenium are viable complexes for the activation of propargylic alcohols as well. The diastereoselectivity of complex formation is highly dependent on the steric effects of the incoming phosphoramidite ligand. Again the best results were obtained for the *N*,*N*-dibenzyl ligand **41b**. The cylcopentadienyl complex bearing the ligand **41b** (**69b**) can be isolated in diastereomeric purity and forms the stable allenylidene [CpRu(PPh_3)(**41b**)(=C=C=CPh_2)]PF_6 (**71b**) in reaction with 1,1-diphenyl-2-propyn-1-ol (**5a**) after chloride abstraction using $AgPF_6$ or

$(Et_3O)PF_6$ in CH_2Cl_2. The allenylidene is not isolable, however, and the complex is not active in catalytic reactions with propargylic alcohols.

Switching arenes from cyclopentadiene to indene increases the activity of the resultant phosphoramidite complexes in reactions with propargylic alcohols. Utilizing the fragment $[(Ind)Ru(PPh_3)(\mathbf{41b})]^+$ formed by chloride abstraction from $[(Ind)RuCl(PPh_3)(\mathbf{41b})]$ (**111b**), allenylidenes $[(Ind)Ru(PPh_3)(\mathbf{41b})(=C=C=CR^1R^2)]PF_6$ (**116**) can be synthesized in high yield and complete diastereoselectivity with a variety of R groups. The cationic fragment $[(Ind)Ru(PPh_3)(\mathbf{41b})]^+$ is also active in a Friedel-Crafts type reaction involving propargylic alcohols. The reaction is believed to proceed by protonation of an intermediate allenylidene to give the alkenylcarbyne electrophile.

Steric tuning via the substituents on the N atom of the phosphoramidite ligand shows a clear effect on the catalytic activity and diastereoselectivity of the piano-stool ruthenium complexes. Electronic tuning, however, is a much more difficult challenge. Electronic tuning via the phosphoramidite ligand shows little effect; substitution of the BINOL backbone does not give significant alteration of activity (Chapters 2, 3). Exchanging the O-atoms of the phosphoramidite ligand for S-atoms to form a dithiaphosphoramidite resulted in a ligand and subsequent complex of low stability, prone to hydrolysis and alcoholysis. Alteration of the indenyl substituent by the addition of electron-withdrawing groups failed to give a viable complex for test reactions.

By far the most effective way to electronically tune piano-stool ruthenium complexes with phosphoramidite ligands is by substitution of the phosphine in mixed phosphine/phosphoramidite complexes. Substitution of PPh_3 by a relatively electron-poor, monodentate phosphine ($PPyr_3$) is possible, but using this method a broad range of electronically tuned complexes was shown to not be readily available. Bidentate phosphoramidite ligands utilizing a pyridyl moiety can coordinate in a chelating fashion, favoring the double substitution due to entropic reasons. A potentially general synthetic route to this new class of ligands has been developed. The effectiveness of this method of electronic tuning is still uncertain, as the coordination chemistry of the analogous ligands is dissimilar due to steric reasons. Synthesis of a small library of tuned, bidentate phosphoramidite ligands will give greater insight into the usefulness of this ligand class and will allow further tuning of the catalytic activity of the respective complexes.

---

[1] Costin, S.; Rath, N. P.; Bauer, E. B. *Tetrahedron Lett.* **2009**, *50*, 5485.

[2] Costin, S.; Rath, N. P.; Bauer, E. B. *Adv. Synth. Catal.* **2008**, *350*, 2414.

[3] (a). Gamasa, M. P.; Gimeno, J. Gonzalez-Bernardo, C.; Borge, J.; García-Granda, S. *Organometallics* **1997**, *16*, 2483; (b). Sridevi, V. S.; Leong, W. K. *J. Organomet. Chem.* **2007**, *692*, 4909.

[4] (a). Kündig, E. P.; Saudan, C. M.; Alezra, V.; Viton, F.; Bernardinelli, G. *Angew. Chem. Int. Ed.* **2001**, *40*, 4481; (b). Iizuka, Y.; Li, Z.; Satoh, K.; Kamigaito, M.; Okamoto, Y.; Ito, J.; Nishiyama, H. *Eur. J. Org. Chem.* **2007**, 782; (c). Ng, S. Y.; Fang, G.; Leong, W. K.; Goh, L. Y.; Garland, M. V. *Eur. J. Inorg. Chem.* **2007**, 452.

[5] (a). Prasad, K. T.; Gupta, G.; Chandra, A. K.; Pavan, M. P. ; Rao, K. M. *J. Organometallic Chem.* **2010**, *695*, 707; (b). Gupta, G.; Prasad, K. T.; Das, B.; Rao, K. M. *Polyhedron* **2010**, *29*, 904; (c). García-Fernández, A.; Gimeno, J.; Lastra, E.; Madrigal, C. A.; Graiff, C.; Tiripicchio, A. *Eur. J. Inorg. Chem.* **2007**, 732; (c). Mebi, C. A.; Nair, R. P.; Frost, B. J. *Organometallics* **2007**, *26*, 429.

[6] Álvarez, P.; Gimeno, J.; Lastra, E.; García-Granda, S.; Van der Maelen, J. F.; Bassetti, M. *Organometallics* **2001**, *20*, 3762.

[7] Hata, E.; Yamada, T.; Mukaiyama, T. *Bull. Chem. Soc. Jpn.* **1995**, *68*, 3629.

---

[8] Back, T. G.; Collins, S. *J. Org. Chem.* **1981**, *46*, 3249.

[9] Billups, W. E.; Buynak, J. D.; Butler, D. *J. Org. Chem.* **1980**, *45*, 4636.

[10] Cristau, H.-J.; Ouali, A.; Spindler, J. F.; Taillefer, M. *Chem. Eur. J.* **2005**, *11*, 2483.

[11] Oro, L. A.; Ciriano, M. A.; Campo, M.; Foces–Foces, C.; Cano, F. H. *J. Organometallic Chem.***1985**, *289*, 117.

[12] Jackstell, R.; Klein, H.; Beller, M.; Wiese, K.-D.; Rottger, D. *Eur. J. Org. Chem.* **2001**, 3871.

[13] (a). Coe, B. J.; Meyer, T. J.; White, P. S.; *Inorg. Chem.* **1995**, *34*, 3600; (b). Chen, D.; Zhang, X.; Xu, S.; Song, H.; Wang, B. *Organometallics* **2010**, *29*, 3418.

[14] www.aldrich.com

[15] Niu, J.-L.; Chen, Q.-T.; Hao, X.-Q.; Zhao, Q.-X; Gong, J.-F.; Song, M.-P. *Organometallics* **2010**, *29*, 2148.

[16] Zheng, Z.; Zhao, G.; Fablet, R.; Bouyahyi, M.; Thomas, C. M.; Roisnel, T.; Casagrande, O. Jr.; Carpentier, J.-F. *New J. Chem.* **2008**, *32*, 2279.

[17] Hulst, R.; de Vries, N. K.; Feringa, B. L. *Tetrahedron: Asymmetry* **1994**, *5*, 699.

[18] Pizzuti, M. G.; Minaard, A. J.; Feringa, B. L. *J. Org. Chem.* **2008**, *73*, 941.

Experimental Section

General. Chemicals were treated as follows: THF, toluene, diethyl ether (Et_2O), distilled from Na/benzophenone; CH_2Cl_2, MeOH, distilled from CaH_2. (R)-1,1'-binaphthyl-2,2'-diol ((R)-BINOL) (Strem), phosphorus trichloride (PCl_3), *N*-methyl-2-pyrrolidinone (NMP) (Acros), 1,1-diphenyl-2-propyn-1-ol (**5a**) (Aldrich), 2-phenyl-3-butyn-2-ol (**5b**) (Aldrich), BuLi (1.6 M in hexanes, Aldrich), anhydrous DMF (Acros) and other materials used as received. "(R)-BINOL-*N,N*-dimethyl-phosphoramidite" **41a,**[1a] "(R)-BINOL-*N,N*-dibenzyl-phosphoramidite" **41b,**[1b] [RuCl(Ind)(PPh_3)$_2$] (**110**, Ind = indenyl anion)[2] and tripyrrolylphosphine ($PPyr_3$)[3] were synthesized according to literature procedures.

NMR spectra were obtained at room temperature on a Bruker Avance 300 MHz or a Varian Unity Plus 300 MHz instrument and referenced to a residual solvent signal; all assignments are tentative. Exact masses were obtained on a JEOL MStation [JMS-700] Mass Spectrometer. Melting points are uncorrected and were taken on an Electrothermal 9100 instrument. IR spectra were recorded on a Thermo Nicolet 360 FT-IR spectrometer. Elemental Analyses were performed by Atlantic Microlab Inc., Norcross, GA, USA.

"[RuCl(Ind)($PPyr_3$)((R)-BINOL-*N,N*-dibenzyl-phosphoramidite)]" (**132**). To a Schlenk flask containing [(Ind)RuCl(PPh_3)$_2$] (**110**) (0.227 g, 0.292 mmol), **41b** (0.156 g, 0.305 mmol) and $PPyr_3$ (0.201 g, 0.879 mmol), toluene (9 mL) was added and the mixture heated to reflux for 15 h. Upon cooling to rt, the solvent was removed under high vacuum. The resulting residue was purified by flash chromatography (2 x 14 cm silica), eluted with CH_2Cl_2. The first of two orange bands was collected and all volatiles removed under high vacuum to give **132** as an orange solid (0.170 g, 0.172 mmol, 59%), m.p. 154–156 ^{o}C dec. (capillary). An analytically pure sample was obtained by slow diffusion of methanol into a solution of **132** in CH_2Cl_2. Recovered 12 mg from 15 mg original sample, 80% recovery. Anal calcd. for $C_{55}H_{45}N_4O_2P_2ClRu$: C, 67.84 H, 4.68; Found: C, 67.59; H, 4.72.

NMR (δ, $CDCl_3$) ^1H 8.10 (d, $^3J_{HH}$ = 8.8 Hz, 1H, aromatic), 7.99 (d, $^3J_{HH}$ = 9.4 Hz, 1H, aromatic), 7.65 (d, $^3J_{HH}$ = 8.7 Hz, 2H, aromatic), 7.59 (d, $^3J_{HH}$ = 8.2 Hz, 1H, aromatic), 7.51 (d, $^3J_{HH}$ = 8.9 Hz, 1H, aromatic), 7.46 (t, $^3J_{HH}$ = 7.1 Hz, 1H, aromatic), 7.30–7.13 (m, 15H, aromatic), 7.12–6.97 (m, 4H, aromatic), 6.90–6.83 (m, 3H, pyrrolyl), 6.31 (s, br, 1H, pyrrolyl), 6.08 (s, br, 1H, pyrrolyl), 5.90 (s, br 7H, pyrrolyl), 5.53 (s, br, 1H, indenyl), 5.44 (s, br, 1H, indenyl), 4.93 (s, br, 1H, indenyl), 4.51 (d, $^2J_{HH}$ = 10.6 Hz, 1H, C*H*H'), 4.46 (d, $^2J_{HH}$ = 10.6 Hz, 1H, CH*H*'), 3.15 (d, $^2J_{HH}$ = 11.4 Hz, 1H, C*H*H'), 3.10 (d, $^2J_{HH}$ = 11.4 Hz, 1H, CH*H*'); $^{13}C\{^1H\}$ 150.3 (d, J_{CP} = 15.5 Hz, aromatic), 148.6 (d, J_{CP} = 7.0 Hz, aromatic), 138.3 (s, aromatic), 133.9 (s, aromatic), 132.6 (s, aromatic), 131.7 (s, aromatic), 131.1 (s, aromatic), 130.3 (s, aromatic), 129.6 (s, aromatic), 129.5 (s, aromatic), 129.2 (s, aromatic), 128.5 (s, aromatic), 128.2 (s, aromatic), 128.1 (s, aromatic), 127.4 (s, aromatic), 126.9 (s, aromatic), 126.7 (s, aromatic), 126.3 (s, aromatic), 125.9 (s, aromatic), 125.2 (s, aromatic), 125.0 (s, aromatic), 124.1 (s, br, aromatic), 123.3 (s, aromatic), 122.3 (s, aromatic), 121.7 (s, aromatic), 121.5 (s, aromatic), 112.5 (s, aromatic), 112.2 (s, indenyl), 111.4 (s, br, indenyl), 92.0 (s, indenyl), 69.7 (d, $^2J_{CP}$ = 1.5 Hz, indenyl), 65.5 (d, $^2J_{CP}$ = 7.6 Hz, indenyl), 49.7 (s, *C*H_2), 49.6 (s, *C*H_2); $^{31}P\{^1H\}$170.7 (d, $^2J_{PP}$ = 77.6 Hz, phosphoramidite), 124.8 (d, $^2J_{PP}$ = 77.6 Hz, *P*Pyr$_3$).

HRMS calcd for $C_{55}H_{45}N_4O_2P_2ClRu$ 992.1749, found 992.1731. IR (neat solid, cm^{-1}) 3052(w), 3028(w), 1587(m), 1455(m), 1321(m), 1228(s), 1178(s), 1056(s), 1037(s), 730(s).

“6-methoxy-2-pyridinecarboxaldehyde”, (138). To a flame dried Schlenk flask was added THF (30 mL) and 2-bromo-6-methoxypyridine (1.8 mL, 14.6 mmol) and the solution was cooled to –78 °C. BuLi (10.0 mL, 16 mmol, 1.6 M in hexanes) was added dropwise over ca. 10 minutes and the solution stirred for 1.5 h at –78 °C. DMF (1.8 mL, 23 mmol) was added and the solution stirred for 30 min at –78 °C after which the solution was allowed to slowly warm to rt and then stirred for an additional 1 h. A saturated aqueous solution of NH_4Cl (60 mL) was added and the aqueous layer extracted with CH_2Cl_2 (2 × 100 mL). The combined organic layers were dried over Na_2SO_4, filtered and all volatiles were removed under high vacuum (Note: after extended times (> ~1 h) under high vacuum **138** will slowly evaporate reducing the yield). The yellow oil was purified by flash chromatography (4 × 12 cm silica), eluted with CH_2Cl_2/hexanes 1:1 v/v. The fractions ($R_f \approx 0.5$) were collected and volatiles removed under high vacuum to give **138** as a clear, colorless oil (1.44 g, 10.5 mmol, 72%).

NMR (δ, $CDCl_3$) ^1H 9.96 (s, 1H, C*H*O), 7.74 (t, $^3J_{HH}$ = 7.9 Hz, 1H, aromatic), 7.57 (d, $^3J_{HH}$ = 7.2 Hz, 1H, aromatic), 6.98 (d, $^3J_{HH}$ = 8.3 Hz, 1H, aromatic), 4.04 (s, 3H, OCH_3); $^{13}C\{^1H\}$ 193.6 (s, *C*HO), 164.8 (s, pyridyl), 150.8 (s, pyridyl), 139.5 (s, pyridyl), 116.8 (s, pyridyl), 116.0 (s, pyridyl), 54.1 (s, OCH_3).

EI MS 137 (**138**$^+$, 85%), 108 ([**138**-CHO]$^+$, 30%), 93 ([**138**-CHO-CH_3]$^+$, 40%). IR (neat solid, cm^{-1}) 2985(m), 2954(s), 2828(s), 2684 (w), 2594 (w), 1701(s, C=O), 1597 (s, C=C), 1473 (s).

“*N*-benzyl-2-(6-methoxypyridyl)methyl amine”, (139). To a Schlenk flask containing crushed 3 Å MS was added methanol (6 mL) and **138** (0.200 g, 1.46 mmol) followed by benzyl amine (0.180 mL, 1.65 mmol). The resulting solution was allowed to stir overnight at rt (20 h) and then the contents were filtered through a fritted funnel. The filtrate was collected and the volatiles removed under high vacuum. 6 mL methanol was then added and the oil dissolved. $NaBH_4$ (0.115 g, 3.04 mmol) was added and a gas evolved. After 2 h stirring at rt, the solution was decanted into a beaker containing H_2O (50 mL). The solution was acidified with HCl to pH 0 then KOH pellets were added until the pH reached 14. The aqueous layer was extracted with CH_2Cl_2 (4 × 50 mL) and the combined organic layers dried over Na_2SO_4, filtered and the volatiles removed under vacuum. The resulting oil was then purified by flash chromatography (2 × 15 cm silica) using CH_2Cl_2/Et_2O 9:1 v/v followed by CH_2Cl_2/acetone 9:1 v/v as eluent to give **139** as a clear, colorless oil (0.280 g, 1.22 mmol, 84%).

NMR (δ, $CDCl_3$) ^1H 7.40 (t, $^3J_{HH}$ = 7.6 Hz, 1H, pyridyl), 7.38–7.14 (m, 5H, Ph), 6.73 (d, $^3J_{HH}$ = 7.2 Hz, 1H, pyridyl), 6.51 (d, $^3J_{HH}$ = 8.2 Hz, 1H, pyridyl), 3.83 (s, 3H, OCH_3), 3.73 (s, 2H, NCH_2), 3.72 (s, 2H, NCH_2'), 2.05 (s, br, 1H, NH); $^{13}C\{^1H\}$ 164.3 (s, aromatic), 157.8 (s, aromatic), 140.7 (s, aromatic), 139.3 (s, aromatic), 128.8 (s, aromatic), 128.7 (s, aromatic), 127.4 (s, aromatic), 151.2 (s, aromatic), 109.1 (s, aromatic), 54.4 (s, OCH_3), 53.8 (s, NCH_2), 53.7 (s, NCH_2).

EI MS 120 ($PhCH_2NHCH_2^+$, 5%), 106 ($PhCH_2NH^+$, 100%), 91 ($PhCH_2^+$, 40%), 77 (Ph^+, 35%). IR (neat solid, cm^{-1}) 3028(w), 2948(w), 1599(m), 1578(s), 1464(s), 1414(m), 1305(m), 1030(m).

"(R)-BINOL-*N*-benzyl-*N*-(2-pyridyl)methyl-phosphoramidite" (**135a**). To a Schlenk flask containing (R)-BINOL (0.503 g, 1.76 mmol), PCl_3 (0.600 mL, 6.88 mmol) was added followed by NMP (0.010 mL) and the mixture was heated to reflux for 1 h. After cooling to rt, the excess PCl_3 was removed under high vacuum. Residual PCl_3 was removed by coevaporation with Et_2O (3 × 3 mL) under high vacuum. THF (10 mL) was added followed by Et_3N (0.350 mL, 2.64 mmol) and *N*-benzyl-*N*-(2-pyridyl)methyl amine (0.348 g, 1.76 mmol). After 2.5 h stirring at rt, the slurry was filtered over Celite® and the volatiles were removed under high vacuum. Et_2O (15 mL) was added and the resulting slurry was filtered over Celite® to give **135a** in ca. 90% spectroscopic purity (0.720 g, 1.40 mmol, 80%), m.p. 60-62 ^{o}C dec. (capillary).

NMR (δ, $CDCl_3$) ^1H 8.46–8.42 (m, 1H, aromatic), 7.93 (d, $^3J_{HH}$ = 8.8 Hz, 1H, aromatic), 7.84 (d, $^3J_{HH}$ = 8.9 Hz, 1H, aromatic), 7.74–7.72 (m, 1H, aromatic), 7.68 (d, $^3J_{HH}$ = 8.8 Hz, 1H, aromatic), 7.65–7.59 (m, 1H, aromatic), 7.56 (d, $^3J_{HH}$ = 8.7 Hz, 1H, aromatic), 7.40–7.34 (m, 2H, aromatic), 7.31–7.20 (m, 9H, aromatic), 7.18–7.10 (m, 2H, aromatic), 6.99 (d, $^3J_{HH}$ = 8.8 Hz, 1H, aromatic), 4.29–4.10 (m, 2H, CH_2), 3.72–3.50 (m, 2H, CH_2'); $^{13}C\{^1H\}$ 158.7 (s, aromatic), 149.6 (d, J_{CP} = 21.6 Hz, aromatic), 149.4 (s, aromatic), 137.8 (s, aromatic), 136.7 (s, aromatic), 133.1 (s, aromatic), 132.7 (s, aromatic), 131.7 (s, aromatic), 131.0 (s, aromatic), 130.5 (d, J_{CP} = 5.1 Hz, aromatic), 129.3 (s, aromatic), 128.7 (s, aromatic), 128.6 (s, aromatic), 127.7 (s, aromatic), 127.2 (d, J_{CP} = 16.7 Hz, aromatic), 126.5 (s, aromatic), 126.3 (d, J_{CP} = 4.5 Hz, aromatic), 122.8 (s, aromatic), 122.3 (s, aromatic), 121.7 (s, aromatic) 50.2 (d, $^2J_{CP}$ = 8.1 Hz, CH_2), 49.6 (d, $^2J_{CP}$ = 24.1 Hz, CH_2'); $^{31}P\{^1H\}$ 145.8 (s).

HRMS calcd for $C_{33}H_{25}N_2O_2P$ 512.1653, found 512.1669. IR (neat solid, cm^{-1}) 2963(m), 1589(w), 1507(w), 1259(s), 1066(s), 1016(s).

“(R)-BINOL-*N*-benzyl-*N*-(2-(6-methoxypyridyl))methyl-phosphoramidite” (**135b**). To a Schlenk flask containing (R)-BINOL (0.202 g, 0.705 mmol), PCl_3 (0.500 mL, 5.73 mmol) was added followed by NMP (0.010 mL) and the mixture was heated to reflux for 1 h. After cooling to rt, the excess PCl_3 was removed under high vacuum. Residual PCl_3 was removed by coevaporation with Et_2O (3 × 3 mL). THF (4 mL) was added followed by Et_3N (0.150 mL, 1.13 mmol) and **139 (**0.161 g, 0.706 mmol). After 2.5 h stirring at rt, the slurry was filtered over Celite® and the volatiles were removed under high vacuum. The yellow solid was purified by flash chromatography (2 x 18 cm silica). The column was first neutralized using 50 mL hexanes/Et_3N 9:1 v/v then eluted with CH_2Cl_2/hexanes/Et_3N 1:3:0.2 v/v/v to give **135b** as a white solid (0.153 g, 0.282 mmol, 40%), m.p. 58-60 ºC (capillary).

NMR (δ, $CDCl_3$) ^1H 8.07 (d, $^3J_{HH}$ = 8.8 Hz, 1H, aromatic), 8.00 (d, $^3J_{HH}$ = 8.13 Hz, 1H, aromatic), 7.88 (d, $^3J_{HH}$ = 7.8 Hz, 1H, aromatic), 7.82 (d, $^3J_{HH}$ = 8.7 Hz, 1H, aromatic), 7.69 (d, $^3J_{HH}$ = 9.9 Hz, 1H, aromatic), 7.67–7.60 (m, 1H, aromatic), 7.51–7.40 (m, 6H, aromatic), 7.36–7.24 (m, 5H, aromatic), 7.10 (d, $^3J_{HH}$ = 8.7 Hz, 1H, aromatic), 6.98 (d, $^3J_{HH}$ = 7.5 Hz, 1H, aromatic), 6.75 (d, $^3J_{HH}$ = 8.4 Hz, 1H, aromatic), 4.32–4.22 (m, 2H, CH_2), 4.07 (s, 3H, CH_3), 3.81–3.57 (m, 2H, CH_2); $^{13}C\{^1H\}$ 164.0 (s, aromatic), 156.2 (s, aromatic), 149.9 (d, J_{CP} = 5.6 Hz, aromatic), 149.6 (s, aromatic), 139.0 (s, aromatic), 138.1 (s, aromatic), 133.0 (s, aromatic), 132.7 (s, aromatic), 131.6 (s, aromatic), 130.9 (s, aromatic), 130.4 (d, J_{CP} = 15.6 Hz, aromatic), 129.1 (s, aromatic), 128.53 (s, aromatic), 128.46 (s, aromatic), 128.4 (s, aromatic), 127.4 (s, aromatic), 127.2 (s, aromatic), 127.1 (s, aromatic), 126.2 (d, J_{CP} = 3.5 Hz, aromatic), 125.0 (s, aromatic), 124.8 (s, aromatic), 124.2 (d, J_{CP} = 5.1 Hz, aromatic), 122.9 (d, J_{CP} = 2.0

Hz, aromatic), 122.3 (s, aromatic), 121.7 (s, aromatic), 115.6 (s, aromatic), 109.3 (s, aromatic), 53.7 (s, CH_3), 50.3 (d, J_{CP} = 24.7 Hz, CH_2), 48.7 (d, J_{CP} = 13.6 Hz, CH_2); $^{31}P\{^1H\}$ 146.1 (s).

HRMS calcd for $C_{34}H_{27}N_2O_3PNa^4$ 565.1657, found 565.1677. IR (neat solid, cm^{-1}) 3064(w), 2974(w), 1578(s), 1464(s), 1229(s), 933(m).

"[(Ind)RuCl((R)-BINOL-*N*-benzyl-*N*-(2-pyridyl)methyl-phosphoramidite)]" (**136a**). To a Schlenk flask containing $[(Ind)RuCl(PPh_3)_2]$ (**110**) (0.248 g, 0.319 mmol) and **135a** (0.164 g, 0.319 mmol), toluene (5 mL) was added and the mixture heated to reflux for 14 h. Upon cooling to rt, the solvent was removed under high vacuum. The resulting residue was purified by flash chromatography (2 × 15 cm silica), eluted with CH_2Cl_2/Et_2O (9:1 v/v) and then CH_2Cl_2/Et_2O (4:1 v/v). The second of two orange bands was collected and all volatiles removed under high vacuum to give **136a** as an orange solid (0.146 g, 0.191 mmol, 60%), m.p. 178–179 ^{o}C dec. (capillary).

NMR (δ, $CDCl_3$) ^1H 8.34 (d, $^3J_{HH}$ = 8.8 Hz, 1H, aromatic), 8.03 (d, $^3J_{HH}$ = 8.8 Hz, 1H, aromatic), 7.97–7.92 (m, 3H, aromatic), 7.46–7.35 (m, 6H, aromatic), 7.28–7.23 (m, 4H, aromatic), 7.16–7.15 (m, 2H, aromatic), 6.87–6.84 (m, 1H, aromatic), 6.80–6.74 (m, 2H, aromatic), 6.70–6.71 (m, 1H, aromatic), 6.63 (d, $^3J_{HH}$ = 8.1 Hz, 1H, aromatic), 6.54 (d, $^3J_{HH}$ = 7.3 Hz, 2H, aromatic), 6.43 (d, $^3J_{HH}$ = 7.1 Hz, 1H, aromatic), 4.78–4.77 (m, 1H, indenyl), 4.66–4.54 (m, 2H, C*H*H', indenyl), 4.34 (s, br, indenyl), 3.82–3.53 (m, 3H, CH*H*', C*H*$_2$); $^{13}C\{^1H\}$ 157.8 (s, aromatic), 156.4 (s, aromatic), 149.4 (d, J_{CP} = 12.6 Hz, aromatic), 148.5 (d, J_{CP} = 5.1 Hz, aromatic), 137.7 (s, aromatic), 134.8 (s, aromatic), 132.5 (s, aromatic), 132.1 (s, aromatic), 131.2 (s, aromatic), 130.9 (s, aromatic), 129.8 (s, aromatic), 129.5 (s, aromatic), 128.3 (s, aromatic), 128.0 (s, aromatic), 127.5 (s, aromatic), 127.4 (s, aromatic), 127.0 (d, J_{CP} = 6.6 Hz, aromatic), 126.5 (d, J_{CP} = 7.1 Hz, aromatic), 126.0 (s, aromatic), 125.7 (s, aromatic), 125.5 (s, aromatic), 124.9 (s, aromatic), 124.6 (s, aromatic), 124.4 (s, aromatic). 123.4 (s, aromatic), 122.9 (s, aromatic), 122.4 (s, aromatic), 122.2 (s, aromatic), 121.9 (s, aromatic), 121.1 (s, aromatic), 114.9 (d, $^2J_{CP}$ = 7.1 Hz, indenyl), 112.2 (d, $^2J_{CP}$ = 9.6 Hz, indenyl), 84.9 (s, indenyl), 61.7 (s, indenyl), 53.3 (d, $^2J_{CP}$ = 18.2 Hz, CH$_2$), 51.7 (s, indenyl), 51.1 (d, $^2J_{CP}$ = 4.0 Hz, CH$_2$); ^{31}P{^{1}H} 183.6 (s).

HRMS calcd for $C_{42}H_{32}N_2O_2PClRu$ 764.0933, found 764.0916. IR (neat solid, cm^{-1}) 3049(w), 1588(w), 1458(m), 1321(m), 1226(s), 1066(m), 945(s), 746(s).

“[(Ind)RuCl(PPh$_3$)((R)-BINOL-*N*-benzyl-*N*-(2-(6-methoxypyridyl))methyl-phosphoramidite]” (**140**). To a Schlenk flask containing [(Ind)RuCl(PPh$_3$)$_2$] (**110**) (0.102 g, 0.132 mmol) and **135b** (0.077 g, 0.143 mmol), toluene (2 mL) was added and the mixture heated to reflux for 14 h. Upon cooling to rt, the solvent was removed under high vacuum. Crude NMR analysis revealed that the monosubstituted complex **140** was the major product.

NMR (δ, CDCl$_3$, partial) ^{1}H 5.83 (s, 1H, indenyl), 5.46 (s, 1H, indenyl), 5.02–4.92 (m, 1H, C*H*H’), 4.86–4.76 (m, 1H, CH*H*’), 4.40–4.30 (m, 1H, C*H*H’), 4.27 (s, 1H, indenyl), 4.14–4.02 (m, 1H, CH*H*’), 3.96 (s, 3H, CH_3); ^{31}P{^{1}H} 175.4 (d, $^2J_{PP}$ = 61.2 Hz, phosphoramidite), 47.9 (d, $^2J_{PP}$ = 61.2 Hz, *P*Ph$_3$).

“[(Ind)Ru(PPh$_3$)((R)-BINOL-*N*-benzyl-*N*-(2-(6-methoxypyridyl))methyl-phosphoramidite]BF$_4$” (**141a**). To a Schlenk flask containing [(Ind)RuCl(PPh$_3$)$_2$] (**110**) (0.150 g, 0.194 mmol) and **135b** (0.107 g, 0.198 mmol), toluene (3 mL) was added and the mixture heated to reflux for 14 h. Upon cooling to rt, $AgBF_4$ (0.040 g, 0.206 mmol) was added, forming a precipitate (AgCl). After filtration of the resulting slurry, the volatiles were removed under high vacuum. The resulting residue was purified by flash chromatography (2 × 15 cm silica), eluted with CH_2Cl_2/Et_2O 9:1 v/v then CH_2Cl_2/Et_2O 4:1 v/v. The orange band was collected and all volatiles removed under high vacuum to give **141a** in ca. 90% spectroscopic purity.

NMR (δ, $CDCl_3$, partial) ^1H 6.31–6.24 (m, 2H, CH_2), 5.92–5.86 (m, 2H, CH_2), 5.26 (s, br, 1H, indenyl), 5.12 (s, br, 1H, indenyl), 3.43–3.38 (m, 2H, indenyl + 1H), 3.15 (s, 3H, CH_3), 1.28–1.17 (m, 1H); $^{31}P\{^1H\}$ 174.5 (d, $^2J_{PP}$ = 69.6 Hz, phosphoramidite), 63.5 (d, $^2J_{PP}$ = 69.6 Hz, PPh_3).

X-ray Structure Determination for 132: X-ray quality crystals of **132** were obtained by slow diffusion of MeOH into a solution of **132** in CH_2Cl_2 at –10 °C.

Preliminary examination and X-ray data collection were performed using a Bruker Kappa Apex II single crystal X-Ray diffractometer equipped with an Oxford Cryostream LT device. Intensity data were collected by a combinations of ϖ and ϕ scans. Apex II, SAINT and SADABS software packages (Bruker Analytical X-Ray, Madison, WI, 2008) were used for data collection, integration and correction of systematic errors, respectively.

Crystal data and intensity data collection parameters are listed in Table 1. Structure solution and refinement were carried out using the SHELXTL- PLUS software package.[5] The structure was solved by direct methods and refined successfully in the space group $P2_12_12_1$. The non-hydrogen atoms were refined anisotropically to convergence. All hydrogen atoms were treated using appropriate riding model (AFIX m3).

---

[1] (a). Hulst, R.; de Vries, N. K.; Feringa, B. L. *Tetrahedron: Asymmetry*, **1994**, *5*, 699; (b). Duursma, A.; Boiteau, J.-G.; Lefort, L.; Boogers, J. A. F.; de Vries, A. H. M.; de Vries, J. G.; Minnaard, A. J.; Feringa, B. L. *J. Org. Chem*. **2004**, *69*, 8045.

[2] Oro, L. A.; Ciriano, M. A.; Campo, M. *J. Organomet. Chem*. **1985**, *289*, 117.

[3] Jackstell, R.; Klein, H.; Beller, M.; Wiese, K.-D.; Rottger, D. *Eur. J. Org. Chem.* **2001**, 3871.

[4] The molecule had to be sodiated to give a molecular ion of appropriate intensity.

[5] G. M. Sheldrick, *Acta Cryst*. **2008**, *A64*, 112.